ANALYTICA CHIMICA ACTA

International monthly devoted to all branches of analytical chemistry
Revue mensuelle internationale consacrée à tous les domaines de la chimie analytique
Internationale Monatsschrift fur alle Gebiete der analytischen Chemie

ELSEVIER SCIENTIFIC PUBLISHING COMPANY

AMSTERDAM

Anal. Chim. Acta, Vol. 73, No. 2, 225–440, December 1974

Published monthly

Completing Volume 73

Publication Schedule for 1974

Vol. **68**, No. **1**	January 1974	
Vol. **68**, No. **2**	February 1974	**(completing Vol. 68)**
Vol. **69**, No. **1**	March 1974	
Vol. **69**, No. **2**	April 1974	**(completing Vol. 69)**
Vol. **70**, No. **1**	May 1974	
Vol. **70**, No. **2**	June 1974	**(completing Vol. 70)**
Vol. **71**, No. **1**	July 1974	
Vol. **71**, No. **2**	August 1974	**(completing Vol. 71)**
Vol. **72**, No. **1**	September 1974	
Vol. **72**, No. **2**	October 1974	**(completing Vol. 72)**
Vol. **73**, No. **1**	November 1974	
Vol. **73**, No. **2**	December 1974	**(completing Vol. 73)**

Subscription price: Dfl. 492.00 plus Dfl. 36.00 postage. Subscribers in the U.S.A. and Canada receive their copies by airmail. Additional charges for airmail to other countries are available on request. For advertising rates apply to the publishers.

Subscriptions should be sent to:
Elsevier Scientific Publishing Company, P.O. Box 211, Amsterdam, The Netherlands.

GENERAL INFORMATION

Languages

Papers will be published in English, French or German.

Submission of papers

Papers should be sent to:

PROF. PHILIP W. WEST,
Coates Chemical Laboratories,
College of Chemistry and Physics,
Louisiana State University,
Baton Rouge 3,
La. 70803 (U.S.A.)

or to:

DR. A. M. G. MACDONALD,
Department of Chemistry,
The University,
P.O. Box 363
Birmingham B15 2TT (Great Britain)

Reprints

Fifty reprints will be supplied free of charge. Additional reprints (minimum 100) can be ordered at quoted prices. They must be ordered on order forms which are sent together with the proofs.

PRINTED IN THE NETHERLANDS

AUTOMATIC AIR QUALITY MONITORING SYSTEMS

Proceedings of the Conference held at the National Institute of Public Health, Bilthoven, The Netherlands, 5-8 June, 1973.

edited by **T. SCHNEIDER,** National Institute of Public Health, Bilthoven, The Netherlands.

1974. 284 pages. Dfl. 42.00 (about US$15.30) ISBN 0-444-41202-6

This symposium was organized by the National Institute of Public Health in Bilthoven, The Netherlands. Its purpose was to set up an exchange of knowledge on existing and planned automated air quality monitoring systems and the analysis of the air pollution data. It comprised the following subjects: monitors for measurement of air pollution and their use in the systems approach; design and application of automatic systems; data handling and data evaluation in connection with large systems; use of models for the determination of dispersion of air pollution; and application of monitoring systems within the existing international cooperation. As a result of the symposium a plan has been developed for future international cooperation between national research institutes and governmental agencies in the field of monitoring of pollution with a systematic and harmonized approach.

CONTENTS:

Elsevier
P.O. BOX 211
AMSTERDAM, THE NETHERLANDS
1292 E

Optimal Substance Separation with Pre-packed Columns

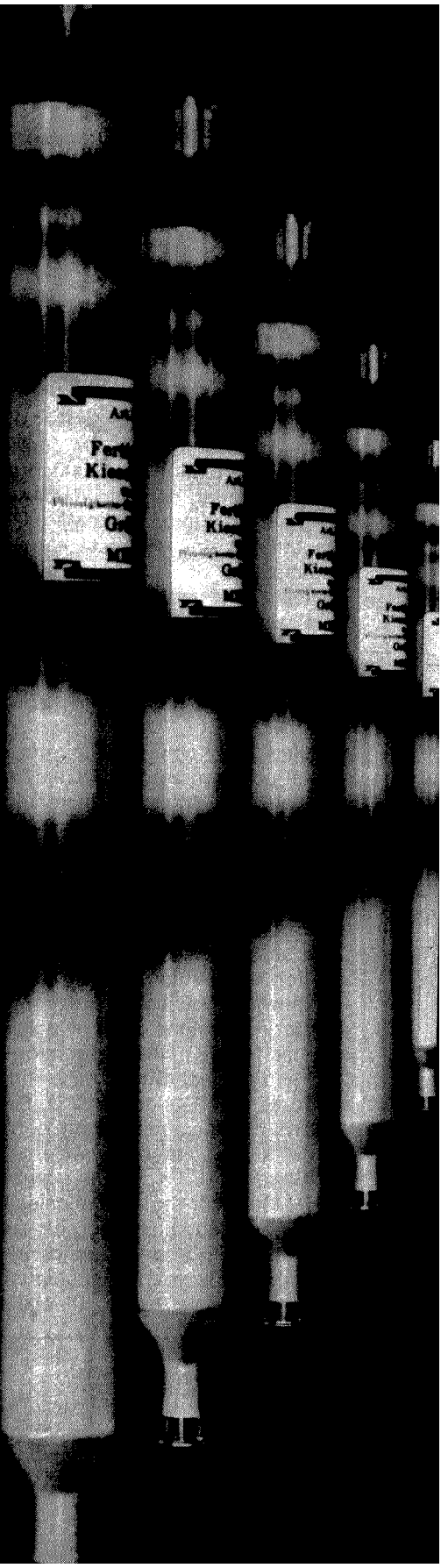

Analytica Chimica Acta, 73 (1974) 225–234

NON-DESTRUCTIVE DETERMINATION OF SILVER IN LEAD BY NEUTRON ACTIVATION WITH A ^{227}Ac–Be ISOTOPIC NEUTRON SOURCE

L. ALAERTS*, J. VAN SCHUERBEEK, J. P. OP DE BEECK and J. HOSTE
Institute for Nuclear Sciences, Rijksuniversiteit Gent, Proeftuinstraat 86, B-9000 Gent (Belgium)
(Received 2nd July 1974)

There are many potential systematic errors in the cupellation process as part of the fire-assay technique, which is commonly used in industrial routine analysis for silver, hence a fast and accurate new method for the determination of silver in lead, in concentrations ranging from a few hundred up to several thousand p.p.m., should have numerous applications.

As described earlier[1–5], non-destructive neutron activation analysis with the aid of an isotopic neutron source has proved to be a powerful tool for the fast, precise and accurate determination of some major constituents in ores and alloys.

In this paper, it will be shown, that, by applying this technique to the determination of silver in lead and by exploiting the favourable properties of some silver nuclides, a relative precision of 1% or better on the mean of four analyses can be reached within 10 min, with relatively small samples (*ca.* 17.4 g) containing 1000 p.p.m. silver or more.

The determination of silver by neutron activation

In Table I the nuclear properties of the silver isotopes are summarized. Only three radioisotopes give rise to measurable activities after irradiation of natural silver with thermal and epithermal neutrons.

All of these isotopes have already been used for the determination of silver, in a wide range of concentrations, in various materials, by activation analysis based on nuclear reactors, neutron generators and isotopic neutron sources[9].

TABLE I

NUCLEAR DATA FOR NATURAL SILVER[6–8]

Stable isotopes	*Abundance (%)*	*(n, γ) Product*	σ_0 *(barn)*	I_0 *(barn)*	$T_{\frac{1}{2}}$	*Main γ-energies and intensity (MeV)*
^{107}Ag	51.83	^{108}Ag	37	143	2.41 min	0.632 (1.7%) 0.434 (0.5%)
^{109}Ag	48.17	^{110}Ag	88	1400	24.6 s	0.658 (4.5%)
		^{110m}Ag	4	70	252 day	0.658 (96%)

* Aspirant of the N.F.W.O.

Nuclear reactors are powerful tools for determining very low amounts of silver, but they cannot provide the inherent precision required in the present case, and can hardly if at all be adapted to an industrial environment.

Kusaka[10] originally used a relatively modest ^{226}Ra–Be source, containing only 50 mg of radium, for the determination of silver in samples in which it was present as a major constituent. Senftle *et a* .[11] have described a mobile system consisting of a ^{252}Cf isotopic neutron source, a 3-MeV deuterium accelerator and NaI(Tl) detectors for *in situ* activation analysis of silver in silver ores. Concentrations as low as 6 p.p.m. could be detected, but in view of the complexity of the spectra, little could be said about the precision. Vakhtin and Filippov[12] described the determination of silver in geological samples, with the aid of a 10^7 n s^{-1} ^{238}Pu–Be source, by absorption of resonance neutrons. They obtained a straight line for silver concentrations between 0 and 2500 p.p.m., but the standard error of $\pm$500 p.p.m. that was obtained did not allow quantitative conclusions to be drawn from these data.

Nuclear interferences

Some elements, occurring as minor or trace constituents in lead, give rise to short-lived activities. The nuclear properties of the potential interfering nuclides are summarized in Table II, together with the range of concentrations of the corresponding elements in the available lead samples. Taking into account the irradiation, waiting and counting periods actually used, one can calculate the apparent silver concentrations corresponding to the given concentrations of interfering elements.

TABLE II

INTERFERING ACTIVITIES[6–8]

Stable isotope	*Abundance (%)*	*(n, γ) Product*	σ_{th} *(barn)*	I_0 *(barn)*	$T_{\frac{1}{2}}$ *(min)*	*% γ Detected*	*Concn. in Pb samples (%)*	*Apparent Ag concn (p.p.m.)*
^{65}Cu	30.9	^{66}Cu	2.17	2.2	5.1	9.25	0.1–0.4	5.2–21
^{121}Sb	57.3	^{122m}Sb	0.06	1.96	4.2	67	0.01–0.13	0.5–7.0
^{123}Sb	42.7	^{124m}Sb	0.04	1.07	1.6	20		0.2–3.0
^{124}Sn	5.8	^{125m}Sn	0.13	7	9.2	100	0.01	0.1
^{70}Zn	0.62	^{71}Zn	0.09	0.04	2.4	19.5	0.5–1.1	0.1–0.2

As can be seen from the last column of Table II, the ^{71}Zn and ^{125m}Sn activities can be neglected. As to ^{122m}Sb, the low γ-energies (61 and 75 keV) emitted by this isotope mean that a large fraction is absorbed by the lead sample. The only interferences that finally must be taken into account are ^{66}Cu and ^{124m}Sb. In practice, an amount of 1000 p.p.m. of copper or antimony in lead results in, respectively, 5.2 and 2.3 p.p.m. of apparent silver content. For high concentrations of copper, this interference can be reduced by irradiating under a cadmium thermal neutron filter.

EXPERIMENTAL

Neutron source and counting equipment

All irradiations were carried out with the annular ^{227}Ac–Be isotopic neutron source described previously[3]. During the actual analysis the thermal and epithermal neutron flux at the irradiation site amounted to $4.1 \cdot 10^5$ n cm^{-2} s^{-1} and $2.2 \cdot 10^4$ n cm^{-2} s^{-1}, respectively.

A 7.5 × 7.5-cm NaI(Tl) detector with a well of 3.3-cm diameter and 4.3-cm depth was used for all measurements. The detector assembly was coupled to a Canberra model 1418 amplifier and model 1431 single channel analyser. Counts were collected with a N.E. 4613 scaler. The automatic irradiation, waiting and counting cycle-time was controlled by three N.E. 4624 timers. At the end of the counting cycle, the results were printed automatically on a teletype printer.

Sample preparation

Cylindrical samples of 5 ± 0.1 mm height and 20 ± 0.1 mm diameter were machined from the available lead and from the standard lead ingots. A high precision on the sample geometry is necessary to avoid systematic errors arising from differences in irradiation and counting geometry in the presence of rather sharp flux gradients at the irradiation site[3].

Optimization of the irradiation conditions

Ten 17.5-g lead samples containing *ca.* 2500 p.p.m. of silver were irradiated one after the other for 60 s, and counted during 60 s after a delay of 10 s. The

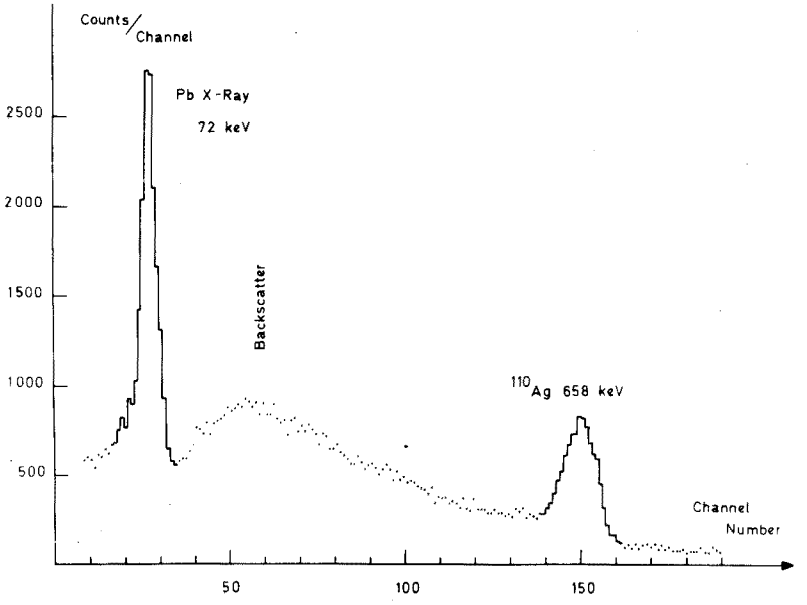

Fig. 1. Sum of 10 NaI(Tl) spectra of a lead sample containing 2500-p.p.m. silver. Irradiation time. 60 s; cooling time, 10 s; counting time, 60 s.

spectra were accumulated with a 400-channel analyser. The channel-by-channel sum was made as shown in Fig. 1. An intensive lead x-ray fluorescence peak at 72 keV can be seen, apart from the 658-keV γ-rays of ^{110}Ag. The decay of both peaks as well as of the whole spectrum was followed with a 400-channel analyser in the multiscaler mode (steps of 4 s). As can be seen from Fig. 2, which gives the decay of the whole spectrum, only silver isotopes are present, whereas the contribution of the 632-keV γ-rays of ^{108}Ag is small. In view of the data in Table I, it can be decided that longer irradiations would not result in a significant gain in the number of counts, and would only increase the danger of interference by longer-lived isotopes from impurities in the lead.

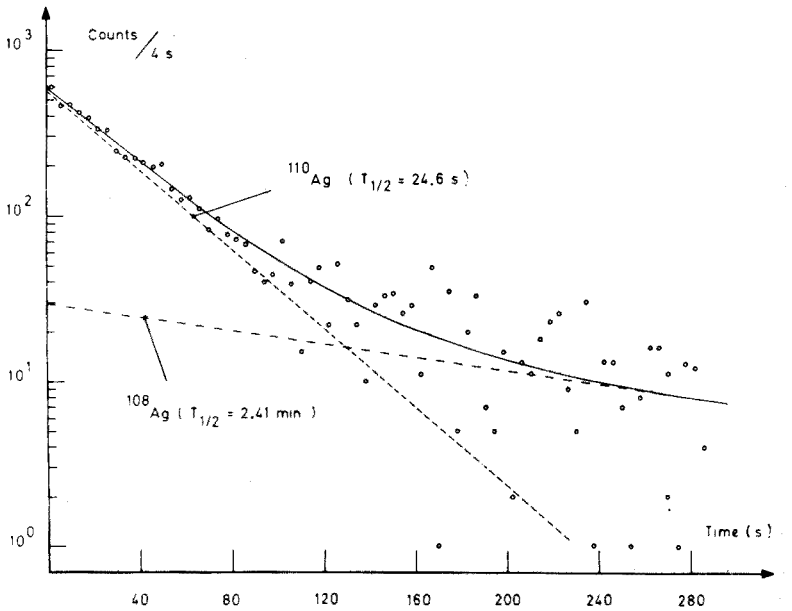

Fig. 2. Decay curve of a lead sample containing 2500 p.p.m. silver. Irradiation time, 60 s; cooling time, 10 s; steps of 4 s.

In order to optimize the geometry of irradiation, the activity of a silver-containing lead sample, after irradiation at different positions in the rabbit, was plotted against the height from the bottom of the irradiation tube. As shown in Fig. 3 the activation curve goes through a maximum at a height of 3.2 cm from the bottom. This is completely in agreement with a calculated activation curve for the reaction ^{109}Ag (n, γ) ^{110}Ag by means of the following equation:

$$A_t = k(\Phi_{th} \cdot \sigma_0 + \Phi_{epi} \cdot I_0) \tag{1}$$

where A_t = activity of the sample after irradiation at a fixed position
Φ_{th} = thermal neutron flux at that position
Φ_{epi} = epithermal neutron flux at that position
σ_0 = thermal neutron cross section for the given reaction
I_0 = resonance integral for the given reaction
k = proportionality constant

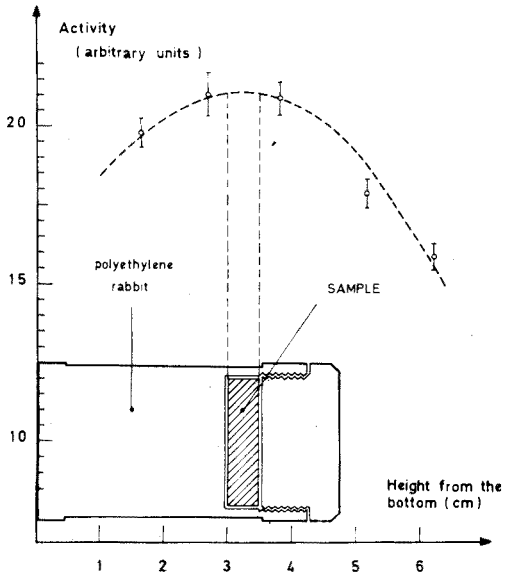

Fig. 3. Activity of a silver-containing lead sample as a function of the irradiation position. (○) Experimental, (---) calculated.

On the basis of this information, a polyethylene irradiation container was constructed, such as shown in Fig. 3, in order to fix the position of the sample during irradiation at the maximum of the activation curve.

Preparation of standards

The history and the method of preparation of the lead samples to be analyzed was not known, hence it was decided to prepare standards with an accurately known amount of silver, instead of making high-precision analyses on the available samples by chemical methods.

Originally, an attempt was made to produce standards by spontaneous deposition of silver on lead grains from an aqueous $Ag[S_2O_3]_2^{3-}$ solution. After washing and drying, pellets were pressed from the lead powder having the same dimensions and density as the samples. These precipitations of silver were quantitative and reproducible within 0.5%, as was proved in tracer experiments with ^{110m}Ag. The activity measurements after irradiation, however, showed deviations of more than 10% from the correct calibration curve when the silver content exceeded 2000 p.p.m. (Fig. 4). This effect is probably due to local high concentrations of silver in the lead pellets resulting in excessive neutron shadow effects.

Subsequently, standards were prepared by melting in a quartz crucible high-purity silver foil (99.99%; thickness: 0.5 mm), cut into fine bits, together with the lead grains with dimensions between 150 and 750 μm. To avoid the formation of yellow lead oxide (PbO), which readily attacks quartz at high temperature, all fusions were carried out under a hydrogen atmosphere. The silver cuttings were weighed on a microbalance and mixed with 80–100 g of accurately weighed lead grains, previously etched in 0.06 *M* nitric acid, washed with water and dried. After

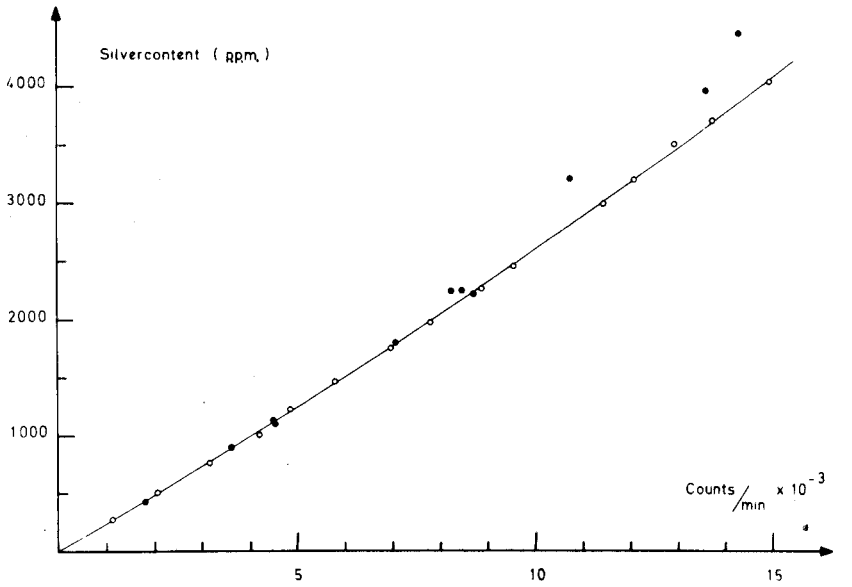

Fig. 4. Calibration curve for the determination of silver in unknown samples, established with standards obtained by melting. (○) Standards obtained by melting; (●) standards obtained by spontaneous deposition. $P.P.M. = 4.7 + 239.21\ x + 3.026\ x^2 - 0.1891\ x^3 + 0.01476\ x^4 - 0.000348\ x^5$.

heating for 50 min over a Bunsen burner under a hydrogen stream, at a temperature of *ca.* 550°C, the liquid mass was poured into a graphite mould. By pre-heating the mould to a temperature just above the melting point of lead before the casting, immediate solidification and trapping of air bubbles in the ingots were avoided. By gradually cooling the melt, the solidification starts inwards from the graphite–molten-lead boundary. As a result silver gradients were observed, pointing to an enrichment of silver in the solid phase. Differences of up to 3% in induced activity were noticed between the top and bottom discs (20-mm diam.; 5-mm height; weight, *ca.* 17.4 g), that were machined out of the lead ingots (23-mm diam.; 30-mm height). These gradients, however, could be avoided by immersing the hot graphite mould, containing the melt, suddenly and completely in cold water after the air bubbles formed by the pouring of metal had been allowed to escape from the melt. This fast quenching produced lead ingots with homogeneously distributed silver, but often containing cavities, owing to the sudden shrinkage on solidification, in the upper part where the melt came in direct contact with the water. As a precaution only one standard was machined out of the bottom part of each ingot intended for establishing a calibration curve.

In this way, fifteen standards with silver concentrations between 250 and 4000 p.p.m. were prepared. A blank lead sample was prepared in an identical way in order to correct for the silver content (< 10 p.p.m.) of the lead grains.

Calibration curve

The optimized irradiation conditions described above were used to establish a calibration curve for the determination of silver in unknown samples. Each

standard was irradiated for 60 s at the maximum of the activation curve. A delay time of 10 s allowed for the transfer of the container from the neutron source, via the receiving station of the pneumatic transport system, into the detector. The container was put into the detector upside down, in order to optimize the counting geometry. To save time, each standard was irradiated while the previous one was still being counted. The whole series of standards was analysed four times, resulting in sixty experimental data points.

By means of a computer program, based on the subroutine POLFIT taken from Bevington[13], the degree and the coefficients of the best polynomial approximation through these points (number of counts as a function of silver content) were determined. The program is based on a minimization of χ^2. By means of a second program the obtained polynomial was inverted in order to obtain concentration values as a function of the number of counts. A polynomial of the fifth order resulted in the smallest χ^2 value:

$$P.P.M. = \sum_{i=0}^{5} a_i A^i \tag{2}$$

where *P.P.M.* is the silver content in p.p.m.; A is the net activity divided by 1000, of a 17.4-g sample or standard after irradiation and counting under standardized conditions; and a_i are the coefficients calculated by the computer (Fig. 4).
The calibration curve is presented in Fig. 4 and shows the precision that can be obtained, as well as the lack of accuracy for standards obtained by spontaneous silver deposition for high silver concentrations. The curve obtained deviates from a straight line because of neutron self-shielding effects.

RESULTS AND DISCUSSION

In Table III the results of the analyses are given for 12 industrial lead

TABLE III

RESULTS OBTAINED FOR COMMERCIAL LEAD SAMPLES

Sample code	*Fire assay result (p.p.m.)*	*N.a.a. result with stand. dev. (p.p.m.)*	*[N.a.a.−fire assay] (p.p.m.)*
47/1	948	971±14	+23
444/1	1064	1184±6	+120
444/2	1072	1230±1	+158
222/1	1161	1185±16	+24
528/2	1266	1297±7	+31
528/3	1295	1350±16	+55
152/2	1595	1625±10[a]	+30
494/4	2156	2081±14	−75
1	193	222±5	+29
2	480	535±6	+55
3	1126	1145±13	+19
4	2345	2331±20	−14

[a] Corrected for ^{66}Cu (0.4% Cu in the sample).

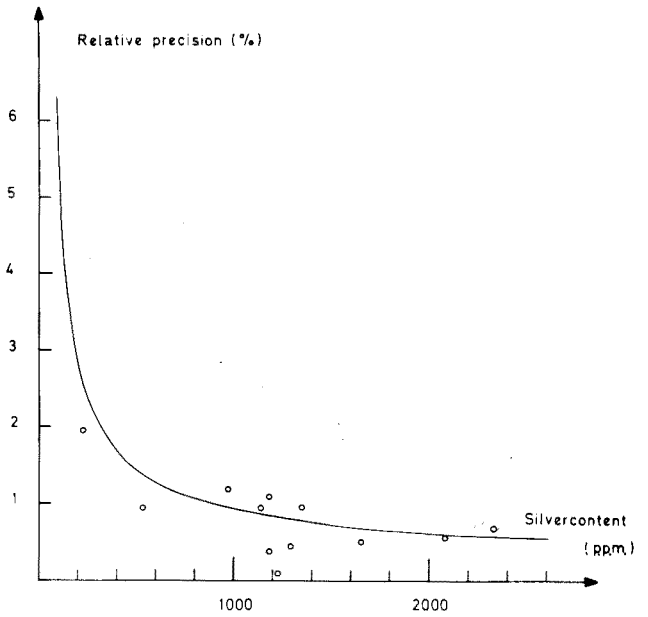

Fig. 5. Relative precision as a function of the silver concentration. (○) Experimental points (without t-factor); calculated line (counting statistics).

samples, with silver concentrations between 200 and 2400 p.p.m. The standard deviation on the mean of 4 analyses, taking into account Student's t-factor for a 70% confidence level, is indicated. A comparison is made between the results obtained by n.a.a., calculated by means of eqn. (2), and the chemical results in industry by the fire-assay technique. From the first eight samples, two discs were made and each was analysed twice, whereas for the last four samples four analyses were made of a single disc from each sample.

For samples with silver concentrations of *ca.* 1000 p.p.m. or more, a mean relative precision, calculated from the indicated standard deviations, of 0.8% was obtained. This precision is an improvement over the one that can be reached by the fire-assay[14] procedure. The available precision is, of course, a function of the silver concentration in the lead sample, since it is determined by the counting statistics on the induced activity. Figure 5 shows the precision as a function of the silver concentration for the irradiating and counting conditions, as well as sample size, used in this work. The counting statistics on the background of 725 counts min^{-1}, cause a significant deterioration of the relative precision on samples with silver contents lower than *ca.* 500 p.p.m. From the background activity, one can calculate a detection limit of 26 p.p.m. by means of the equation for the "well-known blank" as defined by Currie[15].

Table IV gives the results for four discs made from two particular lead samples. It is obvious that the silver was not homogeneously distributed over these samples. In particular, for sample 470/2 the difference between the chemical result and the n.a.a. result strongly suggests that the inhomogeneity is even greater than can be deduced from the n.a.a. results.

TABLE IV

RESULTS FOR INHOMOGENEOUS SAMPLES

Sample code	*Fire assay result (p.p.m.)*	*N.a.a. result (p.p.m.)*	*Mean with stand. dev. (p.p.m.)*	*[N.a.a.–fire assay] (p.p.m.)*
470/2	755	A {379, 349}	423±43	−322
		B {486, 478}		
494/1	2521	A {2434, 2437}	2492±41	−29
		B {2557, 2540}		

[a] A and B denote two different discs from the same sample.

From the comparison of the chemical and the n.a.a. results it appears that usually, the fire-assay treatment gives a systematic negative bias.

Considering both the possibility of preparing standards from pure elements as well as the precision obtained on the calibration curve, it may be concluded with regard to the irreproducibility of the differences between the n.a.a. and chemical results, that not only the precision but also the accuracy of the proposed method are superior to those of the fire-assay technique.

X-Ray fluorescence spectrometry with radioisotope excitation (45 mCi ^{241}Am) has been proposed as an alternative method for the instrumental determination of silver in lead[16]. However, both the detection limit (160 p.p.m.) and the attainable precision, because of counting statistics, for a silver concentration range of 1000–2500 p.p.m. (1340 counts per hour for a lead sample containing 0.1% silver) are considerably lower than those of the n.a.a. method proposed in this work. Moreover, correction factors for differences in matrix absorption, mainly owing to the occurrence of tin and antimony in the samples, have to be introduced, so that systematic errors become possible.

CONCLUSIONS

In spite of their relatively low neutron density, isotopic neutron sources appear to be very suitable for determining silver in lead by i.n.a.a. with high precision, accuracy and speed.

For a lead sample containing 0.1% of silver, a relative precision of 0.9% can be reached within 10 min. For the same sample, the fire-assay procedure would result in a precision between 1 and 2% and require an analysis time of 3–4 hours[14].

Since standards can be prepared from the pure elements, and as ^{110}Ag can be measured free of interference in the lead matrix, provided that copper and antimony do not exceed *ca.* 1000 p.p.m., an excellent accuracy is guaranteed, if the measurements are carried out with stable counting equipment, and if a small correction for the decay of the ^{227}Ac in the neutron source ($<0.01\%$ per day) is taken into account.

In view of the simplicity of the proposed n.a.a. method, the high precision and accuracy can be maintained for routine analyses with an automated system in an industrial laboratory without the necessity for highly qualified personnel. With adequate shielding, the neutron source does not present any radiation hazard, whereas the activity induced in the samples is so small that no shielding is required at all, and the samples can be handled manually immediately after irradiation. Furthermore, the induced activity decays away extremely quickly and no radioactive waste build-up can occur.

All this places the n.a.a. technique above competition among the currently used routine analytical methods for silver.

Thanks are due to the "Nationaal Fonds voor Wetenschappelijk Onderzoek" for partial financial support, and to Dr G. Kraft (Metall Geselschaft) and Dr. R. De Neve (Metalurgie Hoboken) for providing the lead samples.

SUMMARY

A method has been developed for the determination of silver in lead by instrumental neutron activation analysis with the aid of a ^{227}Ac–Be isotopic neutron source. The samples are irradiated for 60 s, allowed to decay for 10 s, and counted for 60 s. ^{110}Ag can be measured free of interferences provided that copper and antimony do not occur in concentrations higher than *ca.* 1000 p.p.m. A calibration curve was established for silver concentrations between 0 and 4000 p.p.m. by means of standards prepared by melting together high-purity silver and lead under a hydrogen atmosphere. For 17.5-g lead samples, containing between 1000 and 2500 p.p.m. of silver, a mean relative precision of 0.8% was obtained after a 10-min analysis.

REFERENCES

1 J. P. Op de Beeck, L. Alaerts and J. Hoste, *Report No. 11*, Eurisotop Office, Brussels, 1972.
2 L. Alaerts, J. P. Op de Beeck and J. Hoste, *J. Radioanal. Chem.*, 15 (1973) 601.
3 L. Alaerts, J. P. Op de Beeck and J. Hoste, *Anal. Chim. Acta*, 69 (1974) 1.
4 L. Alaerts, J. P. Op de Beeck and J. Hoste, *Anal. Chim. Acta*, 70 (1974) 253.
5 L. Alaerts, J. P. Op de Beeck and J. Hoste, *Anal. Chim. Acta*, 73 (1974) 53.
6 N. E. Holden and F. W. Walker, *Chart of the Nuclides*, General Electric Company, Schenectady, N. Y., 1972.
7 C. M. Lederer, J. M. Hollander and I. Perlman, *Table of Isotopes*, Wiley, New York, 1967.
8 R. Van der Linden, Ph. D. Thesis, University of Gent, Belgium, 1974.
9 R. Gijbels and J. Hoste, *Report No. 66*, Eurisotop Office, Brussels, 1971.
10 Y. Kusaka, *Bunseki Kagaku*, 8 (2) (1959) 111.
11 F. E. Senftle, P. W. Philbin and P. Sarigianis, *Isotop. Radiat. Technol.*, 7 (1970) 411.
12 B. S. Vakhtin and E. M. Filippov, *Sov. J. Non-Ferrous Metals*, 9 (12) (1968) 19.
13 P. R. Bevington, *Data Reduction and Error Analysis for the Physical Sciences*, McGraw Hill, New York, 1969, p. 140.
14 H. Pohl, *Report No. 64*, Eurisotop Office, Brussels, 1971.
15 L. A. Currie, *Anal. Chem.*, 40 (1968) 586.
16 J. De Neef, F. Adams and J. Hoste, *Anal. Chim. Acta*, 62 (1972) 71.

Analytica Chimica Acta, 73 (1974) 235–244

THE DETERMINATION OF MERCURY IN WATER SAMPLES FROM THE ENVIRONMENT BY NEUTRON ACTIVATION ANALYSIS

H. A. VAN DER SLOOT and H. A. DAS
Stichting Reactor Centrum Nederland, Petten (The Netherlands)
(Received 12th June 1974)

The possibility of determining even small changes in the mercury content of natural waters is important for pollution control. This requires a sensitive method, which is capable of detecting mercury at concentrations well below 100 ng l^{-1}. In this region, activation analysis is superior to atomic absorption[1–3] owing to its greater sensitivity, if a suitable way of concentrating mercury on a solid adsorber can be found. This preconcentration is necessary, as the irradiation of water samples in a nuclear reactor is cumbersome. Olafsson collected inorganic mercury from sea water by reduction with tin(II) chloride, volatilization and amalgamation with a gold foil[4]. This method is not applicable to organic mercury compounds. Moreover, gold is not a convenient matrix for activation analysis.

A diluted tin(II) solution, acetone and twice-distilled nitric acid are the only reagents used in the method presented here. These reagents can be stripped of mercury easily so that there is no contamination by the reagents[5,6]. Any losses by adsorption on the walls of the storage bottles[7–9] or volatilization of organic mercury compounds are minimized by performing the preconcentration step at the sampling site. The behaviour of some organic mercury compounds throughout the whole procedure has been studied with ^{197}Hg-labelled compounds.

The proposed method is an extension of the procedure described earlier[10] for the determination of mercury in air. As in the previous method, extensive use is made of activated charcoal as an absorbent for mercury compounds.

EXPERIMENTAL

Reagents and apparatus

A 1% (w/v) tin(II) chloride solution was aerated before use to remove any mercury.

Acetone (analytical-grade) was percolated through a charcoal column before use. Analytical-grade nitric acid was twice-distilled before use. The standard mercury(II) solution contained 0.1 mg Hg ml^{-1}. Activated charcoal (0.5–0.75-mm grain size) was of chromatographic quality (Merck).

A well-type NaI detector was mounted in a sample changer and connected to a 400-channel analyser with electric typewriter or punchtape read-out.

Separation of different forms of mercury

The following separation of different species of mercury has been made (*cf.* Fig. 1).

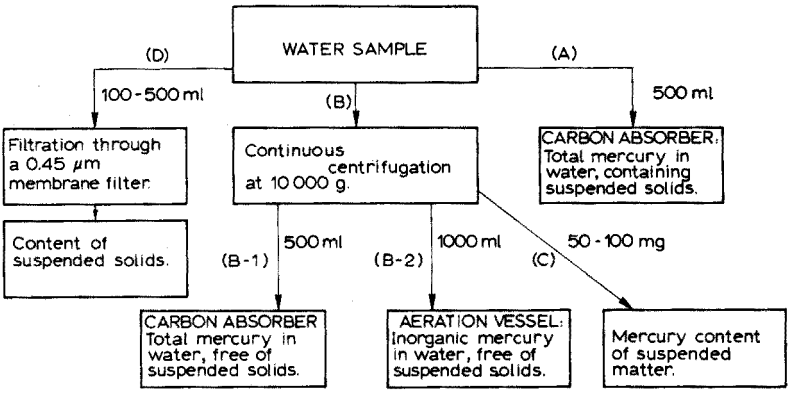

Fig. 1. Scheme for the sampling of inorganic, organic and particulate mercury.

The total amount of mercury in the water sample is collected by passing a known volume of the crude sample through an activated charcoal column (amount A). The mercury in solution and that adsorbed on suspended matter is concentrated as follows. Part of the water sample is freed from particulate matter by continuous centrifuging at 10000*g*. A known fraction of the clear liquid is passed through a charcoal column to collect the total amount of mercury present in water stripped of suspended solids (amount B1). The difference between the mercury concentrations for A and B1 gives the amount of mercury adsorbed on suspended matter.

Another fraction of the clear liquid is transferred to an aeration vessel. After reduction with tin(II) chloride, aeration and subsequent absorption on activated charcoal, the concentration of inorganic mercury is determined (amount B2). The organic mercury content can be derived from the difference between the two mercury concentrations determined for the samples B1 and B2.

The amount of mercury bound to suspended matter can also be determined in another way. Some of the solid concentrated by centrifugation is weighed after equilibration at constant relative humidity, thus obviating dubious drying procedures. Then the solid is mixed with charcoal and irradiated (amount C). Finally the amount of suspended matter is determined by weighing, after filtration of a known volume through a pre-weighed membrane filter (0.45 μm).

The collection of inorganic mercury

For the determination of inorganic mercury in water, the apparatus shown in Fig. 2 is used. The procedure is based on reduction to metallic mercury with tin(II) chloride and subsequent aeration with a stream of air, which carries the mercury to an activated charcoal absorber. The influence of the most important parameters on the recovery of mercury in the charcoal absorbers was studied with ^{197}Hg tracers.

Concentration of tin(II) chloride. High concentrations of tin(II) chloride (1.5 g/50 ml), such as are used in atomic absorption determinations, were found to be quite unnecessary, when reduction of only inorganic mercury is involved. A final concentration of 10 mg $SnCl_2\ l^{-1}$ is sufficient for complete reduction.

Flow rate of the air stream. The percentage of mercury remaining in the vessel

was determined as a function of the flow rate for solutions containing 0.18 μg Hg l^{-1}. Complete removal of mercury from the solution was obtained at flow rates higher than 3 l min^{-1}. However, to prevent any break-through in the charcoal absorber, the flow rate should not exceed 6 l min^{-1}. At flow rates between 3 and 6 l min^{-1}, complete collection of metallic mercury on the charcoal absorber was obtained (see also ref. 10).

Time of aeration. It was found that under normal conditions all mercury was volatilized within 5 min, hence this time was used in further experiments unless otherwise stated. At 4, 20 and 40 °C, complete volatilization took, respectively, 5, 3 and <2 min. This is in accordance with data published in literature[2,11].

Acidity and salinity of the sample. At high acid concentrations, a considerable amount of mercury will be retained in solution[11]. Between pH 1 and 7, no influence of acidity on aeration was observed. Salt concentrations up to 2 *M* sodium chloride showed no influence on the yield.

Volume of the sample. When small volumes (relative to the volume of the vessel) were processed, recoveries decreased. The recovery fell to 80 % in the case of a 100-ml sample.

Amount of charcoal. The amount of activated charcoal necessary for complete collection of volatilized mercury was determined by loading a 5.6-g charcoal bed with metallic mercury at a flow-rate of 5 l min^{-1}, and dividing it in fractions of 0.5 g each. The first fraction contained 96 %, and the second 4 %; the others did not contain any mercury. These and other results proved that the use of 2.5 g of charcoal is satisfactory.

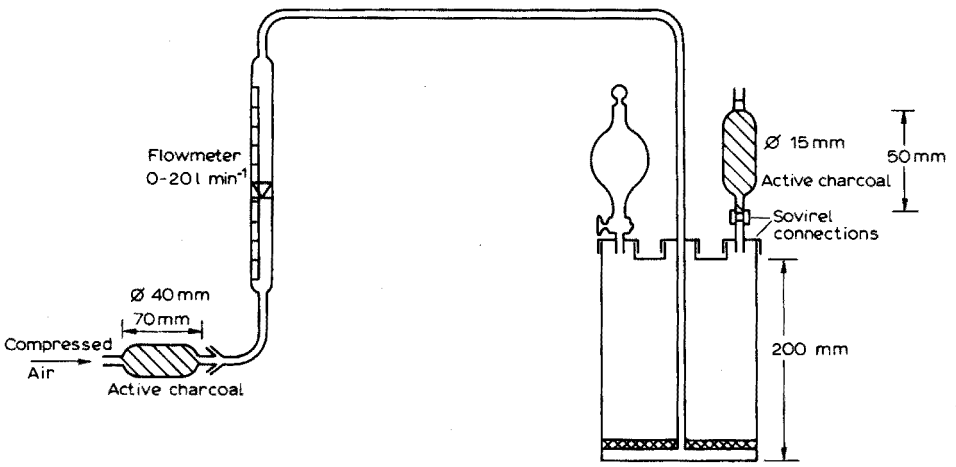

Fig. 2. The aeration vessel.

The reduction of organic mercury compounds. Only a small fraction (less than 0.5 %) of organic mercury compounds is reduced under the conditions recommended for the determination of inorganic mercury. Under more severe conditions (*e.g.* stronger reduction, or oxidation followed by reduction, combined with long aeration times), the results given in Table I were obtained. It can be concluded that a separation between the two species of mercury by the standard procedure is achieved.

TABLE I

VOLATILIZATION OF ORGANIC MERCURY COMPOUNDS FROM DILUTE AQUEOUS SOLUTIONS

Compound	*Concentration* ($\mu g\ l^{-1}$)	*Percentage found on charcoal absorber after*		
		Aeration[a]	*Reduction*[b]	*Oxidation–reduction*[c]
$(C_6H_5)_2Hg$	2.66	0.4	8.6	25.7
$(C_6H_5)HgCl$	0.67	0.2	3.5	13.4
$(C_6H_5)HgAc$	0.19	0.1	8.7	17.3
CH_3HgCl	1.39	0.2	5.8	20.7
$(CH_3)_2Hg$	22.6	0.14	0.07	—

[a] Aeration time was 5 min at a flow rate of 5 l min^{-1}.
[b] Reduction with $SnCl_2$ (final concentration 1 g l^{-1}) for 15 min. Aeration time was 20 min.
[c] Oxidation with $KMnO_4$ (final concentration 0.1 g l^{-1}) for 15–20 min, followed by reduction with $SnCl_2$ as described above.

Collection of total mercury

The apparatus shown in Fig. 3 was used for the determination of the total amount of mercury in untreated and centrifuged water samples. The mercury, either inorganic or organic, is adsorbed quantitatively on the charcoal column. A small

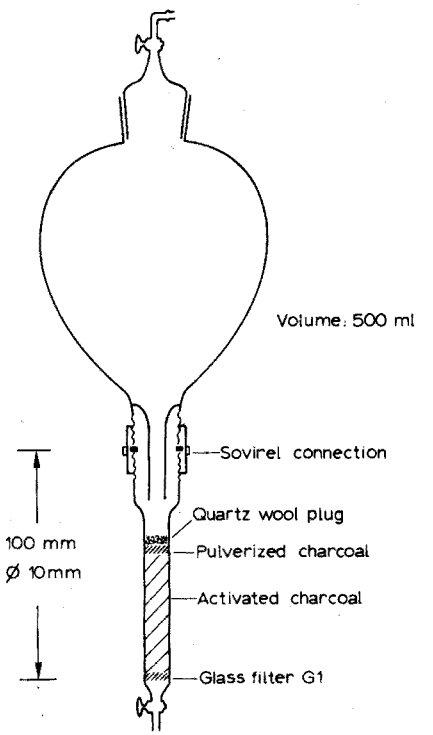

Fig. 3. Apparatus for the preconcentration of mercury on charcoal.

layer of pulverized charcoal is put on top of the column to retain the suspended matter present in the untreated water sample. The influence of the various parameters on the adsorption efficiency was measured with ^{197}Hg and ^{197}Hg-labelled compounds.

Acidity and salinity of the water sample. In spite of the high salt content of sea water, no influence on the absorption of mercury (compounds) at concentrations ranging from 10 ng l^{-1} to 10 μg l^{-1} was observed. At the normal pH of sea water (*ca.* 8) and for low mercury concentrations (50 ng l^{-1}), incomplete absorption on charcoal sometimes occurred. Such losses could be prevented by acidification. After adjustment of the pH to 1 with twice-distilled nitric acid, absorption was complete.

Flow rate through the column. At flow rates up to 4 ml min^{-1} absorption of mercury was complete, as checked with mercury tracers.

Absorption of mercury compounds. The absorption of metallic mercury, mercury chloride and some organomercury compounds was investigated. The results are summarized in Table II. It can be said that losses are negligible.

TABLE II

THE ABSORPTION OF SOME MERCURY COMPOUNDS ON ACTIVATED CHARCOAL[a]

Compound	*Dissolved in*	*Concentration (μg l^{-1})*	*Percentage absorbed*
Hg(II)	Water	0.1	99.8
Hg(II)	Acetone	0.1	98.3
Hg(0)[b]	Water	0.1	93.5
$(C_6H_5)_2Hg$	Water	12.7	98.9
C_6H_5HgCl	Water	4.3	100.4
C_6H_5HgAc	Water	1.3	100.6
C_6H_5HgAc	Benzene	1.3	99.7
CH_3HgCl	Water	1.5	98.9
$(CH_3)_2Hg$	Water	15.4	97.1

[a] The labelled organic compounds were prepared by exchange of the unlabelled species with ^{197}Hg.
[b] The Hg(0) was obtained by reduction of mercury(II) with $SnCl_2$. Losses by volatilization may have occurred. The mercury content of the effluent was 0.2% of the original value.

Collection of particulate matter

The mercury content of suspended matter can be determined in two ways: either from the difference between the total mercury contents of the unprocessed and the centrifuged samples (see above) or directly from a certain quantity of suspended matter collected from the rotor of the centrifuge. The second method is to be preferred.

To determine the mercury content of a sample of suspended solids or sediments, various methods have been used[12,13]. The method applied in this work was to mix sediment or suspended matter with some charcoal and, after irradiation, to transfer the mercury, by heating the sediment–charcoal mixture in a tube furnace to 900°C with a stream of nitrogen, to a second charcoal absorber. From experiments with a ^{197}Hg tracer, it was found that mercury absorbed on suspended matter can be recovered quantitatively in this way. Weighing of the sampled suspended matter

should be done before heating. Drying of the material for 1 h at 110°C cannot be applied; experiments with labelled organic mercury compounds showed that severe losses could occur:

Compound	*Percentage loss after 1 h at 110 °C*
CH_3HgCl	8–10
$(CH_3)_2Hg$	80–90
Hg(II)	0

Therefore, samples were weighed after equilibration (in a desiccator containing 48% sulphuric acid) at 52% relative humidity for at least 16 h; this avoided mercury losses by volatilization. The determination of the content of suspended matter in the water sample (mg l^{-1}) by filtration should be performed by weighing under the same conditions.

Purification of charcoal and its absorption capacity

The mercury content of commercially available "activated" charcoal is 15–20 ng Hg g^{-1}. This content can be lowered considerably by heating the charcoal in a quartz tube (40 mm o.d. and 300 mm long), placed inside a tube furnace in a vertical position. The temperature of the furnace is maintained at 950–1000°C and a stream of nitrogen, previously purified by a charcoal scavenger, is passed through the glowing carbon for 30–60 min. Activated charcoal purified in this way contains only 0.1–0.2 ng Hg g^{-1}. This residual mercury content determines the lower limit of the determination. A slight increase of the specific absorption capacity was observed after this treatment. The specific absorption capacity of charcoal for mercury(II) and methylmercury chloride can be calculated from absorption isotherms determined with ^{197}Hg–labelled compounds. The Langmuir plots for metallic mercury (II) ion and methylmercury chloride are shown in Fig. 4. The slow solubility in water of the latter compound limits the concentration range which can be studied in this way. The

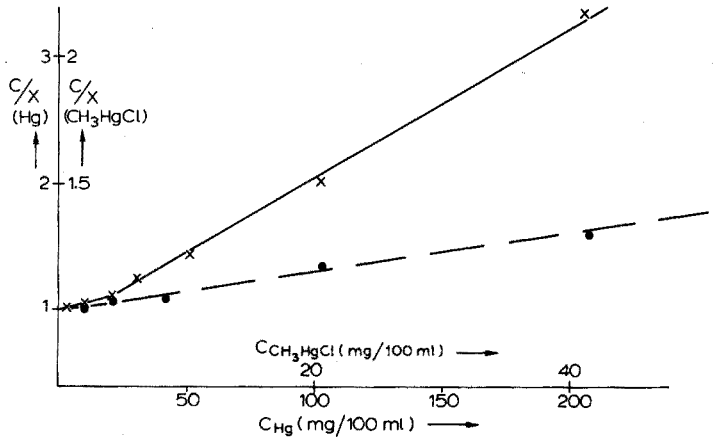

Fig. 4. Langmuir absorption plots for mercury(II) on 250 mg of charcoal (×), and CH_3HgCl on 150 mg of charcoal (●). $C/X=(1/X_m k)+(C/X_m)$ where X = amount of Hg(II) or CH_3HgCl absorbed, and C = amount of mercury in the original solution.

collection of mercury(II) ion and methylmercury chloride on 250 mg of charcoal was quantitative for concentrations below 1 mg Hg(II)/100 ml and 2.5 mg CH_3Hg/100 ml, respectively. Methylmercury chloride is probably completely ionized. From the slopes of the Langmuir plots, the absorption capacities per gram of activated charcoal for complete monomolecular coverage were found to be: Hg(II), 330 mg g^{-1}, and CH_3Hg(I), 820 mg g^{-1}.

Irradiation of the charcoal samples

The different charcoal samples obtained as described above were packed in quartz capsules (10 mm i.d., 70 mm long) and irradiated together with a standard for 8–12 h at a thermal neutron flux of $3 \cdot 10^{12}$ cm^{-2} s^{-1}. The standards were prepared by putting 20 μl of a solution of mercury(II) nitrate (2.03 μg Hg/20 μl) in quartz capsules which already contained some activated charcoal. The capsules were sealed and the contents homogenized by vigorous shaking.

Irradiation was done in a dry rotating facility which could hold 19 quartz capsules of the type used. To check flux variations, thin iron rods were placed at different positions throughout the irradiation flask. After irradiation, the samples were cooled for 24 h, to allow for the decay of short-lived nuclides.

Separation of mercury from radioactive charcoal

After irradiation, the matrix activity of the charcoal prevents the direct instrumental determination of mercury. For the separation of mercury, the apparatus described previously[10,13] was used. When the quartz capsules were opened, cooling with liquid nitrogen was used to avoid risks of explosion arising from pressure build-up during irradiation. The contents of a capsule were transferred to the quartz tube that fits into the first tube furnace (25 mm i.d. and 200 mm long; *cf.* Fig. 2 of ref. 10). The apparatus described previously[10] was modified by the insertion of a tube (150 mm long, 16 mm i.d.) containing glass wool coated with silver and maintained at 400°C, between the furnace for the irradiated carbon and the final activated charcoal trap at room temperature. In the present work, the temperature of the tube furnace for the irradiated carbon was maintained at 700–800°C.

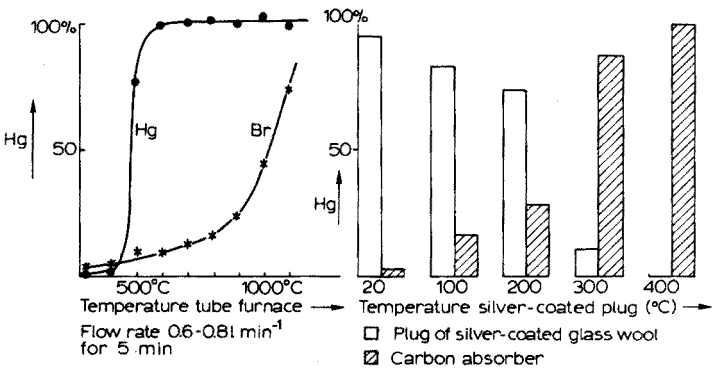

Fig. 5. (a) The influence of temperature on the amount of mercury and bromine released from charcoal; flow rate 0.6–0.8 l min^{-1} for 5 min. (b) The influence of temperature on the amount of mercury retained in the silver-coated plug; □, plug of silver-coated glass wool; ▨, carbon absorber.

The choice of these temperatures becomes apparent from Fig. 5. Two requirements must be fulfilled: complete removal of mercury from the irradiated charcoal matrix, and absolutely no absorption on the silver-coated glass wool plug. A stream of nitrogen, purified by a charcoal scavenger[10], was passed through the system at a flow rate of 0.6–0.8 l min^{-1}. This carries the mercury, volatilized at 700–800°C, to the second absorber. ^{82}Br ($T_{\frac{1}{2}}$ = 35.4 h), which is partially released at this temperature, is retained in the silver-coated plug. Although only a small percentage of the bromine present in the sample is absorbed on charcoal, and although at 700–800°C only 10–15% of the bromine is released, the amount of bromine absorbed on the second charcoal layer would prevent the determination of mercury in sea water if the silver-coated plug were omitted.

Experiments with labelled organic mercury compounds showed that, whatever the chemical form of mercury in the sample, quantitative volatilization was obtained.

Procedure for the determination of inorganic, total and particulate mercury

Collection of inorganic mercury. Transfer a 1-l sample of centrifuged water to the aeration vessel and mount a 2.5-g charcoal absorber on top of the vessel (Fig. 2). Add 1 ml of 1% tin(II) chloride solution and close the vessel. Adjust the flow rate to 4–6 l min^{-1}. After 5 min, stop aeration and transfer the charcoal to a quartz capsule which is then sealed off.

Collection of total mercury. Transfer a water sample, either unprocessed or centrifuged, to a receiver connected to a column containing 1.5 g of purified charcoal (Fig. 3). For an unprocessed water sample, place about 100 mg of pulverized charcoal on top of the granulated charcoal. Wet the charcoal with twice-distilled water before use. Acidify the sample with about 1 ml of concentrated nitric acid to pH 1. Adjust the flow rate of the sample through the column to below 4 ml min^{-1}. Pass 5 ml of previously purified acetone through the column and dry the column with a gentle stream of air. Transfer the carbon to a quartz capsule, cool with liquid nitrogen and then seal off.

Collection of particulate matter. Take 50–100 mg of suspended matter from the centrifuge tube, and transfer to a previously weighed quartz capsule. Place the capsule in a desiccator containing a 48% sulphuric acid solution (relative humidity 52%) for at least 16 h. Determine the weight of the suspended matter in the capsule and add 0.5 g of purified charcoal. Homogenize the mixture and seal the capsule off.

Irradiation of charcoal samples. Place different charcoal samples in an irradiation can together with mercury standards and flux monitors. Irradiate for 8–12 h at a thermal neutron flux of $3 \cdot 10^{12}$ n cm^{-2} s^{-1}. After irradiation, cool the samples for 24 h.

Separation of mercury from the radioactive charcoal. Open the quartz capsules, under cooling with liquid nitrogen, and transfer the radioactive charcoal to a quartz tube connected with two glass tubes containing silver-coated glass wool and a fresh charcoal adsorber (see above and Fig. 2 of ref. 10); connect up the whole system and pass a stream of nitrogen through the system at a flow rate of 0.6–0.8 l min^{-1}. Keep the temperatures of the furnaces at 700–800°C and 400°C as indicated above.

After 5 min remove the tubes from the system and transfer the carbon of the second absorber to a test tube (16 × 160 mm). Process mercury standards in the

same way as the samples.

Count samples and standards for at least 5 min in a 3 × 3-in. well-type NaI detector, connected to a 400-channel analyzer. The spectra are read out on punchtape or on an electrical typewriter. Count the flux monitors in a 1.5 × 2-in. NaI detector connected to a single-channel analyzer.

The observed specific count-rate under the 0.077 MeV photopeak of ^{197}Hg ($T_{\frac{1}{2}} = 66$ h) is about $1.6 \cdot 10^5$ c.p.m./μg Hg after an irradiation of 12 h at $3 \cdot 10^{12}$ n cm^{-2} s^{-1} and a cooling period of 24 h. Figure 6 gives the γ-spectrum of the second charcoal absorber, containing all mercury originally present in the water sample.

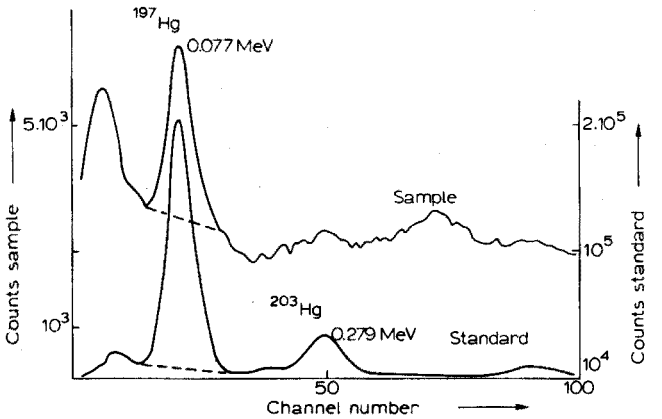

Fig. 6. Gamma spectra of a sample and standard. Integrated thermal neutron flux $4 \cdot 10^6$ n cm^{-2}, counting time 30 min, sample 36.1 ng (500 ml), standard 2.033 μg, decay 3 days.

RESULTS

Mercury content of tap water

From one large sample of tap water, twelve 500-ml aliquots were taken and analysed separately. The following results were obtained.

Total mercury: 31.0, 36.2, 22.9, 35.3, 20.7, 25.1, 27.1, 31.8 and 22.9 ng l^{-1}. Average: 28 ($\pm$5) ng l^{-1}.

Inorganic mercury: 4.2, 3.5, 4.5 and 3.9 ng l^{-1}. Average: 4.0 ($\pm$0.4) ng l^{-1}.

Organic mercury: 24 ($\pm$5) ng l^{-1}

Mercury content of distilled water

Twice-distilled water was prepared from demineralized water in a quartz apparatus, which had been continuously in operation for a few years. The total mercury contents of three aliquots, taken on various days, were 7.4, 7.6 and 4.6 ng l^{-1}.

Mercury content of sea water

Three aliquots of a large sample, taken at the beach at Petten, were analysed. The results obtained were as follows.

Total mercury: 55.1, 53.6 and 46.8 ng l^{-1}. Average: 52 ($\pm$4) ng l^{-1}.

Total mercury in the centrifuged sample: 14.4, 16.2 and 22.0 ng l^{-1}. Average: 17.5 ($\pm$3.5) ng l^{-1}.

Inorganic mercury: 4.7, 4.2 and 4.3 ng l^{-1}. Average: 4.4 ng l^{-1}.

Mercury content of the particulate matter: 0.35 μg g^{-1}. Dissolved organic mercury: 13 ng l^{-1}.

Mercury in surface waters

A large sample was taken in a semi-industrial region in the western part of the Netherlands. Three aliquots were analysed separately. The results were as follows.

Total mercury: 78.2, 67.0 and 74.3 ng l^{-1}. Average: 73 ($\pm$6) ng l^{-1}.

Total mercury in the centrifuged sample: 39.2, 41.1 and 46.5 ng l^{-1}. Average: 42 ($\pm$4) ng l^{-1}.

Inorganic mercury: 7.0 and 7.3 ng l^{-1}. Average: 7.1 ($\pm$0.2) ng l^{-1}.

Mercury content of the particulate matter: 0.70 and 0.58 μg g^{-1}. Dissolved organic mercury: 35 ng l^{-1}.

SUMMARY

A sensitive method for the determination of mercury in sea and surface waters is presented. A distinction is made between inorganic, organic and particulate mercury. In the determination of inorganic mercury, the element is isolated by reduction and volatilization, followed by absorption on a charcoal column. The total mercury content of the water with and without suspended solids is determined by absorption from the solution onto a column of charcoal. In all cases, the mercury on the absorber is determined by thermal neutron activation analysis. The limit of detection is 1 ng l^{-1}.

REFERENCES

1 A. E. Moffitt and R. E. Kupel, *Amer. Ind. Hyg. Ass. J.*, (1971) 614.
2 T. R. Gilbert and D. N. Hume, *Anal. Chim. Acta*, 65 (1973) 461.
3 R. E. Cranston and D. E. Buckley, *Environ. Sci. Technol.*, 6 (1971) 274.
4 J. Olafsson, *Anal. Chim. Acta*, 68 (1974) 207.
5 D. E. Robertson, *Anal. Chem.*, 40 (1968) 1067.
6 A. R. Byrne, M. Dermelj and L. Kosta, *J. Radioanal. Chem.*, 6 (1970) 325.
7 R. V. Coyne and J. A. Collins, *Anal. Chem.*, 44 (1972) 1093.
8 D. E. Robertson, *Anal. Chim. Acta*, 42 (1968) 533.
9 R. M. Rosain and C. M. Wai, *Anal. Chim. Acta*, 65 (1973) 279.
10 H. A. van der Sloot and H. A. Das, *Anal. Chim. Acta*, 70 (1974) 439.
11 Y. Kimura and V. L. Miller, *Anal. Chim. Acta*, 27 (1962) 325.
12 I. K. Iskander, J. K. Syers, L. W. Jacobs, D. R. Keeney and J. I. Gilmour, *Analyst (London)*, 97 (1972) 388.
13 L. Kosta and A. R. Byrne, *N.I.J.S. Report R-554*, 1968.

Analytica Chimica Acta, 73 (1974) 245–254

METAL COMPLEXES OF AROMATIC SCHIFF BASE COMPOUNDS

PART II. THE FLUORESCENCE OF BERYLLIUM AND SCANDIUM COMPLEXES AND THEIR USE IN FLUORIMETRY

KIYOTOSHI MORISIGE

Department of Fundamental Education, Faculty of Science and Technology, Kinki University, Kowakae, Higashi – Osaka (Japan)

(Received 24th May 1974)

Quinalizarin[1], 2-methyloxine[2], morin[3] and some Schiff bases[4,5] are useful fluorimetric reagents for beryllium; morin[6], 5,7-dichlorooxine[7] and Schiff bases[8,9] are available for scandium. In attempts to establish more sensitive and precise fluorimetric methods, about ninety Schiff bases were synthesized in the present work. These were derivatives of salicylidene-*o*-aminophenol or salicylaldehyde semicarbazone, and fluorimetric determinations of aluminium and gallium with some of these compounds have already been reported[10].

In this research, the fluorescence properties of beryllium complexes with salicylidene-*o*-aminophenol and eight derivatives, and the properties of scandium complexes with salicylaldehydesemicarbazone and seven derivatives were studied (see Table I), and procedures for fluorimetric determinations were established.

EXPERIMENTAL

Apparatus and materials

Fluorescence measurements were made with a Hitachi Fluorescence spectrophotometer, Model 204 (exciting source: 150 W Xenon lamp). A Hitachi–Horiba glass electrode pH Meter, Model M-5, was used for pH measurements.

Schiff base compounds. The seventeen Schiff bases used in this investigation are listed in Table I. Compounds II–IX are derivatives of 2-hydroxyaniline-N-salicylidene (compound I), and compounds X–XVII are 2-hydroxybenzaldehyde-semicarbazones. These compounds were synthesized by condensation of aldehydes with amino compounds at 100°C for 30 min[11]. The aldehydes which were not commercially available were prepared by the Duff reaction[12]. The products obtained were purified by repeated recrystallizations from ethanol, and were dried at room temperature over silica gel.

Schiff base solution. 0.1 g of Schiff base was dissolved and diluted to 100 ml with N,N-dimethylformamide (Dotite Spectrosol Solvents).

Standard solutions of beryllium and scandium. A stock solution of beryllium was prepared by dissolving 0.2774 g of BeO (99.9%) with 10 ml of concentrated sulfuric acid and diluting to 100 ml with water (1 mg Be ml^{-1}). A stock solution of scandium was prepared by dissolving 0.1537 g of Sc_2O_3 (99.9%) with 20 ml of

TABLE I

ELEMENTAL ANALYSIS OF SCHIFF BASES USED

Compd. no.	*Schiff base*		*Result of elemental analysis (%)*			*m.p. (°C)*
			C	*H*	*N*	
I	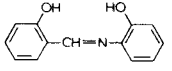	2-Hydroxyaniline-N-salicylidene	*Found* 72.90 *Calcd.* 73.16	5.10 5.16	6.65 6.75	185
II	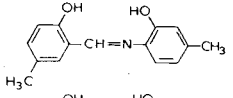	2-Hydroxy-4-methylaniline-N-2-hydroxy-5-methylbenzylidene	*Found* 74.50 *Calcd.* 74.61	6.18 6.22	5.64 5.80	
III	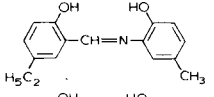	2-Hydroxy-5-methylaniline-N-2-hydroxy-5-ethylbenzylidene	*Found* 75.02 *Calcd.* 75.15	6.43 6.55	5.22 5.37	
IV	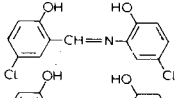	2-Hydroxy-5-chloroaniline-N-2-hydroxy-5-chlorobenzylidene.				201
V	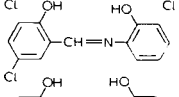	2-Hydroxyaniline-N-2-hydroxy-5-chlorobenzylidene				184
VI	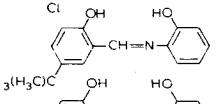	2-Hydroxyaniline-N-2-hydroxy-5-tert-butylbenzylidene	*Found* 75.55 *Calcd.* 75.76	6.98 7.06	5.04 5.20	
VII	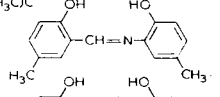	2-Hydroxy-5-methylaniline-N-2-hydroxy-5-methylbenzylidene				185
VIII	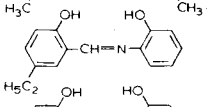	2-Hydroxyaniline-N-2-hydroxy-5-ethylbenzylidene	*Found* 74.53 *Calcd.* 74.61	6.20 6.22	5.76 5.80	
IX	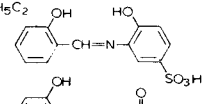	2-Hydroxy-5-sulfoaniline-N-salicylidene	*Found* 53.15 *Calcd.* 53.40	3.70 3.75	4.90 4.77	
X	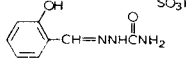	2-Hydroxybenzaldehyde-semicarbazone				224

XI	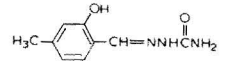	2-Hydroxy-4-methylbenzaldehyde-semicarbazone	*Found* 55.84 *Calcd.* 55.96	5.60 5.70	21.53 21.76	
XII	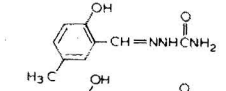	2-Hydroxy-5-methylbenzaldehyde-semicarbazone				239
XIII	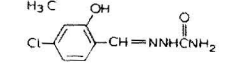	2-Hydroxy-4-chlorobenzaldehyde-semicarbazone				214
XIV	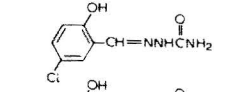	2-Hydroxy-5-chlorobenzaldehyde-semicarbazone	*Found* 45.01 *Calcd.* 44.97	3.83 3.75	19.78 19.67	
XV	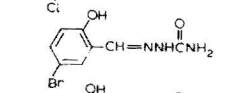	2-Hydroxy-5-bromobenzaldehyde-semicarbazone	*Found* 37.03 *Calcd.* 37.21	3.00 3.10	16.13 16.28	
XVI	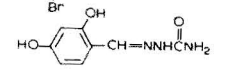	2,4-Dihydroxybenzaldehyde-semicarbazone	*Found* 49.30 *Calcd.* 49.23	4.71 4.62	21.68 21.54	
XVII	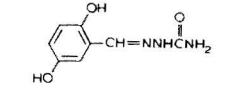	2,5-Dihydroxybenzaldehyde-semicarbazone				247.5

concentrated hydrochloric acid and diluting the solution to 100 ml with water. Working solutions were prepared by dilution with 0.1 *M* hydrochloric acid.

Quinine standard solution. 0.1 g of quinine (Nakarai Chemicals Ltd.) was dissolved in 100 ml of 0.1 *M* sulfuric acid, and this solution was diluted with 0.1 *M* sulfuric acid to give solutions containing 0.1–0.5 μg ml^{-1}. These solutions were employed as reference standards in adjusting the sensitivity of the instrument.

General procedure

To 10–15 ml of a sample solution containing an appropriate amount of beryllium or scandium ion, 1–2 ml of a 0.1% Schiff base solution and 2 ml of 20% ammonium acetate or 5 ml of 20% ammonium chloride solution were added. The pH was adjusted to the required value with dilute hydrochloric acid or ammonia solution, and then the solution was diluted to 25 ml with water. The fluorescence intensity was measured at the optimal excitation and maximal fluorescence wavelengths, with a quinine solution as the reference standard. (The fluorescence spectra were not corrected, since the present research was done principally for analytical purposes.)

RESULTS AND DISCUSSION

Fluorescence properties of metal–Schiff base complexes

The fluorescence properties of the beryllium and scandium complexes formed with 87 Schiff bases were investigated. Generally, beryllium formed fluorescent complexes with salicylidene-*o*-aminophenols in alkaline solution, whereas scandium formed such complexes with salicylaldehydesemicarbazones in weakly acidic solution. Table I shows the 17 Schiff bases which gave relatively intense fluorescence with beryllium or scandium. Their fluorescence characteristics obtained under the optimal conditions are summarized in Table II. Of the bases mentioned salicylidene-*o*-aminophenol (compound I) and the chloro-, methyl-, ethyl-, tert-butyl-, and sulfo-substituted derivatives (compounds II–IX) reacted with beryllium to show intense blue fluorescence. Salicylaldehydesemicarbazone (compound X) and the chloro-, bromo-, methyl- and hydroxy- substituted products (compounds XI–XVI) formed blue fluorescent complexes with scandium; compound XVII, however, scarcely fluoresced.

The fluorescence intensities of the beryllium complexes decreased in the following order: compound II > VIII > III = IV = V > VI ⩾ VII = IX > I. With regard to the substituent group at the *m*-position (to –CH=N–) in the α-ring, C_2H_5 > Cl > $C(CH_3)_3$ > H, *i.e.* VIII > V > VI > I. However, the Schiff bases had a weak point as reagents for beryllium, in that the fluorescence of the complexes was usually unstable. 2-Hydroxy-5-sulfoaniline-N-salicylidene can be recommended, because the change in the fluorescence intensity on standing is relatively small, although this reagent was the least sensitive for beryllium.

The fluorescence intensities of the scandium complexes decreased in the order: XVI ⩾ XII > XIV ⩾ X = XI > XIII > XV > XVII. With regard to the substituent group at the *m*-position or *p*-position to the –CH=N– group, CH_3 > Cl > H > Br > OH, *i.e.* XII > XIV > X > XV > XVII; and OH > H = CH_3 > Cl, *i.e.* XVI > X = XI > XIII. With respect to the substituted position, *m*-substitution provided increased

TABLE II

OPTIMAL FLUORESCENCE CONDITIONS FOR BERYLLIUM AND SCANDIUM COMPLEXES WITH SCHIFF BASES

(The metal–ligand ratio is 1:1 in all cases.)

Compd. no.	*λ excitation max. (nm)*	*λ emission max. (nm)*	*pH*	*Relative fluorescence intensity*[a]	
				Net fluor. for 1 μg metal	*Reagent blank*
Beryllium					
I	337	440	10.5	59.4	10.3
II	353	450	10.0	104.0	14.5
III	355	450	8.5	94.6	4.8
IV	353	445	9.5	94.0	12.4
V	353	445	9.7	93.4	19.7
VI	350	450	8.7	91.0	3.6
VII	350	450	9.5	90.0	4.0
VIII	355	450	8.7	97.0	3.6
IX	343	430	9.7	89.2	8.0
Scandium					
X	365	450	6.0	62.6	23.5
XI	368	450	6.3	62.4	17.3
XII	375	470	6.2	69.4	25.0
XIII	365	435	6.5	40.0	178.0
XIV	375	455	6.5	64.4	276.0
XV	370	455	6.0	16.3	30.5
XVI	360	425	6.0	70.8	6.5
XVII	395	507	2.5	4.8	10.0

[a]Fluorescence intensities were measured at maximal fluorescence wavelength. The sensitivity of the fluorimeter was regulated by setting the fluorescence of the standard quinine solution (0.25 μg ml^{-1}) at 100 div., 353 nm/445 nm.

sensitivity compared to *p*-substitution except in the case of hydroxyl groups. From the results, 2,4-dihydroxybenzaldehyde-semicarbazone seems to be the most useful reagent for scandium.

The excitation and emission spectra of the beryllium and scandium complexes are shown in Figs. 1 and 2. Figures 1 and 2 indicate that excitation at a wavelength of 337–355 nm is effective for beryllium complexes, and excitation at 360–395 nm for scandium complexes. Emission bands lie in the region 370–580 nm, and the fluorescence maxima occur near 440 nm. As shown in Fig. 1, the fluorescence of beryllium complexes with salicylidene-*o*-aminophenol derivatives, which are substituted in the α-ring, show a red shift, while those substituted in the N-ring show a blue shift, compared with the beryllium–salicylidene-*o*-aminophenol complex; complexes having substituent groups in both the α-ring and the N-ring also show the red shift.

In the case of the scandium–salicylaldehydesemicarbazone complexes, the fluorescence maxima of the complexes with a substituent group at the *m*-position to the –CH=N– bond, shift to longer wavelengths, but the maxima of the *p*-substituted complexes shift to shorter wavelength. The tendency in the shift increases in the order of $CH_3 < Cl < OH$.

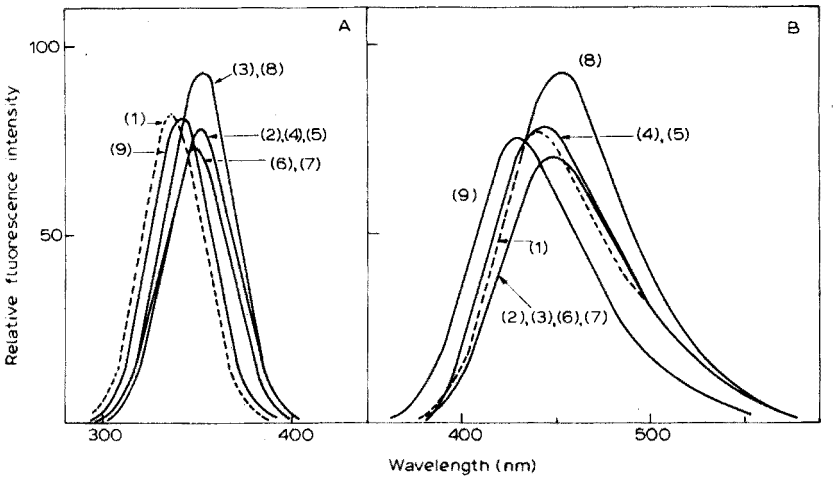

Fig. 1. Excitation spectra (A) and emission spectra (B) of beryllium complexes with Schiff bases. (1) Compound I, λ_{em} 440 nm, λ_{ex} 337 nm. (2) compound II, λ_{em}, 450 nm, λ_{ex} 353 nm; (3) compound III, λ_{em}, 450 nm, λ_{ex} 355 nm; (4) compound IV, λ_{em}, 445 nm, λ_{ex} 353 nm; (5) compound V, λ_{em}, 445 nm, λ_{ex} 353 nm; (6) compound VI, λ_{em}, 450 nm, λ_{ex} 350 nm; (7) compound VII, λ_{em}, 450 nm, λ_{ex} 350 nm; (8) compound VIII, λ_{em}, 450 nm, λ_{ex} 355 nm; (9) compound IX, λ_{em}, 430 nm, λ_{ex} 343 nm.

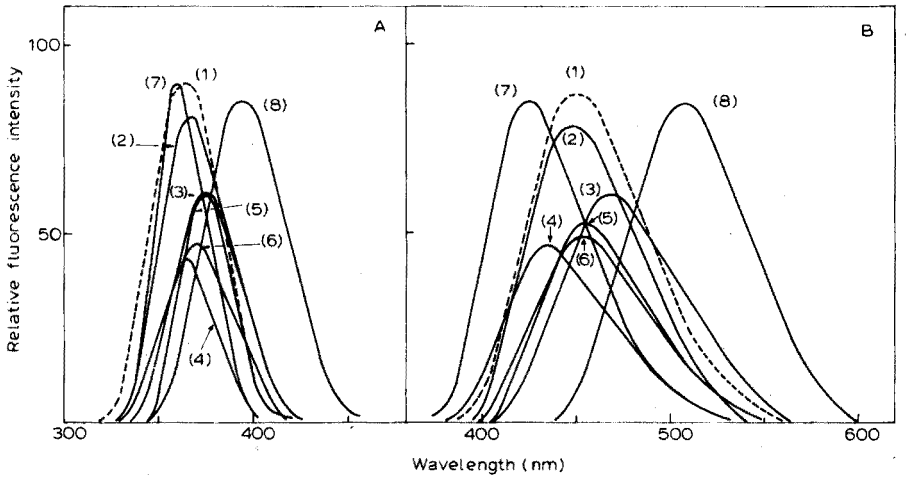

Fig. 2. Excitation spectra (A) and emission spectra (B) of scandium complexes with Schiff bases. (1) Compound X, λ_{em}, 450 nm, λ_{ex} 365 nm; (2) compound XI, λ_{em}, 450 nm, λ_{ex} 368 nm; (3) compound XII, λ_{em}, 470 nm, λ_{ex} 375 nm; (4) compound XIII, λ_{em}, 435 nm, λ_{ex} 365 nm; (5) compound XIV, λ_{em}, 455 nm, λ_{ex} 375 nm; (6) compound XV, λ_{em}, 455 nm, λ_{ex} 370 nm; (7) compound XVI, λ_{em}, 425 nm, λ_{ex} 360 nm; (8) compound XVII, λ_{em}, 507 nm, λ_{ex} 395 nm.

FLUORIMETRIC DETERMINATION OF BERYLLIUM AND SCANDIUM WITH SCHIFF BASES

As described above, Schiff bases provide some useful fluorimetric reagents for beryllium and scandium, and therefore, the analytical conditions were investigated in further detail.

Effect of pH

The effect of pH on the fluorescence intensity of the metal complexes is indicated in Fig. 3. Beryllium complexes show maximal fluorescence in the pH region 8.5–10.5, and scandium complexes in the region 2.5–6.5.

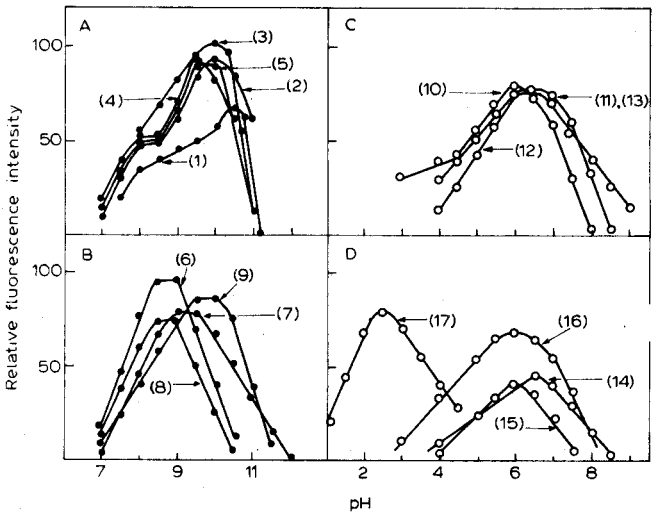

Fig. 3. Effect of pH on fluorescence intensity. *Beryllium complexes.* A-(1) Compound I; A-(2) compound II; A-(3) compound III; A-(4) compound IV; A-(5) compound V; B-(6) compound VI; B-(7) compound VII; B-(8) compound VIII; B-(9) compound IX. *Scandium complexes.* C-(10) Compound X; C-(11) compound XI; C-(12) compound XII; C-(13) compound XIII; D-(14) compound XIV; D-(15) compound XV; D-(16) compound XVI; D-(17) compound XVII.

Effect of standing time

The fluorescence of the beryllium and scandium complexes develops fully immediately after the pH adjustment (Fig. 4). The fluorescence of the scandium complexes is stable for 3 h at least, while that of the beryllium complexes becomes weaker on standing. With compound IX, the change is comparatively slow, and this may be the best reagent. However, the measurements must be made as rapid as possible.

Effect of reagent concentration

Various amounts of 0.1% Schiff base solution were added to solutions containing 3–5 μg of beryllium or 5 μg of scandium, and the fluorescence intensities were measured at the optimal pH. Figure 5 shows the results which were obtained for the beryllium–compound II, VII and IX systems and the scandium–compound X, XII and XVI systems. The results indicate that 1 ml of 0.1% Schiff base solution is required for 3–5 μg of beryllium in 25 ml, and 2 ml is required for 5 μg of scandium.

Calibration curves

Figures 6 and 7 present the calibration curves for the beryllium–compound II, VII and IX systems and the scandium–compound X, XII and XVI systems, respectively. The sensitivity of the fluorimeter was set by using a 0.1–0.5 μg ml^{-1}

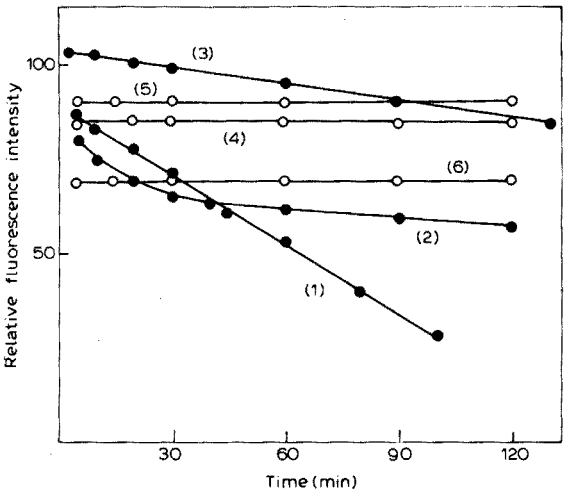

Fig. 4. Effect of standing time. (1) Be-compound II system, Be 2 μg, 353 nm/450 nm (40 div); (2) Be-compound VII system, Be 4 μg, 350 nm/450 nm (20 div); (3) Be-compound IX system, Be 5 μg, 343 nm/430 nm (20 div); (4) Sc-compound X system, Sc 5 μg, 365 nm/450 nm (20 div); (5) Sc-compound XII system, Sc 5 μg, 375 nm/470 nm (10 div); (6) Sc-compound XVI system, Sc 5 μg, 360 nm/425 nm (15 div). The number of divisions in brackets indicates the setting against a reference standard of 0.25 μg quinine/ml.

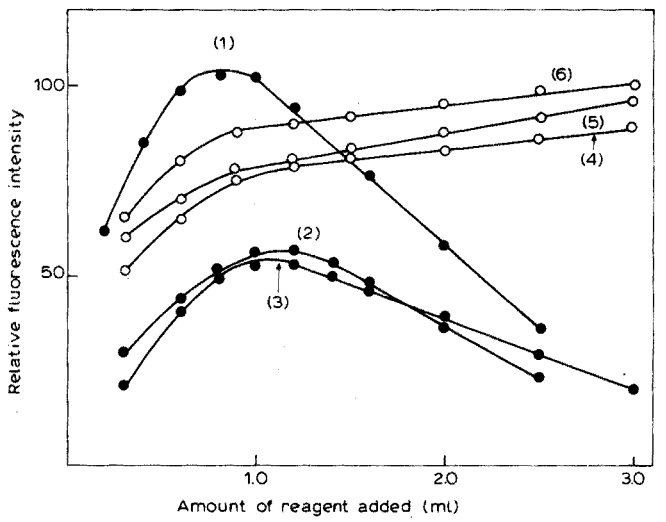

Fig. 5. Effect of reagent concentration. (1) Be-compound II, Be 5 μg (20 div.); (2) Be-compound VII, Be 3 μg (20 div.); (3) Be-compound IX, Be 5 μg (10 div.); (4) Sc-compound X, Sc 5 μg (20 div.); (5) Sc-compound XII, Sc 5 μg (10 div.); (6) Sc-compound XVI, Sc 5 μg (20 div.). Wavelengths as in Fig. 4. Setting (in divisions) against a standard of 0.25 μg quinine/ml.

quinine solution (in 0.1 *M* sulfuric acid) as the reference standard.

Beryllium and scandium can be determined within a relative error of 3 % in the following concentration range: beryllium, 0.01–5 μg/25 ml with compound II, VII and IX; scandium, 0.05–10 μg/25 ml with compound X or XII, and 0.02–10 μg/25 ml with XVI.

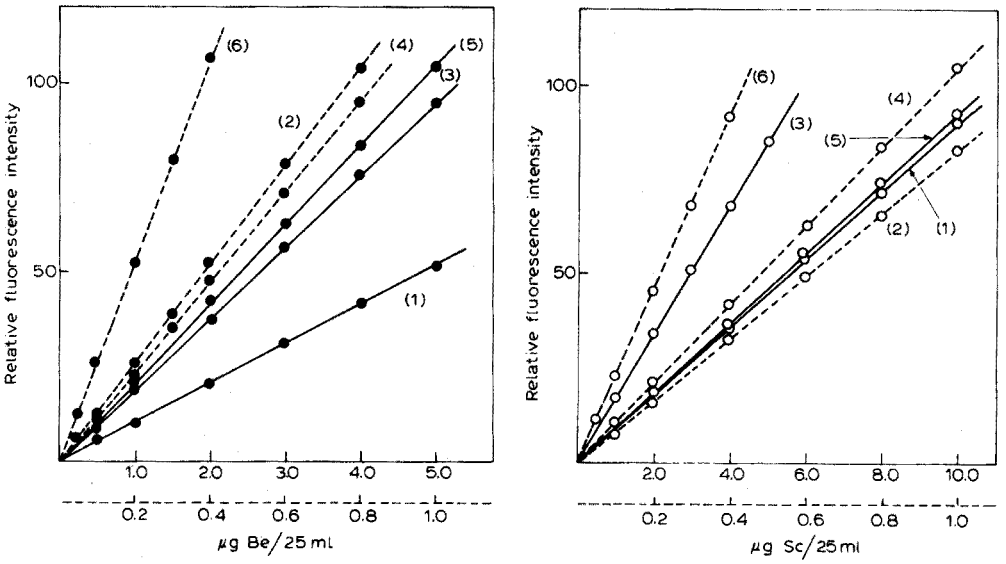

Fig. 6. Calibration curves for beryllium. (1) Be–compound II system, 10 div. *vs.* 0.25 μg quinine/ml; (2) Be–compound II system, 50 div. *vs.* 0.1 μg quinine/ml; (3) Be–compound VII system, 20 div. *vs.* 0.25 μg quinine/ml; (4) Be–compound VII system, 50 div. *vs.* 0.1 μg quinine/ml; (5) Be–compound IX system, 20 div. *vs.* 0.25 μg quinine/ml; (6) Be–compound IX system, 100 div. *vs.* 0.1 μg quinine/ml. Wavelengths as in Fig. 4.

Fig. 7. Calibration curves for scandium. (1) Sc–compound X system, 10 div. *vs.* 0.25 μg quinine/ml; (2) Sc–compound X system, 40 div. *vs.* 0.1 μg quinine/ml; (3) Sc–compound XII system, 10 div. *vs.* 0.25 μg quinine/ml; (4) Sc–compound XII system, 50 div. *vs.* 0.1 μg quinine/ml; (5) Sc–compound XVI system, 10 div. *vs.* 0.25 μg quinine/ml; (6) Sc–compound XVI system, 100 div. *vs.* 0.1 μg quinine/ml. Wavelengths as in Fig. 4.

Effect of diverse ions

The interferences of 100-fold amounts of foreign cations were studied. Antimony(III), arsenic(III), boron(III), bismuth(III), cadmium(II), calcium(II), magnesium(II), mercury(II), thallium(I), tungsten(VI), uranium(VI) and zinc(II) did not interfere the determination of beryllium. Aluminium(III), chromium(VI), copper(II), gallium(III), indium(III), iron(III), manganese(II), nickel(II), scandium(III), tin(II) vanadium(V) and yttrium(III) caused negative errors.

For the determination of scandium, antimony(III), arsenic(II), barium(II), beryllium(II), boron(III), bismuth(III), cadmium(II), calcium(II), cerium(IV), europium(III), germanium(IV), indium(III), lanthanum(III), magnesium(II), manganese-(II), selenium(IV), strontium(II), thallium(I) and tungsten(VI) did not interfere. Chromium(VI), cobalt(II), copper(II), gallium(III), iron(III), nickel(II) and tin(II) caused negative errors. Aluminium(III), yttrium(III) and zinc(II) showed positive errors.

Determination of metal–ligand ratio

The mole ratio of metal to ligand in the metal complexes (of Schiff base compounds) was determined fluorimetrically by the continuous variation method.

TABLE III

ANALYSIS OF METAL–SCHIFF BASE COMPLEXES

Compound	*Chemical formula*	*N(%)*		*Be(%)*	
		Found	*Calcd.*	*Found*	*Calcd.*
I	$C_{13}H_9NO_2 \cdot Be \cdot H_2O$	5.80	5.88	3.70	3.78
II	$C_{15}H_{13}NO_2 \cdot Be \cdot H_2O$	5.10	5.26	3.21	3.38
IV	$C_{13}H_7NO_2Cl_2 \cdot Be \cdot H_2O$	4.34	4.56	2.81	2.93
VII	$C_{15}H_{13}NO_2 \cdot Be \cdot H_2O$	5.34	5.26	3.45	3.38
VIII	$C_{15}H_{13}NO_2 \cdot Be \cdot H_2O$	5.18	5.26	3.25	3.38
IX	$C_{13}H_{11}NO_5S \cdot Be \cdot H_2O$	4.25	4.40	2.74	2.83

Both beryllium and scandium formed 1 : 1 complexes. Table III summarizes the results of the elemental analysis of the beryllium complexes with compounds I, II, IV, VII, VIII and IX; the results also indicate that the metal–ligand ratios are 1:1 in these crystalline complexes.

The author wishes to thank Professor Tsunenobu Shigematsu (Kyoto University), Professor Yasuharu Nishikawa and Assistant Professor Keizō Hiraki (Kinki University), and Professor Masayuki Tabushi (Tohoku Women's College) for their kind advice and suggestions.

SUMMARY

The fluorescence properties of the beryllium and scandium complexes with 17 Schiff bases were studied and the conditions for fluorimetric determinations of these metals were established. 2-Hydroxy-5-sulfoaniline-N-salicylidene proved a good reagent for beryllium on account of the stability of fluorescence, and 2,4-dihydroxybenzaldehydesemicarbazone seemed to be the best for scandium. Optimal pH and wavelength conditions and interferences are reported. Beryllium can be determined in the range 0.4–200 ng ml^{-1} and scandium in the range 2–400 ng ml^{-1}.

REFERENCES

1 M. H. Fletcher and C. E. White, *Ind. Educ. Chem., Anal. Ed.*, 18 (1946) 179.
2 M. Ishibashi, T. Shigematsu and Y. Nishikawa, *Nippon Kagaku Zasshi*, 78 (1957) 1143.
3 I. May and F. S. Grimaldi, *Anal. Chem.*, 33 (1961) 1251.
4 I. M. Korenman and V. S. Efimychev, *Tr. Khim. Khim. Tekhnol.*, (1961) 323.
5 V. S. Efimychev, *Tr. Khim. Khim. Tekhnol.*, (1962) 126.
6 E. B. Sandell, *Colorimetric Determination of Trace of Metals*, Interscience, New York, 2nd edn., 1950, p. 536.
7 Y. Nishikawa, K. Hiraki and T. Shigematsu, *Nippon Kagaku Zasshi*, 90 (1969) 483.
8 Z. Urner, *Anal. Abstr.*, 17 (1969) 773.
9 G. F. Kirkbright, T. S. West and G. Woodward, *Analyst (London)*, 91 (1966) 23.
10 K. Morisige, *Anal. Chim. Acta*, 72 (1974) 295.
11 C. Donald, J. Freeman and C. E. White, *J. Amer. Chem. Soc.*, 78 (1956) 2678.
12 J. C. Duff, *J. Chem. Soc., (London)*, (1941) 547.

Analytica Chimica Acta, 73 (1974) 255–264

DOSAGE DE TRACES DE CUIVRE, DE NICKEL ET DE COBALT DANS LES ROCHES PAR UNE TECHNIQUE COMBINÉE EXTRACTION–FLUORESCENCE-X*

O. F. GÜLAÇAR

Département de Minéralogie, Section des Sciences de la Terre, 13 rue des Maraîchers, 1211 Genève (Suisse)

(Reçu le 17 juin 1974)

Lors de la détermination des éléments traces dans des matrices de composition variable par la spectrométrie de fluorescence-x l'exactitude, la sensibilité et la limite de détection dépendent beaucoup des effets de matrice, rendant souhaitables des séparations préalables. On a proposé diverses techniques de séparation des éléments à doser telles que les séparations sur échangeurs d'ions[1–4], la coprécipitation[5], l'extraction par solvant organique[6], etc.

Ce mémoire décrit une technique de séparation de traces de cuivre, de nickel et de cobalt dans des roches, combinée avec l'analyse de ces éléments par fluorescence-x. La séparation est réalisée par extraction des complexes diéthyldithiocarbamiques des éléments cités dans le chloroforme.

Un nombre important de publications se rapporte à l'étude de divers complexes métalliques ($Me(DDC)_n$) que forme l'ion diéthyldithiocarbamate (DDC^-) et à l'utilisation de ceux-ci à des fins analytiques. On peut citer, à titre d'exemple, l'article de revue publié par Délepine[7] et les travaux de Bode et Neumann[8]. Différentes études montrent que l'ion DDC^- est un agent complexant très peu sélectif mais qu'en utilisant des agents masquants appropriés on peut effectuer des séparations sélectives. Chilton[9] décrit par exemple une technique de séparation simultanée, sélective et quantitative du cuivre, du nickel et du cobalt en présence de nombreux autres métaux. C'est cette technique, qui consiste à extraire dans CCl_4 les $Me(DDC)_n$ formés à pH 8,5–9,0 et en présence d'ions citrates et pyrophosphates, qui a été modifiée ici pour l'appliquer aux solutions obtenues par décomposition d'échantillons de roches. En effet la technique telle que la décrit Chilton se révèle insatisfaisante, notamment avec les roches contenant beaucoup de fer et de magnesium comme par exemple les roches basiques et ultrabasiques.

PARTIE EXPÉRIMENTALE

Appareillage et réactifs

L'appareil utilisé pour les analyses par fluorescence-x est un spectromètre Philips, type 1540 modifié, muni d'un discriminateur à hauteurs d'impulsions. Un

* Cette méthode a été mise au point dans le cadre d'un travail de thèse intitulée "Contribution à la Géochimie du Cu, du Ni et du Co dans les Roches Ultrabasiques" par l'auteur, thèse No 1619 de l'Université de Genève (1973).

tube à anticathode d'Ag de 1600 W a été utilisé comme source de rayons x primaires. Le cristal analyseur était le LiF (200) de distance réticulaire $d = 2{,}01$ Å. L'intensité des radiations a été mesurée par une sonde à scintillation munie d'un cristal de NaI activé au thallium. Une installation de pastillage, similaire à celle décrite par Volborth[10], qui permet d'obtenir des pastilles de 31 mm de diamètre a été employée.

Les mesures de la radioactivité du ^{60}Co ont été faites avec un spectromètre-γ Paccard (modèle 3002) qui comporte un scintillomètre muni d'un cristal de NaI activé au thallium.

Sauf indication contraire les réactifs utilisés sont des produits Merck de qualité pro anal. La cellulose (cellulose pour chromatographie de Roth) et le $LiCO_3$, utilisés pour la préparation des pastilles, ont une granulométrie inférieure à 200 meshs.

Les solutions mères de Cu, de Ni et de Co à 2 mg ml^{-1} ont été préparées à partir de $CuSO_4 \cdot 5\ H_2O$, $NiCl_2 \cdot 6\ H_2O$ et $CoCl_2 \cdot 6\ H_2O$ respectivement par dissolution dans HCl 0,5 *M*. Les solutions standard sont obtenues par dilution avec de l'eau bidistillée.

La solution aqueuse de ^{60}Co est fournie par The Radiochemical Centre, Amersham G.B. avec une activité spécifique de 50–150 mCi mg^{-1} Co et 1 mCi ml^{-1}. La solution de traceur a été préparée à partir de celle-ci par dilution avec H_2O de façon à présenter une activité d'environ $1{,}5 \cdot 10^5$ cpm ml^{-1}.

Attaque des échantillons de roche

Le procédé décrit ci-dessous permet une décomposition complète de toutes les espèces de roches analysées au cours de ce travail. Peser exactement environ 500 mg de roche (broyée à $\leqslant 150$ meshs) dans un creuset de platine de 35–40 ml. Ajouter 2 ml de HNO_3 concentré, 2 ml de $HClO_4$ concentré et environ 15 ml de HF 40%. Chauffer sur une plaque jusqu'à siccité. Laisser refroidir, ajouter à nouveau 2 ml de $HClO_4$ et évaporer à sec. Après refroidissement reprendre avec 2 ml de HCl 2 *M* et 10 ml d'eau. Couvrir et mettre au bain-marie pour décomposer le résidu. Si, à ce stade, la dissolution est complète, transférer la solution dans un bécher de 100 ml pour l'analyse. Si, au contraire, il reste un résidu, transférer la solution par pipetage en laissant le résidu dans le creuset puis sécher ce dernier à l'étuve. Ajouter sur le résidu environ 0,5 g de $KHSO_4$ et chauffer doucement sur une flamme jusqu'à fusion puis graduellement jusqu'au rouge. Laisser refroidir puis reprendre avec 2 ml de HCl 2 *M* et 5 ml d'eau et décomposer le culot par chauffage. Rajouter la solution à celle de l'attaque humide. Généralement une seule fusion suffit à décomposer tout le résidu de l'attaque humide. Si ce n'est pas le cas il faut répéter la fusion.

Notons que pendant l'attaque le silice est éliminé sous forme de SiF_4 et que le fer(II) originellement présent dans la roche est transformé en fer(III).

Procédé analytique

Principe de la méthode. Après l'extraction des complexes diéhyldithiocarbamiques de Cu, de Ni et de Co dans le solvant organique, ce dernier est évaporé sur un support solide en poudre fine et insoluble. Dans ce support, homogénéisé et comprimé en pastille, on dose les éléments par fluorescence-x en comparant l'intensité de leur raie $K\alpha$ à celle donnée par les pastilles standard.

Préparation des standards et des blancs. Les pastilles standard avec des teneurs

en Cu (10–500 p.p.m.), en Ni (10–1200 p.p.m.) et en Co (10–200 p.p.m.) en proportions variables ont été préparées de la manière suivante. On prépare une solution aqueuse contenant des quantités connues de Cu, de Ni et de Co et on ajuste le pH à 7 ± 1 avec NaOH ou HCl dilués. On transfère dans une ampoule d'extraction et on ajoute 2 ml de solution aqueuse de NaDDC·3 H_2O 1% (p/v). On agite une fois avec 10 ml et deux fois avec 3 ml de $CHCl_3$ (chaque fois pendant 3 min) pour extraire quantitativement les trois éléments. On introduit l'extrait chloroformique dans une cuve en verre à fond plat contenant exactement 1 g d'un mélange cellulose: $LiCO_3$ (7:3) et on laisse dans une chapelle ventilée pour évaporer le solvant. On ajoute alors environ 5 ml d'acétone et évapore à nouveau en homogénéisant. Le mélange est enfin séché à 105°C et comprimé en pastille selon une technique décrite par Delaloye[11].

L'échantillon à blanc a été préparé par pastillage du mélange pur cellulose–$LiCO_3$.

chloroformiques obtenues par extraction du Cu, du Ni et du Co des échantillons de roches se fait de la même manière que celle décrite pour les standards. Le procédé d'extraction est décrite plus loin.

Mode opératoire de l'analyse par fluorescence-x. La détermination des trois éléments dans les pastilles a été faite dans les conditions instrumentales données dans le Tableau I

TABLEAU I

CONDITIONS INSTRUMENTALES

Source	Tube à anticathode d'Ag (57 kV—28 mA)			
Cristal	LiF (200)			
Détecteur	Scintillateur H.T. = 910 V			
Collimateur	D'entrée: 480 μm			
	Du compteur: 160 μm			
Discriminateur	Seuil: 1,1 V			
	Fenêtre: 1,0 V			
Attenuation	2^2			
Spectromètre	Non évacué (air)			
Raies analytiques		*Co*	*Ni*	*Cu*
	2θ raies $K\alpha$	52,79°	48,66°	45,02°
	2θ pour BF	53,79°	49,66°	46,02°

Pour chaque élément l'intensité est mesurée à deux positions; $2\theta_{pic}$ pour l'intensité du pic (R_{pic}) et $2\theta + 1°$ pour l'intensité du bruit de fond (R_{BF}). Chaque mesure représente la moyenne de 10 mesures de 10 s chacune. Le porte-échantillon du spectromètre est chargé avec 4 pastilles; un standard (ou blanc) et trois inconnues. Le goniomètre est réglé à l'une des 6 positions 2θ données dans le tableau I et les 4 pastilles sont mesurées successivement. On passe ensuite à la position 2θ suivante, on répète les mesures et ainsi de suite.

Les courbes d'étalonnage établies à partir des mesures des standards et des blancs montrent que la méthode de préparation des pastilles est satisfaisante. L'in-

tensité du pic R_n, qui est proportionnelle à la concentration de l'élément dans la partie irradiée de la pastille, est calculée d'après:

$$R_n = (R_{pic} - R_{BF})_{standard} - (R_{pic} - R_{BF})_{blanc}$$

ou R_{pic} = intensité mesurée à la position $2\theta_{pic}$, et
R_{BF} = intensité mesurée à la position $2\theta_{pic} + 1°$.

A titre d'exemple la droite d'étalonnage pour le cobalt est illustrée dans la Fig. 1 ainsi que les performances de la méthode sont données dans le Tableau II. Les précisions données ci-dessus ont été calculées en mesurant 10 pastilles contenant chacune 100 p.p.m. de l'élément à doser et sont valables jusqu'à une teneur minimum de 50 p.p.m. environ. En dessous de cette teneur elles sont de ± 2 p.p.m. en valeur absolue. La limite de détection donnée dans le Tableau II est définie comme étant la

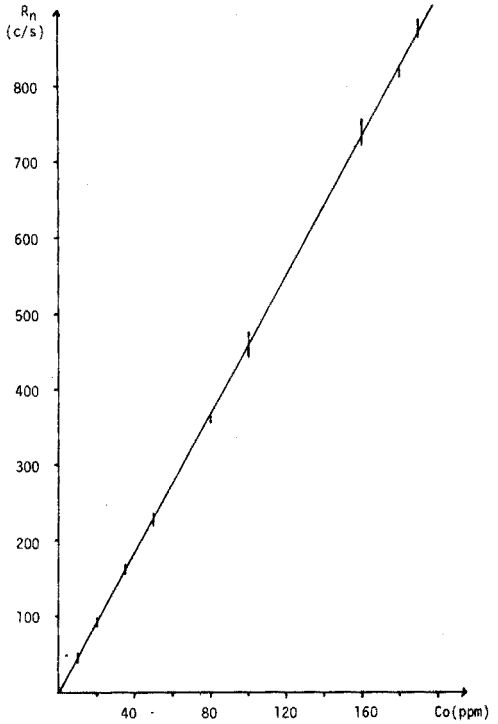

Fig. 1. Droite d'étalonnage pour le cobalt. Chaque standard a été mesuré 2 ou plus de fois. Les traits verticaux montrent la dispersion des mesures effectuées sur un même standard. La pente de la droite a été déterminée par calcul de la droite de régression.

TABLEAU II

PERFORMANCES DE LA MÉTHODE

	Co	*Ni*	*Cu*
Sensibilité (c/s/p.p.m.)	4,58	5,70	7,20
Précision (%)	4,9	5,0	4,8
Limite de détection (p.p.m.)	1,5	1,6	2.1

concentration minimum qui donne une intensité nette R_n trois fois supérieure à la déviation standard de la détermination de l'intensité du bruit de fond.

Aucune interférence entre les trois éléments n'a été observée dans les marges de concentrations dosées.

RÉSULTATS ET DISCUSSION

Application du procédé de Chilton

Le procédé d'extraction de Chilton a été appliqué systématiquement aux solutions obtenues par décomposition de la roche étalon PCC-1 dont la composition chimique est donnée par Flanagan[12]. $CHCl_3$ a été préféré à CCl_4 du fait de meilleure solubilité des complexes diéthyldithiocarbamiques des éléments à extraire[13]. La solution qui provient de l'attaque de 500 mg de roche est additionnée de 100 μg de cuivre (PCC-1 a une teneur en cuivre de 10 p.p.m. seulement; ajouter du cuivre permet de mieux suivre son extraction). On ajoute un volume mesuré d'acide citrique 2 *M* et on neutralise avec l'ammoniaque concentrée. Après avoir ajusté le pH avec NH_3 ou HCl, on complète à un volume connu. Cette solution, contenant 28,5 mg de Fe, 105 μg de Cu, 1200 μg de Ni et 56 μg de Co, est transférée dans une ampoule à extraction et additionnée de 2 ml de solution aqueuse de NaDDC. 3 H_2O 1% (ce qui correspond environ à un excès de complexant de 20 fois). On extrait une fois avec 10 ml et trois fois avec 5 ml de $CHCl_3$ en agitant chaque fois pendant 15 min, puis on procède au pastillage et à l'analyse par fluorescence-x.

Une première constatation à laquelle cette expérience conduit est que le masquage du fer n'est pas effectif à pH 8,5–9,0 même en présence de concentrations de citrate de l'ordre de 0,5 *M*, ce qui est de loin supérieure à la concentration maximum utilisée par Chilton. La concentration en citrate a alors été portée à 1 *M*. D'autre part, des pastilles standard avec des teneurs en fer de 100 à 1000 p.p.m. ont été préparées de la même manière que les standards de Cu, Ni et Co. Il a ainsi été possible de déterminer la quantité de fer coextrait en mesurant l'intensité de la raie $K\alpha$ du fer à $2\theta = 57{,}51°$. Cette étude a montré que, dans les conditions décrites et avec une phase aqueuse de:

pH de 8,5 à 9,5: Cu et Ni sont quantitativement extraits mais de 1000 à >1500 μg de fer sont coextraits ce qui perturbe le dosage du cobalt;

pH de 9,6 à 10,3: Cu et Ni sont quantitativement extraits. Le masquage du fer est meilleur (généralement $\leqslant 100$ μg de fer sont coextraits); mais le cobalt n'est extrait que partiellement (80–90%);

pH 10,3: Cu et Ni sont extraits partiellement (60–90%). Le masquage du fer est bon ($\leqslant 10$ μg de fer en phase organique. Le rendement d'extraction du cobalt varie de 20 à 50%.

La technique de Chilton est donc inapplicable aux solutions obtenues par la décomposition de roches; une recherche plus détaillée des conditions permettant un masquage efficace du fer en même temps qu'une extraction quantitative des 3 éléments était nécessaire.

Étude du masquage du fer

Une étude par colorimétrie visuelle a été faite sur des solutions synthétiques pour comparer l'efficacité du masquage par le tartrate à celle par le citrate.

Une solution aqueuse (5 ml) contenant du fer(III) en concentration connue et 1 *M* en citrate ou en tartrate et dont le pH a été ajusté par adjonction de NaOH ou de HCl, sont agités avec 5 ml de solution fraîchement préparée de diéthyldithiocarbamate de diéthylammonium dans $CHCl_3$. Après une durée d'agitation t_{ag}, on laisse se séparer les deux phases et on compare l'intensité de la couleur de la phase organique à celle d'une solution de $Fe(DDC)_3$ dans $CHCl_3$ contenant 5 μg Fe ml^{-1}.

Les résultats rassemblés dans le Tableau III montrent que l'ion tartrate masque le fer plus efficacement que ne le fait l'ion citrate; en outre, prolonger la durée d'agitation défavorise le masquage. Il est évident que l'extraction du fer est régie par la cinétique de formation du $Fe(DDC)_3$ en phase aqueuse. Le passage du

TABLEAU III
MASQUAGE DU FER PAR L'ION CITRATE OU TARTRATE 1 *M*
($T = 22 \pm 3°C$, $V_{org} = V_{aq}$.)

pH	*Ion*	t_{ag}					
		30 s	*5 min*	*10 min*	*20 min*	*1 h*	*6 h*
(a) $[Fe^{+3}] = 100\ \mu g\ ml^{-1}$, $[DDC^-] = 2 \cdot 10^{-2}\ M$							
8,6	Citrate	b[a]	m	n			
8,6	Tartrate	b	b	m	n		
8,9	Citrate	b	b	m	n		
8,9	Tartrate	b	b	b	b	m	n
9,2	Citrate	b	b	b	b	n	
9,2	Tartrate	b	b	b	b	b	b
9,5	Citrate	b	b	b	b	b	n
9,8	Citrate	b	b	b	b	b	n
10,3	Citrate	b	b	b	b	b	b
(b) $[Fe^{+3}] = 400\ \mu g\ ml^{-1}$, $[DDC^-] = 2 \cdot 10^{-2}\ M$							
8,6	Citrate	n					
8,6	Tartrate	b	m	n			
9,3	Citrate	b	m	n			
9,3	Tartrate	b	b	b	b	m	n
9,5	Citrate	b	m	n			
9,5	Tartrate	b	b	b	b	b	b
9,8	Citrate	b	m	n			
10,0	Citrate	b	b	m	n		
10,3	Citrate	b	b	b	b	m	n
10,6	Citrate	b	b	b	b	b	b
(c) $[Fe^{+3}] = 1\ mg\ ml^{-1}$, $[DDC^-] = 3 \cdot 10^{-2}\ M$							
8,9	Tartrate	b	m	n			
9,3	Tartrate	b	b	m	n		
9,7	Tartrate	b	b	b	m	n	
10,1	Tartrate	b	b	b	b	m	n
10,3	Tartrate	b	b	b	b	b	m
10,5	Tartrate	b	b	b	b	b	b

[a] b—Bon masquage: $Fe_{org} < 5\ \mu g\ ml^{-1}$; m—masquage moyen: $Fe_{org} \sim 5\ \mu g\ ml^{-1}$; n—mauvais masquage: $Fe_{org} > 5\ \mu g\ ml^{-1}$.

complexe dans la phase organique est rapide; une fois qu'il est formé une agitation de 2 à 3 min suffit à l'extraire quantitativement. En effet quelques expériences conduites en incorporant le complexant dans la phase aqueuse, laissant au repos pendant une durée t_r (durée réactionnelle) puis en agitant pendant 3 min avec $CHCl_3$ de façon à avoir $t_r + 3$ min $= t_{Ag}$, ont donné les mêmes résultats que ceux du Tableau III.

Étude comparative de l'extraction du cobalt

Pour étudier l'effet du citrate et celui du tartrate sur les rendements d'extraction, il suffit d'effectuer cette étude avec le cobalt seulement, car c'est cet élément qui systématiquement est extrait avec le plus faible rendement. La détermination du cobalt étant plus rapide par traçage isotopique avec ^{60}Co que par fluorescence-x, c'est cette première méthode qui a été choisie. Le procédé utilisé est le suivant. Une portion de 5 ml de solution de PCC-1 est additionnée de 2 ml de solution de traceur et de x ml de solution aqueuse d'acide citrique ou d'acide tartrique 2 M. On neutralise avec NH_3 concentrée et ajuste le pH avant de completer à 20 ml avec de l'eau. Dans 4 ml de cette solution on ajoute 1 ml de solution aqueuse de NaDDC 0,05 M et on laisse au repos pendant la durée t_r. On extrait en agitant pendant 3 min avec 5 ml de $CHCl_3$. Après la séparation des deux phases on détermine le rendement d'extraction du cobalt en mesurant l'activité du ^{60}Co dans 1 ml de chacune des phases.

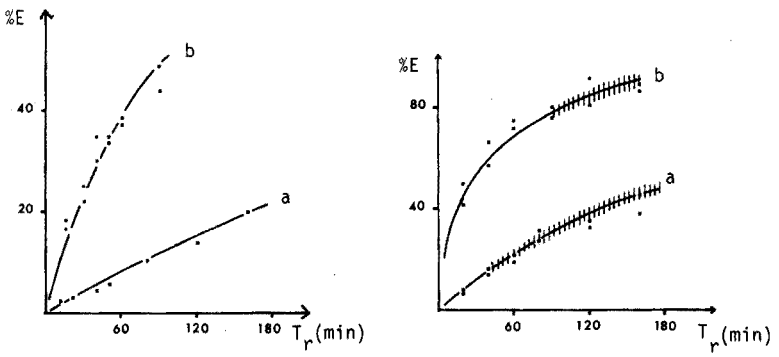

Fig. 2. Rendement d'extraction du Co en fonction de la durée réactionnelle à pH = 11,7; $V_{org} = V_{aq}$, [DDC] = 10^{-2} M, $T = 22 \pm 3$°C; (a) en présence de citrate 0,32–0,64 M (pour $t_r = 12$ h, $\%E = 65$), (b) en présence de tartrate 0,32–0,64 M (pour $t_r = 12$ h, $\%E = 98$).

Fig. 3. Rendement d'extraction du Co en fonction de la durée réactionnelle à pH = 10,5; $V_{org} = V_{aq}$, [DDC] = 10^{-2} M, $T = 22 \pm 3$°C; (a) en présence de citrate 0,4 ou 0,8 M, (b) en présence de tartrate 0,4 ou 0,8 M. Les parties hachurées indiquent une coextraction de Fe observée visuellement en présence de citrate ou de tartrate 0,4 M. Avec 0,8 M d'agent masquant on n'observe plus cette coextraction.

Les Figures 2, 3, 4 et 5 montrent l'influence de divers facteurs sur le rendement d'extraction du cobalt. Il en ressort que ce rendement est lié à la cinétique de formation du complexe $Co(DDC)_3$ en phase aqueuse. Dans les conditions de concentrations employées, la concentration de l'agent masquant (0,3–0,8 M) n'influence pas la cinétique, mais toutes autres conditions égales, cette cinétique est beaucoup plus rapide en présence de tartrate qu'en présence de citrate (Figs. 2, 3 et 4). Le pH a aussi une grande influence sur la cinétique (Fig. 4). Enfin l'augmenta-

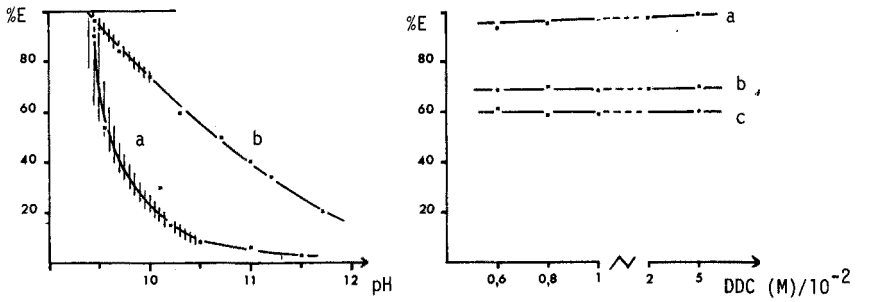

Fig. 4. Rendement d'extraction du Co en fonction du pH; $V_{org} = V_{aq}$, $[DDC] = 10^{-2}$ *M*, $T = 22 \pm 3°C$, $t_r = 15$ min; (a) en présence de citrate 0,4 *M*, (b) en présence de tartrate 0,4 *M*.

Fig. 5. Rendement d'extraction du Co en fonction de la concentration du complexant; $T = 22 \pm 3°C$; (a) en présence de tartrate 0,6 *M*, pH = 11,5, $t_r = 12$ h, (b) en présence de citrate 0,6 *M*, pH = 11,5, $t_r = 12$ h, (c) en présence de tartrate 0,6 *M*, pH = 11,0, $t_r = 1$ h.

tion de l'excès du complexant n'a pas d'influence significative sur le rendement de l'extraction du Co (Fig. 5). En ce qui concerne le masquage du fer, les résultats obtenus avec les solutions synthétiques sont qualitativement confirmés.

Conclusions et description du procédé d'extraction adopté

L'extraction quantitative du cuivre, du nickel et du cobalt avec un masquage optimal du fer nécessite les conditions suivantes: concentration en tartrate $\geqslant 0{,}5$ *M*, pH = 10,5–11,7, concentration en DDC^- 10–40 fois en excès par rapport à la somme des métaux à extraire, et au moins 12 h de repos après l'incorporation du complexant dans la solution.

Cependant, puisque le rendement de l'extraction est lié à la cinétique de formation du complexe en phase aqueuse, on peut prévoir que la température favorisera l'extraction. L'influence de la température n'a pas fait l'objet d'une étude systématique, mais plusieurs essais, comportant une étape d'ébullition de la solution aqueuse après l'introduction du complexant, ont montré que la formation des complexes diéthyldithiocarbamiques de cuivre, de nickel et de cobalt était quantitative déjà après 5 min d'ébullition. Le procédé d'extraction retenu est le suivant. Dans la solution provenant de la décomposition de 350 à 500 mg de roche ajouter 15 ml de solution aqueuse d'acide tartrique 40%. Alcaliniser avec l'ammoniaque concentrée jusqu'à pH $\geqslant 10{,}5$. Ajouter 2 ml de solution aqueuse de $NaDDC \cdot 3\,H_2O$ 1% et chauffer 5 min à ébullition douce. Laisser refroidir avant de transférer le contenu du bécher dans une ampoule d'extraction. Rincer le bécher soigneusement une fois avec une quantité minimum d'eau et deux fois avec des portions de 5 ml de $CHCl_3$ et rajouter les solutions de rinçage dans l'ampoule. Agiter pendant 3–5 min et séparer la phase organique. Répéter l'extraction encore 3 fois avec chaque fois 5 ml de $CHCl_3$.

Les trois éléments sont ensuite dosés par fluorescence-x. Pour tenir compte des contaminations possibles par les réactifs utilisés, les pastilles standard ont été de nouveau préparées en utilisant le procédé d'extraction finalement adopté.

Avec ce procédé on coextrait dans la phase organique de 0 à 100 μg de Fe et de 0 à 200 μg de Mn, ces deux éléments étant dosés par fluorescence-x à l'aide de quelques standards dans lesquels on a incorporé des quantités connues de Fe et de Mn en plus de Cu, de Ni et de Co. Des concentrations dans cet ordre de grandeur

de ces deux éléments ne perturbent pas le dosage par fluorescence-x.

La soude peut remplacer l'ammoniaque comme agent d'alcalinisation mais ce dernier est préférable. En effet, en milieu alcalin contenant du tartrate, $Mg(OH)_2$ précipite lentement (Mg est très abondant dans certaines roches telles que les roches ultrabasiques) et, bien qu'il reste en phase aqueuse après l'agitation, ce précipité ralentit considérablement la séparation des deux phases. Cette précipitation est beaucoup plus lente en présence de NH_4OH que de NaOH.

Application

La méthode décrite ici a été appliquée à plusieures roches étalon provenant de l'United States Geological Survey (U.S.G.S.) et du National Institute of Metallurgy, Johannesburg, South Africa (N.I.M.). Les résultats obtenus sont rassemblés dans le Tableau IV.

AU IV

TATS D'ANALYSE DE QUELQUES ROCHES ETALON

n^a	*Co (p.p.m.)*			*Ni (p.p.m.)*			*Cu (p.p.m.)*		
	Litt.[b]	*Trouv.*	*Préc.*[c]	*Litt.*	*Trouv.*	*Préc.*	*Litt.*	*Trouv.*	*Préc.*
8	50	44,1	2	78	82	3	110	126	7
8	112	103	3	2430	2370	54	10,4	14,0	5
2	132	128	6	2330	2370	118	7,9	11	4
2	7,5	8	4	10,7	7	4	35,2	36	4
2	35,5	34	4	15,0	11	4	22,4	17	4
2	15,5	14	4	17,8	21	4	63,7	62	4
2	—	196	10	—	2020	100	—	9	4
4	—	98	5	—	575	29	—	18	4
2	—	<3	—	—	3	4	—	10	4
2	—	4	4	—	5	4	—	20	4
2	—	56	4	—	124	6	—	9	4

nbre d'analyses.
/aleurs recommandées par Flanagan[12].
précision absolue (±).

Je remercie les professeurs A. Buchs, M. Delaloye et W. Haerdi de l'intérêt qu'ils ont manifesté pour ce travail, et le Fonds National Suisse pour la Recherche Scientifique qui a mis à ma disposition l'appareillage nécessaire.

RÉSUMÉ

La méthode combinée extraction–fluorescence-x décrite élimine toute source d'erreur liée aux effets de matrice et l'exactitude du dosage d'un élément vaut la précision de sa détermination par fluorescence-x. En utilisant 500 mg de roche, on peut doser de 3 à 2400 p.p.m. Ni, de 3 à 400 p.p.m. Co et de 4 à 1000 p.p.m. Cu dans la roche avec une précision de ±4 p.p.m. jusqu'à une teneur de 100 p.p.m. et de ±5% au-delà. Dans un laboratoire bien équipé une seule personne peut doser les trois éléments dans 48 roches en 10 jours de travail effectif. L'application de la méthode à d'autres matériaux que des roches doit être possible.

SUMMARY

An extraction–x-ray fluorescence method is described for the determination of copper, nickel and cobalt in roc .s. Matrix effects are eliminated, and the precision corresponds to that of the x.r.f. determination itself. If 500 mg of rock is used, 3–2400 p.p.m. Ni, 3–400 p.p.m. cobalt and 4–1000 p.p.m. copper can be determined with a precision of ±4 p.p.m. up to 100 p.p.m. and ±5% at higher values. One person can determine the 3 elements in 48 rocks in 10 working days. The proposed method should be applicable to other materials.

BIBLIOGRAPHIE

1 K. Hickson et R. J. Leech, *5th Conference on X-Ray Analytical Methods, Swansea, 1966*, p. 98.
2 E. F. Spano et T. E. Green, *Anal. Chem.*, 38 (1966) 1341.
3 W. C. Campbell, E. F. Spano et. T. E. Green, *Anal. Chem.*, 38 (1966) 987.
4 D. Doly, *8ème Colloque sur l'Analyse de la Matière, Florence, 1969*, p. 75.
5 L. G. Sear, *7th X-Ray Analytical Conference, Durham, 1970*, p. 11.
6 F. J. Marcie, *Environ. Sci. Technol.*, 1 (1967) 164.
7 M. Délepine, *Bull. Soc. Chim. Fr.*, (1958) 5.
8 H. Bode et F. Neumann, *Z. Anal. Chem.*, 172 (1960) 1.
9 J. M. Chilton, *Anal. Chem.*, 25 (1953) 1274.
10 A. Volborth, *Elemental Analysis in Geochemistry*, Elsevier, New York, 1969.
11 M. Delaloye, *C.R. Seances Soc. Phys. Hist. Natur. Geneve*, 4(2) (1969) 156.
12 F. J. Flanagan, *Geochim. Cosmochim. Acta*, 33 (1969) 81.
13 V. Sedivec et J. Flek, *Chem. Listy*, 52 (1958) 545.

Analytica Chimica Acta, 73 (1974) 265–272

THE DIFFERENTIATION OF SUBMICROGRAM AMOUNTS OF INORGANIC AND ORGANOMERCURY IN WATER BY FLAMELESS ATOMIC ABSORPTION SPECTROMETRY

RICHARD J. BALTISBERGER and CURTIS L. KNUDSON
University of North Dakota, Grand Forks, North Dakota 58201 (U.S.A.)
(Received 18th April 1974)

Methods for the determination of mercury traces in aqueous solutions have generally lacked the selectivity to differentiate and determine both inorganic and organomercury (RHg^+) compounds at the p.p.b. level. Numerous methods have been used for the determination of total mercury in substances, as reported in a review by Reimers *et al.*[1]. Various oxidizing agents have been used in sample preparation including hot acids[2], acidic peroxide media[3], permanganate[4], vanadium pentoxide[5] and ozone[6]. The mercury(II) content of an aqueous solution at the p.p.b. level can then be measured by the flameless atomic absorption method[7]. Gas chromatographic techniques have been used to separate and measure RHgX compounds which are detected by electron capture[8,9] or u.v. detection of mercury metal produced in a reduction after g.c. separation[10]. The direct g.c. technique is not useful for mercury(II) determinations. One of the first techniques reported for determinations of Hg(II) and RHg(II) individually was the method of Miller *et al.*[11], which is based on dithizone extraction but is satisfactory only at p.p.m. levels. Recently, Umezaki and Iwamoto[12] reported a method in which inorganic mercury in a mixture containing Hg(II) and RHg(II) was measured by selective reduction with acidic tin(II) chloride. The total mercury present was then measured by reduction with tin(II) in 1 *M* sodium hydroxide in the presence of a small amount of copper(II). The mercury vapor in each case was measured by a flameless atomic absorption technique. The organic mercury content of the aqueous solution was determined by difference. The method was reported to be satisfactory in the range 0.2–7 p.p.b. with a standard deviation of 2% at 5 p.p.b.; but it requires that two mercury reduction vessels be used in conjunction with the flameless atomic absorption device, or that one vessel be used which must be cleaned between each analysis for inorganic and total mercury, respectively.

This paper reports a method based on the use of acidic hydrogen peroxide for the determination of the individual concentrations of inorganic and organomercury compounds present in an aqueous sample. The advantage of the technique is that the two determinations can be carried out in the same reaction vessel without change of reduction media: the inorganic mercury present is first determined by reduction with tin(II) in sulfuric acid solution in the absence of hydrogen peroxide. No organomercury compounds are reduced in this step. The total mercury content of the sample is then measured after oxidation with hydrogen peroxide of a second aliquot before injection into the same tin(II) reduction

solution. The mercury metal produced by the reduction steps is measured by a flameless atomic absorption technique. The method is satisfactory at the 1–15 p.p.b. level with a standard deviation of 1 p.p.b. at 15 p.p.b., and permits the analysis of 10–20 samples in an hour if the oxidation step is completed. The oxidation step with hydrogen peroxide requires 15 min in a separate reaction vessel.

EXPERIMENTAL

Reagents

Reagent-grade sulfuric, perchloric and hydrochloric acids, tin(II) sulfate and 30% hydrogen peroxide were used in this study. Mercury(II) perchlorate (G. F. Smith Chemical Co.) methylmercury acetate and phenylmercury acetate (Alfa Chemical Co.) were used to prepare 1-p.p.m. stock solutions of the mercury compounds in 0.1 *M* perchloric acid. Methylmercury(II) and phenylmercury(II) have no tendency to adsorb on glassware and can be stored in glass containers at 0°C in the dark to prevent photodecomposition[13]. Mercury(II) adsorbs on glassware from perchlorate media, but the adsorption was insignificant at the 1-p.p.m. level. Adsorption problems will be discussed later.

Tin(II) solution. Tin(II) sulfate (10 g; Alfa Chemicals) was dissolved in 80 ml of water containing 20 ml of 10 *M* sulfuric acid. This solution was prepared weekly. Before use this solution was aereated to remove background u.v. readings. The aeration chamber (percolator) contained 5 ml of tin(II) solution initially and was replaced after about ten 0.2-ml injections or five 0.4-ml injections, except where noted.

Hydrochloric acid solution. Hydrochloric acid must be added to environmental water samples in order to obtain a quantitative release of mercury(II). The solution was prepared by adding 20 ml of concentrated hydrochloric acid to 10 ml of the tin(II) solution. Aeration of the solution for a few minutes eliminated any blank mercury reading when used in the percolator[4].

Apparatus

Mercury vapor was determined with a Laboratory Data Control system which consisted of a model 1235 UV Monitor, model 3300 recorder, model 900073 long path-length gas cell, and a mercury aereation vessel (impinger type percolator). The percolator was connected to the gas cell by Chromatronix model T125063 Cheminert (1/16 in. i.d.) tubing. Initially, a calcium sulfate drying tube was placed between the percolator and the gas cell, but this caused dust contamination of the gas cell, necessitating its cleaning, and caused decreased sensitivity and reproducibility. The drying tube was therefore removed. No difficulties were experienced with the water vapor background at the mercury levels used. The aereation vessel was cleaned periodically with basic peroxide solution in order to obtain a stable baseline.

A constant 920 ml min^{-1} air supply filtered through calcium sulfate and ascarite was obtained by means of a Masterflex model 7540 constant speed pump fitted with a model 7015 head. Sample injections were made with Plasticpak, 5602, 1-ml TB disposable syringes to which were glued 2-in. Hamilton, N722,

stainless steel needles. Repeated rinsing with hydrochloric acid solution and distilled water cleaned the syringes. Scotch tape was used to cover the markings on the syringes to allow their repeated usage.

Data analysis

The peak shape depended on the volume of the solution in the percolator, the speed of injection, and the volume of solution injected[6,14]. Rather than attempt to control these variables so that peak height could be used for analysis, the concentrations were determined by comparison of peak areas. This method was found to be reproducible from day to day, and eliminated the need for continuously running extensive instrument standardizations. Over two years of study, the maximal expected error for a single injection was $\pm 10\%$. As observed in Table I, standard deviations for multiple injections at the 29, 22, and 16-p.p.b. levels were $\pm 4\%$, $\pm 5\%$, and $\pm 7\%$, respectively, which compares favorably with other techniques[6,15].

TABLE I

ACIDIC WATER ANALYSIS[a]

Type of sample	*Total Hg[b] added (p.p.b.)*	*Mercury(II) found (p.p.b.)*	*Total Hg found (p.p.b.)*	*Total RHg[c] found (p.p.b.)*
Hg^{2+}	30	—	29 ± 1 (1, 6)	—
CH_3Hg^+	15	—	16 ± 1 (2, 4)	—
$C_6H_5Hg^+$	22	—	23 ± 1 (2, 9)	—
Mixture 1	45	29 ± 0.5 (1, 2)	47 ± 2 (1, 4)	18
Mixture 2	68	31 ± 4 (1, 5)	68 ± 4 (1, 4)	37

[a] Values in parentheses are the number of the mixtures and the total number of injections from which the standard deviation was calculated. Mixture 1 contained mercury(II) and methylmercury(II) ions. Mixture 2 contained mercury(II), methylmercury(II), and phenylmercury(II) ions.

[b] Known concentrations were obtained by weight and dilution.

[c] Total organomercury values were obtained by subtracting the amount of mercury(II) found from the total mercury found.

Peroxide reaction

Mercury(II) can be determined in the presence of methyl- and phenylmercury(II) by direct injection of an aqueous sample into the percolator[12]. Methyl- and phenylmercury(II) in 0.1 *M* perchloric acid gave no detectable mercury if injected into the percolator without prior oxidation steps. In this study it was found that under certain conditions hydrogen peroxide would yield quantitative decomposition of these organomercury species. Various hydrogen peroxide concentrations and injection techniques were investigated to determine the optimal conditions for organomercury analysis.

Prior oxidation of methyl- and phenylmercury was carried out in 15-ml graduated pyrex centrifuge tubes that could be capped and used as reaction vessels. To 10-ml samples containing 25 p.p.b. mercury as methylmercury(II) in 0.1 *M* perchloric acid was added 0.1, 0.3, 0.5, 1.0, or 2.0 ml of 30% hydrogen peroxide. These samples were controlled to 30 ± 0.2°C. Sample volumes of 0.2 ml were

removed at various times from 15 min to 12 h with a syringe that had never been in contact with tin(II) solution and directly injected into the percolator, which contained 5 ml of freshly added tin(II) solution. Fresh tin(II) solution was needed in the percolator since injections of undecomposed 30% peroxide would yield additional mercury peaks if any unreacted organomercury from a previous injection was present in the percolator. Only partial recovery of mercury in up to 12 h was observed as shown in Fig. 1. For 1-ml and 2-ml additions of peroxide per 10 ml of sample, the recovery was more erratic. The remainder of the methylmercury seemed to remain in the percolator and would not react unless a large concentration of hydrogen peroxide was added in a subsequently injected sample.

In order to recover the methylmercury(II) quantitatively as mercury vapor, it was necessary to add 0.1–0.2 ml of tin(II) solution to the syringe containing 0.2 ml of sample with hydrogen peroxide and to shake the syringe for 10–15 s just before injection. The quantitative recovery of methylmercury(II) obtained by this technique is shown in Fig. 1.

The reactions of methyl- and phenylmercury(II) acetate with peroxide (0.4 ml/10 ml of sample) were observed at 27 ± 1°C and 60 ± 2°C, in order to determine the effects of temperature. As observed in Fig. 2, an essentially constant recovery of only 35% with time was obtained at 27°C for both species. At 60°C the recovery varied linearly with time from 40% to 90% during an observation period of 15 min to 3 h. This constant recovery or steady increase in recovery that exhibits temperature-dependence is presently being investigated. If at any time, 0.1–0.2 ml of tin(II) solution was pre-mixed with a sample in the syringe, quantitative data were obtained.

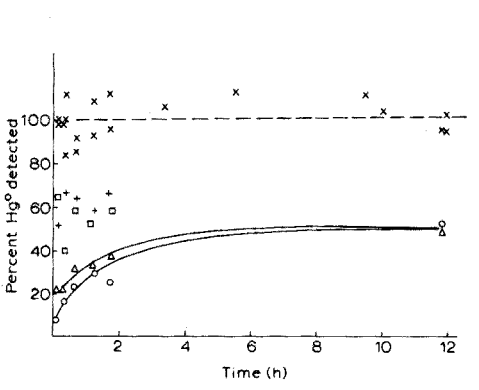

Fig. 1. Percentage of mercury detected as a function of time for 25 p.p.b. Hg as methylmercury(II) acetate in 0.1 *M* perchloric acid in the presence of hydrogen peroxide. Samples containing 0.1, 0.3, and 0.5 ml of peroxide per 10 ml of sample are represented as (⊙), (△), and (⊡), respectively, when directly injected, and as (+) for 0.1 ml and (×) for 0.3 ml and two 0.5 ml additions when pre-mixed with tin(II) solution before injection.

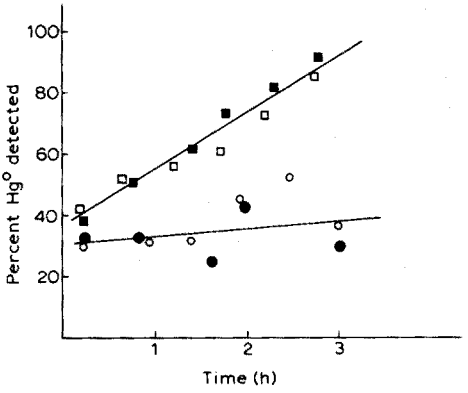

Fig. 2. Percentage of mercury detected as a function of time for 14 p.p.b. Hg as methylmercury(II) acetate in 0.1 *M* perchloric acid in the presence of 0.4 ml of hydrogen peroxide per 10 ml of sample at 27 ± 1°C (⊙) and at 60 ± 2°C (⊡). The same conditions were observed for 21 p.p.b. phenylmercury(II) acetate at 27°C (⊗) and at 60°C (⊠).

Recommended procedure for a mixture of mercury(II) and RHg(II)

Solutions containing mercury(II), methylmercury(II) and phenylmercury(II) were prepared with distilled water separately and as mixtures in 0.1 *M* perchloric acid by dilution. These were analyzed by direct injection of 0.2 ml of solution containing 1–25 p.p.b. Hg into the percolator containing 5 ml of the tin(II) solution. The mercury(II) content was determined by the u.v. reading at 254 nm. In order to determine the total mercury content of a sample, 0.2 ml of 30% hydrogen peroxide was added to 5 ml of the sample containing 0.1 *M* perchloric acid. After standing for 15 min, 0.2 ml of the solution was removed by syringe, 0.1–0.2 ml of tin(II) solution was added to the syringe, the syringe was shaken for 15 s, and the mixture was injected into the percolator.

Glassware adsorption

Adsorption and desorption of mercury(II) species on glassware has been observed to occur[3,16,17,18]. In this work, desorption problems were eliminated by choosing the glassware to be used. Glassware to be checked for possible mercury contamination was filled with dilute hydrochloric acid and allowed to stand overnight, and the solution was then analyzed for mercury. Glassware giving a blank greater than 0.2 p.p.b. was considered to be too contaminated for use; and was either re-cleaned with chromic acid or rejected. Rapid desorption of mercury(II) was observed; for example, a 15 p.p.b. methylmercury(II) solution was placed in an unchecked and contaminated volumetric flask. The initial analysis of the solution gave 15 p.p.b. RHg(II) in the flask, but after 1 h, analysis of the solution gave a concentration of 6 p.p.b. mercury(II) and 22 p.p.b. total mercury. The value of 0.2 p.p.b. used as the measure of contamination is the limit of detectability of the method. Adsorption of 10–20% mercury(II) by selected glassware was observed with standing overnight. Since the analytical technique is rapid, adsorption is not a problem unless the sample must be transported some distance before analysis. Solutions of methyl- and phenylmercury(II) showed no observable adsorption even after storage for 1 month. Adsorption of mercury(II) in stock solutions in 0.1 *M* perchloric acid of even 1–100 p.p.b. was negligible, if the glassware was preequilibriated with mercury of the same concentration. This decreasing adsorption with use of containers has been reported by Rosain and Wai[18].

Natural water analysis.

Water samples from the Red and Red Lake rivers were obtained from the Grand Forks Water Department. Analysis indicated that these samples contained 140, 116, and 194 p.p.m. of calcium, magnesium, and carbonate (as calcium carbonate), respectively. Mixtures of almost equal concentrations of mercury(II) and methylmercury(II) from 0–200 p.p.b. mercury in 0.1 *M* perchloric acid were prepared by diluting small volumes of stock solutions and concentrated perchloric acid with river water. These samples were analyzed for inorganic, total, and organomercury content. It was found necessary to add 0.1–0.2 ml of the hydrochloric acid solution and to shake for 20–30 s before direct injection or before addition of tin(II) solution to obtain quantitative mercury(II) recoveries (see Figs. 3 and 4).

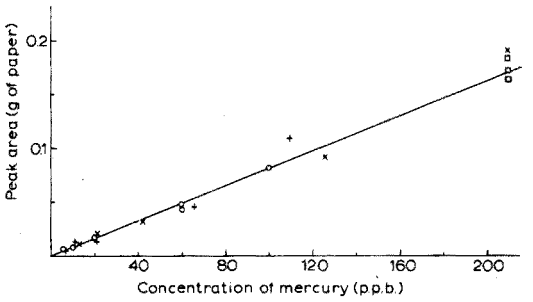

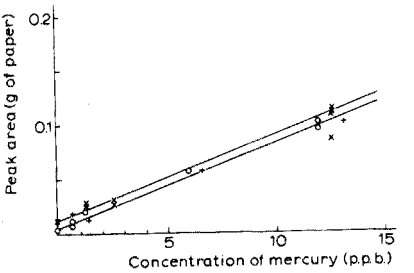

Fig. 3. Comparison of total mercury (×), mercury(II) (⊙), and methylmercury(II) (+) determinations in spiked river water samples. A 21 p.p.b. mercury(II) (⊡) stock solution is presented for comparison at ten times its concentration.

Fig. 4. Comparison of under 15 p.p.b. spiked river water samples in which the total mercury (×), mercury(II) (⊙), and methylmercury(II) (+) concentrations were determined.

Interferences

The interference of sulfide on the determination of both mercury(II) and methylmercury(II) was measured. The tolerable limit of sulfide (present as H_2S in 0.1 *M* perchloric acid media) is 10^{-4} *M*. Chloride ion or *L*-alanine have no effect on the reduction reactions up to 0.1 *M*. Earlier studies have noted interferences of 0.2 *M* hydrochromic acid, 0.01 *M* thiosulfate, 0.05 *M* iron, 1 p.p.m. iodide and 1 p.p.m. nitrite on the reduction of mercury(II) by tin(II) in flameless atomic absorption analysis[6,12,19,20,21]. The presence of any volatile u.v. absorbing volatile species would cause problems since no prior oxidation is possible in the two-step analysis proposed here. On this point, it can only be stated that the river water samples used in this work presented no problem in the range 1–15 p.p.b. Below 0.2 p.p.b., the limit of detectability is reached. The presence of interfering u.v.-absorbing species could be checked by a prior oxidation of the sample and a comparison with the total mercury analysis done by the proposed peroxide method. This was unnecessary with the Red River water samples used here.

In the river water study, analysis for total mercury, where peroxide was used, yielded consistent data whereas analysis for mercury(II) tended to be low unless the hydrogen chloride solution was utilized as described. There was considerable suspended clay material in the river samples. Analysis of spiked solutions before and after settling yielded similar results. Analysis of the clay yielded essentially no detectable mercury. The presence or absence of suspended matter also had no effect on the syringe or other apparatus. Thus, the stock river and spiked solutions were shaken and treated as homogeneous mixtures. Loss of mercury was observed if the treated solutions were allowed to stand overnight. Re-use of the same volumetric glassware with the same stock river water and mercury concentrations yielded smaller losses, indicating that mercury was adsorbed by the glass.

RESULTS AND DISCUSSION

An interesting result of this work is that in acidic media, hydrogen peroxide will not completely oxidize the organomercury ion so that the resulting

mercury(II) can be reduced in the percolator. A small quantity of tin(II) must be added with the hydrogen peroxide in the syringe. A correct concentration of hydrogen peroxide and pre-mixing with tin(II) solution were needed to obtain quantitative recoveries for organomercury compounds. Injecting peroxide solutions directly without pre-mixing with tin(II) solution did not give quantitative recoveries even after 12 h at 30 °C or 3 h at 60 °C (see Figs. 1 and 2). However, for 0.3 and 0.5 ml of peroxide per 10 ml of sample, pre-mixing with tin(II) yielded quantitative results with a standard deviation of $\pm 8\%$ (see Fig. 1) at the 25-p.p.b. level for 17 injections from 3 solutions over a 10 min–12 h period of observation. For 0.1 ml of peroxide additions, quantitative results were not obtained even with tin(II) pre-mixing. On this basis, a ratio of 0.4 ml of peroxide to 10 ml of sample is recommended for the analysis of a solution containing organomercury compounds.

Results obtained for determinations of total mercury, inorganic mercury and organomercury in 0.1 *M* perchloric acid are presented in Table I. The data indicate that the procedure is selective in that, without the addition of peroxide and pre-mixing with tin(II) solution only inorganic mercury is determined. The relative standard deviation ranges from 4% at 67 p.p.b. to 6% at 15 p.p.b. for individual injections. Comparisons between solutions yield similar values.

Examples of 15-min analyses of spiked river water solutions are presented in Figs. 3 and 4. For concentrations greater than 5 p.p.b., the error was similar to that observed in distilled water determinations. In Fig. 4, it can be observed that the spiked solutions containing less than 15 p.p.b. mercury yielded non-zero intercepts, possibly because of the presence of mercury or u.v.-absorbing species in the original water sample. If this absorbance was due to mercury, the intercepts indicate that the solution contained 0.7 ± 0.2 p.p.b. inorganic and 1.2 ± 0.3 p.p.b. organomercury.

In natural water analysis, low results for mercury(II) ion were obtained when the hydrochloric acid solution was not utilized. This seemed to indicate that a complex had been formed with species present in river water that would not rapidly decompose to yield elemental mercury. This effect has been reported in earlier papers[6,19,20]. The use of the hydrogen chloride solution did not interfere, when used as described, with the organomercury analysis.

The method described above facilitates the rapid determination and differentiation of mercury(II) and RHg(II) in the range 1–15 p.p.b. in environmental water samples. A single reduction percolator is needed in the flameless atomic absorption train. The method can be adapted to most water samples unless volatile u.v. absorbing species are present. Prior oxidation of the organic matter, followed by determination of total mercury could be used to determine the extent of such interferences. The limit of detection is 0.2 p.p.b. for a 0.2-ml injection of sample. To extend the method below 0.2 p.p.b. two problems become more severe: adsorption and desorption of mercury(II) on container materials and u.v. interferences. Hume and Gilbert[14] by carefully controlling aereation variables have determined 0.04 p.p.b. total mercury in 100 ml of solution.

This work was supported by Grant B-020 NDAK from the Office of Water Resources Research Institute, Fargo, North Dakota.

SUMMARY

A method for the determination of the individual concentrations of mercury(II) and RHg(II) in aqueous solutions is described. The mercury metal produced by reduction with tin(II) is measured by flameless atomic absorption. Selective reduction of mercury(II) is achieved in the presence of RHg(II) in sulfuric acid media with tin(II). The total mercury content is then measured after oxidation with acidic hydrogen peroxide solution just before injection into the tin(II) solution of the mercury analyzer. The method is useful in the range 1–15 p.p.b. with a standard deviation of 1 p.p.b. at 15 p.p.b. The method was satisfactory for river water samples.

REFERENCES

1 R. S. Reimers, W. D. Burrows and P. A. Krenkel, *J. Water Pollut. Contr. Fed.*, 45 (1973) 816.
2 T. T. Gorsuch, *Analyst (London)*, 84 (1959) 142.
3 D. Polley and V. L. Miller, *Anal. Chem.*, 27 (1955) 1162.
4 S. H. Omang, *Anal. Chim. Acta*, 53 (1971) 415.
5 F. D. Deitz, J. L. Sell and D. Bristol, *J. Off. Anal. Chem.*, 56 (1973) 378.
6 L. Lopez-Escobar and D. N. Hume, *Anal. Lett.*, 6 (1973) 343.
7 W. R. Hatch and W. L. Ott, *Anal. Chem.*, 40 (1968) 2085.
8 J. A. Ealy, W. D. Shults and J. A. Dean, *Anal. Chim. Acta*, 64 (1973) 235.
9 R. C. Dressman, *J. Chromatogr. Sci.*, 10 (1972) 468.
10 R. C. Dressman, *J. Chromatogr. Sci.*, 10 (1972) 472.
11 V. L. Miller, D. Polley and G. J. Gould, *Anal. Chem.*, 23 (1951) 1286.
12 Y. Umezaki and K. Iwamoto, *Bunseki Kagaku*, 20 (1971) 173.
13 P. L. Goggen and L. A. Woodward, *Trans. Faraday Soc.*, 58 (1962) 1495.
14 T. R. Gilbert and D. N. Hume, *Anal. Chim. Acta*, 65 (1973) 461.
15 B. W. Bailey and F. C. Lo, *Anal. Chem.*, 43 (1971) 1525.
16 C. Feldman, *Anal. Chem.*, 46 (1974) 99.
17 M. R. Greenwood and T. W. Clarkson, *J. Amer. Ind. Hyg. Assoc.*, 31 (1970) 250; *Chem. Abstr.*, 73, 33502a.
18 R. M. Rosain and C. W. Wai, *Anal. Chim. Acta*, 65 (1973) 279.
19 M. J. Fishman, *Anal. Chem.*, 42 (1970) 1462.
20 N. S. Poluektov, R. A. Vitkun and Yu. V. Zelyukova, *Spektral. Anal. Geol. Geokhim., Mater. Sib. Soveshch. Spektrosk., 2nd I.* 1963 (Pub. 1967) 200; *Chem. Abstr.*, 72 28106z.
21 G. Lindstedt, *Analyst (London)*, 95 (1970) 264.

Analytica Chimica Acta, 73 (1974) 273–281

DETERMINATION OF TRACE METALS IN POLYMERS BY FLAMELESS ATOMIC ABSORPTION WITH A SOLID SAMPLING TECHNIQUE

EARL L. HENN

Calgon Corporation, Box 1346, Pittsburgh, Pa. 15230 (U.S.A.)

(Received 25th March 1974)

The distribution of trace metals in the environment has become a matter of increasing concern to health officials and environmentalists in recent years. Consequently, much work has been done in developing analytical techniques to measure very small concentrations of heavy metals[1]. The atomic absorption method of determining trace metal constituents has been found to be sensitive and reliable and is used in the analysis of many different substances[2]. However, few applications of this technique to the analysis of trace metals in polymers are reported in the literature.

Slavin[3] and Druckman[4] have reported a method in which the polymer is ashed and the residue is taken up in acid solution. The solution is then analyzed by conventional atomic absorption methods. This technique, although providing low detection limits, suffers from the need for time-consuming sample preparation and the possibility of loss of volatile elements during the ashing step. Olivier[5] has reported a method in which concentrated solutions of the polymers are prepared in acids or organic solvents and then aspirated directly into a flame. Although this method provides a distinct advantage in speed of analysis, detection limits by this technique are often insufficient to provide reliable data in the low p.p.m. range. This is because there is a limit on how concentrated a polymer solution may be before the viscosity of the solution prevents efficient aspiration. When the viscosity of the solution affects the uptake rate of the nebulizer, either a metal-free solution of the polymer must be used for preparation of standards, or the analysis must be performed by the method of standard addition to compensate for the changes in sensitivity which result from the slower rate of nebulization.

The difficulties associated with the analysis of polymers by flame atomic absorption prompted an investigation into the feasibility of using flameless methods for the analysis. Flameless atomic absorption has been amply described elsewhere. In addition to the increased sensitivity available by flameless methods, a unique advantage of this technique is that solid samples can be analyzed directly. The use of solid sampling in the determination of trace metallic constituents in solid polymers provides distinct advantages in speed and convenience over other methods. Solid sampling eliminates the necessity of preparing a concentrated solution of the polymer, a procedure which is often tedious and time-consuming. This is especially true of water-soluble polyelectrolytes which tend to swell rapidly in the presence of water and go into solution very slowly. In addition, there is always the possibility of contaminating a solution with trace metals during preparation.

It would be expected that much lower detection limits could be achieved with solid sampling because a much larger amount of sample can be used. Inasmuch as solid sampling is a new technique and very little information regarding its reliability is available, it was felt that an in-depth study of the method was necessary before any reliance could be placed on results.

In evaluating the solid sampling technique a number of basic questions had to be answered. Is it possible to obtain accurate results with solid samples by comparing the absorption peaks obtained to a calibration curve which must be prepared from aqueous standards? In preparing the calibration curve, what volume of aqueous standard solution should be used to provide the absolute sensitivity which most closely approximates the absolute sensitivity being obtained with the solid sampling method? If it is assumed that trace metals are distributed in a heterogeneous manner in most solids, how many analyses must be performed in order to obtain an average value which represents the overall distribution of the metal in the solid? What is the largest practical sample size that can be used in order to obtain maximal sensitivity?

The approach that was used in obtaining answers to these questions was to analyze solid polymer samples for iron, copper and chromium both in solution and by the solid-sampling technique by flameless atomic absorption, with the same calibration curve for the solid samples as for the solutions. Recovery studies were then performed on the solutions to assess the accuracy of these values and the results obtained by both methods were compared.

EXPERIMENTAL

Apparatus

A Perkin-Elmer Model 305B atomic absorption spectrophotometer, equipped with an HGA-2000 heated graphite atomizer, deuterium background corrector and strip chart recorder, was used for all measurements.

A tantalum solid-sampling spoon (Perkin-Elmer) was used for injection of solid samples into the furnace. Liquid samples were injected with Eppendorf microliter pipets. Solid samples were weighed to the nearest microgram on a Cahn Model G electrobalance before placement in the furnace.

Single-element hollow-cathode lamps were used as line sources for all metals.

Instrument settings

The spectrophotometer settings used for analysis of the three metals are listed in Table I. Background correction was used for all measurements.

The drying, charring and atomization time and temperature settings used on the HGA-2000 heated graphite atomizer for analyzing both solid and liquid samples are listed in Table II.

Reagents

A solution of 0.16 *M* nitric acid was used as a solvent for solid polymers and standard metal solutions. The 1000 mg l^{-1} stock solutions used in preparing standards were obtained from Fisher Scientific Co., Pittsburgh, Pa.

TABLE I

SPECTROPHOTOMETER SETTINGS USED FOR METALS IN POLYMERS BY FLAMELESS ATOMIC ABSORPTION

Metal	*Wavelength (nm)*	*Source current (mA)*	*Spectral bandpass (nm)*
Copper	324.7	15	0.7
Iron	248.3	30	0.2
Chromium	357.9	25	0.7

.E II

·2000 SETTINGS USED IN ATOMIZING BOTH SOLID AND LIQUID SAMPLES FOR 1ELESS ATOMIC ABSORPTION

	Time (s)						*Temperature (°C)*		
	Solid samples			*Liquid samples*			*Dry*	*Char*	*Atomize*
	Dry	*Char*	*Atomize*	*Dry*	*Char*	*Atomize*			
:r	20	60	15	60	60	15	125	700	2500
	20	60	15	60	60	15	125	1000	2500
nium	20	60	15	60	60	15	125	1350	2700

Polymer types

The polymers used were all water-soluble and some can be classified as polyelectrolytes. Included are alginates, polyacrylamide (PAM) in varying degrees of hydrolysis, polyethylene oxide, the sodium salt of 2-acrylamido-2-methylpropanesulfonic acid (AMPSA), copolymers of AMPSA and PAM and terpolymers of acrylamide, dimethyldiallylammonium chloride (DMDAAC) and diethyldiallylammonium chloride (DEDAAC).

Sample preparation

Solutions of the polymers were prepared in the range of 0.25–1.0% by dissolving the appropriate amount of polymer in 0.16 *M* nitric acid.

Sample analysis

The tantalum spoon used for injecting solid samples into the graphite furnace is designed to deliver the sample at the center of the tube. The spoon containing the sample is inserted into one end of the tube and then inverted when it reaches the center. The sample then drops off the spoon into the tube. Occasionally, sample particles tend to adhere to the tantalum spoon and the barrel of the spoon holder has to be tapped after insertion and inversion, to empty the spoon completely. Solid samples were analyzed in triplicate, absorption values were referred to the same calibration curve as used for the solutions, and the results were averaged.

In analyzing the polymer solutions a 50-μl sample volume was used for

TABLE III COMPARISON OF SOLID SAMPLING WITH SOLUTION ANALYSIS IN DETERMINING CHROMIUM, COPPER AND IRON IN POLYMERS

Sample	*Cr Found (p.p.m.)*			*Cu found (p.p.m.)*			*Fe found (p.p.m.)*		
	Solution	*Solid*		*Solution*	*Solid*		*Solution*	*Solid*	
		Average	*Range*		*Average*	*Range*		*Average*	*Range*
Xanthan gum	0.7	0.8	0.7–1.0	1.5	1.5	1.4–1.7	16.5	31.8	30.0–34.6
Propylene glycol alginate	0.5	0.6	0.5–0.6	0.2	0.2	0.2–0.3	22.0	21.9	20.6–23.4
Sodium alginate	0.4	0.4	0.3–0.5	0.4	0.4	0.3–0.4	16.7	13.0	4.6–17.6
Polyethylene oxide	0.5	0.1	0.1–0.1	0.6	<0.1	<0.1–<0.1	3.2	2.8	2.5–3.3
Polyacrylamide (5% hydrolyzed)	0.3	0.3	0.1–0.5	1.2	2.2	1.6–2.6	6.6	6.6	5.9–7.8
Polyacrylamide (35% hydrolyzed)	0.2	0.2	0.1–0.2	5.4	3.8	3.8–3.8	7.9	5.7	3.5–8.1
47.5% DMDAAC, 2.5% DEDAAC, 50% PAM terpolymer (4.5% hydrolyzed)	0.3	0.2	0.1–0.2	4.0	3.3	2.8–4.0	15.9	4.3	3.5–5.4
Polyacrylamide (15% hydrolyzed)	0.2	0.1	0.1–0.2	0.9	0.7	0.6–0.8	17.8	16.8	14.6–20.3
47.5% DMDAAC, 2.5% DEDAAC, 50% PAM terpolymer	0.3	1.2[a]	0.1–6.0	0.4	0.6	0.5–0.8	13.8	11.2	9.8–12.4
Poly AMPSA	0.6	0.5	0.5–0.5	0.5	0.3	0.2–0.3	13.3	14.0	13.2–15.1
PAM–AMPSA copolymer	0.4	0.9	0.3–2.8	2.3	2.3	1.6–3.0	21.3	18.4	16.7–20.0
Polyacrylamide (unhydrolyzed)	1.4	1.3	0.7–2.5	2.9	2.0	1.7–2.5	11.7	9.9	9.2–10.7
Polyacrylamide (35% hydrolyzed)	<0.4	0.4	0.4–0.5	20.0	17.6	15.3–18.6	10.7	13.2	11.6–14.6
Polyacrylamide (15% hydrolyzed)	0.6	0.2	0.2–0.2	11.5	9.1	4.5–14.3	15.7	15.9	14.2–19.0
37.5% DMDAAC, 2.5% DEDAAC, 60% PAM terpolymer	0.9	0.5	0.3–0.8	3.8	0.7	0.6–0.7	8.8	8.1	7.5–9.5
57.5% DMDAAC, 2.5% DEDAAC, 40% PAM terpolymer	1.0	0.3	0.2–0.6	1.4	0.3	0.3–0.4	16.8	14.2	11.4–16.9

samples and standards in tests for copper and chromium. For iron determinations, a 25-μl sample volume was used in most cases. The metal concentration was taken from the average absorption value obtained from triplicate injections.

RESULTS AND DISCUSSION

Comparative studies

The chromium, copper and iron concentrations found in all solid samples by both the solid sampling and solution techniques are listed in Table III. The average values listed for the solid sampling method represent an average of at least three analyses. The range values listed represent the range of concentration covered by the three or more analyses by the solid sampling technique and are an indication as to how homogeneously the metals are distributed in the sample. It should be noted that, in the majority of cases, fairly good agreement was obtained between the two methods, indicating that the sensitivity obtained by the solid sampling technique was close to that obtained with the standard solutions, and that, in most cases, triplicate analysis is sufficient to provide a measure of the overall distribution of the metal in the solid. It was noted, however, that the results by the solid sampling technique were generally somewhat lower than those obtained by the solution method. At first it was thought that this was due to contamination of the solution in preparation. However, a statistical analysis of the data revealed that this was not the case. In Fig. 1 the solid analyses values for chromium, copper and iron are plotted *versus* the solution analyses values on linear graph paper. The dotted line represents the line that would be formed by the points if perfect agreement had been obtained between the two methods. The solid line represents the line actually formed by the points as calculated by the method of least squares. If the higher solution analyses values were due primarily to contamination

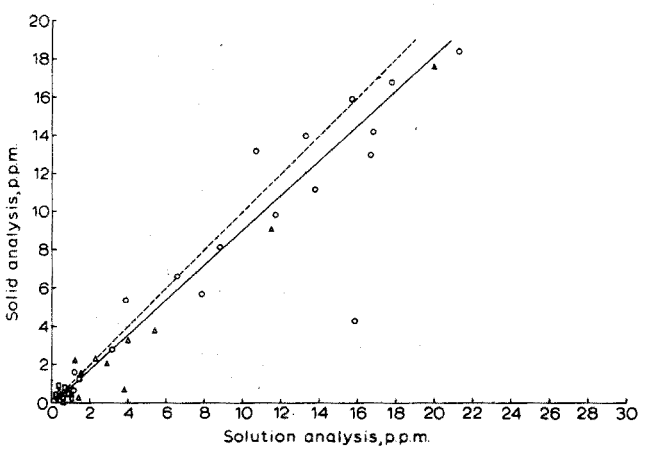

Fig. 1. Graphical representation of the degree of congruence between the results obtained by the solid sampling technique and solution analysis of metals in polymers. (---), the line that would have been formed by the points if perfect agreement had been obtained between the two methods; (—), the line actually formed by the points as calculated by the method of least squares; (△), copper; (⊙), iron; (⊡), chromium.

TABLE IV

RECOVERY OF METAL ADDED TO POLYMER SOLUTIONS

Sample	*Cr in 50 μl of solution (pg)*			*% Recovery of added Cr*
	Found	*Added*	*Recovered*	
Xanthan gum	350	2500	1790	72
Propylene glycol alginate	225	2500	1900	76
Sodium alginate	200	2500	1475	59
Polyethylene oxide	125	2500	2000	80
Polyacrylamide (5% hydrolyzed)	80	2500	2535	101
Polyacrylamide (35% hydrolyzed)	60	2500	2615	104
47.5% DMDAAC, 2.5% DEDAAC, 50% PAM terpolymer	80	2500	2720	109
Polyacrylamide (15% hydrolyzed)	60	2500	2430	98
47.5% DMDAAC, 2.5% DEDAAC, 50% PAM terpolymer	80	2500	2370	95
Poly AMPSA	140	2500	2560	102
PAM–AMPSA copolymer	110	2500	2540	101
Polyacrylamide (unhydrolyzed)	350	2500	2420	97
Polyacrylamide (35% hydrolyzed)	< 50	2500	2500	100
Polyacrylamide (15% hydrolyzed)	80	2500	2445	98
37.5% DMDAAC, 2.5% DEDAAC, 60% PAM terpolymer	110	2500	2660	107
57.5% DMDAAC, 2.5% DEDAAC, 40% PAM terpolymer	125	2500	2575	103
		Average	*% recovery*	94

[a] A 10-μl sample was used for the alginate polymers.

of the solution, the percentage difference would be much greater at the lower concentrations than at the higher concentrations. However, the percentage difference between the two values (about 10%) remains essentially constant at all concentrations, indicating that the difference between the two methods is due primarily to somewhat less sensitivity being obtained with solid analysis compared to solution analysis.

The absolute sensitivity that is achieved for a metal by flameless atomic absorption with aqueous standards will vary considerably with sample volume. This variation in sensitivity is probably due to the different ways the element is distributed in the graphite tube after drying. This variation is more pronounced with some metals than with others. Figure 2 illustrates the variation in absolute sensitivity that occurs with different sample volumes for chromium, iron and copper. Note that maximum sensitivity is achieved in all cases with a sample volume of

μl of solution (pg)		% Recovery of added Cu	Fe in 25 μl of solution (pg)			% Recovery of added Fe
Added	Recovered		Found	Added	Recovered	
1000	380	38	1800	1000	470	47
500	410	82	2200	2500	1600	65
500	505	101	1670[a]	2000[a]	1160[a]	59
500	480	96	400	2500	1920	77
2500	2440	98	830	2500	2890	116
1000	610	61	980	2500	1920	77
1250	1775	142	1980	5000	5320	106
500	320	64	2200	5000	5000	100
1000	550	55	1730	5000	7580	152
1000	600	60	1670	5000	4900	92
1000	810	81	2660	5000	3490	70
1000	940	94	1470	5000	5480	109
5000	3500	71	670	5000	2980	60
1500	2233	149	985	5000	4830	96
1000	930	93	550	5000	4680	94
500	650	130	1050	5000	7350	147
Average	*% recovery*	88		*Average % recovery*		92

50 μl. The lowest sensitivity for iron and copper occurs at the maximal sample volume of 100 μl. The most drastic change in absolute sensitivity with sample volume was observed with copper, for which the sensitivity with a 100-μl sample volume was found to be about 35% less than that obtained with a 50-μl sample volume.

Inasmuch as the results by solid sampling are somewhat low, greater accuracy could be achieved with this method by using a standard volume which would provide a reduction in absolute sensitivity below that obtained with a 25- or 50-μl standard volume. In most cases this would be obtained with a standard volume of 100 μl.

Recovery studies

The percent recovery of added known amounts of metal to polymer solutions for all samples analyzed is listed in Table IV. No consistent pattern can be seen

in the recovery values with some samples causing some negative interference and others showing a positive interference. The only metal for which generally consistent recovery values were obtained was chromium. With the exception of xanthan gum and the alginate polymers, the recovery values for chromium ranged from 80 to 109%, with the majority of the values in the 95–105% range. The average percent recoveries were fairly good for all three metals. However, it is apparent that matrix interferences are a serious problem in flameless atomic absorption. For highly accurate results, some samples should be analyzed by the method of standard additions. In the case of solid sampling, an appropriate correction factor, carefully calculated from recovery studies, would have to be applied to the final result to correct for matrix interference effects.

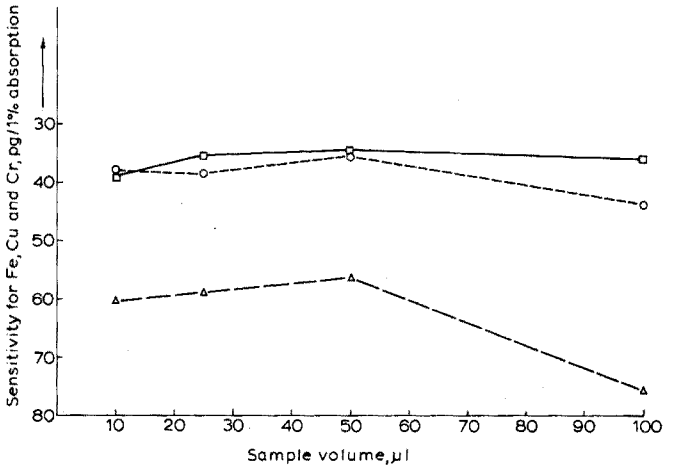

Fig. 2. Variation in absolute sensitivity with change in sample volume: (⊡), chromium; (⊙), iron; (△), copper.

Maximal sample size

The maximal sample size that can be used for solid sampling will vary depending on the nature of the sample. If a sample is too large, it is sometimes difficult to decompose completely during the charring stage. Also, the larger the sample size, the more inorganic constituents will remain after charring, and inorganics sometimes cause background absorption during the atomization stage. Experience has shown that, for most samples, 5000 μg is the largest practical sample size that can be used.

Detection limits

The mass of metal which can be detected depends on the amount of sample taken. In most of the analyses the sample weight involved when the solution analysis technique was used was 500 μg. In solid sampling, the sample weight varied considerably but rarely exceeded 5000 μg. The absolute detection limits of the three metals tested were very close, about 500 pg. Based on a solution sample weight of 500 μg and a solid sample weight of 5000 μg, the respective detection limits were 0.1 p.p.m. for solution analysis and 0.01 p.p.m. for solid analysis.

CONCLUSIONS

Solid sampling has been demonstrated to be a rapid and sensitive sampling technique for determining trace levels of iron, copper and chromium in polymers by flameless atomic absorption. In most cases, triplicate analysis is sufficient to obtain a value representing the overall distribution of the metal in the solid. Detection limits for the metals tested are about 0.01 p.p.m. when the solid sampling method is used. The method is subject to the numerous matrix interferences encountered in flameless atomic absorption; consequently, care must be exercised in interpreting results.

Although this study has been limited to the analysis for iron, copper and chromium, there is no doubt that other metals could be determined by the same technique.

SUMMARY

A method for determining trace metals in polymers which combines flameless atomic absorption with a solid sampling technique is described. The method is applied to the analysis of iron, copper and chromium and is compared with results obtained from analysis of solutions of the polymers. Optimal conditions for achieving maximal accuracy and sensitivity are discussed. The effects of various matrix interferences and the heterogeneous distribution of trace metals in polymers are discussed.

REFERENCES

1 *J. Water Pollut. Contr. Fed.*, 45 (1973) 979.
2 R. J. Reynolds and E. L. Pierson, *Amer. Lab.*, August 1971, p. 27.
3 W. Slavin, *At. Absorption Newslett.*, 4 (1965) 192.
4 D. Druckman, *At. Absorption Newslett.*, 6 (1967) 113.
5 M. Olivier, *At. Absorption Newslett.*, 10 (1971) 12; *Z. Anal. Chem.*, 257 (1971) 135.

Analytica Chimica Acta, 73 (1972) 283–292

DETERMINATION OF (*d,l*)-6-CHLORO-α-METHYLCARBAZOLE-2-ACETIC ACID IN BLOOD AND URINE BY SPECTROFLUORIMETRY AND ELECTRON-CAPTURE GAS CHROMATOGRAPHY

J. ARTHUR F. DE SILVA, NORMAN STROJNY and MARVIN A. BROOKS

Department of Biochemistry and Drug Metabolism, Hoffmann–La Roche, Inc., Nutley, N.J. 07110 (U.S.A.)

(Received 17th May 1974)

The compound (*d,l*)-6-chloro-α-methylcarbazole-2-acetic acid (I, Fig. 1) synthesized by Berger[1] has shown marked anti-inflammatory activity in the rat[2,3]. Blood levels determined in the rat, associated with anti-rheumatic activity were reported to be comparable to indomethacin[4]. The compound is of clinical interest as an anti-inflammatory agent.

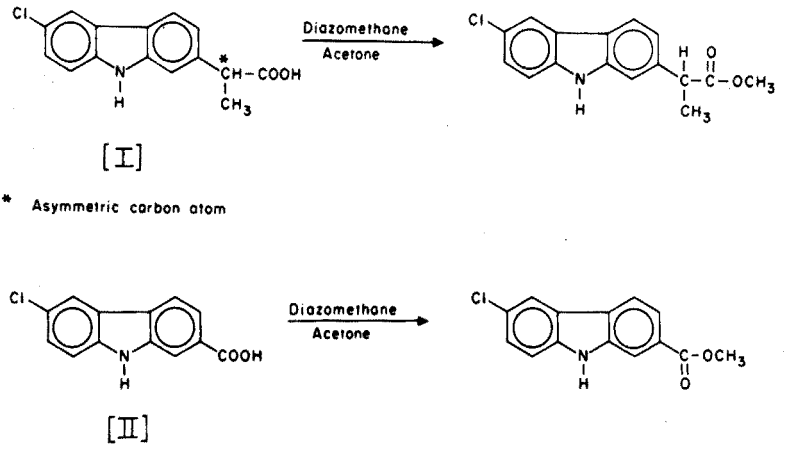

Fig. 1. Chemical reactions of compounds [I] and [II].

A sensitive and specific spectrofluorimetric assay was developed for the determination of the compound in blood and urine based on its intense intrinsic fluorescence in 1% acetic acid in ethanol (Fig. 2). The fluorescence is linear with concentration over the range of 0.05–10.0 μg/5 ml of 1% glacial acetic acid in ethanol. A thin-layer chromatographic step is used not only to impart specificity to the assay but also as a necessary clean-up step. The compound can also be determined by electron-capture gas chromatography of its methyl ester with the analogous compound, 6-chloro-2-carbazole carboxylic acid (II, Fig. 1) as the reference standard.

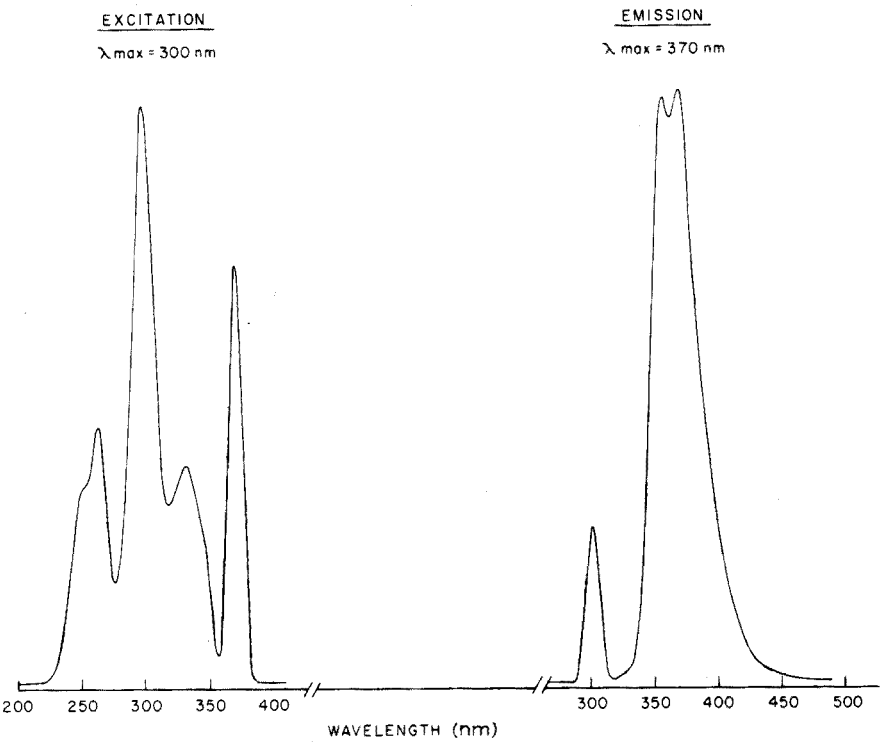

Fig. 2. Excitation and emission spectra of [I] in 1% glacial acetic acid in absolute ethanol. Concentration, 1·0 μg/5 ml. Attenuation, 10×.

The spectrofluorimetric assay was used in the determination of blood levels and the urinary excretion of [I] in a dog, and in toxicity studies of the compound in the rat and the dog[4].

EXPERIMENTAL

Spectrofluorimetric analysis

Analytical standard. Compound [I] $C_{15}H_{12}NO_2Cl$, m.w. 273.72, m.p. 192–194 °C, of pharmaceutical-grade purity (>99%) was used as the analytical standard.

Standard solutions. Prepare a stock solution (A) of compound [I] by dissolving 10 mg in 100 ml of methanol, and make a (1+9) dilution in methanol to yield a working solution (B) containing 10 μg [I] ml^{-1}. Suitable aliquots of solution (B) are added to blood or urine as internal standards.

Reagents. Prepare 1.0 *M* (pH 6.8–7.2) potassium phosphate buffer by mixing equal volumes of 1 *M* $K_2HPO_4 \cdot 3H_2O$ (228.23 g l^{-1}) and 1 *M* KH_2PO_4 (136.09 g l^{-1}). Mix well and check the final pH with a pH meter. Diethyl ether (Mallinckrodt, absolute analytical reagent), ethyl acetate (reagent grade) and a solution of 1% glacial acetic acid in absolute ethanol (1+99) as the solvent for fluorimetry are the other reagents used.

Analysis of blood. Into a 50-ml centrifuge tube add 1 ml of oxalated whole

blood, 5 ml of 1.0 *M* pH 6.8 potassium phosphate buffer and 10 ml of diethyl ether. Along with the unknowns run internal standards of 1.0, 5.0, and 10 μg of [I] (0.10, 0.50, and 1.0 ml of solution B evaporated to dryness under nitrogen) added to control blood. Extract all the samples by shaking on a reciprocating shaker for 10 min, centrifuge at 2000 r.p.m. for 10 min, transfer the supernatant ether extracts into 15-ml centrifuge tubes, and evaporate off most of the ether (to about 1 ml) under nitrogen in a 50°C water bath. Repeat the extraction with another 10-ml portion of ether, centrifuge, combine the ether extracts, evaporate the ether to dryness and dissolve the residues in 100 μl of chloroform. Transfer the chloroform extracts onto a 20×20 cm E. Merck [F_{254}]-60 μm silica gel chromatoplate. Rinse each tube with an additional 50 μl of chloroform and transfer to the t.l.c. plate to effect a quantitative transfer of the sample. Develop the plate for 15 cm ascending in a vapor saturated tank containing chloroform–diethylamine (90:10) to move the "lipids" away from the origin. Air-dry the plate, then redevelop in chloroform–ethanol–formic acid (90:10:5) to move the compounds. Compound [I] (R_F Ω 0.33) is identified by reference to the R_F of 10 μg of the authentic standard run alongside the sample extracts (Fig. 3A) as a dark u.v.-absorbing spot when viewed under short-wave u.v. radiation.

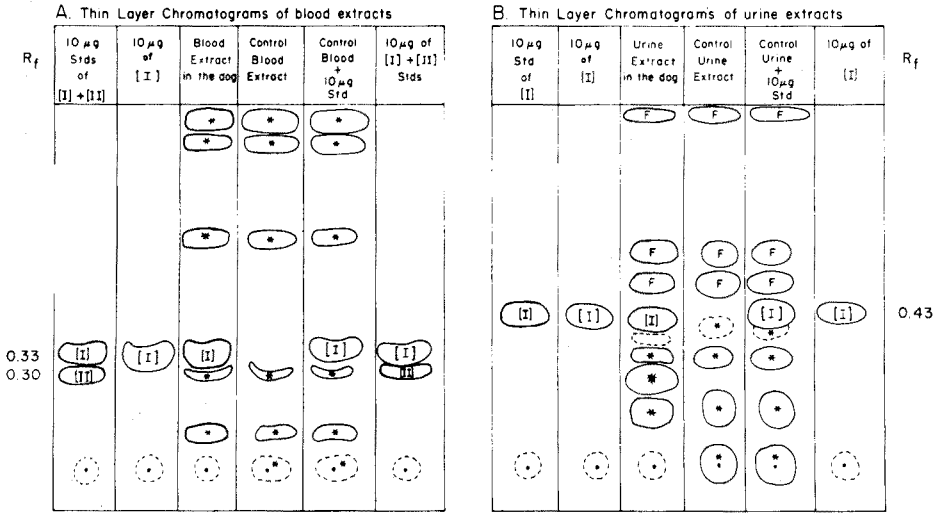

Fig. 3. Thin-layer chromatograms of (A) compound [I] recovered from blood and (B) [I] recovered from urine. Asterisked spots absorb under short-wave u.v. Spots marked F fluoresce under short-wave u.v.

Elute the silica gel areas containing [I] with 5 ml of 1% glacial acetic acid in ethanol by shaking for 5 min to effect complete elution. Centrifuge the samples and transfer the supernates quantitatively to fresh 15-ml tubes. Read the fluorescence of the solution in a 1-cm path cell at 370 nm, with excitation at 300 nm (Fig. 2). Any unknown sample whose fluorescence is greater than the 10-μg internal standard must be diluted (1+9) and re-read. The mean recovery of 0.5–10-μg amounts of internal standards of [I] was 85±5.0%.

Analysis of urine. Into a 50-ml centrifuge tube add 1 ml of urine and 5.0 ml of pH 6.8 buffer, and extract with 3 × 5-ml portions of ethyl acetate; then centrifuge and combine the ethyl acetate extracts by transferring successively into a 15-ml centrifuge tube, and evaporate in a water bath at 50°C under a stream of nitrogen. Along with the unknowns run internal standards of 1.0, 5.0, and 10.0 μg of [I] prepared as described in the assay in blood. Dissolve each residue in 100 μl of chloroform and transfer quantitatively onto a 20 × 20 cm E. Merck [F_{254}]-60 μm silica gel chromatoplate. Rinse each tube with 50 μl of ethanol to effect quantitative transfer. Develop the plate first for 15-cm ascending in a vapor-saturated tank containing acetone–ammonia liquor (100:1) to move extracted impurities from the origin. Air-dry the plate and redevelop in chloroform–ethanol–formic acid (90:10:5) to move the compound and any metabolites present. Compound [I] ($R_F \simeq 0.4$, Fig. 3B) is again identified as in the blood assay. Elute [I] and determine as described in the blood assay. The recovery of [I] from urine is similar to that from blood.

Calculations. All fluorescence readings (*TM*: transmittance *(T)* × meter multiplier factor *(M)*) are corrected for blood or urine blank readings and for any dilutions made.

(a) Concentrations of [I] in the unknowns are calculated either from the formula:

$$\frac{TM\,(\text{unknown})}{TM\,(\text{int. std.})} \times \frac{\text{conc. of int. std.}(\mu g)}{\text{ml of sample}} = \mu g\ [\text{I}]\ \text{ml}^{-1} \text{ of blood or urine}$$

or by interpolation from a calibration curve of the recovered internal standards.

(b) Recovery of [I] is obtained either from the slope of the calibration curve or by using the formula:

$$\frac{(TM/\mu g\ \text{ml}^{-1})\ \text{int. std.}}{(TM/\mu g\ \text{ml}^{-1})\ \text{ext. std.}} \times 100 = \%\ \text{recovery}$$

The percent recovery should be calculated routinely as a check on analytical precision and reproducibility.

Electron-capture gas chromatographic analysis of [I] in blood

Compound [I] is determined as its methyl ester after selective extraction from blood, thin-layer chromatographic separation as a clean-up step, and elution from the silica gel.

Preparation of the diazomethane reagent[5,6]. The reagent is prepared fresh weekly from N,N-nitrosomethylurea in a modification of a generator[6] which is used to distil the reagent into diethyl ether. The preparation is chemically pure and well suited for esterification of submicrogram amounts of carboxylic acids for e.c.–g.l.c. analysis[6].

The diazomethane generator (Fig. 4) consists of a 20 × 150 mm side-arm test tube with a 2-hole rubber stopper. Through one hole of the stopper is inserted a 50-ml separatory funnel with a teflon stopcock. Filtered nitrogen is delivered through an inlet of glass tubing which is bent and inserted through the other hole of the stopper to extend to the bottom of the generator.

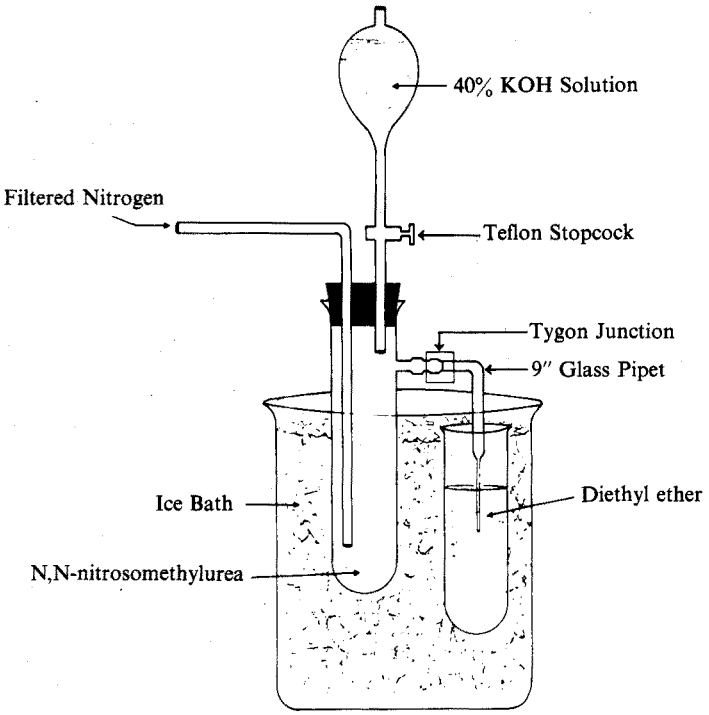

Fig. 4. Modified diazomethane generator[5].

Diazomethane formed in the generator is swept into diethyl ether through a bent glass capillary pipet connected to the side arm of the generator with tygon tubing. The generator is installed in a fume hood behind an explosion-proof shield.

Add 2.5 g of N,N-nitrosomethylurea to the generator and wash with 10 ml of diethyl ether, which is then aspirated off. Insert the rubber stopper to cap the generator and pass filtered nitrogen through the system for 30 s. Add 10 ml of ether-washed aqueous 40% potassium hydroxide solution to the separatory funnel. Partially immerse the generator in ice water (0–5°C), and immerse the delivery tube in 30 ml of fresh diethyl ether [Mallinckrodt, peroxide-free ($< 0.00005\%$) anhydrous analytical-reagent grade] contained in a 50-ml test tube.

Interrupt the flow of nitrogen momentarily and add the 40% hydroxide solution to the generator. Close the stopcock and allow the reaction to proceed for 5 min, then resume the nitrogen flow at a rate of 1–3 bubbles per s to sweep out the diazomethane produced in the generator into the diethyl ether. Transfer the "diazomethane reagent" in ether to a 50-ml centrifuge tube, stopper lightly with a teflon stopper and store in a freezer. The reagent must be handled with care as it is toxic, explosive, and degenerates on standing. Prepare fresh reagent weekly. When using the reagent, place the tube in an ice-water bath to arrest decomposition. Diazomethane prepared in this manner is free of extraneous impurities that are usually present in commercially available N,N-nitrosomethylurea which would otherwise contaminate the esterified sample.

Standards. In addition to compound [I], the analogous compound 6-chloro-2-carbazole-carboxylic acid [II] ($C_{13}H_8NO_2Cl$, m.w. 245.66, m.p. 328–329°C, Fig. 1) of pharmaceutical-grade purity (>99% was used as the reference standard for e.c.–g.l.c. analysis.

Standard solutions. Prepare separate stock solutions (A and A^1) of compounds [I] and [II] by dissolving 10 mg in 100 ml of methanol. Make serial (1+9) dilutions of these stock solutions in methanol to yield working solutions (B and B^1) containing 1.0 μg [I] and [II] ml^{-1}, respectively.

G.l.c. standard solutions. Prepare the following standard solutions by combining suitable aliquots of the working solutions (B and B^1) to contain 50, 100, 150 or 200 ng of [I], each containing 75 ng of [II] (reference standard). Evaporate the solutions to dryness and esterify by adding 0.5 ml of acetone to dissolve the residue followed by 0.5 ml of the diazomethane reagent, and mix well on a super mixer. React at room temperature for 15 min; then evaporate to dryness at 60°C under a stream of nitrogen.

After esterification, dissolve the residue of each sample in 100 μl of 20%

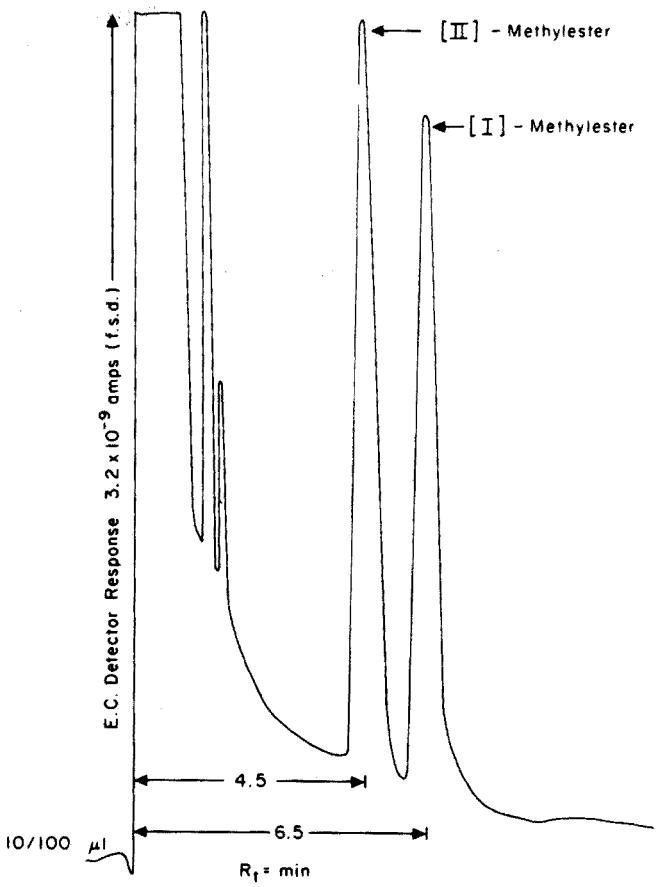

Fig. 5. Chromatograms of the e.c.-detector response to the methyl esters of [I] and [II] recovered from blood and analyzed on a 4-ft column of 3% OV-17 on Gas Chrom Q.

acetone–n-hexane solution and transfer the sample to a 200-μl conically tapered micro sample vial (Hewlett-Packard, Cat. No. 4330-0540), cap immediately with the silicone caps and seal by crimping the aluminum cover.

Inject 10-μl aliquots of these solutions for e.c.–g.l.c. analysis. A typical chromatogram is shown in Fig. 5. Establish a calibration curve of [I]–methyl ester using the conditions described below by plotting the peak-area ratio of [I]:[II] *vs.* concentration of [I] as shown in Fig. 6 to determine the linearity of the e.c.-detector response and the reproducibility of the esterification reaction. The non-zero intercept of the curve is probably due to incomplete esterification of [I] below 25 ng.

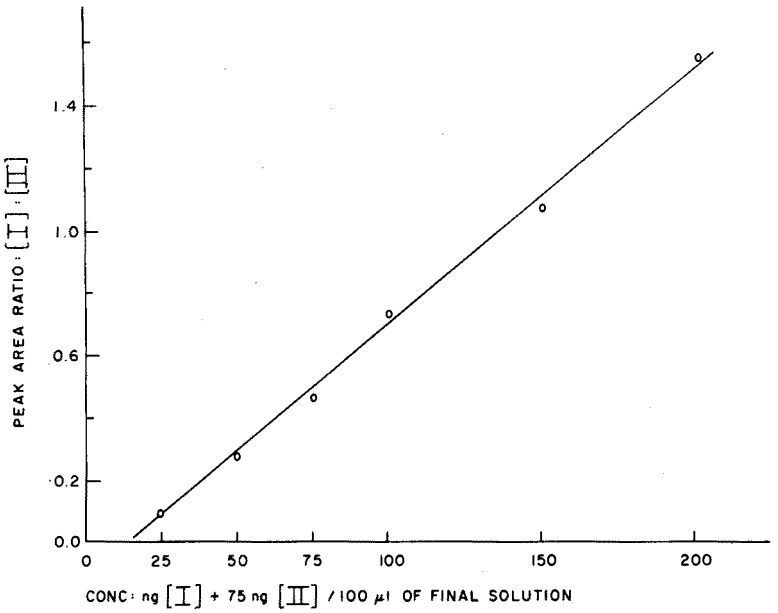

Fig. 6. E.c.–g.l.c. calibration curve of the peak area ratio of the methyl esters of [I]:[II] *vs.* concentration of [I] containing 75 ng of [II] as the reference standard.

Conditions for the e.c.–g.l.c. analysis of the methyl esters of [I] and [II].

A 4-foot, 4-mm i.d. borosilicate glass column containing 3% OV-17 on 60/80 mesh Gas Chrom Q (Applied Science Labs., State Park, Pa.) was used. The column was conditioned as previously described[7,8].

A Micro-Tek Gas Chromatograph, Model MT-220 equipped with a 15-mCi ^{63}Ni electron-capture detector was used. The carrier gas used was argon–methane (90:10) (Matheson), the column head pressure was 40 p.s.i.g. and the flow rate was 90 ml min^{-1} with the detector purge at 20 ml min^{-1}. The temperature settings were as follows: oven 240°C, injection port 280°C, detector 325°C. Under these conditions, the retention times of [I] and [II] were 6.5 min and 4.5 min, respectively (Fig. 5). The response of the solid-state electrometer (model 8169) was $3.2 \cdot 10^{-9}$ A for full-scale deflection (f.s.d.). The time constant on the 1.0-mV Honeywell recorder (Model 194) was 1 s (f.s.d.) and the chart speed was 30

in h^{-1}. The response of the ^{63}Ni e.c. detector (operated in the pulsed mode) to the methyl esters of [I] and [II] showed maximal sensitivity at 60 V d.c. with a 300-μs pulse rate and a 4-μs pulse width. Under these conditions 30 ng of [I] and 15 ng of [II] per 10/100 μl injected gave full-scale response on the 1.0-mV recorder. The sensitivity was 0.20–0.25 μg of [I] or [II]/ml of sample analyzed.

Analysis of blood. The extraction of a specimen of blood is carried out exactly as described in the fluorimetric assay along with separate internal standards of 250, 500, 750 or 1000 ng of [I], each containing 750 ng of the reference standard [II] added per ml of blood. Separate the residues of the ether extracts of blood on a 20×20 cm plate [E. Merck F_{254}-60 μm silica gel-G] by developing first in chloroform to move the lipid-like interferences up to the solvent front, followed by a second development in chloroform–ethanol–formic acid (95:5:3) to move the compounds to be analyzed. Scrape off compound [I] (R_F 0.35) and the reference standard [II] (R_F 0.30) together and co-elute with ethanol, the residue of which is dissolved in acetone and esterified with diazomethane. Dissolve the methyl esters of [I] and [II] in the final residue in 100 μl of 20% acetone–n-hexane, transfer to the micro-vials as previously described, and inject a 10-μl aliquot for e.c.–g.l.c. analysis. The methyl esters are eluted as completely resolved Gaussian shaped peaks on a 4-ft column of 3% OV-17 on Gas Chrom Q (60/80) (Fig. 5). The overall recovery of [I] and [II] by this procedure is of the order of 60–65%, and the sensitivity is 0.20–0.25 μg of [I]/ml of blood analyzed.

Calculations. The concentration of [I] present in the unknowns is determined by interpolation from the internal standard curve (Fig. 7).

RESULTS AND DISCUSSION

The intense u.v. absorption and luminescence properties of the carbazole class of compounds is well documented[9,10]. Consequently, compound [I] was examined in several solvents for its intrinsic u.v. absorption and luminescence properties. The u.v. absorption spectrum of [I] in methanol, showed a major absorption band at 237–238 nm with an absorptivity of about 194. Compounds [I] and [II] are weak acids and are quantitatively extractable below pH 7.0 into diethyl ether or ethyl acetate. Their extractability above pH 7.0, however, declines dramatically and they are not extracted at pH 14.0, owing to salt formation.

The intrinsic luminescence properties of [I] were examined visually, *in situ* on a silica gel thin layer plate, which was oversprayed with ethanol, immersed in a trough containing liquid nitrogen and examined under short and long-wave u.v. light. An intense blue-green fluorescence and a green-yellow phosphorescence was observed at 77°K at concentrations less than 50 ng of the compound. Although the fluorescence of [I] in ethanol at room temperature is weak, it is greatly enhanced in the presence of acid or alkali. The fluorescence of [I] in acid is more intense and stable than that in alkali. A solution of 1% glacial acetic acid in absolute ethanol showed optimal fluorescence and chemical stability for [I] and was preferred.

The excitation and emission spectra of [I] show several bands (Fig. 2) characteristic of carbazoles[9,10] and attest to the high degree of aromaticity of these molecules. The intense fluorescence of [I] ($TM/\mu g\ ml^{-1} = 1000$) and its linear

range of fluorescence, enables determination in the concentration range 0.05–10.0 μg of [I]/5 ml of 1% glacial acetic acid in ethanol. The sensitivity of the assay is of the order of 0.20–0.30 $\mu g\ ml^{-1}$ of blood or urine, and may be increased by extracting up to 4 ml of blood or 5 ml of urine per analysis.

The diacidic nature and polarity of these compounds necessitates derivatization of at least one functional group to render them sufficiently volatile for gas chromatographic analysis. The carboxylic acid group of these compounds is readily esterified with diazomethane[5,6] to produce methyl esters which yield well resolved symmetrical peaks on g.l.c. analysis with nanogram sensitivity to the electron-capture detector. Gas chromatographic analysis of these compounds with a ^{63}Ni electron-capture detector was investigated for extending the limits of detection below that of the fluorimetric assay; the analogous compound, 6-chloro-2-carbazole-carboxylic acid [II] (Fig. 1) was used as the reference standard. The assay involved the t.l.c. separation of the residue of a diethyl ether extract of blood buffered to pH 7.0 (as in the fluorimetric assay) to resolve the compounds of interest from lipid-like impurities to obtain optimal esterification, and further to ensure specificity. The esterification of varying amounts of authentic standards of [I] and [II] was apparently quantitative and reproducible.

After t.l.c. separation, compounds [I] and [II] (whose common R_F was 0.30–0.35) were scraped off together and co-eluted with ethanol; the residue was dissolved in acetone, esterified with diazomethane and analyzed by e.c.–g.l.c. The methyl esters of [I] and [II] were eluted as completely resolved Gaussian-shaped peaks on a 4-ft column of 3% OV-17 on Gas Chrom Q (60/80).

The poor overall recovery of [I] by this procedure of 60–65% was due to

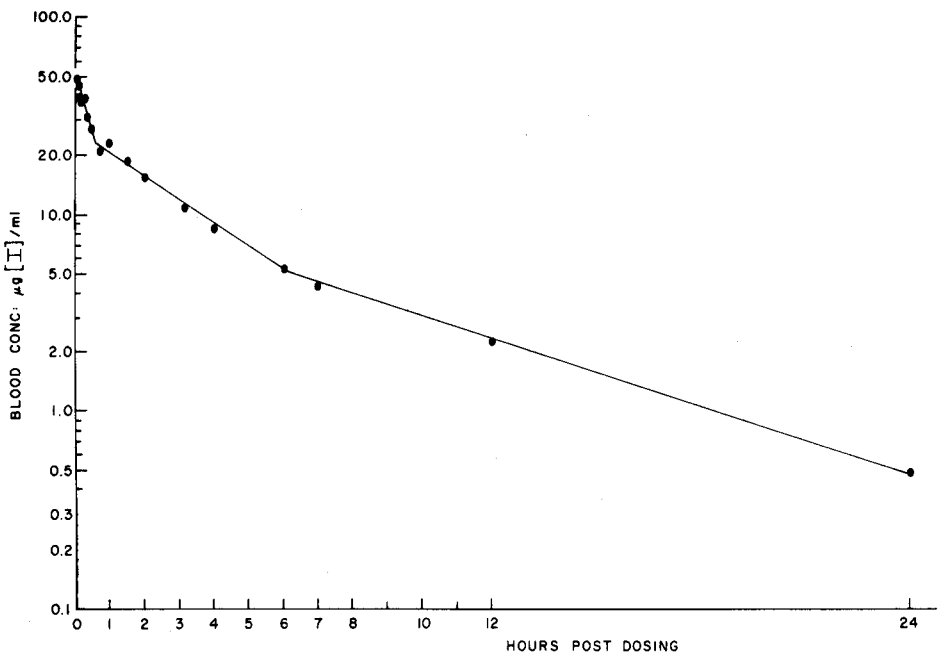

Fig. 7. Blood level fall-off curve of [I] in a dog after administration of a single dose.

impaired esterification because of the presence of trace amounts of lipid-like impurities from the extract which were co-eluted with the compounds; the sensitivity was 0.20–0.25 μg [I] ml^{-1} of blood. No significant improvement in sensitivity over that of the fluorimetric assay was therefore achieved by the e.c.–g.l.c. assay; consequently, the simpler fluorimetric assay was preferred.

Application of the spectrofluorimetric method to biological specimens

Blood levels and the urinary excretion of [I] were determined in a pilot study in a dog, after the intravenous administration of a 10 mg kg^{-1} dose. The blood level data are shown in Fig. 7. A triphasic fall-off curve was seen with blood levels ranging from 48.5 μg ml^{-1}, at 2 min after injection, to 0.50 μg ml^{-1} at 24 h.

The urinary excretion of [I] in the dog accounted for 6–8% of the dose in the 0–24-h excretion period. The drug levels were not measurable in the 24–48-h urine. Neither incubation with glucuronidase–sulfatase nor acid hydrolysis to deconjugate any hippurate-like conjugates yielded any measurable amounts of [I] as a conjugate.

SUMMARY

A sensitive and specific fluorimetric assay was developed for the determination of (*d,l*)-6-chloro-α-methyl-carbazole-2-acetic acid [I] in blood and urine, based on the intrinsic fluorescence of the compound in 1% acetic acid in ethanol. The compound can also be determined by gas chromatography based on the response of its methyl ester to electron-capture detection. A t.l.c. step is used in the assay, not only to ensure specificity, but also as a necessary clean-up step. The fluorimetric method was applied to the determination of blood levels and the urinary excretion of the compound in a dog after intravenous administration of a single 10 mg kg^{-1} dose.

REFERENCES

1 L. Berger, Unpublished data, Chemical Research Dept., Hoffmann-La Roche Inc., Nutley, N.J. 07110, 1972.
2 H. Baruth and L. O. Randall, *Fed. Proc. Fed. Amer. Soc. Exp. Biol.*, 33 (3) (1974) Abstract 1953.
3 W. R. Pool, D. L. Hane and G. K. S. Roberts, *Fed. Proc., Fed. Amer. Soc. Exp. Biol.*, 33 (3) (1974) Abstract 1952.
4 J. A. Cheripko, C. B. Coutinho and B. H. Min, *Fed. Proc., Fed. Amer. Soc. Exp. Biol.*, 33 (3) (1974) Abstract 1954.
5 A. H. Blatt in F. Arndt (Ed.), *Org. Synthesis Coll.*, Vol. 2, Wiley, New York, 1943, pp. 165–166.
6 M. J. Levitt, *Anal. Chem.*, 45 (1973) 618.
7 J. A. F. de Silva and C. V. Puglisi, *Anal. Chem.*, 42 (1970) 1725.
8 J. A. F. de Silva, I. Bekersky and C. V. Puglisi, *J. Chromatogr. Sci.*, 11 (1973) 547.
9 D. F. Bender, E. Sawicki and R. M. Wilson, Jr., *Anal. Chem.*, 36 (1964) 1011.
10 M. Zander in *Phosphorimetry*, Academic Press, New York, 1968, pp. 96–100.

Analytica Chimica Acta, 73 (1974) 293–300

THE SEPARATION OF PHENOL FROM DILUTE, ALKALINE AQUEOUS SOLUTION BY SOLVENT EXTRACTION, SOLVENT SUBLATION, AND FOAM FRACTIONATION

R. B. GRIEVES, W. CHAREWICZ* and S. M. BRIEN

Department of Chemical Engineering, University of Kentucky, Lexington, Ky. 40506 (U.S.A.)

(Received 3rd April, 1974)

Adsorptive bubble separation methods are effective in the removal and concentration from dilute aqueous solution of non-surface-active and weakly surface-active (such as phenol) ions and molecules by interaction with a surface-active agent; numerous analytical applications are included in a comprehensive review edited by Lemlich[1]. Foam fractionation of an ionic species relies principally on specific attraction to an oppositely charged surfactant, together with adsorption of the soluble ion pair at the gas–liquid interfaces of generated bubbles and carriage into the foam phase formed atop the bulk solution[2,3]. Solvent sublation is a method in which the ion pair or soluble complex (or even precipitate at sufficiently high concentrations), raised to the surface by gas bubble attachment, is extracted into a thin layer of a relatively immiscible organic solvent which has been spread on the surface of the bulk solution[4–8]. Solvent sublation may couple the mechanisms of foam fractionation and of solvent extraction. Depending upon the extent of mixing at the solvent–bulk aqueous solution interface, and also throughout the bulk solution, a greater amount of sublate (ion pair, soluble complex, or precipitate) may be removed from the bulk solution by solvent sublation than by solvent extraction, and there may be less dissolution of solvent into the aqueous phase than in the case of extraction. A molecular or ionized species which is too weakly surface-active to be separated by foam fractionation, owing to foam instability, may be effectively solvent-sublated even in the absence of a surfactant.

Phenol is an example of a weakly surface-active compound, the extent of ionization of which can be controlled with the pH of its aqueous solution. The pK value has been reported[9] as 9.9. Phenol is of significance as a water pollutant, causing severe taste and odor problems in very dilute solutions containing some chlorine. As a result, phenol analyses have to be conducted in quite dilute (frequently 10^{-8} M) solutions. Several extraction studies are reported[10–12], but all of these were performed in acidic solution. A variety of solvents was considered by Korenman[12] but he did not consider their solubility in the aqueous phase. Phenol has been foam-fractionated on a batch basis[13–15] and in a continuous flow foam fractionation unit[16]; all of the studies were carried out with a cationic

* Institute of Inorganic Chemistry and Metallurgy of Rare Elements, Technical University of Wroclaw, 50-370, Wroclaw, Poland.

surfactant and established the effects on the separation achieved of several operational and solution variables. Phenol has not been subjected to solvent sublation, perhaps the most promising technique of the three.

The objective of this study is a comparison of the solvent extraction, solvent sublation, and foam fractionation of phenol from $2.0 \cdot 10^{-4}$ *M*, neutral and alkaline solutions, with a quaternary ammonium surfactant, ethylhexadecyldimethylammonium bromide, and a satisfactory solvent, amyl acetate. Results from the three processes are compared on the basis of phenol removal from the aqueous phase, and mechanistic aspects of the three methods are discussed.

EXPERIMENTAL

The foam fractionation studies and solvent sublation studies were carried out in a Pyrex, batch foam separation unit, 4.3 cm in diameter and 80-cm high. Filtered and water-saturated air was dispersed through a sintered glass diffuser of 30–60-μm nominal porosity, at a flow rate of 0.030 l min^{-1} and with an average bubble size in the range 100–300 μm. The 0.50 l of initial solution volume provided an initial liquid height of 30.3 cm, and in the foam fractionation experiments the foam was removed at an initial height 7.0 cm above the initial solution height. The 0.50-l aqueous solution was $2.0 \cdot 10^{-4}$ *M* in phenol, 0–$2.0 \cdot 10^{-4}$ *M* in the quaternary ammonium surfactant, ethylhexadecyldimethylammonium bromide (EHDA-Br), and 0–0.10 *M* in added ionic strength, using NaOH and/or NaCl. In the solvent sublation experiments, a layer of an organic solvent, almost always amyl acetate and generally 0.050 l in volume, was pipetted atop the initial solution. The solvent was pre-saturated with water. At time equal zero the air flow was initiated and the experiment was continued until foam no longer was formed atop the bulk solution or solvent layer, which required *ca.* 2 h. Temperature was maintained at 23 ± 1.0°C.

The solvent extraction studies were conducted in 0.125-l cylindrical separatory funnels, with 0.050 l of aqueous phenol solution (as above) and 0.010 l of organic solvent. Seven solvents were used altogether; the best was amyl acetate which was employed in most of the experiments. Equilibrium extraction was achieved in a matter of minutes.

The residual aqueous solution, after foam fractionation, solvent sublation, or solvent extraction, was analyzed for phenol by a modified aminoantipyrene method[17] and for the surfactant (EHDA-Br) by a two-phase titration technique[18]. The aqueous phase was analyzed for amyl acetate dissolution by a Beckman total organic carbon analyzer, the carbon contribution of amyl acetate being determined by subtracting the known contribution of phenol. All reagents were analytical-reagent grade, with the exception of EHDA-Br which analyzed 97% on a bromide basis and *ca.* 93% on a carbon basis.

RESULTS AND DISCUSSION

Solvent extraction

A preliminary series of experiments was conducted to determine the most suitable solvent for phenol extraction. The pH of the initial aqueous solution was

LE I

VENT COMPARISON FOR EXTRACTION OF PHENOL FROM ALKALINE AQUEOUS SOLUTIONS

nt	*Mol. wt.*	*B.p.* (°C)	*Density* ($g\ ml^{-1}$)	*Solubility in* H_2O (wt.%)	*Initial phenol concentration* (*M*)	*Initial surfactant concentration* (*M*)	*Phenol removal* (%)
ene	78.1	80.1	0.88	0.18	$1.0 \cdot 10^{-4}$	$5.0 \cdot 10^{-4}$	21
ene	92.3	110.6	0.87	0.05	$2.0 \cdot 10^{-4}$	$1.0 \cdot 10^{-4}$	53
l alcohol	88.2	137.9	0.82	2.2	$1.0 \cdot 10^{-4}$	$5.0 \cdot 10^{-4}$	34
nol	130.2	195.2	0.82	0.03	$1.0 \cdot 10^{-4}$	$5.0 \cdot 10^{-4}$	73
ıtanone	86.1	101.7	0.81	6.0	$2.0 \cdot 10^{-4}$	$1.0 \cdot 10^{-4}$	53
opyl ether	102.2	67.5	0.78	1.2	$2.0 \cdot 10^{-4}$	$1.0 \cdot 10^{-4}$	17
l acetate	130.2	149.2	0.88	0.17	$1.0 \cdot 10^{-4}$	$5.0 \cdot 10^{-4}$	77
l acetate					$2.0 \cdot 10^{-4}$	$1.0 \cdot 10^{-4}$	67

11.0, the ionic strength was 0.1 *M*, the phenol concentration was either $2.0 \cdot 10^{-4}$ *M* or $1.0 \cdot 10^{-4}$ *M*, the EHDA-Br concentration was either $1.0 \cdot 10^{-4}$ *M* or $5.0 \cdot 10^{-4}$ *M*, and the phase volume ratio of solvent to water was 1:5. Results are given in Table I, which also includes the significant properties of the solvents. The extractions of phenol with benzene or 2-pentanone were poor, and the water solubility of amyl alcohol and isopropyl ether were excessive. The selection of amyl acetate over toluene was based on the improved extraction of phenol, in spite of the lower water solubility of toluene. The selection over octanol was based on the greater boiling point difference of amyl acetate from phenol (for solvent recovery) compared to the difference from octanol, and on the greater stability of esters compared to alcohols in alkaline aqueous solutions. Actually, either octanol, toluene, or amyl acetate would have been an acceptable choice.

At a constant initial phenol concentration of $2.0 \cdot 10^{-4}$ *M* (ionic strength 0.1 *M*, amyl acetate–water volume ratio 1:5, and in the absence of surfactant), the effect of pH on phenol extraction is presented in Fig. 1. The phenol removal

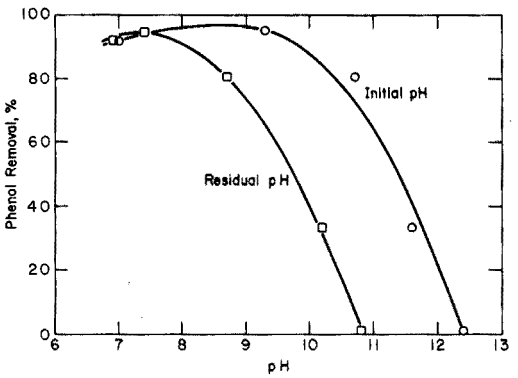

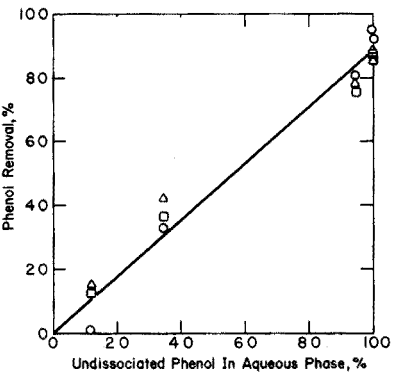

Fig. 1. Solvent extraction of phenol as a function of pH.

Fig. 2. Solvent extraction of phenol related to the calculated percent undissociated phenol present in the aqueous phase; in the absence (○) and in the presence of $1.0 \cdot 10^{-4}$ *M* (□) or $2.0 \cdot 10^{-4}$ *M* (△) ethylhexadecyldimethylammonium bromide.

is related to the initial pH_i (before extraction) and to the residual pH_r (after extraction). Removal of 80% or greater was achieved up to *ca.* pH_i 11 and then the removal fell off abruptly.

Two additional series of extraction experiments were carried out, the only difference from those in Fig. 1 being the presence of $1.0 \cdot 10^{-4}$ *M* or $2.0 \cdot 10^{-4}$ *M* surfactant. The surfactant was included to enable a comparison with solvent sublation and foam fractionation. The presence of surfactant caused a slight decrease in extraction removal at neutral pH (from 91 to 85%) and a modest increase at high pH: from 1 to 15% at pH_i 12.3, and from 32 to 42% at pH_i 11.7. The presence of surfactant in solutions with no added NaCl (with ionic strength varying with pH_i) improved the removal somewhat more.

The decline in removal with pH in Fig. 1, coupled with the fact that $pH_r < pH_i$, can be explained on the basis of high extractability of undissociated phenol and low extractability of sodium phenolate. Figure 2 presents the phenol removal *versus* the percent undissociated phenol present in the residual solution at pH_r (with $pK_{phenol} = 9.9$). A linear fit is good for zero, $1.0 \cdot 10^{-4}$, and $2.0 \cdot 10^{-4}$ *M* surfactant present. For an ideal situation of only undissociated phenol present in the solvent phase and no solvent–solute interaction in the aqueous phase (and at a constant phase volume ratio), it can be shown readily that phenol removal/(100 − phenol removal) should be linear with the undissociated phenol present at pH_r. Therefore the linearity of Fig. 2 could indicate solvent–solute interaction. The formation of a phenol–amyl acetate adduct,

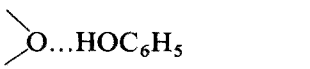

has been reported[19,20], together with a standard heat of formation[20] of −4.0 kcal $mole^{-1}$. Adduct formation would decrease with an increase in pH and could significantly influence the extraction behavior. The hydrolysis of amyl acetate in aqueous sodium hydroxide solution has also been reported[21].

In the extraction studies, the equilibrium solubility of amyl acetate in the aqueous phase was determined to be 0.0095 *M* over pH_i 7–11. The data for surfactant extraction scattered somewhat, ranging from 10 to 40% removal.

Solvent sublation

The results of the first series of solvent sublation experiments are given in Fig. 3. The ionic strength was 0.1 *M*, the amyl acetate volume was 0.050 l (atop the solution volume of 0.50 l), and no surfactant was present. The justification for the use of the 1:10 phase volume ratio (compared to 1:5 for extraction) is discussed below. The effects of pH were rather similar to those shown for extraction, except that the phenol removal was only about half of that obtained by extraction. The sharp decreases in pH during solvent sublation indicate that phenol was sublated as an undissociated molecule.

In contrast to the extraction results, Fig. 4 shows a significant effect of the presence of even a low ($0.2 \cdot 10^{-4}$ *M*) concentration of the surfactant EHDA-Br, for experiments at a constant pH_i of 10.7. This effect was evident both with 0.1 *M* ionic strength and with no NaCl added. The fact that the phenol removal did not bear a stoichiometric relation to the surfactant dosage shows that ion pairing

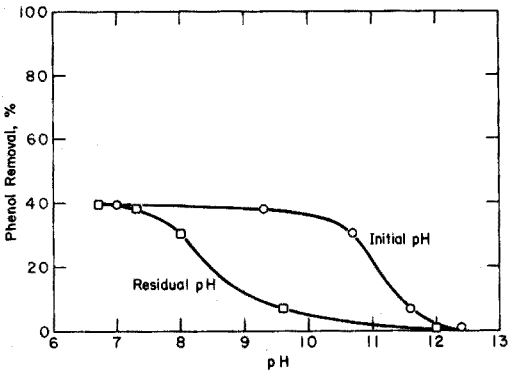

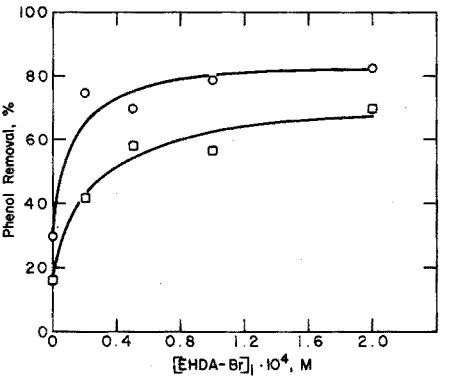

Fig. 3. Solvent sublation of phenol as a function of pH.

Fig. 4. Effect of initial surfactant concentration on the solvent sublation of phenol, at constant 0.1 *M* ionic strength (○) and at variable, low ionic strength (□). Initial pH, 10.7.

between phenolate and $EHDA^+$ was not significant in the sublation of phenol into the amyl acetate layer except possibly above pH_i 11.0. The surfactant may have facilitated the separation by promoting greater air–liquid interfacial area (per unit air rate), thereby promoting the adsorption of phenol at the bubble interfaces and the levitation of phenol to the top of the aqueous phase. Also the surfactant may have provided greater phase contact at the amyl acetate–water interface, promoting the extraction of the phenol–amyl acetate adduct. Solvent sublation was consistently more efficient at high ionic strength than at low ionic strength (note the two curves in Fig. 4), principally because of a salting-out effect.

Table II presents the influence of the amyl acetate phase to aqueous phase volume ratio on the solvent sublation of phenol at pH 9.3, ionic strength 0.1 *M*, and with the optimum surfactant concentration of $0.5 \cdot 10^{-4}$ *M*. For ratios from 1:20 to 1:10, an appreciable effect of the volume ratio was exhibited, in contrast to the results of other solvent sublation studies[6].

In the sublation experiments, the solubility of amyl acetate in the aqueous phase was determined to be 0.0056 *M*, only about half of the equilibrium value of 0.0095 *M* determined in the extraction studies. Again assuming the sublation of a phenol–amyl acetate adduct, the decreased concentration of amyl acetate in the aqueous phase may have brought about the reduced removal (*versus* extraction)

TABLE II

EFFECT OF PHASE VOLUME RATIO ON THE SOLVENT SUBLATION OF PHENOL AT pH_i 9.3

Organic to aqueous phase volume ratio	*Phenol removal (%)*
1:20	67
1:10	82
1:5	90

indicated in Fig. 3. The sublation of the surfactant ranged from 10 to 40% removal, being consistently somewhat greater than the removal of surfactant by extraction. This is in agreement with previous extraction–sublation studies[6,7], but the lower phenol removal in sublation *versus* extraction is in contrast to the behavior of the particular solutes investigated in those same studies.

Foam fractionation

The final series of experiments involved no extractant; the aqueous solutions were $2.0 \cdot 10^{-4}$ *M* in both phenol and surfactant and the ionic strength was either 0.1 *M* or was permitted to vary with pH (no NaCl was added). Results are presented in Fig. 5, *versus* pH_i ($pH_r \simeq pH_i$). At high ionic strength, the phenol removal was consistently poor because of chloride competition with the phenolate anions for ion pair formation with the surfactant cations ($EHDA^+$). The increased removal above pH 12 was due to the replacement of most of the chloride by hydroxide, presumably a poorer competitor with phenolate for $EHDA^+$.

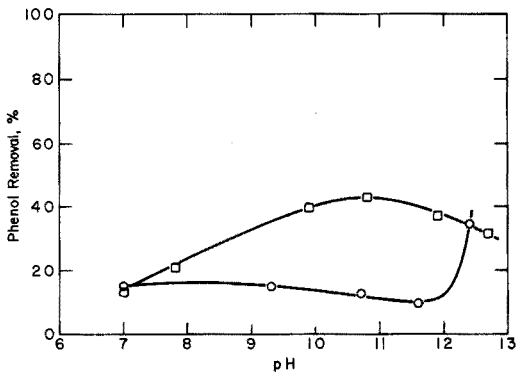

Fig. 5. Foam fractionation of phenol as a function of pH, at constant 0.1 *M* ionic strength (○) and at variable, low ionic strength (□).

At low (and variable) ionic strength, the increased phenol removal above pH 9 was evidently promoted by the dissociation of phenol, with ion pair formation with $EHDA^+$ increasing the removal from 25 to 40%. A small amount of undissociated phenol was foam fractionated at pH_i 7–8 due to the surface activity of phenol itself. The fact that the removal above pH 9 was 40%, instead of the much higher value that might be expected in the presence of the stoichiometric EHDA-Br concentration, was due to the competition of bromide (the surfactant counterion) with phenolate for $EHDA^+$. In the foam fractionation experiments, the foam volume (collapsed, as liquid) was only about 0.025 l.

The removal of surfactant was 65–80% with no added NaCl, and approximately 90% at an ionic strength of 0.1 *M*. The foam fractionation data for surfactant and phenol are generally in agreement with results reported previously[13–16].

CONCLUSIONS

Solvent extraction with amyl acetate provides 80–95% removal of phenol

from $2.0 \cdot 10^{-4}$ *M* aqueous solutions, at an ionic strength of 0.1 *M*, with a phase volume ratio of 1:5, and over the pH range 7.0–10.7. The presence of a cationic surfactant does not substantially modify the extraction behavior. A possible mechanism is phenol–amyl acetate adduct formation, with the formation (and extraction) dropping off abruptly above pH 11, although undissociated phenol should be extracted much more readily than sodium phenolate even in the absence of an adduct.

Phenol removals of the same order are achieved by solvent sublation, but the presence of approximately 1/4 the stoichiometric concentration of a cationic surfactant is required. Two advantages of solvent sublation over solvent extraction are: (1) the lower solubility of amyl acetate in the aqueous phase (owing to non-equilibrium conditions); (2) the requirement of a lower phase volume ratio. In solvent sublation, the extraction mechanism appears to predominate, with possible surfactant–phenol interaction only at pH 11 and above.

Ionic strength has a strong influence on foam fractionation, depressing the phenol removal from 40 to 12% over the pH range 10–12. Some undissociated phenol is removed by foam fractionation, but most of the removal is due to phenolate–surfactant cation ion pairing; the ionic strength effect is due to chloride competition with phenolate for the surfactant cations. Three decided advantages of foam fractionation over extraction and sublation are the high removal of surfactant, the elimination of the problem of organic solvent dissolved in the aqueous phase, and the concentration of phenol in a foam that is only 1/20th the volume (as liquid) of the aqueous phase. However, foam fractionation should be considered only for phenol solutions of low ionic strength.

SUMMARY

An experimental investigation is presented of the separation of phenol from aqueous $2.0 \cdot 10^{-4}$ *M* solutions over the pH range 7.0–12.3 at an ionic strength of 0.1 *M*. Extraction with amyl acetate provides 80–95% removal over pH 7.0–10.7, with the removal falling off sharply above pH 11.0. Solvent sublation, with a thin layer of amyl acetate atop the aqueous phase in a cylindrical foam separation column, results in equivalent removals, but about 1/4 of the stoichiometric (*versus* phenol) concentration of a quaternary ammonium surfactant is required. The advantages of sublation over extraction are non-equilibrium dissolution of the solvent in the aqueous phase and the use of a phase volume ratio lower than that for extraction. Foam fractionation, with the stoichiometric surfactant concentration, produces 40% removal over pH 10–12, but is strongly influenced by ionic strength. Possible mechanisms for extraction, sublation, and foam fractionation are suggested.

REFERENCES

1 R. Lemlich (Ed.), *Adsorptive Bubble Separation Techniques*, Academic Press, New York, 1973.
2 R. B. Grieves, D. Bhattacharyya and P. J. W. The, *Can. J. Chem. Eng.*, 51 (1973) 173.
3 W. Charewicz and R. B. Grieves, *J. Inorg. Nucl. Chem.*, in press.
4 F. Sebba, *Ion Flotation*, Elsevier, Amsterdam, 1962.
5 B. L. Karger, A. B. Caragay and S. B. Lee, *Separ. Sci.*, 2 (1967) 39.
6 B. L. Karger, T. A. Pinfold and S. E. Palmer, *Separ. Sci.*, 5 (1970) 603.

7 P. E. Spargo and T. A. Pinfold, *Separ. Sci.*, 5 (1970) 619.
8 I. Sheiham and T. A. Pinfold, *Separ. Sci.*, 7 (1972) 43.
9 E. A. Braude and F. C. Nachod, *Determination of Organic Structures by Physical Methods*, Academic Press, New York, 1955.
10 L. Coin and M. Mathis, *Eau*, 40 (1953) 61.
11 S. Kell and N. Vlasie, *Met. Constr. Masini*, 10 (1958) 104.
12 A. I. Korenman, *Tr. Khim. Khim. Tekhnol.*, 1 (1968) 118.
13 R. B. Grieves and R. C. Aronica, *Int. J. Air Water Pollut.*, 10 (1966) 31.
14 C. Jacobelli-Turi and M. Palmera, *Gazz. Chim. Ital.*, 113 (1966) 1432.
15 R. B. Grieves and R. C. Aronica, *Nature (London)*, 210 (1966) 901.
16 E. D. Ervin and R. P. Danner, *Separ. Sci.*, 8 (1973) 179.
17 *Standard Methods*, American Public Health Association, Washington, D.C., 1971.
18 J. T. Cross, *Analyst (London)*, 90 (1965) 315.
19 A. Aarna and L. Melder, *Tr. Tallin. Politekh. Inst., Ser. A*, (1962) 15.
20 D. G. Brown, R. S. Drago and T. F. Bolles, *J. Amer. Chem. Soc.*, 90 (1968) 5706.
21 A. I. Kravcenko and J. E. Penzova, *Zh. Obshch. Khim.*, 20 (1950) 20706.

Analytica Chimica Acta, 73 (1974) 301–309

CHROMOFOAMS* QUALITATIVE AND SEMI-QUANTITATIVE TESTS WITH CHROMOGENIC ORGANIC REAGENTS IMMOBILIZED IN PLASTICIZED OPEN-CELL POLYURETHANE FOAMS

T. BRAUN and A. B. FARAG

Institute of Inorganic and Analytical Chemistry, L. Eötvös University, 1443 Budapest P.O. Box 123 (Hungary)

(Received 31st May 1974)

This paper describes the work which has been carried out in an attempt to use open-cell polyurethane foams loaded with various organic reagents as new universal media for the detection of very low amounts of metal ions. The idea depends basically on the possible physical immobilization of hydrophobic organic solvents (especially plasticizers) containing different insoluble chromogenic organic reagents in the thin membranes and strands forming the foam material (Chromofoams). Shaking the produced loaded foams with aqueous solutions of metal ions allows the collection and detection of these ions on the proposed reagent foams. Insofar as the colour of the reaction products can be observed more easily on the relatively high surface area of the reagent foam membranes, the process allows the detection of very low amounts of metal ions in high volumes of their aqueous solutions in batch experiments. Also, the proposed reagent foams can be packed in suitable columns to produce foam beds which can be used for the detection and semiquantitative determination of metal ions from extremely dilute solutions. This may be achieved by passing a high volume of the test solution through the proposed foam bed, which functions as a collector for the metal ion to be detected, and by observing the length of the developed colour zone. The detection and semiquantitative determination of several metal ions with the proposed reagent foams have been examined in detail in both batch and column experiments.

EXPERIMENTAL

Static method

For the detection of metal ions by the static method, 1–2 ml of the test solution is mixed with one cube of the reagent foam (see below) in a normal test tube. The test tube is then shaken for 1–2 min and the colour change of the foam is observed.

For the semiquantitative determination of metal ions, a standard foam colour scale is prepared with standard solutions of different concentrations of the metal ion in question. The colour of the foam cube produced from the unknown solution is then compared with the standard colour scale.

* Patent pending.

Dynamic method

Glass columns of 5 mm diameter and 12 cm length are used.

A standard series of metal ion solutions of different concentrations is allowed to pass through previously prepared reagent foam columns at 10–15 ml cm^{-2} min^{-1} (100-ml solutions were used for each column but the volume can be increased as necessary). The aqueous solution of the unknown sample (100 ml) is allowed to pass through a reagent foam column under the same experimental conditions. The length of the colour zone, produced from the reaction of the metal ion in the aqueous solution and the reagent foam bed, is then compared with those of the standard series.

General reagents and materials

Except where otherwise mentioned, all the chemicals used were of analytical-reagent grade. α-Dinonyl phthalate (phthalic acid-di-3,5,5-trimethylhexylester, pure grade) was used without further purification. The polyurethane foam used was a polyether of open-cell type (North Hungarian Chemical Works, Sajóbábony, Hungary and Greiner-K.G. Schaumstoffwerk-Kremsmünster, Austria). The volume weight of the Austrian foam was 30 kg m^{-3}. The foam (cubes of about 4 mm edge) was washed with 1 *M* hydrochloric acid followed by distilled water until the washings were free from chloride ion. Then the foam material was washed with acetone and dried at 80°C.

Stock solutions (1 mg ml^{-1}) of zinc(II), lead(II) and copper(II) were prepared by dissolving zinc sulphate, lead nitrate and copper sulphate in distilled water, respectively. The stock solution of cobalt(II) was prepared by dissolving its chloride salt in 0.01 *M* hydrochloric acid. All the solutions were standardized titrimetrically by EDTA. Series of standard zinc, lead or copper solutions were prepared by diluting the stock solutions of these elements with water. The standard series of cobalt(II) solutions was prepared by diluting the stock solution with 0.01 *M* hydrochloric acid. All the solutions were stored in polyethylene bottles.

For the purpose of studying the influence of various cations and anions on the detection of cobalt with Amberlite LA-1 foam, stock solutions of various metals were prepared from their nitrates, chloride or sulphate, so as to contain 10–50 mg of each cation per ml. To avoid hydrolysis of metal ions, the salts were dissolved in dilute acids. Stock solutions of anions were prepared from their alkali or ammonium salts.

A 50%(v/v) Amberlite LA-1 (N-dodecyl-(trialkylmethyl)amine, BDH Laboratory reagent) solution was prepared in α-dinonyl phthalate. The solution was conditioned by washing successively with 0.3 *M* nitric acid, distilled water, aqueous 0.1 *M* sodium hydroxide to convert to the hydroxide form, and finally with 0.1 *M* hydrochloric acid to convert to the chloride form. Water purified by distillation and cellulose ion exchange was used throughout the work. Dithizone solution was prepared by dissolving 0.05 g of dithizone (Merck) in 100 ml of α-dinonyl phthalate. The saturated rubeanic acid (Merck) solution was prepared by dissolving the solid reagent in α-dinonyl phthalate (the concentration of rubeanic acid is less than 0.1%).

Reagent foam preparation

The dried foam cubes (white coloured foam was used whenever possible) are equilibrated with the required reagent solution (3 ml g^{-1} dry foam) with efficient stirring, and then allowed to remain in contact with the solution for about 1 h to ensure complete saturation. The loaded foam material is then dried between two sheets of filter paper to remove the excess of the reagent solution. The colours of the dithizone, rubeanic acid and Amberlite LA-1 foams are green, yellow and white, respectively.

Column preparation

The loaded foam material (0.5 g) is packed into the column by applying gentle pressure with a glass rod. To avoid bubbles during packing, air should be withdrawn with a suction pump. After about 2 min of evacuation, distilled water is allowed to fill the column gradually through the funnel tap.

RESULTS AND DISCUSSION

Preliminary experiments on plastic foams commercially available here (PVC, viscose, rubber and polyurethane), concerning chemical resistance towards acids, bases and organic solvents, and also the hydrodynamic properties of columns packed with them, showed that polyurethane foam (polyether of open-cell type) is the most appropriate. Consequently, this foam material was subjected to more thorough examination.

Polyurethane foam was found to retain a considerable amount of various organic solvents by swelling; the organic solvents are firmly retained in the produced swollen foam. Thus the foam material can be loaded with various organic reagents simply by dissolving these organic reagents in the hydrophobic organic solvent before allowing the foam material to swell in the latter. With this method, it was possible to immobilize chloroform or carbon tetrachloride solutions of, *e.g.*, dithizone on or in polyurethane foam. Although this method was successful in the preparation of several reagent foams, yet the rapid volatilization of the solvent (carbon tetrachloride or chloroform) affected the homogeneity of the loaded foam, because of precipitation of the solid reagent on the external surfaces of the foam material. Obviously, this would have serious draw-backs in application of the reagent foams, especially in semiquantitative analysis which requires homogeneous distribution of the reagent in the foam matrix.

Attention was therefore directed towards the possibility of using non-volatile organic solvents (*e.g.* α-dinonyl phthalate) for dissolving the organic reagent and loading the foam material. It was found that polyurethane foam retains α-dinoyl phthalate firmly by swelling, and that the swollen foam contains 65–70% (w/w) of this organic solvent. At the same time, several hydrophobic organic reagents could be dissolved in α-dinonyl phthalate to a considerable extent, *e.g.* dithizone, rubeanic acid and Amberlite LA-1. Accordingly, it was possible to prepare several reagent foams by means of this non-volatile organic solvent. The prepared reagent foam was found to retain both the solvent and the reagent firmly, so that no leaching of the organic reagent solution occurred on shaking the loaded foam with aqueous solutions of various acid concentrations (up to 2 *M* hydrochloric acid) for more than 1 h.

It is worth mentioning that α-dinonyl phthalate not only serves as a non-volatile solvent for the organic reagents but also as a plasticizer for the foam material. Plasticizers are defined as essentially non-volatile liquids used to modify synthetic resins[1]; plasticizer molecules reduce the secondary valence forces (Van der Waals) between the polymeric chains, thus increasing the mobility of the molecular segments and decreasing the glass transition temperature of the system. Above the glass transition temperature the mobility of plasticizer molecules within the polymeric network may be quite high[2]. The plasticized resin is generally considered as a dynamic system in which the individual plasticizer molecules have varying degrees of mobility within the resin matrix[1]. Actually, plasticizers are generally employed for controlling the physical properties of synthetic resins, *e.g.* flexibility, rigidity, etc.

Recently, however, considerable attention has been directed towards the application of plasticizers in the so-called "solvent membranes"[3–5]; it has been reported that the diffusion of ions through the membrane is enhanced by the plasticizer[6]. Similar effects may be present in the case of plasticized reagent foam; rapid attainment of equilibrium between the metal ion in the aqueous solution and the organic reagent in the foam was expected, owing to the enhanced solid-phase mass transfer.

The sensitivity of spot tests can often be increased by shaking the aqueous solution of metal ions with water-immiscible organic solutions[7]. Obviously, it would be advantageous to render the organic solution immobile by retention on or in a solid foam support, because the liquid–liquid extraction process can be replaced by a batch liquid–solid extraction. In the latter case, the organic reagent solution, which is homogeneously distributed on the relatively high surface area of the foam material, can function as an effective collector for traces of metal ions from relatively high volumes of aqueous solution. This can be achieved simply by shaking one or more cubes of the reagent foam with the aqueous solution of metal ion in a normal test tube. This can allow the detection of traces of metal ions in more than 1 ml of their aqueous solutions, which may significantly improve the sensitivity and dilution limit of the usual spot reactions.

A further advantage of the proposed reagent foams is that they can be easily packed in columns, which provide good hydrodynamic properties. These columns can be used for the retention of metal ions in dynamic experiments. A column technique which is originally based on a series of successive equilibrations between the metal ion in the aqueous solution and the organic reagent on or in the foam support is generally considered to have advantages over liquid–liquid or liquid–solid extraction processes. Low concentrations of metal ions can be collected from high volumes of aqueous solutions by passing the aqueous solution through the proposed reagent foam columns; this is basically a multistage extraction technique. Observation of the change of colour of the foam bed, which is due to reaction of the collected metal ion with the reagent foam, can serve as a test for the semiquantitative analysis of extremely dilute solutions.

In order to examine the practical utility of the proposed plasticized reagent foams for the detection and semiquantitative determination of metal ions in batch and column experiments, the following examples are investigated in comparison with the usual spot tests.

Static technique

Detection and semiquantitative determination of zinc(II) with dithizone foam cubes. Diphenylthiocarbazone (dithizone) forms highly coloured chelates with numerous metal ions[8]. These chelates are insoluble in water but easily soluble in many organic solvents. Dithizone forms a primary complex[9] with zinc(II) in neutral solution and it was proved that this complex is extractable in α-dinonyl phthalate. When the zinc–dithizone reaction is carried out on foam material by mixing a cube of α-dinonyl phthalate–plasticized dithizone foam with 1 ml of an aqueous solution of zinc(II) at pH *ca.* 6.2, 0.05 μg of zinc can be detected by the red colour which appears on the foam after shaking for 1–2 min. A comparison with the results reported[7] with the usual spot tests shows that the proposed foam test is more sensitive (Table I).

TABLE I

SENSITIVITY OF TESTS FOR ZINC(II) WITH DITHIZONE

Method	*Amount of zinc detected (p.p.m.)*	*Ref.*
Spot-test on spot plate	1	7, p. 513
Spot-test with dithizone(CCl_4)-impregnated paper	8	7, p. 513
Dithizone foam cubes	0.05	Present work

The semiquantitative determination of zinc with the dithizone foam was possible by comparing the colour which appears on a dithizone foam cube added to 1 ml of the unknown solution, with a standard foam colour scale (0.5, 1, 10 and 100 p.p.m.).

Detection and semiquantitative determination of lead(II) with plasticized dithizone foam cubes. Dithizone forms a primary red complex with lead(II) in neutral solution[10]. Detection of lead with the previously described dithizone foam test is possible. As little as 0.25 p.p.m. of lead can be detected by the change of the foam colour from green to brick-red. This result is slightly better than that reported[7] (0.8 p.p.m.) by the usual spot test with one drop of the lead solution and one drop of a carbon tetrachloride solution of dithizone. With the foam test, lead can be determined semiquantitatively by comparison with a standard colour scale (0.25, 1, 10 and 100 p.p.m.).

Detection and semiquantitative determination of copper(II) with rubeanic acid foam cubes. Copper(II) in ammoniacal or weakly acidic solutions reacts with alcoholic solutions of rubeanic acid (dithiooxamide) to form a dark green, nearly black, chelate, which can be used to identify copper[7]. In the present work, rubeanic acid solution in α-dinonyl phthalate was immobilized on polyurethane foam cubes and this foam was tested for the detection of copper from ammoniacal solution. It was found that as little as 0.5 p.p.m. copper can be detected by shaking 1 ml of the copper solution with one cube of rubeanic acid foam for 1–2 min. This sensitivity is very similar to that reported with rubeanic acid-impregnated paper (0.4 p.p.m.)[7]. Again, the semiquantitative determination of copper

was also possible with the proposed foam test. The standard colour scale covered the range 0.5, 1, 10 and 50 p.p.m.

Detection and semiquantitative determination of cobalt(II) with Amberlite LA-1 foam cubes. The above examples show that the foam tests are generally at least as sensitive as the usual spot tests. The present example represents a more comprehensive comparison between the proposed foam test and the resin spot test method[11], with the detection of cobalt(II) as a model.

Cobalt(II) ions form a pink-coloured thiocyanate complex which can be extracted as a blue complex with amines and long chain ammonium salts[12]. Fujimoto and Nakatsukasa[11] examined the detection of cobalt in the presence of thiocyanate solution using various concentrations of liquid anion exchanger (Amberlite LA-1) in carbon tetrachloride. They claimed that 5 p.p.m. of cobalt can be detected with a 5% solution of Amberlite LA-1 in carbon tetrachloride, or with Amberlite LA-1-impregnated paper, these tests being regarded as modifications of the resin-spot method.

In the present work, the rapid detection of as little as 0.3 p.p.m. cobalt in slightly acidic thiocyanate solution was possible with Amberlite LA-1 foam cubes. Also, the semiquantitative determination of cobalt was possible with a standard colour scale based on 0.5, 2.5, 25, 50, 250 and 500 p.p.m. cobalt.

It is worth mentioning that the sensitivity of the proposed foam test for cobalt is not only better than that of the resin-spot method but also superior to the commercially available Merckoquant stick (see Table II). The cobalt foam test was satisfactory in the pH range 1–6.

TABLE II

SENSITIVITY OF COBALT DETECTION BY VARIOUS METHODS

Method	*Amount of cobalt detected (p.p.m.)*	*Note*
Resin-spot test method with strongly basic anion-exchange resin beads	5	Colour appears after 1 h[11]
Modified resin-spot test with Amberlite LA-1 impregnated paper	5	
Modified resin-spot test with Amberlite LA-1 in CCl_4	5	Colour appears after 10 min[11]
Merckoquant cobalt test	10	
Amberlite LA-1 foam cubes	0.3	Colour appears after 1–2 min

The effects of foreign ions on this detection of cobalt were studied as an example for the selectivity of the proposed foam test. The selectivity of the foam test for cobalt was quite good (Table III).

Dynamic technique

The hydrodynamic properties of columns packed with reagent foams was

ABLE III

FECT OF DIVERSE IONS ON THE DETECTION OF 1 μg OF COBALT(II)

cept where mentioned otherwise, the colour of the foam in a blank test was white. In case of ions which erfere by their own colours in solution, it was found better to take out the foam cube (after shaking with the t solution) and to shake it with few ml of water. The blue colour, which appears in the presence of balt(II), was then better observed.

reign ion	*Compound added*	*Amount added (mg)*[a]	*Vol. of aq. soln. (ml)*	*Cobalt: foreign ion*	*Notes*
tions forming thiocyanate complexes					
(II)	$Fe(NH_4)_2(SO_4)_2$	1.0	2	$1:1.0\cdot10^3$	One drop of satd. KF soln. added
(III)	$FeCl_3$	2.0	3	$1:2.0\cdot10^3$	1 ml satd. KF soln. added
(II)	$CuSO_4$	2.0	3	$1:2.0\cdot10^3$	Traces of solid KI and $Na_2S_2O_3$ added
(II)	$Pb(NO_3)_2$	40.0	2	$1:4.0\cdot10^4$	White ppt. formed, but did not interfere
n(II)	$MnSO_4$	4.0	2	$1:4.0\cdot10^3$	Yellow foam in blank
(II)	$CdSO_4$	4.0	2	$1:4.0\cdot10^3$	
(II)	$Ni(NO_3)_2$	1.0[b]	2	$1:1.0\cdot10^3$	Pale green foam in blank
(I)	$AgNO_3$	10.0	2	$1:1.0\cdot10^4$	
I)	Tl_2SO_4	20.0	3	$1:2.0\cdot10^4$	White ppt. formed
(II)	$Hg(NO_3)_2$	2.0	2	$1:2.0\cdot10^3$	
III)	$Bi(NO_3)_3$	2.0	2	$1:2.0\cdot10^3$	White ppt. formed
(III)	$AuCl_3$	1.0[b]	2	$1:1.0\cdot10^3$	Pale orange foam in blank
ions forming cobalt(II) complexes					
O_3^{2-}	$Na_2S_2O_3$	20.0	3	$1:2.0\cdot10^4$	
alate	$Na_2(COO)_2$	5.0	2	$1:5.0\cdot10^3$	
tate	CH_3COONa	20.0	3	$1:2.0\cdot10^4$	
trate	$KHC_4H_4O_6$	10.0	2	$1:1.0\cdot10^4$	
her ions					
(II)	$BaCl_2$	20.0	3	$1:2.0\cdot10^4$	
(II)	$CaCl_2$	20.0	3	$1:2.0\cdot10^4$	
(II)	$MgCl_2$	20.0	3	$1:2.0\cdot10^4$	
II)	$Sr(NO_3)_2$	20.0	3	$1:2.0\cdot10^4$	
IV)	$Ce(SO_4)_2$	1.0	2	$1:1.0\cdot10^3$	Yellow foam in blank
IV)	$Zr(SO_4)_2$	2.0	2	$1:2.0\cdot10^3$	
(I)	RbI	20.0	3	$1:2.0\cdot10^4$	
I)	LiBr	2.0	3	$1:2.0\cdot10^3$	
III)	As_2O_3	2.0	2	$1:2.0\cdot10^3$	
III)	$KCr(SO_4)_2$	1.0[b]	2	$1:1.0\cdot10^3$	Violet foam in blank
O_3^-	NH_4VO_3	7.0[b]	2	$1:7.0\cdot10^3$	Satd. KF soln. (0.1 ml) added. Yellow foam in blank
O_4^{2-}	Na_2WO_4	5.4	3	$1:5.4\cdot10^3$	
O_3^{2-}	Na_2SeO_3	16.0	2	$1:1.6\cdot10^4$	
HO_4^{2-}	Na_2HPO_4	16.0	2	$1:1.6\cdot10^4$	
	KBr	20.0	3	$1:2.0\cdot10^4$	
O_4^-	$NaClO_4$	20.0	3	$1:2.0\cdot10^4$	
	KI	20.0	3	$1:2.0\cdot10^4$	

(continued)

TABLE III (*continued*)

Foreign ion	*Compound added*	*Amount added (mg)*[a]	*Vol. of aq. soln. (ml)*	*Cobalt:foreign ion*	*Notes*
$S_2O_5^{2-}$	$K_2S_2O_5$	20.0	3	$1:2.0\cdot10^4$	
ClO_3^-	$NaClO_3$	20.0	3	$1:2.0\cdot10^4$	
SO_3^{2-}	Na_2SO_3	20.0	3	$1:2.0\cdot10^4$	
$S_2O_8^{2-}$	$K_2S_2O_8$	1.0	2	$1:1.0\cdot10^3$	
MnO_4^-	$KMnO_4$	2.0[c]	2	$1:2.0\cdot10^3$	
F^-	NaF	20.0	3	$1:2.0\cdot10^4$	
BrO_3^-	$KBrO_3$	20.0	3	$1:2.0\cdot10^4$	
ascorbate	L-ascorbic acid	20.0	3	$1:2.0\cdot10^4$	

[a] The amount of the foreign ion below which the detection of 1 μg of cobalt can easily be achieved.
[b] Value obtained by comparison with a blank test.
[c] 0.5 ml 1 *M* HCl and 1 ml $Na_2(COO)_2$ (10 mg ml^{-1}) added, and mixture heated to *ca.* 80 °C. After cooling, 1 ml KSCN solution added; cobalt is then detected as usual with reagent foam.

found to be extremely favourable. Flow-rates as high as 15 ml cm^{-2} min^{-1} can be easily attained by gravity flow. These properties together with the known advantages of multistage operation with columns make the reagent foam columns very favourable for the detection of very low concentrations of metal ions in extremely dilute solutions. However, it should be noted that the preparation of foam columns requires some technical skill in order to obtain homogeneous beds.

Semiquantitative determination of cobalt on Amberlite LA-1 foam columns. Columns packed with 0.5 g of Amberlite LA-1 foam were used for the detection of cobalt(II) in solutions which contained 2% (w/v) potassium thiocyanate adjusted to pH 2–4. The length of the colour zone formed in the column is proportional to the concentration of cobalt in the aqueous solution. This colour scale was successfully used for the semiquantitative determination of cobalt in the range 50–500 p.p.b. The detection of 5 μg of cobalt(II) in 1 l of aqueous solution (*i.e.* 5 p.p.b.) was possible when the aqueous solution was percolated through the foam column at 10 ml cm^{-2} min^{-1}. Thus the scope of application of the foam test can be increased to cover p.p.b. concentrations. Solutions more dilute than 5 p.p.b. could be analyzed by passing higher volumes of the aqueous solution through the foam column.

Semiquantitative determination of copper(II) on rubeanic acid foam columns. As in the case of cobalt, as little as 5 p.p.b. copper(II) can be detected by percolating 1 l of the copper solution through a rubeanic acid foam column at a flow-rate of 10–15 ml cm^{-2} min^{-1}. Semiquantitative determination of copper is possible by using a standard scale of 20, 100, 200, 300 and 400 p.p.b.

Semiquantitative determination of lead(II) on dithizone foam columns. Dithizone foam columns were used for the semiquantitative determination of lead-(II). The colour scale covered 50, 100, 200, 300, 400 and 500 p.p.b.

SUMMARY

Polyurethane foams treated with organic reagents in a plasticizer solution can be used for simple, rapid, sensitive and selective detection and semiquantitative determination of metal ions from dilute aqueous solutions. Batch techniques can be used for simple tests which provide sensitivity as good as, or better than, that attainable by normal spot tests. The application of reagent-treated foam columns for the detection and semiquantitative determination of metal ions from extremely dilute aqueous solutions is advantageous; ions in the p.p.b. range can be detected after passage of 1 l of solution at a fast rate. The use of these techniques for zinc(II) and lead(II) with dithizone, copper(II) with rubeanic acid, and cobalt(II) with thiocyanate–Amberlite LA-1, is described.

REFERENCES

1 J. Frados and S. Gross (Eds.), *Modern Plastics Encyclopedia*, Vol. 45, McGraw-Hill, New York, 1968, p. 428.
2 R. Kosfeld in R. F. Gould (Ed.), *Plasticization and Plasticized Processes*, American Chemical Society, Washington, D.C., 1956, p. 43.
3 R. Bloch, A. Finkelstein, O. Kedem and D. Vofsi, *Ind. Eng. Chem., Process Des. Develop.*, 6 (1967) 231.
4 J. Jagur-Grodzinski, S. Marian and D. Vofsi, *Separ. Sci.*, 8 (1973) 33.
5 S. Lal and G. D. Christian, *Anal. Chem.*, 45 (1971) 410.
6 G. D. Christian and G. L. Stucky, *Amer. Lab.*, Oct. 1970.
7 F. Feigl and V. Anger, *Spot Tests in Inorganic Analysis*, Elsevier, Amsterdam, 6th ed., 1972.
8 A. K. De, S. M. Khopkar and R. A. Chalmers, *Solvent Extraction of Metals*, Van Nostrand–Reinhold, London, 1970.
9 D. Monnier and G. Prod'hom, *Anal. Chim. Acta*, 30 (1964) 358.
10 S. S. Cooper and J. O. Hibbits, *J. Amer. Chem. Soc.*, 75 (1953) 5084.
11 M. Fujimoto and Y. Nakatsukasa, *Anal. Chim. Acta*, 27 (1962) 373.
12 H. Watanabe and K. Akatsuka, *Anal. Chim. Acta*, 38 (1967) 547.

Analytica Chimica Acta, 73 (1974) 311–319

SELECTIVE SEPARATIONS BY REACTIVE ION-EXCHANGE WITH COMMON POLYSTYRENE-TYPE RESINS*

PART I. GENERAL CONSIDERATIONS

GILBERT E. JANAUER, GEORGE O. RAMSEYER and JOYCE W. LIN
Department of Chemistry, SUNY-Binghamton, New York 13901 (U.S.A.)
(Received 14th May 1974)

The eternal quest for superior selectivity has led to some spectacular advances in the area of novel ion-exchange materials "tailor-made" for specific problems. However, the fact remains that, for obvious practical reasons, the polystyrene-type resins (microporous and macroporous) will continue to constitute a major fraction of all exchangers to be made and used for some years to come.

High selectivity is not easy to attain with the common resins, but the presence of complexing ions and/or the introduction of a second solvent component often enhance intrinsic selectivity differences for the species to be separated[1–4]. The use of chelating agents in conjunction with common resins has been very successful where applicable, and chelating ion-exchange resins have shown much potential for selective separations of heavy metal ions[5]. Other reactions can also be combined with ion exchange. Thus, some interesting studies of redox systems have earlier been made[6,7] and the principle of "redox ion exchangers" was discussed in detail by Helfferich[4]. Neutralization reactions involving weakly acidic and basic resins are quite common. The formation of a precipitate on an ion exchange column has been utilized by Ruch *et al.*[8] for trace concentrations. The fact that counterions from several resins can simultaneously participate in reactions with each other and/or with species present in solution is being exploited in the mixed-resin-bed demineralization of water and, occasionally, in the dissolution of sparingly soluble solids[4]. Reactions of colored complexes on ion-exchange resins have been proposed as a means for the colorimetric determination of metal ion traces[9]. Recent results obtained in this laboratory[10–12] have successfully demonstrated with several different reaction types the tremendous practical potential of procedures that can all be taken as examples of a general category for which we have introduced the term "reactive ion-exchange"[10]. In this context it should be mentioned that reactive steps combined with ion-exchange are of considerable interest in the theoretical treatment of ion-exchange rates. Helfferich[13] has discussed the effect of "accompanying reactions" on the rates of ion-exchange processes and has mentioned *e.g.*, the cases of hydrolysis, neutralization, and complex formation as distinguished from the simple case when "the overall process is exclusively a

* This paper was presented in part at the 168th National Meeting of the American Chemical Society, Division of Analytical Chemistry, Atlantic City, September 13th, 1974.

redistribution of counter-ions" and "the exchanging ions retain their identity".

In view of the considerable number of different reactions which might be exploited together with ion-exchange processes, it is hardly surprising that so far no attempt has been made to unify and treat reactive ion-exchange as such in a general and systematic way. It is the aim of this paper to bring into focus the common features and underlying principles of reactive ion-exchange processes with the purpose of developing a general (but practical) approach to realizing some of the hitherto untapped opportunities for selective and quantitative separations offered by such procedures.

As this paper is mainly concerned with an assessment of the unexploited separation potential of reactive ion-exchange, an operational definition is needed. It is suggested that reactive ion-exchange shall encompass all such ion-exchange processes which are accompanied by reactions resulting in the production of new chemical species and/or the consumption or transformation of initially present species (particularly counter-ions) in any number of participating phases. This definition will include even a hypothetical situation where several ion-exchanger phases are involved in reactions with one or two solution phases, several other solid phases, and a gas phase. Such situations may well prove to be of practical interest in the future.

A SIMPLE THERMODYNAMIC APPROACH TO REACTIVE ION-EXCHANGE

Equilibrium aspects of ion-exchange and model approaches to resin selectivity have been reviewed in detail[14–16]. The classical work of Boyd and collaborators has contributed much to our understanding of the thermodynamics of ion-exchange. These authors have determined via calorimetric measurements the exact free energy values for various ion-exchange equilibria—all found to be in the order of one or (at most) a few kcals per mole of exchange[17]. The values for $\Delta G_{\text{exchange}}$ may be assumed (for the purposes of this paper) to result for an exchange

$$A_{\text{resin}} + B_{\text{solution}} \rightleftharpoons A_{\text{solution}} + B_{\text{resin}}$$

as the sum of the two differences[14]

$$\Delta G^{B/A}_{\text{total}} = (\Delta G^{B}_{\text{coulomb}} - \Delta G^{A}_{\text{coulomb}}) + (\Delta G^{B}_{\text{solvation}} - \Delta G^{A}_{\text{solvation}})$$

$|\Delta G^{B/A}_{\text{total}}|$ is rather small as compared to $|\Delta G|$ values for chemical reactions such as, for instance, chelate formation. Therefore, it is possible greatly to change intrinsic ion-exchange selectivities, force to completion exchange equilibria having a small negative ΔG_{total}, and even to reverse "natural" selectivity sequences by means of suitable chemical reactions involving counter-ions. The problem of separating two ions A and B by reactive ion exchange can thus be viewed as the task of finding suitable chemical reaction(s) which will result in an overall negative ΔG_{total} of sufficient magnitude. Since

$$\Delta G^{B/A}_{\text{total}} = \Delta G^{B/A}_{\text{exchange}} + \Sigma \Delta G^{B/A}_{\text{reactions}}$$

and because of the fact that, usually, $\Delta G_{\text{reaction}} > \Delta G_{\text{exchange}}$, it follows that often $\Delta G^{B/A}_{\text{total}} \approx \Sigma \Delta G^{B/A}_{\text{reactions}}$. This means that in such typical cases the totalling up of ΔG

values for all chemical reactions undergone by each of two ions to be separated (followed by subtraction) will yield a reasonable estimate of $\Delta G^{B/A}_{total}$ which in turn will tell how good a separation one may expect (very similar considerations apply to the removal or preconcentration of ionic species or indeed to any practical application of reactive ion-exchange). To illustrate this approach, two different types of reactive ion-exchange processes will be considered briefly.

(a) The deionization of hard water by the mixed bed process (bars over symbols denote, as usual, "resin phase") may simply be represented as follows:

$$(1)\ 2\overline{H}^+ + Ca^{2+} \rightleftharpoons \overline{Ca}^{2+} + 2H^+ \qquad \Delta G_1 < 0 \quad \text{(ion-exchange)}$$

$$(2)\ 2\overline{OH}^- + 2X^- \rightleftharpoons 2\overline{X}^- + 2OH^- \qquad \Delta G_2 < 0 \quad \text{(ion-exchange)}$$

$$(3)\ 2H^+ + 2OH^- \rightleftharpoons 2H_2O \qquad \Delta G_3 \ll 0 \quad \text{(reaction)}$$

$$2\overline{H}^+ + 2\overline{OH}^- + Ca^{2+} + 2X^- \rightleftharpoons Ca^{2+} + 2\overline{X}^- + 2H_2O, \quad \Delta G_T \ll 0$$

In order to make a reasonable estimate of the overall free energy of this process, only the value of ΔG_3 is needed (-19 kcal mole^{-1} of water under standard conditions) and it is possible to neglect all effects caused by electrolytes and polymer present, or by changes in temperature, since ΔG_1 and ΔG_2 are considerably smaller and have both the same sign as ΔG_3. Thus (as we already knew) the deionization of water proceeds to a very high degree of completeness. For a more accurate calculation, values for $\Delta G^{Ca/H}$ and $\Delta G^{X/OH}$ as a function of resin loading would be needed (probably it is best to estimate average ΔG values from K values of exchange at half resin loading, corrected for solution activity coefficients[14], *i.e.*, $K'_{x=0.5}$). These, as well as all other corrections theoretically required—including accounting for the exchange equilibria of all other ions present in hard water—would not change significantly the first result. Of course, the case of total consumption of all counter-ions is just one special case of many possible ones.

(b) The reducing adsorption of oxyions was recently investigated in this laboratory on suitable resinates (of ions in their lower oxidation states) with the objective of preconcentration of trace ions, or their separation (trace or macro) from concomitant ions[12]. Consider the reducing adsorption of chromium(VI) from acidic solution onto a cation-exchange resin in the iron(II) form (which, incidentally, avoids attack on the resin by chromium(VI) at any pH and results in quantitative separation from all non-reducible anions because of their being subject to Donnan exclusion).

$$(1)\ Cr_2O_7^{2-} + 14H^+ + 6Fe^{2+} \rightleftharpoons 2Cr^{3+} + 7H_2O + 6Fe^{3+} \qquad G_1 \ll 0 \text{ (reaction)}$$

$$(2)\ 2Fe^{3+} + 3\overline{Fe}^{2+} \rightleftharpoons 2\overline{Fe}^{3+} + 3Fe^{2+} \qquad G_2 \gtrless 0 \text{ (ion-exchange)}$$

$$(3)\ 2Cr^{3+} + 3\overline{Fe}^{2+} \rightleftharpoons 2\overline{Cr}^{3+} + 3Fe^{2+} \qquad G_3 \gtrless 0 \text{ (ion-exchange)}$$

$$Cr_2O_7^{2-} + 6\overline{Fe}^{2+} + 14H^+ \rightleftharpoons 2\overline{Fe}^{3+} + 2\overline{Cr}^{3+} + 7H_2O + 4Fe^{3+}, \quad \Delta G_{total} \ll O$$

Reactions (1) to (3) proceed once a small amount of iron(II) ions has been initially displaced from the resin by exchange against any cations accompanying dichromate; $\Delta G_{total} \ll 0$, indicating a quite spontaneous overall process. This is a

straightforward example for a redox case of reactive ion-exchange. Here, and in other cases, there will be numerous (and multiple) side equilibria which one might have to consider. Thus, the actual values of ΔG_2 and ΔG_3, and even ΔG_1 are strongly affected by pH and by the type(s) and concentration(s) of ions present in solution. Depending on pH, some hydrolysis of iron(III) may occur (see below). Furthermore, ΔG_2 will be a function of the Nernst term which incorporates the (local) concentrations of the oxidized and reduced species in the column, and activity effects have not been considered at all. A tremendous local rise of pH in the interstitial space must occur even in acid solution because of extensive proton consumption in reaction (1). This can sometimes result in hydrolysis of iron(III) [which can, however, be prevented by using a mixed bed ($\overline{Fe^{2+}} + \overline{H^+}$) instead of pure $\overline{Fe^{2+}}$ resinate]. All these qualitative (or semiquantitative) considerations are quite straightforward and, again, it was possible to predict from fundamental thermodynamic quantities the overall equilibrium situation and hence the actual separation. In order to examine whether or not a particular separation problem is amenable to reactive ion-exchange, a very simple "recipe" may be followed (which is a straightforward application of the first law of thermodynamics):

(i) Write down in general terms the final result needed or hoped for. For example b (above) this would probably have been: $Cr_2O_7^{2-}$ (in aqueous solution)$\rightarrow\overline{Cr}$ (adsorbed on resin in any form; other anions will not be sorbed).

(ii) Consider various combinations of chemical reactions and ion exchanges which add together to an overall equation which yields the desired result. The actual sequence of reaction steps is, of course, immaterial as long as it is practicable, but reactions with a large negative free energy bias in the desired direction would be chosen whenever feasible. These reactions will usually involve transformations of species such as will be discussed below.

(iii) Estimate ΔG values for all intermediate steps from available fundamental information while keeping in mind theoretical limitations (*e.g.*, resin standard states) and making bold (but appropriate) simplifying assumptions (*e.g.*, about expected changes in activity coefficient ratios, local pH, and relative complex formation tendencies).

(iv) Total up all ΔG values from these reactions. The resultant $\Delta G^{B/A}_{total}$ should be negative and of appreciable magnitude. [Should $\Delta G^{B/A}$ come out small or/and positive one will have to go back to (ii) and find some other (more spontaneous) intermediate reaction(s)].

(v) Considering anticipated rates of reaction and diffusion and other practical aspects, design a trial experiment.

KINETIC ASPECTS OF REACTIVE ION-EXCHANGE

As shown by Helfferich[13], experimental research is needed on the rates of ion-exchanges "accompanied by reactions", and many interesting problems are waiting to be attacked in this area. However, the practitioner of reactive ion-exchange needs at first only a qualitative understanding of the factors involved. All actual exchange processes in strong acid or base polymeric exchange resins are diffusion-controlled. Thus, the use of resin beads of small particle size (no

problem with short columns) should be beneficial for all cases where film-diffusion at the exchanger surface is the slowest step[13] and a reasonably low degree of cross-linkage will help particularly those cases where particle diffusion is controlling. Among parameters such as mobility of counter-ions and co-ions, selectivity of the exchanger, concentration of reactants, and temperature, only the latter two can be changed for a given system. Agitation would help when film-diffusion is controlling, but can only be used in batch experiments. Higher temperature and concentrations will, expectedly, favor a faster exchange.

A slow step in a reactive ion-exchange procedure can also arise from a reaction rather than from diffusion. In some cases, information on the kinetics of ionic reactions in solution is available from the literature. Slow kinetics may be encountered with certain redox-reactions, chelation, and with proton transfer involving weak acids or bases. Frequently, higher temperature or simply excess of reagent (solution or suitable resinate) will accelerate the reaction sufficiently. In certain redox cases a small amount of catalyst ions could be added (in solution or in form of a resinate) if they would not otherwise interfere. Sometimes a potentially promising route may have to be abandoned because of unfavorable rates. Experience so far suggests that many reactions having spontaneous thermodynamic characteristics can also be employed under practical conditions, at least at the trace or minor constituent concentration level of the target species.

SPECIES TRANSFORMATIONS AND REACTIONS

Transformation of species in ion-exchange procedures may serve one of the following primary objectives:

(A) the isolation of individual species from more or less complex matrices as in the preconcentration or removal of toxic metal ions—both selectivity and quantitative exchange are required in most cases;

(B) the separation (from each other) of two or more very similar species – high selectivity is the major objective to be attained by maximizing differences in adsorption–elution behavior for these ions;

(C) the "wholesale" sorption (or desorption) of entire groups of ions (same charge type), or removal of all ions present in solution as in the deionization of water; here, the major objective is to increase the overall driving force for the desired process with little concern for individual selectivities.

There are many instances in practice where both high selectivity and very complete adsorption (elution) are desirable. All this can be attained by reactive, ion-exchange, whenever a suitable reaction can be employed to transform the target species in such a way that a significant differentiation from concomitants and complete exchange result. There are three general ways in which ions may be transformed:

(i) the charge on an ion is changed to a higher or lower value ($UO_2^{2+} \rightarrow U^{4+}$; $Fe^{3+} + SCN^- \rightarrow [FeSCN]^{2+}$; etc.);

(ii) the charge on an ion is changed to the opposite sign ($VO_4^{3-} \rightarrow VO^{2+}$; $Cd^{2+} + 4\ Cl^- \rightarrow [CdCl_4]^{2-}$; etc.);

(iii) the charge is removed from an ion resulting in a species of zero charge ($RCOO^- + H^+ \rightarrow RCOOH$; $M^{n+} + nX^- \rightarrow MX_n$; etc.). (The opposite process is also possible.)

TABLE I

SELECTED EXAMPLES OF REACTIVE ION-EXCHANGE

Main reactants[a]		*Main products*[a]		*Main reactions*[a]	*Mode*[c]	*Application*	*Ref.*
Solution	*Resin*[b]	*Resin*[b]	*Solution*				
A $Cr_2O_7^{2-}$, other anions	$\overline{Cl^-}$	$\overline{Cr_2O_7^{2-}}$; Cl^-, other	Cl^-	Ion-exchange	AD	Cr(VI) preconcn. Cr(VI)/Cr(III)[d]	10
B CH_2O (2 *M* in 1 *M* H_2SO_4)	$\overline{Cr_2O_7^{2-}}$	$\overline{SO_4^{2-}}$	Cr^{3+}, HCOOH	Redox	REL	CrVI/anions	
A MnO_4^-, CrO_4^{2-}, VO_4^{3-}, MoO_4^{2-}, cations, H^+, anions	$\overline{Fe^{2+}}$	$\overline{Mn^{2+}}$, $\overline{Cr^{3+}}$, $\overline{VO^{2+}}$, $\overline{Fe^{3+}}$, $\overline{Fe^{2+}}$	Fe^{2+}, MoO_4^{2-}	Redox	RAD	Sepn from anions; Preconcn. of MnO_4, CrO_4^{2-}, VO_4^{3-}; CrO_4^{2-}, VO_4^{3-}/MoO_4^{2-}	
B EDTA (cold)	$\overline{Mn^{2+}}$, $\overline{Cr^{3+}}$, $\overline{VO^{2+}}$ $\overline{Fe^{3+}}$, $\overline{Fe^{2+}}$	$\overline{Cr^{3+}}$, $\overline{H^+}$	MY (M = Mn, Fe, V)	Chelation (fast)	REL	Cr/Mn, V, Fe	12
C EDTA (hot)	$\overline{Cr^{3+}}$	$\overline{H^+}$	CrY	Chelation (slow)	REL	Cr isolation	
A $[Fe(CN)_6]^{4-}$, other anions, other cations	$\overline{Cu^{2+}}$	$\overline{\{Cu_2[Fe(CN)_6]\}}\downarrow$[e], $\overline{Cu^{2+}}$ others	(Some Cu^{2+} by ion-exchange)	Ppt'n	ISPR	Preconcn. of $[Fe(CN)_6]^{4-}$ sepn/anions	
B HCl	$\overline{\{Cu_2[Fe(CN)_6]\}}\downarrow$[e], $\overline{Cu^{2+}}$ other	$\overline{\{Cu_2[Fe(CN)_6]\}}\downarrow$[e], $\overline{H^+}$	$CuCl_4^{2-}$, other	Ion complex	REL	$[Fe(CN)_6]^{4-}$/ excess Cu^{2+} and other cations	11
C NH_3	$\overline{\{Cu_2Fe(CN)_6\}}\downarrow$[e], $\overline{H^+}$	$\overline{[Cu(NH_3)_4]^{2+}}$, $\overline{NH_4^+}$	$[Fe(CN)_6]^{4-}$	Coordin. complex	REL	Isolation of $[Fe(CN)_6]^{4-}$, sepn/Cu	

TABLE 1 *(contd)*

D HCl	$\overline{[Cu(NH_3)_4]^{2+}}$, $\overline{NH_4^+}$	$\overline{NH_4^+}$	$CuCl_4^{2-}$	Ion complex	REL	Elution of Cu	
A Glyceraldehyde-3-phosphate (GAP) and inorganic phospate (P)	$\overline{HSO_3^-}$	$\overline{GAP\text{–}HSO_3^-}$[f] (addition compound) and $\overline{P}$	HSO_3^-	Formation of charged GAP–bisulfite complex	RAD and Ion-exchange	GAP/P	19
B NaCl	$\overline{GAP\text{–}HSO_3^-}$ $\overline{P}$	$\overline{GAP\text{–}HSO_3^-}$ $\overline{Cl^-}$	P	Ion-exchange (of P)	IEX		

[a] No attempt is made in this Table to give a complete list of all species present, or reactions having occurred; only those important for understanding the processes are given.
[b] Conventional polystyrene type resins of the strongly basic or acidic type used in all cases.
[c] Mode refers to the actual column operation: AD = adsorption, REL = reactive elution, RAD = reactive adsorption, ISPR = *in situ* precipitation with retention.
[d] "/" means separation from.
[e] The sign {}↓ means that a precipitate of this apparent stoichiometry is formed *in situ* (on the column) but the actual composition may be different.
[f] A formula for the addition complex has been given[19].

In reactive ion-exchange, species transformations may be effected during adsorption steps—reactive adsorption; and during elution steps—reaction elution. A combination (or sequence) of reactive adsorption and elution can be employed when necessary. In principle, any reaction(s) achieving those transformations serving the primary objectives (A), (B), or (C) are fair game, no matter how well all participating species are accounted for in terms of exact theories of solution and ion-exchange processes. However, it is from a fundamental understanding of ionic reactions and ion-exchange behavior that many ideas will flow which can lead to new and useful procedures. There remain unrealized opportunities for useful species transformations by means of ion complexing and/or aqueous–organic solvent systems with some excellent monographs and reviews available on these topics[2,3,18]. Very promising are apparently the redox chemistry of elements having several oxidation states which offer a wealth of potentially useful reactions, and the formation (or dissolution) of sparingly soluble solids[11,12].

In any event, it is most important not to limit one's thinking to conventional uses of a single resin and one solution phase. Reduction, oxidation, neutralization, chelation, ion complexing, covalent bond formation, any chemical reaction involving resins and/or counter-ions, mixed resin beds, or sequential beds of different resins, immiscible liquid phases containing potentially reactive species, should be considered in order to realize the full potential of the technique. Table I shows a few of the actual reaction sequences recently employed in this laboratory for trace (and mg) separations of inorganic ions performed with 2.5 cm (0.7 cm diameter) resin beds of conventional resins. Also included is an interesting reactive separation of glyceraldehyde 3-phosphate from inorganic phosphate reported by Koser and Oesper[19] which provides additional evidence for the utility of reactive ion-exchange as a general approach. Work now being completed in this laboratory will describe experimental parameters in various reactive systems studied, detailed separation procedures, and mechanistic aspects of particular systems.

CONCLUSION

Ion-exchange processes carried out with common polymeric exchange resins can be combined with chemical reactions resulting in species transformations which can serve to differentiate target ions (to be separated) from each other or from any matrix. Because of the rather modest free energy changes associated with conventional ion-exchange, chemical reactions such as oxidation, reduction, formation of sparingly soluble compounds, neutralization, and others, including the traditionally used ion complexing and chelation reactions, may be employed to "drive" ion-exchange processes in the direction needed: the greater ΔG of a chemical reaction imparts its own free energy bias on the overall process. Therefore, a correct prediction of the resultant process can usually be made based upon straightforward thermodynamic (and kinetic) considerations based on fundamental information available in the literature. Systematic investigation of the entire field of (what is defined as) reactive ion-exchange, following the general approach developed here, can be expected to show many so far unexplored opportunities for selective and quantitative separations of ionic species, particularly (but not only) at the trace concentration level.

SUMMARY

Ion-exchange processes accompanied by chemical reactions are treated as one general category—reactive ion-exchange. A simple operational approach was developed on the basis of thermodynamics which permits correct semi-quantitative prediction of the overall equilibria resulting from the combination of ion-exchange processes and chemical reactions. Performing transformations of ionic species by chemical reactions was shown to be the key to selective ion-exchange separations. A systematic investigation of the utility of various reaction types and systems is suggested; several actual examples were used to illustrate typical reactive ion-exchange procedures involving redox reactions, precipitation, ionic complexing, and chelation as the "driving" chemical reactions.

REFERENCES

1 F. W. E. Strelow in J. A. Marinsky and Y. Marcus (Eds.), *Ion Exchange and Solvent Extraction*, Vol. V, Marcel Dekker, New York, 1973, Ch. 2
2 Y. Marcus in J. A. Marinsky and Y. Marcus (Eds.), *Ion Exchange and Solvent Extraction, Vol. IV*, Marcel Dekker, New York, 1973.
3 J. Korkisch, *Modern Methods for the Separation of Rarer Metal Ions*, Pergamon, Oxford, 1969.
4 F. Helfferich, *Ion Exchange*, McGraw-Hill, New York, 1962, Ch. 5, pp. 202, 228 and Ch. 12.
5 G. Schmuckler, *Talanta*, 12 (1965) 281.
6 J. Inczedy, *Hung. Acta Chim.*, 27 (1961) 185.
7 H. Dalibor, *Chem. Ber.*, 91 (1960) 1955.
8 R. R. Ruch, F. Tera and G. H. Morrison, *Anal. Chem.*, 37 (1965) 1565.
9 W. E. Miller, *Anal. Chem.*, 30 (1958) 1462.
10 J. F. Pankow and G. E. Janauer, *Anal. Chim. Acta*, 69 (1974) 97.
11 G. O. Ramseyer and G. E. Janauer, in preparation.
12 J. W. Lin and G. E. Janauer, in preparation.
13 F. Helfferich in J. A. Marinsky (Ed.), *Ion Exchange*, Vol. I, Marcel Dekker, New York, 1966, Ch. 2, pp. 86, 82.
14 D. Reichenberg in J. A. Marinsky (Ed.), *Ion Exchange*, Marcel Dekker, New York, 1966, Ch. 7.
15 R. M. Diamond and D. C. Whitney, in J. A. Marinsky (Ed.), *Ion Exchange*, Marcel Dekker, New York, 1966, Ch. 8.
16 Y. Marcus and A. S. Kertes, *Ion Exchange and Solvent Extraction of Metal Complexes*, Wiley–Interscience, London, 1968, Ch. 4, p. 277.
17 G. E. Boyd, F. Vaslow and S. Lindenbaum, *J. Phys. Chem.*, 71 (1967) 2214; 68 (1964) 590.
18 W. R. Heumann, *CRC Critical Reviews in Analytical Chemistry*, Volume II, November 1971, pp. 425–459.
19 B. Koser and P. Oesper, *Anal. Biochem.*, 17 (1966) 119.

Analytica Chimica Acta, 73 (1974) 321–328

REPORTING CONCENTRATION- AND CONCENTRATION RATIO-DEPENDENT SELECTIVITY COEFFICIENTS FOR ION-SELCTIVE ELECTRODES

RICHARD P. BUCK

The William Rand Kenan, Jr. Laboratories of Chemistry, University of North Carolina, Chapel Hill, North Carolina 27514 (U.S.A.)

(Received 8th April 1974)

By general usage the expression

$$E = E^0 + \frac{RT}{zF}\ln(a_i + K_{ij}^{pot} a_j) \qquad (1)$$

is considered a norm[1] for ideal behavior of ion-selective electrodes responsive to two species i and j with charge z. When, for positive ions, response is more positive for pure i than for pure j at equal activities, k_{ij}^{pot} is a number less than unity and the electrode is considered more sentitive to i than to j. In only the most idealized models will k_{ij}^{pot} be derived as a concentration-independent, constant quantity at constant temperature and pressure. The incomplete ion-exchange theory of Nicolsky[2] and the more complete theories of Horowitz[3] and Conti and Eisenman[4] ($n=1$ case) give this result provided that ionic mobilities and activity coefficients are independent of distance and concentration, and that a constant fraction of membrane ions are involved in the diffusion potential generation. Thus, membrane systems composed of solid and concentrated liquid electrolytes can be expected to show concentration-dependent selectivity coefficients through complex formation, ion pairing and the effects of concentration and position on mobilities and activity coefficients. As more precise data are collected on mixture responses, constant selectivity coefficients seem to be the exception rather than the rule[5,6]. Reported values of K_{ij}^{pot} must then be recognized as apparent quantities K_{ij}^{pot} (app), which on closer inspection may vary in some way with a_i and a_j.

There are two distinct types of behavior of K_{ij}^{pot}(app) as a function of ion activities which follow from the Teorell–Meyer–Sievers segmented potential model of membrane responses. When interfacial potentials are at equilibrium, *i.e.* for rapid, reversible interfacial processes, and the differential diffusion potential is exact, K_{ij}^{pot}(app) is a function only of the activity ratio a_j/a_i. This is the case for glass electrodes which obey ideal, n-type nonideal[7–10] and the solid[11,12] models, as shown below. If the interfacial potential is not the equilibrated value or the diffusion potential depends on the path of integration by virtue of co-ion transport, complex ion or ion pair formation or transport by ions of same sign but different valence, then K_{ij}^{pot}(app) depends on individual ion activities, a_j/a_i and a_i or a_j, explicitly. The exact dependences are difficult to work out analytically and digital simulation offers the best approach[13]. Hydroxide interference in the fluoride

response of the LaF_3 membrane[14], magnesium interference in the calcium response of liquid phosphonate electrodes[15], nitrate interference in the chloride response of liquid electrodes[6] and hydrogen and sodium interferences in the calcium-selective electrode[16–18] are examples of more complex responses. Others are noted by Moody and Thomas[6].

For the first category, a single plot of K_{ij}^{pot}(app) or log K_{ij}^{pot}(app) *vs.* log (a_j/a_i) will suffice, but for the second category, a family of curves would be required to specify the responses of the systems. Fortunately, even some systems in the latter categories reduce to a single plot over a practical concentration ratio range, according to theoretical studies. For example, liquid membrane responses to ions of the same charge for limiting cases of weak complexing[19] and very strong 1:1 complexing[20], and completely ionic liquid membrane responses of mixed uni- and bi-valent cations[13] reduce to the simpler category, even though eqns. (2) and (3) are not exact for mixed-valence systems.

$$E = E^0 + \frac{RT}{zF}\ln(a_i + K_{ij}^{pot} a_j^{z/n}) \tag{2}$$

or

$$E^0 + \frac{RT}{nF}\ln(a_i^{n/z} + K_{ij}^{pot} a_j) \tag{3}$$

Measurement and data treatment

Striking and clear examples of the two categories of variable K_{ij}^{pot}(app) values can be found in the interference response characteristics of pH- and cation-sensitive glass membrane electrodes. These systems are chosen for illustration because both theory and mixture responses are more extensive and better documented for these electrodes than the newer ion-selective electrodes. Selectivity coefficients must be computed from mixture responses in the region of values of a_j/a_i such that response is not dominated by a_j or a_i alone. The two-point pure solution method[7] will not suffice because it cannot uncover composition-dependent selectivities. The advantage of the two-solution method is simplicity; but even for systems where responses to pure a_i and a_j give parallel E *vs.* log a_i or a_j characteristics, it can be shown that one obtains only limiting values of K_{ij}^{pot} corresponding to high values a_j/a_i. For this reason, mixture methods with many premixed solutions are necessary. Generally, three or four pure solutions of a_i to establish base response and about 15 mixtures ($5a_i$ levels spaced one half decade apart at 3 levels of a_j, one decade apart) are sufficient. Mixture methods were first used extensively by Lengyel and Blum[21] and later by Eisenman[8]. Srinivasan and Rechnitz[22] examined several methods for selectivity coefficients and Pungor and Toth[23,24] emphasized the validity of the method outlined above for solid electrode selectivity measurements. When dealing with ion-exchanging solid electrodes (including glasses) containing the species i, responses to pure interference a_j are unreliable. Mixtures must be used containing a_i such that surface attack by a_j releases an insignificant activity increment of a_i at the membrane surface. A convenient form of the mixture method is the titration procedure of Dole[25]; and as modified and improved in this laboratory[12], this method provides extensive sets of data for determinations of K_{ij}^{pot}(app). Given a set of mixture responses E_{ij} and pure i responses E_i,

$$\ln K_{ij}^{pot}(\text{app}) = \ln\{\exp[(E_{ij}-E_i)/S]-1\} - \ln(a_j/a_i) \quad (4)$$

where S is the slope of the pure i response curve. When normal behavior is encountered (eqn. 1), $K_{ij}^{pot}(\text{app}) = K_{ij}^{pot}$ and the suggested plot [$\log K_{ij}^{pot}(\text{app})$ *vs.* $\log(a_j/a_i)$] gives a constant value for all a_j/a_i. Equation 4 can be used with any set of E_{ij}, but is restricted to regions of a_i response such that

$$E = E^0 + S \log a_i \quad (5)$$

Systems whose selectivities depend only on a_j/a_i

Glass electrode mixture responses have been treated on the basis of three models in recent years. Non-ideal behavior has been attributed to concentration-dependent activity coefficients[10], distribution of ions between fixed sites and mobile interstitial positions[11] and formation of immobile, undissociated species[26] in glasses. Results of the latter are included within the solid state model. These theories[9,11] lead to descriptive $K_{ii}^{pot}(\text{app})$ equations which are zero-order homogeneous functions of a_j/a_i. The n-type non-ideal behavior of a pH-sensing glass obeys the law

$$E = E^0 + \frac{nRT}{F}\ln\{a_H^{1/n} + [K_{ij}^{pot} a_M]^{1/n}\} \quad (6)$$

where

$$n = \mathrm{d}(\ln a)/\mathrm{d}(\ln c) \quad (7)$$

and a_M is a monovalent interfering ion activity. Even though for pure a_H or a_M solutions, response curves are predicted to be parallel with Nernstian slope, the selectivity coefficient varies with salt activities according to

$$K_{ij}^{pot}(\text{app}) = \frac{a_i}{a_j}\{1+[K_{ij}^{pot} a_j/a_i]^{1/n}\}^n - \frac{a_i}{a_j} \quad (8)$$

and, for typical n values exceeding one, $K_{ij}^{pot}(\text{app})$ exceeds K_{ij}^{pot}. Analysis shows that for $K_{ij}^{pot} a_j/a_i > 1$, the plot of $\log K_{ii}^{pot}(\text{app})$ *vs.* $\log(a_j/a_i)$ is linear with slope $(1/n)-1$. As a_j/a_i becomes very large, $K_{ij}^{pot}(\text{app}) = K_{ij}^{pot}$. These conclusions are illustrated in Fig. 1 for $K_{ij}^{pot} = 10^{-5}$. Buck's theory for pH-sensitive glass electrode response has the form,

$$E = E^0 + \frac{RT}{F}\ln\{a_H + K_{H/M}(K_1 a_H a_M)^{\frac{1}{2}}][1+K_1 a_M/a_H]^{\frac{1}{2}}\} \quad (9)$$

where $K_{H/M}$ is a mobility ratio term and K_1 is the ion-exchange constant for M^+ replacing H^+ on surface silica sites. An equation of similar form applies to heterogeneous-site membranes used for cation-selective membrane electrodes. When the terms in eqn. (9) are multiplied out, equivalent cross terms $(a_H a_M)^{\frac{1}{2}}$ create a response similar but not identical to the n-type non-ideality. If one forces the two eqns. (6) and (9) to pass through common points for large $a_M(a_j) \gg a_H(a_i)/K_{ij}^{pot}$ and at $a_H = K_{ij}^{pot} a_M$, then

$$n \simeq \frac{59.14}{17.7}\log[(1+K_{i/j}^{\frac{1}{2}})(1+1/K_{i/j})^{\frac{1}{2}}] \quad (10)$$

The response at high interference shows that

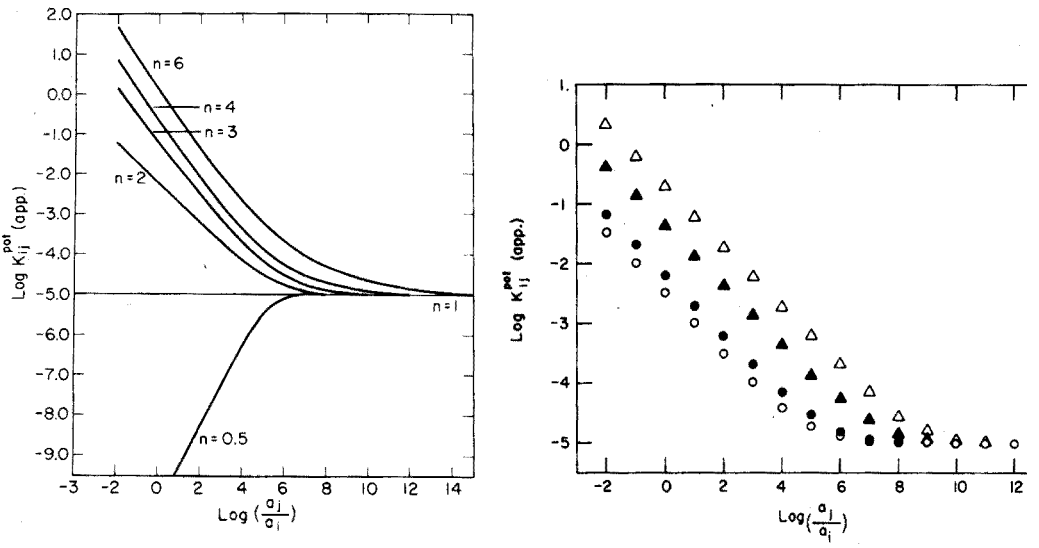

Fig. 1. Dependence of apparent selectivity coefficients on a_j/a_i for systems obeying n-type non-ideality for $K_{ij}^{pot} = 10^{-5}$.

Fig. 2. Dependence of apparent selectivity coefficients on a_j/a_i for systems obeying Buck's solid-state model for non-ideal behavior for $K_{ij}^{pot} = K_{i/j}K_1 = 10^{-5}$ for comparison with Fig. 1. (△) $K_{i/j} = 3.84 \cdot 10^3$, $n \sim 4$; (▲) $K_{i/j} = 225$, $n \sim 3$; (●) $K_{i/j} = 10$, $n \sim 2$; (○) $K_{i/j} = 1$, $n \sim 1$.

$$K_{ij}^{pot} = K_{i/j}K_1 \tag{11}$$

One can deduce that for this solid-state model

$$K_{ij}^{pot}(\text{app}) = \frac{a_i}{a_j}\{[1+K_{i/j}K_1^{\frac{1}{2}}(a_j/a_i)^{\frac{1}{2}}][1+K_1(a_j/a_i)]^{\frac{1}{2}}\} - \frac{a_i}{a_j} \tag{12}$$

For illustration $K_{i/j}K_1 = 10^{-5}$ is chosen, and the two parameters are adjusted so that both theories give the same K_{ij}^{pot}(app) values at $K_{ij}^{pot}a_j/a_i = 1$ in Fig. 2. The important feature of Buck's theory is that log K_{ij}^{pot}(app) is linear with increasing log a_j/a_i with slope $-\frac{1}{2}$ for $K_{ij}^{pot}a_j/a_i \ll 1$, but approaches K_{ij}^{pot} at high a_j/a_i in a fashion similar to the predictions of the Karreman–Eisenman equation.

Systems whose selectivities depend on a_j/a_i and a_i or a_j

Some examples of experimental systems whose responses cannot be reduced to dependences on a_j/a_i alone were listed above. The theoretical interpretations—indeed the physical–chemical sources of the responses—are lacking. For one simple but general type of behavior, the theory is straightforward. Suppose that base reponse to a_i is Nerstian, but the response to a_j is linear with slope S_j. An example is the lithium error at the Beckman sodium-selective glass electrode. For pure Li^+ response (a_j)

$$E \simeq E_j^0 + S_j \log a_{Li^+} \tag{13}$$

and for pure Na^+ response (a_i)

$$E = E_i^0 + S_i \log a_{Na^+} \tag{14}$$

then

$$\log K_{ij}^{pot}(app) = \left(\frac{S_j}{S_i} - 1\right)\log a_j + S_i^{-1}(E_j^0 - E_i^0) \quad (15)$$

In the cases of parallel response curves $S_i = S_j$, one has the usual formula for K_{ij}^{pot} by the two-solution method with unit activity solutions of i and j. The important feature of this equation is that $K_{ij}^{pot}(app)$ increases with increasing interference activity. The lithium error of one sodium-selective glass electrode exhibits this behavior.

EXPERIMENTAL

All responses were measured with the expanded scale on a Beckman Model 76 Century SS pH Meter. The electrodes ere Beckman Type General-Purpose (No. 41263) and Sodium Ion Electrode (No. 39278). The details and procedure have already been published[1,2].

Results

The response–selectivity plot of the general-purpose pH electrode to varying sodium interference by the mixture method is shown in Fig. 3. Although there is some scatter, the log apparent selectivity data follow the $-\frac{1}{2}$ slope predicted by the solid state model. By curve fitting, the limiting K_{ij}^{pot} was previously estimated[1,2]

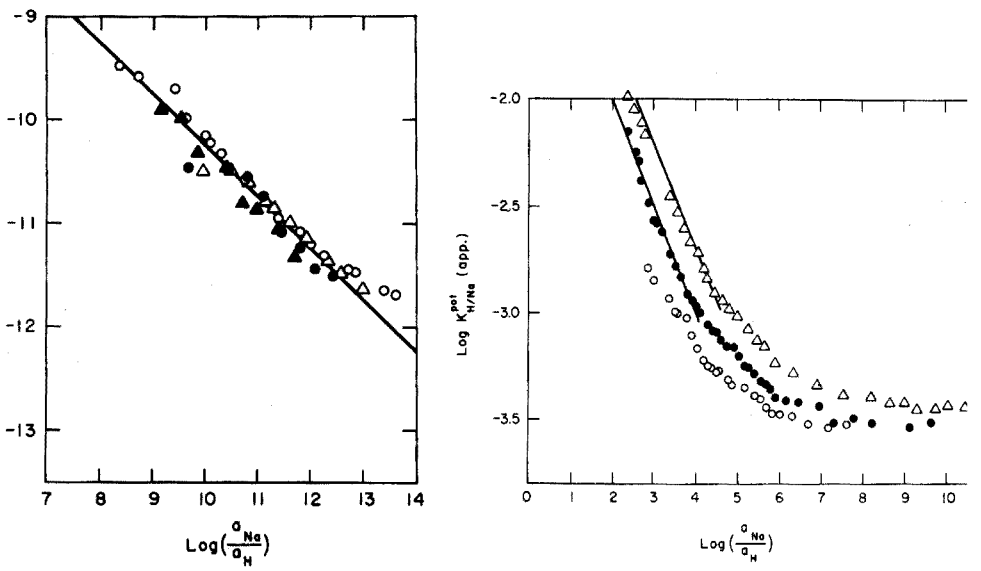

Fig. 3. Apparent selectivity coefficients of the Beckman general-purpose electrode at 25°C for sodium ion interference. (○) 3 *M* sodium chloride, (●) 1 *M* sodium chloride, (△) 0.3 *M* sodium chloride, (▲) 0.1 *M* sodium chloride.

Fig. 4. Apparent selectivity coefficients of the Beckman sodium-selctive electrode at 25°C for hydrogen ion interference. (△) 0.5 *M* NaCl and variable pH, (●) 0.05 *M* NaCl and variable pH, (○) 0.005 *M* NaCl and variable pH.

as about 10^{-12}. Clearly, K_{ij}^{pot} alone is of little value in predicting or describing mixture responses, while K_{ij}^{pot}(app) gives all of the necessary information. From this approach, the need for two parameters $K_{H/M}$ and K_1 or $K_{H/M}$ and K_{ij}^{pot} has been eliminated. Similarly for glasses described by the empirical equation of Eisenman, Rudin and Casby, a need to know both n and K_{ij}^{pot} is avoided by use of K_{ij}^{pot} (app.).

The hydrogen-ion interference of the sodium-selective electrode does not yield a single K_{ij}^{pot}(app) plot at 25°C, as illustrated in Fig. 4. Although the solid-state slopes are correct, the absolute values depend upon a_{Na^+} in a way which is beyond the scatter of the measurement. A plausible explanation, consistent with the low slope of the pNa^+ response is that this electrode does not reach equilibrium rapidly, especially at acidities where the sodium and hydrogen ion terms (surface coverage) are of comparable magnitude. Responses at high a_{Na^+}, low a_{H^+} show less scatter and approach a nearly constant $K_{H/Na}^{pot}$ at the right of the figure; but there is some uncertainty resulting from the assumption that $\gamma_{Na^+} = \gamma_{\pm}$(NaCl). Finally, in Fig. 5 are the computed values for lithium selectivity of the sodium-sensitive electrode. This system is one for which the pure lithium response is significantly super-Nernstian, while the sodium response slope has been found variously as 57 ± 2 mV. The interference by lithium, as a_{Li^+} is increased, is in agreement with predictions of eqn. (15).

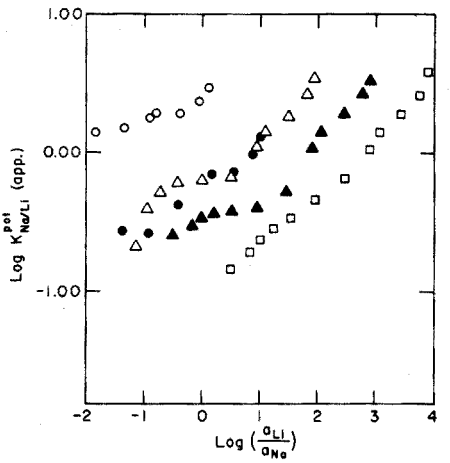

Fig. 5. Apparent selectivity coefficients of the Beckman sodium-selective electrode at 25°C for lithium ion interference. (○) a_{Na} $6.57 \cdot 10^{-1}$ M, (●) a_{Na} $7.78 \cdot 10^{-2}$ M, (△) a_{Na} $9.03 \cdot 10^{-3}$ M, (▲) a_{Na} $1.5 \cdot 10^{-4}$ M, (□) a_{Na} $1.0 \cdot 10^{-4}$ M.

In the past, error responses in pH units, Δ, for pH-sensing electrodes have been reported[27], where

$$\Delta = [E(\text{mixtures}) - E(\text{pure } H^+)]/2.303RT/F \tag{16}$$

For monovalent ion errors of electrodes obeying the two models given above,

$$\Delta = n \log[1 + (K_{ij}^{pot} a_M/a_H)^{1/n}] \tag{17a}$$

or

$$\Delta \doteq \log\{[1 + K_{H/M}(K_1 a_M/a_H)^{\frac{1}{2}}][1 + K_1 a_M/a_H]^{\frac{1}{2}}\} \tag{17b}$$

These are again zero-order homogeneous equations. Lengyel *et al.*[28] reported both the error and $K^{pot}_{H/Na}$(app.) values for MacInnes–Dole glass. The results obey the solid-state model quite accurately with the appropriate slope $-\frac{1}{2}$. However $K^{pot}_{H/Na}$ (app.) values for the Lengyel "Ds" glass obey more nearly the Eisenman–Rudin–Casby form with $n \sim 8$.

It has not been pointed out before that eqns. (17a) and (17b) are implicit in the "empirical" error equaton of Jordan[29]. Errors measured in the vicinity of $a_H = K^{pot}_{H/Na}\, a_M$ permit expansion of the log term so that

$$\log \Delta \simeq (1/n)(\mathrm{pH} + \log a_M) + \text{constant} \tag{18a}$$

or

$$\log \Delta \simeq (1/2)(\mathrm{pH} + \log a_M) + \text{constant} \tag{18b}$$

The empirical equation was given as

$$\log \Delta = A\,\mathrm{pH} + B \log a_M - C \tag{19}$$

The point to be emphasized is that systems obeying the equilibrium models should give error values by Jordan's equation with $A = B$. Lengyel and Csakvari[30] reported these coefficients for fourteen glasses. Glass no. 11, the composition of which is similar to the Beckman general purpose glass gives $A = 0.52$ and $B = 0.50$, in close agreement with Buck's model and the experimental results reported here. An Al_2O_3-containing glass similar to the Beckman sodium electrode gave $A = 0.55$ and $B = 0.64$, which may indicate some deviation from theoretical behavior as noted in connection with Fig. 4. Their accumulated data show that A and B tend to vary together in accordance with eqn. (18a).

Thus, examples of two predicted categories of behavior for equilibrated and unequilibrated systems have been found. Plots for other systems whose apparent selectivities depend on a_j/a_i and a_i or a_j could be prepared from data in the literature[5,6,12–18]. Inasmuch as K^{pot}_{ij} determined by the two-point method describes only ideal systems obeying eqn. (1), it is recommended that K^{pot}_{ij}(app) *vs.* $\log a_j/a_i$, determined by the mixture methods, be reported for characterization of all selective electrodes. Not only does the single parameter remove the need to determine all of the relevant terms in the theoretical model equations as pointed out above, but the actual dependences of K^{pot}_{ij}(app) on activity may aid in diagnosing the presence of *n*-type and solid-state non-ideal behavior, non-equilibrium responses and other, as yet unrecognized, sources of activity-dependent, non-ideal potentiometric response.

The author recognizes support by the National Science Foundation, Grant GP 20524.

SUMMARY

Occurrence and sources of concentration (activity)-dependent selectivity coefficients of ion-selective electrode responses have been interpreted on the bases of equilibrium or nonequilibrium conditions, mixed valence counter ion transport and failure of co-ion exclusion. Equilibrium conditions for common valence counter ions lead to apparent selectivity coefficients which depend only on activity ratios

rather than on individual activities. Plots of K_{ij}^{pot}(app) *vs.* a_j/a_i give unique response characterization. The importance of mixture responses for the determination of K_{ij}^{pot}(app) is emphasized. Examples of the two predicted types of response, *e.g.* apparent selectivity dependent on activity ratios or on individual activities, are illustrated by data for glass membranes.

REFERENCES

1 G. Eisenman in R. A. Durst (Ed.), *Ion Selective Electrodes*, N.B.S. Special Pub. 314, U.S. Government Printing Office, 1969, Ch. 1.
2 B. P. Nicolsky, *Zh. Fiz. Khim.*, 10 (1937) 495.
3 K. Horowitz, *Nature (London)*, 127 (1931) 440.
4 F. Conti and G. Eisenman, *Biophys. J.*, 5 (1965) 247.
5 G. J. Moody and J. D. R. Thomas, *Talanta*, 18 (1971) 125.
6 G. J. Moody and J. D. R. Thomas, *Talanta*, 19 (1972) 623.
7 G. Eisenman, D. O. Rudin and J. U. Casby, *Science*, 126 (1957) 831.
8 G. Eisenman in C. N. Reilley (Ed.), *Advances in Analytical Chemistry and Instrumentation*, Vol. 4, Interscience, New York, 1965.
9 G. Karreman and G. Eisenman, *Bull. Math. Biophys.*, 24 (1962) 413.
10 G. Eisenman, *Biophys. J.*, 2 (1962) 259.
11 R. P. Buck, *Anal. Chem.*, 45 (1973) 654.
12 R. P. Buck, J. H. Boles, R. D. Porter and J. A. Margolis, *Anal. Chem.*, 46 (1974) 254.
13 R. P. Buck and J. R. Sandifer, *J. Phys. Chem.*, 77 (1973) 2122.
14 J. N. Butler in R. A. Durst (Ed.), *Ion Selective Electrodes*, NBS Special Pub. 314, U.S. Government Printing Office, 1969, Ch. 5.
15 J. W. Ross, Jr. in R. A. Durst (Ed.), *Ion Selective Electrodes*, N.B.S. Special Pub. 314, U.S. Government Printing Office, 1969, Ch. 2.
16 J. W. Ross, Jr., *Science*, 156 (1967) 1378.
17 J. Bagg, R. Vinen and O. Nicholson, *J. Phys. Chem.*, 75 (1971) 2138.
18 J. Bagg and R. Vinen, *Anal. Chem.*, 44 (1972) 1773.
19 F. Conti and G. Eisenman, *Biophys. J.*, 6 (1966) 227.
20 J. P. Sandblom, G. Eisenman and J. L. Walker, Jr., *J. Phys. Chem.*, 71 (1967) 3862.
21 B. Lengyel and E. Blum, *Trans. Faraday Soc.*, 30 (1934) 461.
22 K. Srinivasan and G. A. Rechnitz, *Anal. Chem.*, 41 (1969) 1203.
23 E. Pungor and K. Toth, *Anal. Chim. Acta*, 47 (1969) 291.
24 E. Pungor and K. Toth, *Analyst (London)*, 95 (1970) 625.
25 M. Dole, *J. Amer. Chem. Soc.*, 53 (1931) 4260.
26 B. P. Nicolsky, M. M. Shultz, A. A. Belijusten and A. A. Lev in G. Eisenman (Ed.), *Glass Electrodes for Hydrogen and other Cations*, Dekker, New York, 1967, Ch. 6, p. 174.
27 R. G. Bates, *Determination of pH, Theory and Practice*, Wiley, New York, 1964, p. 316.
28 B. Lengyel, B. Csakvari and Z. Boksay, *Ann. Chim., Hung.*, 25 (1960) 225.
29 D. O.Jordan, *Trans. Faraday Soc.*, 34 (1938) 1305.
30 B. Lengyel and B. Csakvari, *Ann. Chim., Hung.*, 25 (1960) 239.

Analytica Chimica Acta, 73 (1974) 329–336

THE SPECTROPOLARIMETRIC BACK-TITRATIONS OF TIN(IV) AND ANTIMONY(III) IONS FROM THEIR D-(−)-*TRANS*-1,2-CYCLOHEXANEDIAMINETETRAACETATE COMPLEXES

K. W. STREET, Jr. and K. H. PEARSON

Department of Chemistry, Cleveland State University, Cleveland, Ohio 44115 (U.S.A.)

(Received 8th April 1974)

Spectropolarimetric titrimetry is a relatively new analytical technique first described by Kirschner *et al.*[1,2]. Continued interest in this technique and its potentialities was enhanced by the introduction of readily available commercial photoelectric polarimeters and later, by improvements in design and versatility[3,4]. Fundamental to this technique is the use of a photoelectric polarimeter to monitor the change in optical rotation of the solution as the titration proceeds. Parameters must be selected so that an inflection in the optical rotation occurs in the vicinity of the end-point. Spectropolarimetric titrimetry has been applied to acid–base titrations, as well as to different metal systems[2]. By utilizing stereospecific titrants, Pearson *et al.* have extensively increased the scope of this technique. The use of D-(−)-1,2-propylenediaminetetraacetic acid (D(−)PDTA) for the spectropolarimetric titrations of various metals has been well characterized[5–8]; sequential titrations are also possible[9]. The stereospecific titrant D-(−)-*trans*-1,2-cyclohexanediaminetetraacetic acid (D(−)CDTA) has also been used for many metal ions[10–12].

For the spectropolarimetric determinations of tin(IV) and antimony(III) ions, the chelating agent D(−)CDTA was selected as the complexing agent because of its stereospecificity, chelating strength, and intrinsic optical activity[11]. Cadmium(II) was chosen as back-titrant because of its large molecular rotation when complexed with D(−)CDTA, and large formation constant for the complex over the pH range necessary for the determination of these metal ions. Spectropolarimetric titrimetric techniques offer several advantages over other complexiметric methods. The most important advantage is that the pH range selected for the titration need only be restricted to where the reactions involving the back-titrant are quantitative and rapid, and where the metal to be determined has a fairly large formation constant. The pH range is not limited by the need for a sharp indicator color transition where the kinetics of the titration are slowest, because the reagents used serve as self-indicators and the end-point is determined by graphical extrapolation. The spectropolarimetric back-titrimetric procedures suggested in this paper for tin(IV) and antimony(III) are rapid, simple, require no external indicator or partially mixed organic solvent system, and the back-titrations are carried out at ambient temperatures.

CDTA forms more stable complexes (generally 1–2 log K units for most metal complexes) with most of the metal ions than does EDTA or PDTA[13]. The greater stability of the CDTA metal complexes compared to the EDTA and PDTA metal

complexes has been attributed to the fact that during chelation, the carbon chain between the nitrogen atoms on both EDTA and PDTA has to be rotated for the nitrogen atoms to be in the same plane as the metal ion for chelation to occur; whereas, the thermodynamically preferred chair configuration of the *trans*-CDTA, with the nitrogen atoms in equatorial positions, requires very little reorientation of the nitrogen atoms for chelation with the metal ion to occur.

Dwyer and Garvan[14] have shown that only two of the possible four isomers of octahedral metal chelates can be obtained, thereby proving that either one of the two optical isomers of *trans*-CDTA is completely stereospecific in its reaction with octahedral coordinated metal ions. The stereospecificity of this ligand has been attributed to the stereochemistry of the cyclohexane ring and its inability to accommodate certain chirality because of the steric hindrance between the methylene groups of the ring and the acetato groups (Fig. 1).

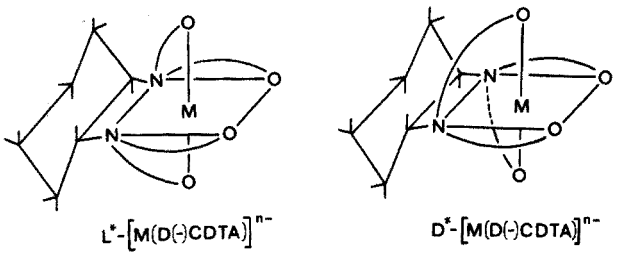

Fig. 1. Stereospecificity of D(−)CDTA to form L*-[M(D(−)CDTA)]$^{n-}$ complexes.

EXPERIMENTAL

Apparatus

A modified Perkin-Elmer Model 141 Photoelectric Polarimeter was used to monitor continuously the optical rotation of the solution during the titrations and to run the optical rotatory dispersion spectra[3–4]. The modifications consisted essentially of (1) attaching a Bausch and Lomb double-grating monochromator and high-intensity xenon light source to the Perkin-Elmer polarimeter and (2) adding a Perkin-Elmer potentiometer and Coleman Model 165 multi-speed, multi-millivolt recorder. The modified instrument has a wavelength range of 650–240 nm and because of the high intensity of the xenon lamp, can handle samples of high absorbances throughout the entire spectrum. A 1-dm flow-through quartz polarimeter cell with optically inactive endplates was used in all titrations. The titration vessel and titrimetric apparatus have been described previously[6]. A Corning Model 104 digital pH meter with a Sargent combination glass electrode was used for all pH measurements.

Reagents

All solutions were prepared from analytical reagent-grade chemicals (usually J. T. Baker), with demineralized water, and stored in polyethylene bottles.

D-(−)-trans-1,2-cyclohexanediaminetetraacetic acid (D(−)CDTA). Prepared by condensation of the resolved D(−)-*trans*-1,2-cyclohexanediamine with sodium chloroacetate in a strongly basic medium, followed by strong cation-exchange techniques to obtain the acid form as described previously[15]. An aqueous

0.5% solution of the D(−)CDTA had a specific rotation of −53.5° at 589 nm; literature values[15,16] for the anhydrous acid are −53.4° and −53.0°, respectively. Prepare all D(−)CDTA solutions by dissolving the appropriate amount of the free acid in enough sodium hydroxide solution to form the disodium species. Standardize against standard lead nitrate solutions at pH 5, with 10% hexamethylenetetramine solution to adjust the pH, with xylenol orange as the indicator[17].

Standard solutions of EDTA. Prepared from dry primary standard disodium dihydrogen ethylenediaminetetraacetate dihydrate (G. F. Smith Chemical Co.).

Aqueous ca. 0.1 M lead nitrate solutions. Standardize against the primary standard EDTA solution by the procedure for standardization of the D(−)CDTA solutions.

Tin(IV) chloride solution ($5.155 \cdot 10^{-2}$ M). Dissolve 6.1246 g of 99.9% pure tin sticks in concentrated hydrochloric acid, treat with 30% hydrogen peroxide and boil. (This ensures that all the tin is in the tin(IV) oxidation state; boiling is necessary to decompose excess of peroxide and tin(IV) peroxide complexes.) Cool and dilute to 1 l with water.

Antimony(III) solution. Dissolve *ca.* 3.4 g of 100.0% pure antimony trioxide in concentrated hydrochloric acid, and filter the insoluble residue through a very fine sintered glass crucible. Standardize iodometrically[18].

Standard iodine solution. Prepare and standardize as described in Skoog and West[18] using *ca.* 0.86 g of iodine dissolved in 1 l water with 1 g of potassium iodide.

Standard arsenic(III) solution. Dissolve 1.5035 g of primary standard arsenic trioxide in 6 *M* sodium hydroxide, adjust to pH 8.0 with dilute hydrochloric acid and dilute to 1 l (ref. 18).

Cadmium(II) perchlorate solutions. Dissolve the approximate amount of cadmium(II) perchlorate in 1 l of water. Standardize against a primary standard EDTA solution at pH 6.0 using 10% hexamethylenetetramine as buffer and xylenol orange indicator.

Acetate pH 5.0 buffer. Dissolve 102 g of sodium acetate in 500 ml of water and adjust the pH to 5.0 with *ca.* 28 ml of glacial acetic acid, before dilution to 1 l.

Acetate pH 3.0 buffer. Prepare as above from 50 g of sodium acetate, adjusting to pH 3.0 with glacial acetic acid.

Spectropolarimetric back-titrimetric procedures

Tin(IV). To an aliquot of the unknown tin(IV) solution to be determined, add an excess of D(−)CDTA and adjust the pH to 5.0 with concentrated sodium hydroxide solution. Boil the solution for 20 min. Allow the solution to cool and dilute to a known volume. Set the optical digital readout of the polarimeter to zero using an aqueous blank at 300 nm. Transfer an aliquot of the test solution to the titration vessel and add 25 ml of pH 5.0 buffer with enough deionized water to dilute to a known volume between 100 and 130 ml. Insert the flow-through polarimeter cell into the cell compartment and titrate the excess of D(−)CDTA with a standard cadmium(II) solution from a 5 ml microburet readable to ±0.001 ml as previously discussed[6]. Best results are obtained when the excess of D(−)CDTA is kept small, less than 10%, so that a dilute (0.01–0.03 *M*) cadmium(II) solution can be used as titrant.

Antimony(III). To an aliquot of the unknown antimony(III) solution to be

determined, add an excess of D(−)CDTA and adjust the pH to 3.0 with concentrated sodium hydroxide solution. Rapid adjustment of the pH causes a white precipitate to form which rapidly dissolves as the antimony complexes with the D(−)CDTA. After all of the precipitate has dissolved, dilute the solution to a known volume. Set the optical digital readout of the polarimeter to zero using an aqueous blank at 310 nm. Transfer an aliquot of the above solution to the titration vessel and add 25 ml of pH 3.0 buffer with enough deionized water to dilute to a known volume between 100 and 125 ml. Proceed from here as described for tin(IV).

RESULTS

The optical rotatory dispersion and absorption spectra for the metal complexes and D(−)CDTA were examined to determine the wavelength giving the maximum optical rotational difference with suitable transmittance. The absorption of D(−)CDTA was never the limiting factor in the selection of a suitable wavelength, but selection was limited, from *ca.* 300 nm down to 250 nm, by the increasing absorption of the metal complexes. Figure 2 shows the optical rotatory dispersion (o.r.d.) spectra of the tin–D(−)CDTA complex, the cadmium–D(−)-CDTA complex and the D(−)CDTA at pH 5.0. To obtain the ORD spectrum of the tin–D(−)CDTA complex, the standard tin(IV) chloride solution was reacted with a known excess of D(−)CDTA and slowly adjusted to about pH 5 with sodium hydroxide, the final pH adjustment being made with acetate buffer. From this spectrum and from the D(−)CDTA spectrum the rotation due to the excess D(−)CDTA in the tin–D(−)CDTA solution was calculated and subtracted from the observed spectrum to give the actual ORD spectrum of the tin–D(−)CDTA complex. From Fig. 2, it can be seen that the known solution titrated should have an initial positive rotation depending upon the relative concentrations of the tin–D(−)CDTA complex and the slight excess of D(−)CDTA. Thus, the ORD spectrum indicates that during tin titrations, the observed rotation will increase at first owing to the formation of the cadmium–D(−)CDTA complex and then remain constant as excess of cadmium(II) perchlorate is added.

Figure 3 shows the spectropolarimetric back-titration of 48.95 mg of tin at pH 5.0. This is a typical spectropolarimetric back-titration where the original metal complex has a large positive rotation, the titrant used in the back-titration forms

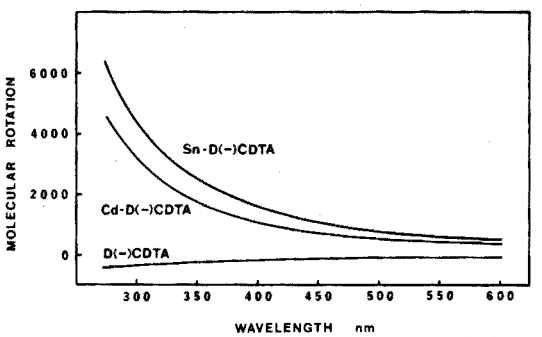

Fig. 2. Optical rotatory dispersion spectra of tin–D(−)CDTA complex, cadmium–D(−)CDTA complex, and D(−)CDTA at pH 5.0.

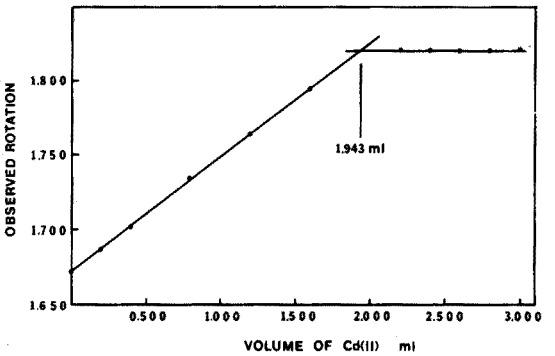

Fig. 3. Spectropolarimetric back titration of 48.95 mg of tin at 300 nm and pH 5.0.

a complex of positive rotation and the excess of titrant itself has no rotation. The back-titration of 11.39 mg of tin at pH 5 and at 300 nm gave a plot of similar shape, and again with a sharp end-point; but as expected, the initial observed rotation had a smaller positive value than that for the titration of 48.95 mg of tin, starting at *ca.* 0.500 and levelling off at *ca.* 0.650.

Figure 4 shows the effect of pH on the molecular rotations of the species involved in the back-titration of antimony(III). Both the antimony–D(−)CDTA complex and the cadmium–D(−)CDTA complex were prepared by reacting the metal and ligand in a 1:1 ratio and then diluting to a known volume. The solutions were titrated with concentrated sodium hydroxide from the 5-ml microburet and volume corrections were applied to obtain the molecular rotations. To obtain the effect of pH on the D(−)CDTA at 310 nm, the optically active free acid was dissolved in demineralized water, concentrated hydrochloric acid was added to adjust the pH and then the solution was titrated with concentrated sodium hydroxide and volume corrections were applied. Inspection of Fig. 4 indicates that antimony(III) must be titrated in the pH range 3.0–5.0. The minimal pH is 3.0 to insure quantitative formation of both the Sb–D(−)CDTA and Cd–D(−)CDTA complexes, and the maximal pH is 5.0 in order to insure complete formation of the antimony–D(−)CDTA complex.

Figure 5 shows the ORD spectra of the species involved in the back-titration of antimony(III) at pH 3.0 (acetate buffer). The selected wavelength for the titration of antimony(III) was 310 nm, where there are large rotational differences between the three species with suitable transmittance. From Figure 5, the back-titration curve for antimony(III) should resemble that of tin(IV); however, the Sb–D(−)CDTA complex is much less stable at pH 3 than the Cd–D(−)CDTA complex. This would lead one to expect that the change in rotation at the beginning of the titration would be positive because of the formation of the Cd–D(−)CDTA complex, as cadmium(II) reacts with the excess of D(−)CDTA. This is not the observed case up to the end-point because cadmium(II) begins to displace antimony(III) from its complex before all of the excess of *D*(−)CDTA has reacted. At pH 4.0 and 5.0 exchange begins almost immediately after the titration is started. At pH 3.0, this displacement before the end-point is much less severe and reliable data points may be collected

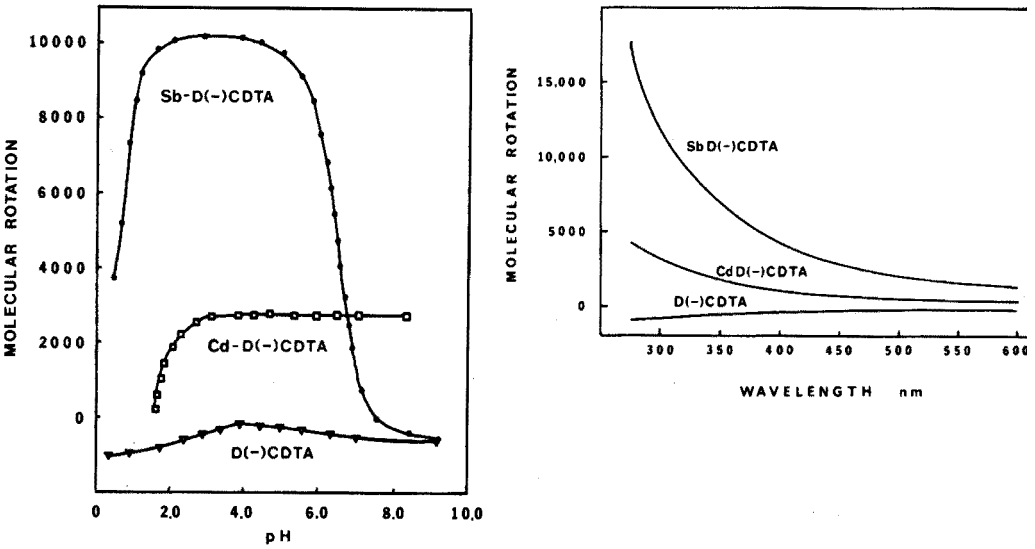

Fig. 4. Effect of pH on the molecular rotations of antimony–D(−)CDTA complex, cadmium–D(−)CDTA complex, and D(−)CDTA at 310 nm.

Fig. 5. Optical rotatory dispersion spectra of antimony–D(−)CDTA complex, cadmium–D(−)CDTA complex, and D(−)CDTA at pH 3.0.

before the end-point (first 50% of titration) when the cadmium(II) reacts with the excess of D(−)CDTA linearly as expected. After the end-point a negative sloping line would be expected as the cadmium–D(−)CDTA complex, which has a much lower positive optical rotational value, forms and the antimony–D(−)CDTA complex of higher positive rotational value is destroyed. In order to obtain the second straight-line portion of the titration curve, points cannot be collected before 150% of the calculated titration end-point. This metal–metal ion exchange with the displacement of the antimony(III) from its D(−)CDTA complex is quantitative and extremely rapid at ambient temperatures at a pH of 3.0.

Figure 6 shows the back-titration plot of 49.59 mg of antimony(III) with

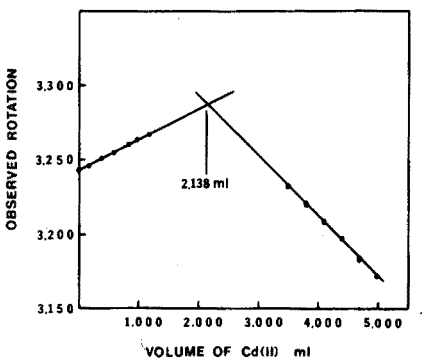

Fig. 6. Spectropolarimetric back-titration of 49.59 mg of antimony at 310 nm and at pH 3.0.

D(−)CDTA as chelating ligand and cadmium(II) perchlorate as the back-titrant at room temperature. All titrations of antimony(III) were performed at 310 nm in order to utilize maximum rotational changes without sacrifice of instrumental response owing to the tremendous amount of light absorption at lower wavelengths of the antimony–D(−)CDTA complex. Titration plots for 10.0 mg of antimony(III) were of similar shape but with observed rotations in the range 0.700–0.850. These titration plots are typical of back-titrations where the initial increased positive rotation is due to the formation of a complex with positive molecular rotation from an optically inactive titrant reacting with the excess of optically active ligand which has a negative molecular rotation; then metal–metal ion exchange occurs where the exchanging metal ion forms a complex which has a positive molecular rotation, which is less than the positive molecular rotation of the original species.

Table I gives the results of the spectropolarimetric back-titrations of tin(IV) and antimony(III). Each value reported is the average of at least three individual titrations.

TABLE I

RESULTS OF SPECTROPOLARIMETRIC TITRATION

Metal	*Amount of metal (mg)*		*Deviation*		*Wavelength (nm)*
	Taken	*Found*	*(mg)*	*(%)*	
Sn(IV)	48.95	48.87±0.04	−0.08	−0.16	300
	11.38	11.40±0.02	+0.02	+0.18	300
	5.689	5.675±0.006	−0.014	−0.25	300
Sb(III)	49.59	49.58±0.08	−0.01	−0.02	310
	24.99	24.95±0.01	−0.04	−0.16	310
	10.00	10.07±0.01	+0.07	+0.70	310

DISCUSSION

The spectropolarimetric back-titrations of tin(IV) are rapid and give very sharp end-points. Although the titrations reported were performed at pH 5.0, they could have been performed at a pH as low as 3.0. The tin(IV) solution should be titrated immediately after being prepared as the complex tends to precipitate in solutions containing more than 1 mg of tin(IV)–D(−)CDTA complex per ml when left overnight at pH 5.0.

The spectropolarimetric back-titrations of antimony(III) are simple, rapid and give very sharp end-points at ambient temperatures. There are few other complexiметric titrations for antimony(III), and none of these seems very satisfactory[17]. In the procedure described here, the second straight-line portion of the titration plot is probably the result of the ligand exchange between the monohydroxy antimony–D(−)CDTA complex, which is expected to have a very low stability constant like its EDTA analog[19], and the cadmium(II) titrant. Thus, spectropolarimetric titrimetry with stereospecific ligands, can accurately and rapidly allow, with a minimum of complications, determinations of both tin(IV) and antimony(III).

SUMMARY

Spectropolarimetric back-titrations are described for tin(IV) and antimony-(III); the optically active ligand D-(−)-*trans*-1,2-cyclohexanediaminetetraacetic acid (D(−)CDTA) is used as the complexing agent and cadmium(II) ion as the back-titrant. The optical rotation is monitored throughout the titration, and the optically active ligand and stereospecifically formed complexes serve as self-indicators. The end-points are determined graphically by straight-line extrapolations from a plot of volume-corrected observed rotations *versus* ml of titrant. The tin(IV) titration plots are representative of normal spectropolarimetric back-titrations and the antimony-(III) titration plots are representative of spectropolarimetric back-titrations where metal–metal ion exchange occurs after the end-point. These analyses are carried out in aqueous systems and the procedures for both the tin and antimony are rapid and simple.

REFERENCES

1 S. Kirschner and D. C. Bhatnager, *Anal. Chem.*, 35 (1963) 1069.
2 K. H. Pearson and S. Kirschner, *Anal. Chim. Acta*, 48 (1969) 339.
3 P. E. Reinbold and K. H. Pearson, *Anal. Chem.*, 43 (1971) 293.
4 S. J. Simon and K. H. Pearson, *Anal. Chem.*, 45 (1973) 620.
5 R. J. Palma, Sr., P. E. Reinbold and K. H. Pearson, *Anal. Chem.*, 42 (1970) 47; *Anal. Lett.*, 2 (1969) 553.
6 R. J. Palma, Sr. and K. H. Pearson, *Anal. Chim. Acta*, 49 (1970) 497.
7 D. L. Caldwell, P. E. Reinbold and K. H. Pearson, *Anal. Chim. Acta*, 49 (1970) 505; *Anal. Chem.*, 42 (1970) 416; *Anal. Lett.*, 3 (1970) 93.
8 K. W. Street, Jr. and K. H. Pearson, *Anal. Chim. Acta*, 63 (1973) 107; 71 (1974) 405.
9 R. J. Palma, Sr., P. E. Reinbold and K. H. Pearson, *Anal. Chim. Acta*, 51 (1970) 329.
10 P. E. Reinbold and K. H. Pearson, *Talanta*, 17 (1970) 391.
11 J. R. Baker and K. H. Pearson, *Anal. Chim. Acta*, 50 (1970) 255.
12 K. H. Pearson, J. R. Baker and P. E. Reinbold, *Anal. Chem.*, 44 (1972) 2090.
13 *Stability Constants of Metal-Ion Complexes*, The Chemical Society, London, 2nd edn., 1964.
14 F. P. Dwyer and F. L. Garvan, *J. Amer. Chem. Soc.*, 81 (1959) 2955.
15 P. E. Reinbold and K. H. Pearson, *Inorg. Chem.*, 9 (1970) 2325.
16 F. P. Dwyer and F. L. Garvan, *J. Amer. Chem. Soc.*, 83 (1961) 2610.
17 G. Schwarzenbach and H. Flaschka, *Complexometric Titrations*, Methuen, London, 1969.
18 D. A. Skoog and D. M. West, *Fundamentals of Analytical Chemistry*, Holt, Reinhart and Winston, New York, U.S.A., 2nd edn., 1969.
19 T. R. Bhat and R. K. Iyer, *Z. Anorg. Allg. Chem.*, 335 (1965) 331.

Analytica Chimica Acta, 73 (1974) 337–354

POLAROGRAPHIC REDUCTION OF ALDEHYDES AND KETONES PART XVIII.* ETHACRYNIC ACID

L. DESHLER** and P. ZUMAN

Department of Chemistry, Clarkson College of Technology, Potsdam, New York 13676 (U.S.A.)

(Received 5th June, 1974)

The α,β-unsaturated carbonyl compounds represent a series of compounds with two reactive centers. To express the relative reactivity of these two centers, a series of α,β-unsaturated compounds must be exposed to an interaction with one particular reagent. The simplest nucleophilic reagent able to attack such systems is the electron.

Electrochemical investigations based on measurement of current–voltage curves with a mercury dropping electrode proved to offer more simplified information about the course of the chemical transformation involved and relative reactivity of individual sites than other techniques. Polarographic investigations have proved that the nature of the group which undergoes transformation in the course of the electrode process depends on the nature of substituents R^1 and R^2 attached to the unsaturated grouping ($R^1CH{=}CH{-}COR^2$). For ketones, where R^2 = alkyl or aryl, the product of the two-electron electroreduction has been repeatedly proved[1–14] to be a saturated ketone. Greater variability has been found for α,β-unsaturated aldehydes ($R^2 = H$): for example with cinnamaldehyde ($R^1 = C_6H_5$), a saturated aldehyde is formed[15], whereas for crotonaldehyde formation of an unsaturated alcohol has been proved[16].

The formation of a saturated compound or unsaturated alcohol should not, however, be taken as evidence that the electron attacks either the double bond or the carbonyl group. In a conjugated system where the electron is transferred to a molecular orbital, it makes little sense to try to identify the point of electron attack. Any reduction of α,β-unsaturated systems in hydroxylic solvents is accompanied by a proton transfer. This proton transfer occurs either before (at lower pH) or after (in more alkaline solutions) the electron transfer. It is the site of this proton transfer which decides about the product formed; this site in turn, may depend on relative electron density—*i.e.* whether the carbonyl oxygen or the α-carbon of the ethylenic bond shows a higher electron density—and on the orientation and/or polarization of the molecule in the vicinity of the electrode.

The reactivity of α,β-unsaturated carbonyl compounds in homogeneous chemical reactions depends on the kind of the nucleophilic reagent involved. Quantitative information about such reactions—*i.e.*, rate and equilibrium constants—are rather scarce.

---

* Part XVII: *J. Electroanal. Chem.*, 46 (1973) 343.

** In partial fulfillment of M.Sc. requirements.

Water as a nucleophile shows little reactivity; most α,β-unsaturated compounds are not significantly hydrated on the carbonyl group[17]. Hydroxyl ions attack the C=C double bond and form ketols or aldols[18] rather than geminal diol anions as do benzaldehydes[19]. Similarly, carbanions in Michael additions attack predominantly the ethylenic bond[20–25], and thiolates add to the double bond[26–28]. However, for nitrogen-containing nucleophiles, formation of azomethine bonds[29] as well as of Mannich bases[30–33] is possible, depending on the amine used.

In most of these systems, there is little information available on the possibility of competitive attacks on both reaction centers. In order to carry out systematic comparison of the reactivity of various nucleophiles, it is necessary to find a model α,β-unsaturated carbonyl compound which is sufficiently soluble in hydroxylic solvents and which also shows limited reactivity towards hydroxyl ions. The nucleophiles frequently react in the conjugate base form which makes the use of higher pH values necessary.

A compound which seemed to fulfill such criteria is ethacrynic acid (I). This compound, the solubility of which is enhanced by the presence of the carboxyl group, shows no measurable change in concentration within 1 h even in 1 *M* sodium hydroxide solution.

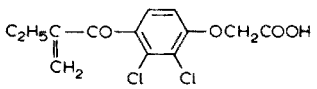

(I)

In order to use the polarographic waves of ethacrynic acid for its determination under various conditions, as needed in the study of kinetics and mechanisms of the reactions with various nucleophiles, it was necessary to investigate its polarographic behaviour over a wide range of pH. A detailed understanding of the changes of polarographic waves with pH and the processes which cause them, is an essential basis for general analytical application.

Ethacrynic acid is used in medicine as a diuretic agent[34]. Although a suitable pH has been reported for determinations of ethacrynic acid in the presence of its dimer[34], a more detailed understanding of its polarographic curves should extend analytical applications of the polarographic method in preparations and for pharmacological studies.

In the present paper, a more detailed examination of the electroreduction of ethacrynic acid is reported and some preliminary investigations of the reaction of this compound with primary amines are described.

EXPERIMENTAL

Apparatus

All d.c. polarographic measurements were carried out on the Sargent Polarograph XVI. A Kalousek cell was used in conjunction with a dropping mercury electrode (DME) and a saturated calomel reference electrode[35]. The electrode drop time (t_1) was 3.4 s in 1 *M* KCl at zero potential and a height of 80 cm of mercury.

Chemicals

Commercial chemicals were used without further purification. The ethacrynic

acid was kindly supplied by Merck, Sharp and Dohme Research Laboratories; acetophenone was a product of Eastman Kodak Co. The standard sulfuric acid and sodium hydroxide solutions were made from the J. T. Baker standard ampoules. All other chemicals for buffers and supporting electrolytes were of Baker Reagent grade.

Solutions

The universal Britton–Robinson buffer[36] was prepared. Simple buffers were prepared so that the ionic strength was constant and greater than 0.1 *M*, and in such a way that one buffer component was held constant while the pH was adjusted by varying concentration of the other buffer component (Table I). Nitrogen introduced into the Kalousek cell for de-aeration and mixing of the sample solution was of high purity, dry type from Linde.

BLE I

FFER COMPOSITION

Buffer	*pH Range*	*Component held constant*		*Variable component conc. range (M)*	*Ionic strength (M)*
		Species	*Conc. (M)*		
Phosphate	1.1– 3.1	NaH_2PO_4	0.100	0.011–0.900	0.10
Acetate	3.6– 5.7	CH_3COOH	0.050	0.005–0.450	0.45
Phosphate	5.5– 7.6	KH_2PO_4	0.015	0.002–0.135	0.50
Borate	7.7– 9.9	NaH_2BO_3	0.020	0.002–0.180	0.02
Borate	8.1–10.0	NaH_2BO_3	0.050	0.005–0.200	0.45
Ammonia	8.6–10.1	NH_3	0.050	0.006–0.450	0.45
Carbonate	8.8–11.1	$NaHCO_3$	0.050	0.006–0.450	1.40
Phosphate	10.4–11.4	Na_3PO_4	0.020	0.002–0.180	0.80
Phosphate	10.6–11.5	Na_3PO_4	0.013	0.001–0.117	0.45

Stock solutions of ethacrynic acid and acetophenone were prepared 0.01 *M* in 95% ethanol. This stock solution for ethacrynic acid was stable up to a period of 14 days after which the polarographic wave heights decreased, probably because of dimerization of the acid[34]. The stock solution of ethacrynic acid for titrimetric p*K* determinations was prepared $1 \cdot 10^{-3}$ *M* in (1+1) ethanol–water.

Procedures

Polarographic curves were recorded in a $2 \cdot 10^{-4}$ *M* solution prepared by addition of 9.8 ml of supporting electrolyte and 0.2 ml of the stock in the Kalousek cell; thus the final solution contained 2% ethanol. Solutions of higher ethanol concentrations (10–60%) were made by the addition of 0.8–5.8 ml of ethanol to a cell containing 0.2 ml of stock and 8.0–4.0 ml of supporting electrolyte. The cell solution was de-aerated and mixed for 3 min before polarographic curves were recorded. Solutions of higher ethanolic content than 2% necessitated longer de-aeration times.

The d.c. polarographic curves were investigated in universal Britton–Robinson buffer (Tables II, III), sulfuric acid and sodium hydroxide solutions and the simple buffers (Tables IV,V). The dependence of polarographic wave heights on

TABLE II

POLAROGRAPHIC DATA IN BRITTON–ROBINSON BUFFER FOR SOLUTIONS OF ETHACRYNIC ACID CONTAINING 60% ETHANOL

(Half-wave potentials $(E_{\frac{1}{2}})_i$ and diffusion current constants I_i)

pH	I_1	$(-E_{\frac{1}{2}})_1$	I_3	$(-E_{\frac{1}{2}})_3$
2.70	0.89	0.905		
2.92	0.89	0.930		
3.92	0.85	1.015		
4.58	0.85	1.060		
5.00	0.89	1.095		
5.15	0.83	1.120		
5.60	0.71	1.160		
5.80	0.54	1.160		
6.15	0.44			1.40
6.40	0.33		1.66	1.41
6.90	0.23		1.83	1.41
7.60	0.15		1.79	1.41
8.20	0.13		1.79	1.41
9.79	0.04		1.89	1.42
11.00	0.0		1.87	1.42
11.75	0.0		1.85	1.44

TABLE III

POLAROGRAPHIC DATA IN BRITTON–ROBINSON BUFFER FOR SOLUTIONS OF ETHACRYNIC ACID CONTAINING 2% ETHANOL

(Half-wave potentials $(E_{\frac{1}{2}})_i$ and diffusion current constants I_i)

pH	I_1	$(-E_{\frac{1}{2}})_1$	I_2	$(-E_{\frac{1}{2}})_2$	I_3	$(-E_{\frac{1}{2}})_3$
1.89	1.54	0.835	1.41	1.015		
2.09	1.67	0.850	1.77	1.045		
2.93	1.80	0.910	1.49	1.055		
3.48					3.31	1.00
3.87					3.31	1.035
4.12					3.36	1.040
4.40					3.23	1.050
4.53					3.34	1.065
4.69					3.31	1.075
4.85					3.44	1.095
5.11					3.54	1.10
6.11					3.70	1.160
6.68					3.81	1.210
7.69					3.88	1.230
8.99					3.47	1.250
9.66					3.67	1.280

concentration of ethacrynic acid was studied by adding 0.2–1.0 ml of the stock to solutions containing a buffer of a chosen pH and ethanol concentration. Addition of ethanolic stock solution resulted in some changes in the final ethanol concentration.

E IV

ROGRAPHIC DATA IN SIMPLE BUFFERS FOR SOLUTIONS OF ETHACRYNIC ACID CONING 60% ETHANOL

wave potentials ($E_{\frac{1}{2}}$)$_i$; currents for $2 \cdot 10^{-4}$ *M* solution in μA, numbers of buffers refer to Table I)

i_1	$(E_{\frac{1}{2}})_1$	i_2	$(E_{\frac{1}{2}})_2$	*pH*	i_3	$(E_{\frac{1}{2}})_3$	*pH*	i_3	$(E_{\frac{1}{2}})_3$
hate buffer (No. 1)				*Borate buffer (No. 4)*			*Ammonia buffer (No. 6)*		
0.36	−0.86	0.53	−1.07	9.70	0.71	−1.45	8.38	0.82	−1.23
0.37	−0.90	0.61	−1.12	10.38	0.72	−1.46	8.60	0.82	−1.26
0.38	−0.92			10.72	0.70	−1.46	8.79	0.78	−1.27
0.38	−0.93			10.92	0.73	−1.48	8.98	0.86	−1.27
0.38	−0.95			11.20	0.76	−1.47	9.15	0.80	−1.29
0.42	−0.96			11.38	0.76	−1.48	9.33	0.80	−1.30
0.34	−0.96			11.62	0.73	−1.48	9.50	0.78	−1.31
0.38	−0.99			11.95	0.73	−1.48	9.72	0.80	−1.32
0.38	−1.02			12.30	0.72	−1.48	10.05	0.82	−1.33
				Borate buffer (No. 5)			*Carbonate buffer (No. 7)*		
i_3	$(E_{\frac{1}{2}})_3$			9.80	0.80	−1.34	10.26	0.88	−1.32
				10.30	0.78	−1.36	10.58	0.78	−1.32
hate buffer (No. 3)				10.58	0.80	−1.36	10.78	0.72	−1.33
0.85	−1.28			10.78	0.70	−1.36	10.97	0.75	−1.33
0.80	−1.29			11.05	0.82	−1.37	11.17	0.70	−1.33
0.76	−1.30			11.25	0.82	−1.38	11.37	0.76	−1.34
0.78	−1.30			11.38	0.76	−1.38			
0.75	−1.29			11.82	0.76	−1.40			
0.75	−1.30								
0.83	−1.30								
0.76	−1.32								
0.74	−1.35								

The dependence of polarographic waves on mercury pressure was measured in solutions containing $2 \cdot 10^{-4}$ *M* ethacrynic acid by adjusting the height of the mercury column between 50 and 100 cm above the capillary tip.

Controlled potential electrolysis

Controlled potential electrolyses were carried out with a dropping mercury electrode on a 1.0- or 2.5-ml sample solution in a vessel designed by Manoušek[37]. The potential source was the Cambridge Polarographic Analyzer 82P. A Hewlett–Packard X–Y recorder Model 135A was used in conjunction with the Cambridge instrument to record polarographic curves at selected time intervals during the electrolysis.

These experiments involved a $1 \cdot 10^{-3}$ *M* concentration of ethacrynic acid. After the addition of 1 ml of the sample into the electrolysis cell, the cell solution was de-aerated and stirred by the introduction of nitrogen gas. The electrolyses were carried out under conditions identical with those of polarography (buffer concentration, percentage ethanol) at specified pH values, and at the potential of the limiting current of the first wave i_3 (Table VI). The electrolysis was interrupted after chosen time intervals to record polarographic *i–E* curves, in order

TABLE V

POLAROGRAPHIC DATA IN SIMPLE BUFFERS FOR SOLUTIONS OF ETHACRYNIC ACID CONTAINING 2% ETHANOL

(Symbols as used in Table IV)

pH	$(E_{\frac{1}{2}})_{a_1}$	i_1	$(E_{\frac{1}{2}})_1$	i_2	$(E_{\frac{1}{2}})_2$
Phosphate buffer (No. 1)					
1.09	−0.64	0.44	−0.77	0.40	−0.95
1.49	−0.66	0.46	−0.81	0.32	−0.97
1.73	−0.69	0.56	−0.85	0.50	−0.99
1.92	−0.69	0.48	−0.83	0.41	−0.97
2.11	−0.71	0.52	−0.85	0.46	−0.99
2.28	−0.72	0.51	−0.85	0.51	−0.99
2.47	−0.73	0.54	−0.87	0.44	−0.99
2.70	−0.73	0.50	−0.88	0.52	−0.99
3.06	−0.76	0.46	−0.89	0.52	−1.015

pH	i_3	$(E_{\frac{1}{2}})_3$	i_{a_2}	$(E_{\frac{1}{2}})a_2$
Phosphate buffer (No. 3)				
5.51	1.06	−1.09	0.24	−1.30
5.86	1.14	−1.13	0.31	−1.30
6.09	1.14	−1.16	0.27	−1.30
6.28	1.13	−1.16	0.27	−1.30
6.48	1.11	−1.17	0.42	−1.29
6.67	1.14	−1.18	0.38	−1.31
6.88	1.13	−1.17	0.31	−1.28
7.16	1.18	−1.18	0.19	−1.30
7.65	1.06	−1.20	0.22	−1.31

pH	i_3	$(E_{\frac{1}{2}})_3$
Borate buffer (No. 4)		
7.72	1.21	−1.24
8.32	1.12	−1.25
8.61	1.09	−1.27
8.80	1.13	−1.28
9.00	1.12	−1.29
9.18	1.12	−1.30
9.38	1.16	−1.31
9.62	1.12	−1.32
9.92	1.10	−1.33
Borate buffer (No. 5)		
8.10	0.95	−1.17
8.55	0.96	−1.19
8.82	0.98	−1.20
8.99	1.18	−1.21
9.22	1.20	−1.22
9.42	1.20	−1.23
9.52	1.18	−1.24
9.95	1.16	−1.25

pH	i_3	$(E_{\frac{1}{2}})_3$	i_4	$(E_{\frac{1}{2}})_4$
Ammonia buffer (No. 6)				
8.59	1.11	−1.16	0.42	−1.52
8.78	1.20	−1.19	0.22	−1.57
8.95	1.20	−1.20	0.21	−1.60
9.12	1.24	−1.21	0.21	−1.59
9.28	1.24	−1.22	0.14	−1.61
9.44	1.16	−1.24	0.21	−1.61
9.61	1.22	−1.24	0.18	−1.62
9.87	1.21	−1.25	0.21	−1.60
10.09	1.24	−1.27	0.18	−1.63
Carbonate buffer (No. 7)				
9.16	1.14	−1.19	0.26	−1.54
9.37	1.11	−1.19	0.37	−1.56
9.56	1.16	−1.20	0.28	−1.58
9.75	1.20	−1.20	0.26	−1.56
9.94	1.18	−1.21	0.36	−1.56
10.15	1.20	−1.22	0.30	−1.57
10.48	1.16	−1.23	0.46	−1.57
11.09	1.18	−1.26	0.73	−1.58
Phosphate buffer (No. 8)				
10.37	1.14	−1.26	0.34	−1.58
10.45	1.20	−1.26	0.35	−1.56
10.82	1.12	−1.28	0.59	−1.57
10.97	1.25	−1.29	0.70	−1.56
11.10	1.06	−1.30	0.42	−1.57
11.21	1.13	−1.29	0.53	−1.56
11.30	1.26	−1.30	0.52	−1.56
11.37	1.15	−1.30	0.56	−1.55

TABLE VI

POTENTIALS USED IN CONTROLLED POTENTIAL ELECTROLYSIS

Buffer	*pH*	*Percent ethanol*	*Ionic strength (M)*	*Potential applied CPE (V)*	*Approximate $E_{\frac{1}{4}}$ of 2nd wave i_4 (V)*
Phosphate	11.06	10	0.80	−1.40	−1.6
Carbonate	9.37	60	1.40	−1.36	−1.7
Borate	9.38	60	0.02	−1.50	−1.8
Ammonia	9.44	60	0.45	−1.30	−1.7

to measure wave heights and the ratio of wave heights. Because the time for electrolysis was long (24 h), nitrogen was passed over the surface of the cell solution continuously.

pH Measurements

The pH values of buffer solutions were determined with a Corning digital 112 pH meter with a combination reference–glass electrode (Sargent 30072-15). The meter was standardized with a standard borax or hydrogen phthalate buffer for aqueous solutions and solutions containing 2% ethanol, and standard borax and acetate solutions in 50% methanol[38] for measurements of relative pH values in 60% ethanolic solutions.

Solutions of ethacrynic acid showed no characteristic changes of absorption band in electronic spectra. To determine the pK value of ethacrynic acid, potentiometric titrations were done in 50% ethanolic solutions with the above pH meter and glass electrode. Since polarographic measurements indicated the possibility of complex formation with boric acid, titrations were also carried out in the presence of varying concentrations of boric acid. The pK value of 4.6 was found to be independent of the boric acid concentration.

i–t Curves

Current–time curves were studied in the Kalousek cell containing $2 \cdot 10^{-4}$ M ethacrynic acid solution and with the Sargent Polarograph XVI as a potential source. A Tektronix Type 564B oscilloscope was placed across a 10 KΩ resistor which was in series with the polarographic cell.

RESULTS AND DISCUSSION

Solutions containing 60% ethanol

Reduction of ethacrynic acid (I) in 60% ethanolic solutions, which are less affected by adsorption phenomena than solutions with lower ethanol content, takes place in a two-electron step. At lower pH values, this process occurs in two one-electron steps i_1 and i_2 (Fig. 1). Above pH 2, the second wave is obscured by the current of supporting electrolyte and cannot be measured. The half-wave potentials of both waves i_1 and i_2 are pH-dependent and shift to negative potentials with 60 mV/pH (Fig. 2). Above pH 4.5 the height of wave i_1 decreases with increasing

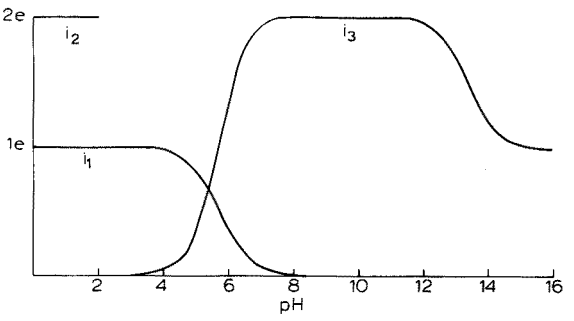

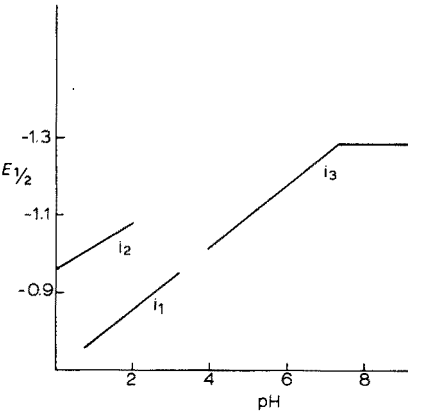

Fig. 1. The dependence of the average values of mean limiting currents i_1 and i_2 on pH for ethacrynic acid in buffer solutions containing 60% ethanol.

Fig. 2. The dependence of half-wave potentials (*vs.* SCE) of ethacrynic acid on pH in buffered solutions containing 60% ethanol.

pH in the shape of a dissociation curve with pK' 5.7. This decrease is accompanied by an increase of wave i_3 at more negative potentials in the shape of a dissociation curve with the same pK' as 5.7. This wave reaches at pH 7 a constant value corresponding to a two-electron reduction. The height of wave i_3 (Fig. 1) remains unchanged up to pH 11 and then decreases somewhat with increasing pH until above pH 14 it reaches a value corresponding to a one-electron process. The half-wave potential of this wave remains practically constant up to pH 12 (Fig. 2).

The pivotal point in the interpretation of this behavior is the pH-independence of both the wave height and the half-wave potential of wave i_3 over the pH range 7–11 (Tables II,IV; borate buffer no. 4). This pH-independence indicates that in the two-electron process a species is reduced which predominates in the bulk of the solution. As the pH in such solutions is higher than the pK of ethacrynic acid (pK 4.6), it can be concluded that the anion II is reduced in wave i_3.

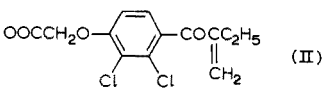

(II)

The pH-dependence of both wave height i_1 and the half-wave potential of this wave indicates reduction of a more protonated form than that present in the bulk of the solution. Principally, reduction of the free acid (I) or of the protonated form (III) can be considered. The fact that the observed dissociation curve in simple buffers has a shape corresponding to the transfer of two rather than of one hydrogen ion indicates reduction of protonated form III. This conclusion also agrees with the fact that form III is one proton richer than the form predominating in the bulk of solution, and also can explain the difference in potentials of waves i_1 and i_3 in the pH range where they coexist. A protonation of II on the carboxyl group to form I alters the electron density on the site so far removed

from the electroactive center COCH=C that it would hardly affect the reactivity of the compound.

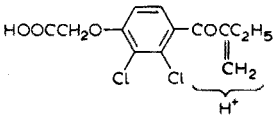

(III)

Hence the proposed reaction scheme is as follows (Ar = 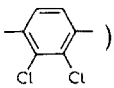)

$$HOOCCH_2O\text{-}Ar\text{-}COCC_2H_5 \underset{\underbrace{CH_2}_{H^+}}{\overset{\parallel}{\rightleftharpoons}} HOOCCH_2O\text{-}Ar\text{-}\underset{CH_2}{\overset{\parallel}{COCC_2H_5}} + H^+ \quad (1)$$
$$pK_1$$

$$HOOCCH_2O\text{-}Ar\text{-}\underset{CH_2}{\overset{\parallel}{COCC_2H_5}} \rightleftharpoons {}^-OOCCH_2O\text{-}Ar\text{-}\underset{CH_2}{\overset{\parallel}{COCC_2H_5}} + H^+ \quad (2)$$
$$pK_2$$

$$HOOCCH_2O\text{-}Ar\text{-}\underset{\underbrace{CH_2}_{H^+}}{\overset{\parallel}{COCC_2H_5}} + e \rightarrow HOOCCH_2O\text{-}Ar\text{-}\underset{\cdot CH_2}{\overset{|}{COCHC_2H_5}} \quad i_1 \quad (3)$$

$$HOOCCH_2O\text{-}Ar\text{-}\underset{\cdot CH_2}{\overset{|}{COCHC_2H_5}} + e + H^+ \rightarrow HOOCCH_2O\text{-}Ar\underset{CH_3}{\overset{|}{COCHC_2H_5}} \quad i_2 \quad (4)$$

$$^-OOCCH_2O\text{-}Ar\text{-}\underset{CH_2}{\overset{\parallel}{COCC_2H_5}} + 2e \rightarrow {}^-OOCCH_2O\text{-}Ar\text{-}\underset{O^-\ CH_2^-}{\overset{|\quad|}{C{=}CC_2H_5}} \quad i_3 \quad (5)$$
(A)

$$^-OOCCH_2O\text{-}Ar\text{-}\underset{O^-\ CH_2^-}{\overset{|\quad|}{C{=}CC_2H_5}} + 2H^+ \underset{k_{-6}}{\overset{k_6}{\rightleftharpoons}} {}^-OOCCH_2O\text{-}Ar\text{-}\underset{OH\ \ CH_3}{\overset{|\quad|}{C{=}CC_2H_5}} \quad (6)$$
(B)

$$^-OOCCH_2O\text{-}Ar\text{-}\underset{O^-\ CH_2^-}{\overset{|\quad|}{C{=}CC_2H_5}} + 2H^+ \underset{k_{-7}}{\overset{k_7}{\rightleftharpoons}} {}^-OOCCH_2O\text{-}Ar\underset{O\ \ CH_3}{\overset{\|\quad|}{C\text{-}CHC_2H_5}} \quad (7)$$
(C)

In the bulk of the solution, pK_1 is several pK units smaller than pK_2, but at the electrode surface, probably owing to the strong adsorption of the cation, the surface value of pK_1 becomes comparable with pK_2 and both proton transfers occur simultaneously.

No reduction wave of the saturated ketone (C) was observed in 60% ethanol. This is not caused by the too negative potential of (C) and overlapping

of the supporting electrolyte current, but rather by the decrease in the rate of keto form formation with rate constant k_7 with increasing ethanol concentration. As protonation with rate constant k_6 produces the electroinactive enol form (B) in a very fast reaction, the height of the reduction wave of the keto form (C) will be governed by the rate of dissociation of the enol (B) with constant k_{-6} (which is usually considered fast) and by the rate of protonation on carbon atoms with constant k_7.

That a saturated ketone (C) rather than an unsaturated alcohol is formed in the two-electron step was proved by the appearance of the more negative reduction wave of the saturated ketone in buffers containing 2% ethanol and by the increase in the height of this more negative wave in the course of controlled potential electrolysis (Fig. 3), where the transformation of the enol into keto form has sufficient time to take place.

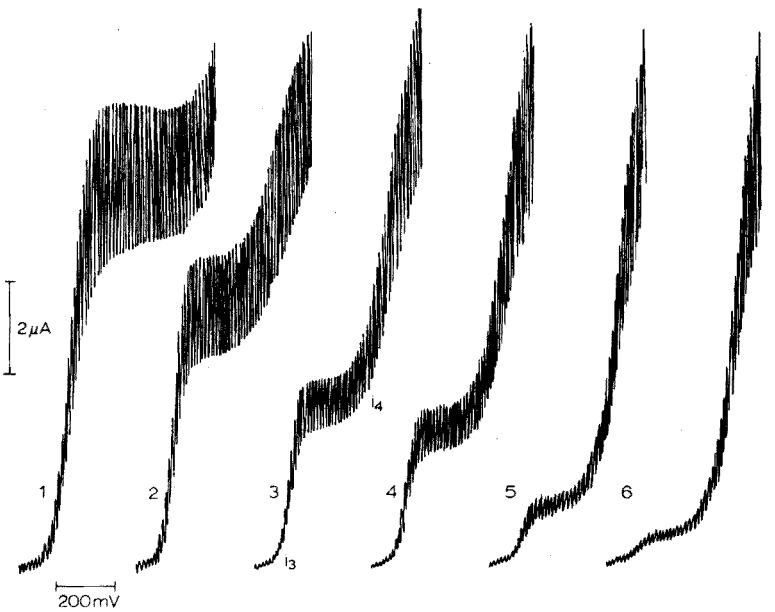

Fig. 3. Decrease of the reduction wave of ethacrynic acid (i_3) and increase of the wave (i_4) of the saturated ketone (C) in the course of controlled potential electrolysis. The electroreduction was carried out at the potential corresponding to the limiting current of wave i_3 (−1.45 V) in 2.5 ml of a solution containing $1 \cdot 10^{-3}$ *M* ethacrynic acid and 60% ethanol. Time of electrolysis: (1) 0, (2) 10, (3) 22, (4) 27.5, (5) 45, (6) 68 h. Curves start at −1.25 V *vs.* SCE.

The observed course of reduction resembles that of other α,β-unsaturated ketones[1–14] in that in the first two-electron step a saturated ketone is formed. Moreover, below pH 2 the reduction takes place in two one-electron steps, as with most other unsaturated ketones.

Contrary to other α,β-unsaturated ketones studied in more detail[4,9] where the half-wave potentials are shifted to more negative values up to pH 10, the half-wave potentials of ethacrynic acid remain pH independent at pH 7–11. Moreover, whereas for chalcone[4] the two one-electron processes remain separated over the whole

pH range, and for phenylvinyl ketone[9] above pH 7, in the case of ethacrynic acid it is possible to observe one two-electron step already above pH 4. Moreover, in none of the cases studied previously was it possible to observe a decrease of the wave of the protonated form with increasing pH, whereas for ethacrynic acid the one-electron wave i_1 decreases above pH 4 and that of the two-electron wave i_3 increases with increasing pH in the shape of a dissociation curve.

These differences may arise from the presence of either an alkyl group on the ethylenic group or the carboxylic group in the side chain. In both cases the orientation at the electrode surface would be affected. It is, in particular, possible that the negative charge of the carboxylate group, when the pH greatly exceeds pK_2, causes a repulsion from the negatively charged surface and prevents surface protonation above pH 5, as observed with chalcone[4], phenyl vinyl ketone[9], or unsaturated ketosteroids[39].

When current–voltage curves were recorded in the pH range between 8 and 11 in buffers prepared from boric acid (No. 5, Table I) or carbonates (No. 7), the total wave height remained constant, corresponding to two electrons, but the wave became more drawn out.

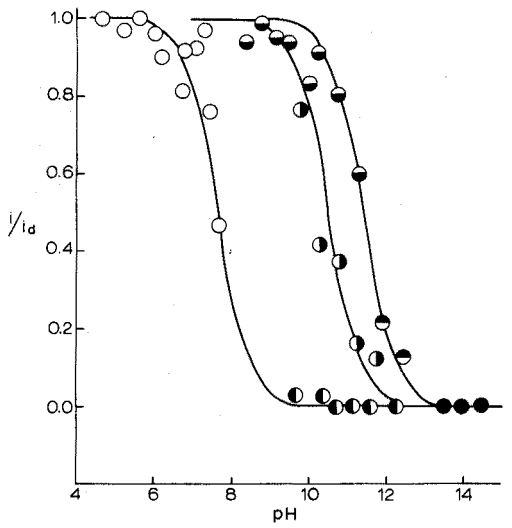

Fig. 4. The dependence of currents at -1.35 V on pH for $2 \cdot 10^{-4}$ *M* ethacrynic acid solutions containing 60% ethanol. Buffers (Table I): (○) No. 2,3, (◐) No. 4, (◑) No. 5, (◒) No 6, (◓) No. 7, (●) NaOH solutions.

When the current was measured at a potential corresponding to the rising portion of the polarographic wave close to the half-wave potential, it was found to decrease with increasing pH in the shape of a dissociation curve (Fig. 4). This dependence together with the formation of two linear pH-dependent sections on the logarithmic analysis indicates formation of two waves. Half-wave potentials of these two waves differ by less than 0.1 V and the height of the more positive wave decreases with increasing pH at the expense of increasing the more negative one. This behavior was not observed in low ionic strength borate buffers (No. 4, Table I).

The decrease of the current can be interpreted as due to the interaction between the buffer component and electroactive species. The observation that the current decreases to zero value (rather than to a value corresponding to a one-electron transfer) indicates that the interaction takes place as a preceding rather than interposed reaction. Borates are known to form complexes with α-hydroxyketones and 1,2-diketones[40–44] but such groups are not present in the acid I. The possibility of complex formation in the α-alkoxycarboxy portion ($R–OCH_2COOH$) of the ethacrynic acid molecule was excluded by the negative result of the study of the effect of boric acid on the pK value of I. At any rate, a relatively small change in the side chain to a benzene ring to which the electroactive group is attached, would not be expected to alter substantially the properties of the electroactive center.

Hence, the alternative possibility, *i.e.* the interaction of the buffer component with the –COC=C grouping, must be considered. The fact that the inflection points of the current–pH plots for borates (about pH 10.5) and carbonates (about pH 11.4) are close to the pK values of the acid dissociations of boric acid and of the HCO_3^- ion indicates that only the conjugate bases of the couples, *i.e.* the borate or carbonate anion, participate in the reaction. A possibility of nucleophilic addition of these anions to the unsaturated ketone must be considered. A similar reaction has been recently observed between carbonates and benzaldehydes[45].

Solutions containing 2% ethanol

In buffered aqueous solutions containing 2% ethanol, reduction waves i_1, i_2, and i_3 showed similar dependence of wave heights and half-wave potentials on pH as observed in 60% ethanol (Figs. 1 and 2). The wave i_1 was, however, preceded by an adsorption prewave (i_{a_1}) at potentials about 150 mV more positive than wave i_1. The height of wave i_{a_1} is concentration-independent at concentrations above *ca.* $7 \cdot 10^{-5}$ M. At a given concentration the height of this wave is a linear function of mercury pressure. Also the shape of the i–t curve, showing the dependence of the instantaneous current on time during the life of a single drop, shows an increase in current followed by a decrease, which is typical for adsorption processes (Fig. 5).

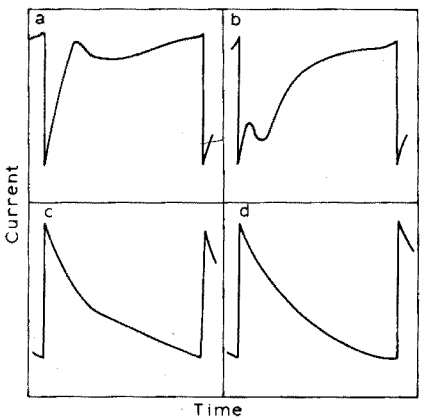

Fig. 5. The dependence of the instantaneous current (i) on time during the life of a single drop in a $2 \cdot 10^{-4}$ M ethacrynic acid solution containing acetate buffer pH 4.20 and 2% ethanol. Potentials: (a) −0.9, (b) −1.1, (c) −1.3, (d) −1.5 V *vs.* SCE (schematic).

The shift of the half-wave potentials of wave i_{a_1} with pH parallelled that of wave i_1.

At potentials about 170 mV more negative than wave i_2, another wave (i_{a_2}) was observed. The shape of the i–t curve in a $1 \cdot 10^{-3}$ M solution of ethacrynic acid at pH 4.2 indicated adsorption processes at the limiting current of wave i_2. It is assumed that this indistinct wave i_{a_2} may correspond to desorption of the product formed in wave i_2. It cannot be excluded that this wave corresponds to the wave attributed[34] to dimer formation.

Contrary to the results in 60% ethanol, the half-wave potentials of wave i_2 above pH 2 became dependent on pH and shifted to more positive values with decreasing pH (Table III; buffer No. 1, Table V). However, the wave i_2 remained measurable even over pH 2–4, where it was overlapped in 60% ethanol.

The most substantial difference between the behavior of ethacrynic acid in 60% and 2% ethanolic solutions lies, however, in the reducibility of the saturated ketone (C) (*cf.* eqn. 7). Whereas no wave was observed in 60% ethanolic solutions, a new wave (i_4) was observed at -1.6 V (*i.e.*, by about 0.3 V more negative than wave i_3) in solutions containing 2% ethanol above pH 8. The half-wave potential of this wave is pH-independent, whereas its height increases with increasing pH in the shape of a dissociation curve with an inflection point at about pH 10.0 (Fig. 6). Above pH 11 the height of this wave becomes pH-independent and corresponds to a one-electron transfer.

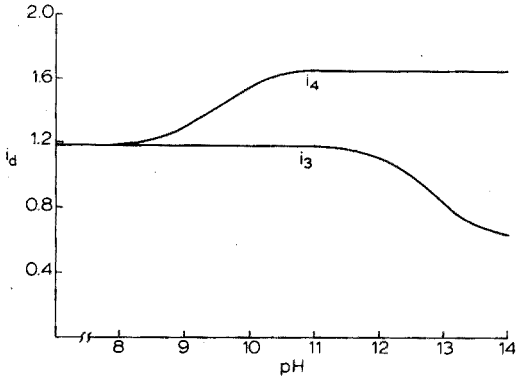

Fig. 6. The dependence of the average values of mean limiting currents i_3 and i_4 on pH for ethacrynic acid in buffer solutions containing 2% ethanol.

The increase in the height of wave i_4 can be interpreted by means of eqns. (5)–(7) as follows: the product of the first two-electron step (5), the dianion (A), is rapidly protonated by reaction (6) with rate constant k_6 to form the enol (B). With increasing pH, the equilibrium (6) is shifted to the left-hand side and the concentration of the anion (A) increases. This, in turn, results in an increase of the rate of protonation, with rate constant k_7. The equilibrium of reaction (7) is under these conditions shifted in favor of the keto-form (C). The inflection of the pH-dependence of wave i_4 at about pH 10.0 thus corresponds to the acid dissociation constant of reaction (6).

This interpretation assumes that the pK_6 (which is the dissociation constant of reaction 6) is smaller than pK_7. This is in agreement with the fact that for aryl

alkyl ketones the equilibrium between the keto and enol form is shifted in favor of the keto form, which is possible[46] when pK_7 greatly exceeds pK_6. Also the pK values of aryl alkyl benzenes are known[47] to be of the order of 19.

Above pH 11, the total height of waves (i_3+i_4) remained constant and corresponded to a three-electron reduction, but the relative heights of waves i_3 and i_4 varied. The height of wave i_3 decreased in a shape of a dissociation curve from a height corresponding to a two-electron process to a height indicating a one electron process (Fig. 6). Simultaneously, the height of wave i_4 increased to reach a value corresponding to a two-electron process. This behavior is in accordance with the following reduction scheme (8)–(14):

$$^{-}OOCCH_2O\text{–}ArCOCC_2H_5 + e \xrightarrow{E_3} [^{-}OOCCH_2O\text{–}ArCOCC_2H_5]^{\cdot} \quad (8)$$
$$\qquad\qquad\qquad\quad \| \qquad\qquad\qquad\qquad\qquad\quad \|$$
$$\qquad\qquad\qquad\quad CH_2 \qquad\qquad\qquad\qquad\qquad\quad CH_2$$

$$[^{-}OOCCH_2O\text{–}ArCOCC_2H_5]^{\cdot} + H^{+} \underset{k_{-9}}{\overset{k_9}{\rightleftharpoons}} {}^{-}OOCCH_2O\text{–}ArCOCC_2H_5 \quad (9)$$
$$\qquad\qquad\qquad\quad \| \qquad\qquad\qquad\qquad\qquad\quad |$$
$$\qquad\qquad\qquad\quad CH_2 \qquad\qquad\qquad\qquad\qquad\quad CH_3$$

$$^{-}OOCCH_2O\text{–}ArCOCC_2H_5 + e \xrightarrow{<E_3} {}^{-}OOCCH_2OArCOCC_2H_5 \quad (10)$$
$$\qquad\qquad\qquad\quad | \qquad\qquad\qquad\qquad\qquad\quad |$$
$$\qquad\qquad\qquad\quad CH_3 \qquad\qquad\qquad\qquad\qquad\quad CH_3$$

$$^{-}OOCCH_2OArC{=}CC_2H_5 + H^{+} \underset{k_{-11}}{\overset{k_{11}}{\rightleftharpoons}} {}^{-}OOCCH_2OArC{=}CC_2H_5 \quad (11)$$
$$\qquad\qquad\qquad\quad | \ \ | \qquad\qquad\qquad\qquad\qquad\quad | \ \ |$$
$$\qquad\qquad\qquad\quad O^{-} \ CH_3 \qquad\qquad\qquad\qquad\qquad\quad OH \ \ CH_3$$

$$^{-}OOCCH_2OArC\text{–}CC_2H_5 + H^{+} \underset{k_{-12}}{\overset{k_{12}}{\rightleftharpoons}} {}^{-}OOCCH_2OArCOCC_2H_5 \quad (12)$$
$$\qquad\qquad\qquad\quad \| \ \ | \qquad\qquad\qquad\qquad\qquad\quad |$$
$$\qquad\qquad\qquad\quad O \ \ CH_3 \qquad\qquad\qquad\qquad\qquad\quad CH_3$$

$$^{-}OOCCH_2OArCOCC_2H_5 + e \xrightarrow{E_4} {}^{-}OOCCH_2OArCOCC_2H_5 \quad (13)$$
$$\qquad\qquad\qquad\quad | \qquad\qquad\qquad\qquad\qquad\quad |$$
$$\qquad\qquad\qquad\quad CH_3 \qquad\qquad\qquad\qquad\qquad\quad CH_3$$

$$[^{-}OOCCH_2O\text{–}ArCOCC_2H_5]^{\cdot} + e \xrightarrow{E_4} {}^{-}OOCCH_2OArC{=}CC_2H_5 \quad (14)$$
$$\qquad\qquad\qquad\quad \| \qquad\qquad\qquad\qquad\qquad\quad | \ \ |$$
$$\qquad\qquad\qquad\quad CH_2 \qquad\qquad\qquad\qquad\qquad\quad O^{-} \ CH_2^{-}$$

Hence, at pH 11 protonation of the radical anion formed in reaction (8), with rate constant k_9, is rapid, and converts during the drop-life all the radical anion into radical which is immediately further reduced in reaction (10) so that a single two-electron wave i_3 results. The carbanion produced in this reaction (10) is then reduced in process (13), where the wave height is governed by the position of equilibrium (11) and rate constant k_{12}.

At pH 14, the reduction of ethacrynic acid proceeds only in step (8) to the radical anion. Its protonation in step (9) is so slow at this pH that no significant amount of the radical anion is converted to radical. The radical is also reduced in

reaction (14), but at more negative potentials. The potential of this reduction is so close to that of reaction (13) that only one wave i_4 is observed, corresponding to the sum of processes (13) and (14).

The increase in the height of wave i_4 in 0.05 *M* sodium hydroxide with increasing sodium ion concentration (Fig. 7) indicates formation of an ion-pair or ketyl in a reaction of the radical anion produced in reaction (13) and sodium ions. The ketyl is evidently reduced at potentials close to or more positive than E_4, as happens, for other aryl alkyl ketones[48].

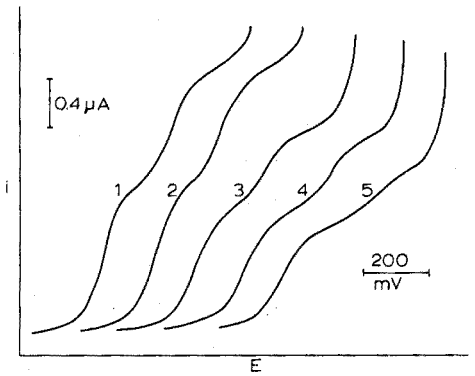

Fig. 7. The dependence of polarographic curves on sodium ion concentration in a 0.05 *M* sodium hydroxide solution. $2 \cdot 10^{-4}$ *M* Ethacrynic acid with sodium ion concentration altered by addition of sodium chloride. Final sodium ion concentration: (1) 2.05, (2) 1.05, (3) 0.35, (4) 0.15, (5) 0.08 *M*.

The rôle of borates and carbonates, forming complexes or adducts with the parent compound at sufficiently high ionic strength, in 2% ethanol is similar to that in 60% ethanol, with the single difference that wave i_4 was observed in the range pH 8–12 in phosphate, carbonate and dilute ammonia–ammonium chloride buffers, but was absent in borate buffers of low (No. 4, Table I) and high (No. 5) ionic strength. Evidently, borate or boric acid reacts with the carbanion–enolate formed in the first two-electron step and prevents formation of the aryl alkyl ketone in reaction (7) or (12).

When the effect of ethanol concentration was followed in acetate buffer pH 3.6 (Fig. 8), the suppression of the adsorption prewave (i_{a_1}) and the separation of waves i_1 and i_2 with increasing ethanol concentration was manifested.

Reaction with amines

When waves of ethacrynic acid were studied in buffers consisting of ammonia and ammonium chloride or ethylamine–ethylammonium chloride, some shifts of half-wave potentials, in particular of wave i_4, were observed with increasing amine concentration at a given pH. Nevertheless, no effect on the wave form or on the heights of waves i_3 and i_4 was observed for ammonium buffer, except in a saturated solution of ammonium chloride in 28% ammonia.

However, with increasing concentration of a buffer containing equal concentrations of ethylamine and ethylammonium chloride (*i.e.*, at pH = p*K*), the formation of a new wave (i_N) was observed at potentials between that of wave i_3 and i_4

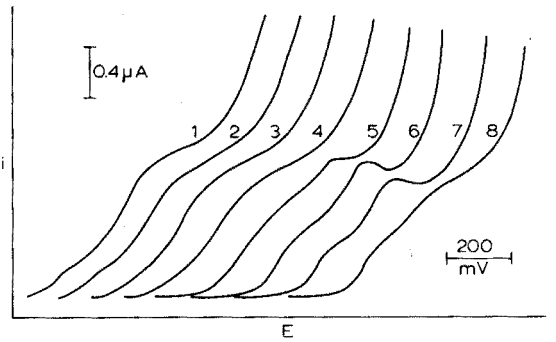

Fig. 8. Polarographic curves as a function of ethanol concentration. $2 \cdot 10^{-4}$ *M* Ethacrynic acid in acetate buffer pH 3.6. Concentration of ethanol: (1) 2, (2) 5, (3) 10, (4) 20, (5) 30, (6) 40, (7) 50, (8) 60 vol %.

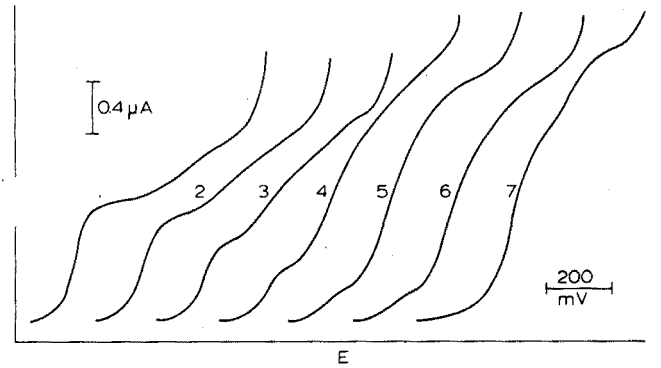

Fig. 9. Dependence of polarographic curves of $2 \cdot 10^{-4}$ *M* ethacrynic acid on ethylamine concentration in a phosphate buffer pH 10.3, containing 2% ethanol. Ethylamine concentration: (1) 0.0, (2) 0.003, (3) 0.01, (4) 0.03, (5) 0.07, (6) 0.10, (7) 0.30 *M*.

(Fig. 9). The height of wave i_N increased with increasing concentration of ethylamine added to a phosphate buffer. Similar dependence on ethylamine concentration was found in the absence of phosphate, when the solution was buffered by the amine buffer only. At lower concentrations of the amine buffer, all three, i_3, i_N and i_4 waves were observed, whereas in solutions containing higher concentrations than 0.3 *M* ethylamine and 0.3 *M* ethylammonium chloride, only wave i_N was observed. Comparison with wave i_3 shows that wave i_N reaches a height corresponding to a four-electron reduction.

The amines can react with both the starting material (the α,β-unsaturated ketone I), and with the aryl alkyl ketone produced in the first two-electron step i_3. The height of the wave i_3 (Fig. 9) indicates that the latter alternative can be excluded and the amine reacts with the α,β-unsaturated ketone.

As the α,β-unsaturated ketone is a system with two reactive centers, an interaction with amines can result in two products: Schiff or Mannich bases. Were the amine added to the C=C double bond[30–33], the resulting Mannich base as a

β-aminoketone would be reduced in a two-electron step, corresponding to the reduction of the carbonyl group[49]. The presence of the four-electron reduction wave indicates formation of a Schiff base; such bases are known[50,51] to undergo four-electron reductions. The product of the four-electron reduction, which might be either a β-arylpropylene or an arylpropylamine, was not identified. The reduction of this α,β-unsaturated Schiff base, however, differs in one respect from azomethine derivatives obtained by condensation of amines with aryl alkyl ketones: for the latter the reduction of the C=N bond occurs regularly at more positive potentials[50] than that of the C=O bond, whereas the Schiff base derived from ethacrynic acid is reduced at a more negative potential than the first wave i_3 of the parent compound.

Conclusions

For analytical purposes the waves of ethacrynic acid in 60% ethanolic solutions of pH 6–10 are most suitable. Alternatively, the four-electron wave in 0.5 *M* ethylamine, 0.5 *M* ethylammonium chloride (prepared by half-titration of 1 *M* ethylamine solution with hydrochloric acid) is suitable for analytical purposes.

Of the two reactive centers in ethacrynic acid, the C=C double bond is attacked first in electroreduction whereas the C=O group is attacked in the reaction with ethylamine. Ethacrynic acid, because of its stability against OH^- attack on the double bond, seems to be a suitable model for the study of addition reactions.

SUMMARY

Investigation of polarographic reduction of ethacrynic acid (I) in 2% and 60% ethanolic solutions showed that acid I is, similarly to other α,β-unsaturated ketones, reduced first on the C=C bond. But the presence of acid–base equilibria for one two-electron reduction wave in the medium pH range, as well as the sensitivity of the reduction wave of the aryl alkyl ketone to the presence of borates and carbonates, makes this reduction process different. Ethacrynic acid proved to be a suitable model compound for the study of addition reactions to a CO–C=C system. Preliminary examination of the reaction of ethylamine indicated that Schiff base rather than Mannich base is formed. A 60% ethanolic solution at pH 6–10 or with 1 *M* ethylamine half-titrated with hydrochloric acid, provided the most suitable conditions for analytical purposes.

REFERENCES

1 R. Pasternak, *Helv. Chim. Acta*, 31 (1948) 753.
2 P. Zuman, D. Barnes and A. Ryvolová-Kejharová, *Discuss. Faraday Soc.*, 45 (1968) 202.
3 Ch. Prévost, P. Souchay and J. Chauvelier, *Bull. Soc. Chim. Fr.*, 18 (1951) 715.
4 A. Ryvolová-Kejharová and P. Zuman, *J. Electroanal. Chem. Interfacial Electrochem.*, 21 (1969) 197.
5 T. A. Geissman and S. L. Friess, *J. Amer. Chem. Soc.*, 71 (1949) 3893.
6 J. Tirouflet and A. Corvaisier, *Bull. Soc. Chim. Fr.*, (1962) 535.
7 Z. S. Ariyan, B. Mooney and H. I. Stonehill, *J. Chem. Soc., London*, (1962) 2239.
8 J. M. Meunier, M. Person and P. Fournari, *Bull. Soc. Chim. Fr.*, (1967) 2872.
9 P. Zuman and J. Michl, *Nature (London)*, 192 (1961) 655.
10 S. Wawzonek and A. Gunderson, *J. Electrochem. Soc.*, 111 (1964) 324.
11 E. Laviron and J. Lucy, *Bull. Soc. Chim. Fr.*, (1966) 2202.

12 R. Rambaud, P. Martinet and J. Simonet, *88th Congress Soc., Savantes, 1963.*
13 P. Martinet and J. Simonet, *Bull. Soc. Chim. Fr.*, (1967) 3533.
14 J. Simonet, *Bull. Soc. Chim. Fr.*, (1970) 1533.
15 D. Barnes and P. Zuman, *Trans. Faraday Soc.*, 65 (1969) 1668, 1681.
16 P. Zuman and D. Barnes, *J. Chem. Soc., London*, (1961) 1118.
17 R. P. Bell, *Advan. Phys. Org. Chem.*, 4 (1966) 1.
18 P. Čársky, P. Zuman and V. Horák, *Collect. Czech. Chem. Commun.*, 30 (1965) 431.
19 W. J. Bover and P. Zuman, *J. Chem. Soc. Perkins II*, (1973) 786.
20 N. H. Cromwell, *Chem. Rev.*, 38 (1946) 83.
21 S. Patai and Z. Rappoport, *J. Chem. Soc., London*, (1962) 377, 383, 392, 396.
22 Z. Rappoport, *J. Chem. Soc., London*, (1963) 4498.
23 S. Patai and Z. Rappoport in S. Patai (Ed.), *The Chemistry of Alkenes*, Interscience–Wiley, New York, 1964, p. 469.
24 Z. Rappoport, Ch. Degani and S. Patai, *J. Chem. Soc., London*, (1963) 4513.
25 S. Patai, S. Weinstein and Z. Rappoport, *J. Chem. Soc., London*, (1962) 1741.
26 K. Sirotanović, M. Bajlon-Rocen and D. Galović, *Bull. Soc. Chim., Beograd*, 25–26 (1960–61) 509.
27 W. E. Truce and A. J. Lewy, *J. Amer. Chem. Soc.*, 83 (1961) 4641.
28 A. Padwa and R. Gruber, *Chem. Commun.*, (1969) 5.
29 V. A. Bren, K. A. Tskhadadze, L. A. Yanovskaya and V. I. Minkin, *Organic Reactiv.*, 8 (1971) 697.
30 N. H. Cromwell and D. J. Cram, *J. Amer. Chem. Soc.*, 65 (1943) 301.
31 H. Riviére, *Bull. Soc. Chim. Fr.*, (1962) 1389.
32 H. Inokawa, *Bull. Soc. Chim. Jap.*, 37 (1964) 568.
33 I. Šestáková, V. Horák and P. Zuman, *Collect. Czech. Chem. Commun.*, 31 (1966) 3889.
34 E. M. Cohen, *J. Pharm. Sci.*, 60 (1971) 1702.
35 J. Heyrovský and P. Zuman, *Practical Polarography*, Academic Press, New York, 1968, pp. 16–23.
36 H. T. S. Britton and R. A. Robinson, *J. Chem. Soc., London*, (1931) 1456.
37 O. Manoušek, unpublished results.
38 M. Paabo, R. A. Robinson and R. G. Bates, *J. Amer. Chem. Soc.*, 87 (1965) 415.
39 P. Zuman, J. Tenygl and M. Březina, *Collect. Czech. Chem. Commun.*, 19 (1954) 46.
40 R. Pasternak, *Helv. Chim. Acta*, 30 (1947) 1948.
41 A. K. Vlček, E. Špalek and L. Krátký, *Tech. Hlidka Koželužská*, 24 (1949) 258.
42 R. Brdička, *Ark. Kemi, Mineral. Geol.*, 26B (19) (1948) 7.
43 W. B. Swann, W. M. McNabb and J. F. Hazel, *Anal. Chim. Acta*, 28 (1963) 441.
44 K. Torssell, *Ark. Kemi*, 3 (1952) 571.
45 W. J. Bover and P. Zuman, *J. Electrochem. Soc.*, in print.
46 G. Schwarzenbach and E. Felder, *Helv. Chim. Acta*, 27 (1944) 1701.
47 H. D. Zook, W. L. Kelly and I. Y. Posey, *J. Org. Chem.*, 33 (1968) 3477.
48 M. Ashworth, *Collect. Czech. Chem. Commun.*, 13 (1948) 229.
49 P. Zuman and V. Horák, *Collect. Czech. Chem. Commun.*, 27 (1962) 187.
50 P. Zuman, *Collect. Czech. Chem. Commun.*, 15 (1950) 839.
51 H. Lund, *Acta Chem. Scand.*, 13 (1959) 249.

Analytica Chimica Acta, 73 (1974) 355–365

A SPECIFIC ENZYME ELECTRODE FOR UREA

G. G. GUILBAULT* and MADS TARP

Chemistry Department A, Technical University of Denmark, 2800 Lyngby, (Denmark)

(Received 21st May 1974)

In the past, Guilbault and co-workers have described several enzyme electrodes for the measurement of nitrogen-containing organic compounds by using an enzyme-catalyzed ammonium-releasing reaction. At first, the ammonium ion was measured with an ammonium-ion glass electrode (Beckman Glass 39137)[1,2]. Unfortunately, this sensor also responds to sodium and potassium ions, which are commonly present in serum and urine (serum contains $5 \cdot 10^{-3}$ *M* urea, $5 \cdot 10^{-3}$ *M* K^+, and 0.14 *M* Na^+). Guilbault and Hrabankova[3] used an ion exchanger to remove interfering sodium and potassium ions, but the use of ion exchangers in blood samples of very small volume, or the complete removal of sodium and potassium from a sample diluted with an ion-free buffer is not easy.

Guilbault and Nagy[4] reported an improved urea electrode made from a silicone rubber membrane containing the antibiotic nonactin as the active ingredient. The improved selectivity of this membrane electrode ($k_{NH_4^+/K^+} = 6.5$, $k_{NH_4^+/Na^+} = 750$) indicated the utility of this electrode, which was prepared by covering the active surface of the solid-type ammonium electrode with an immobilized urease, for the direct assay of urea without an ion-exchanger pre-treatment. Subsequently, Guilbault *et al.*[5] showed that urea can be assayed directly if the electrode is calibrated in a solution of a constant interfering potassium ion level, and a monitored dilution of the blood samples is made to this interference level. About a 5% accuracy was achieved with this method. Unfortunately, all of these electrodes have some limitations in the direct assay of urea in blood or urine.

For total specificity, an ammonia electrode could be used, *i.e.*, an electrode which responds only to gaseous ammonia and not to the ions present in blood or urine, such as sodium or potassium. Such a gaseous electrode is sold by Orion (Cambridge, Mass.), but has several practical difficulties, such as poor mechanical properties of the membrane, giving rise to long response times (5 min at 10^{-4} *M*), and susceptibility to clogging of the pores of the membrane when measuring in biological fluids[6].

Anfält *et al.*[7] found, however, that enough free ammonia is liberated in the urease gel layer placed on top of an Orion gas electrode to permit the direct measurement of urea at physiological pH values. In fact, a super-Nernstian plot (slope 69.5 mV/decade) was observed at pH 7. This indicates that it should be possible in many cases to adapt the sensor to fit the enzyme system, instead of *vice versa*, as many workers have done in the past.

---

* Guest Professor of Analytical Chemistry, on leave from the University of New Orleans, New Orleans, Louisiana.

Recently, Růžička and Hansen[8] have described a new type of gas sensor, the air-gap electrode, which is based on the same principle as other gas sensors, except for the absence of a gas-permeable membrane. This membrane is replaced by an air gap which separates the electrolyte layer (a very thin film of an electrolyte, *e.g.* ammonium chloride for the ammonia sensor, held on the surface of the indicator pH electrode with a hydrophilic wetting agent) from the sample solution. Gaseous ammonia generated in solution diffuses to the electrode surface in a gas-tight measuring chamber, where it reacts with the surfactant electrolyte layer to yield a pH change which is proportional to the concentration of the gas. Depending on the pH of the sample (pH_s), the ammonium ions of the sample can be either quantitatively or partially converted to ammonia gas. Based on these conditions, Hansen and Růžička[9] performed a urea assay using the air-gap electrode in two separate operations: the enzymatic reaction was carried out with soluble urease at pH 7.0 (optimal activity), and then the ammonium ion measurements were made after addition of an excess of strong base to convert all the product to free ammonia (optimal electrode sensitivity).

In this paper, a direct one-step assay of urea by means of chemically immobilized urease is described. The ammonia liberated at pH 8.5 is measured with the air gap electrode, thereby eliminating all interferences commonly associated with the assay. Direct assays in blood serum are performed in 2–4 min, with an accuracy and a precision of about 2.5%. Highly stable Enzygel-urease is used as well as soluble urease.

EXPERIMENTAL

Apparatus

The air gap electrode was constructed as shown in Fig. 1, which is a partial front sectional view. The Teflon body (A) has a diameter of 50 mm and a

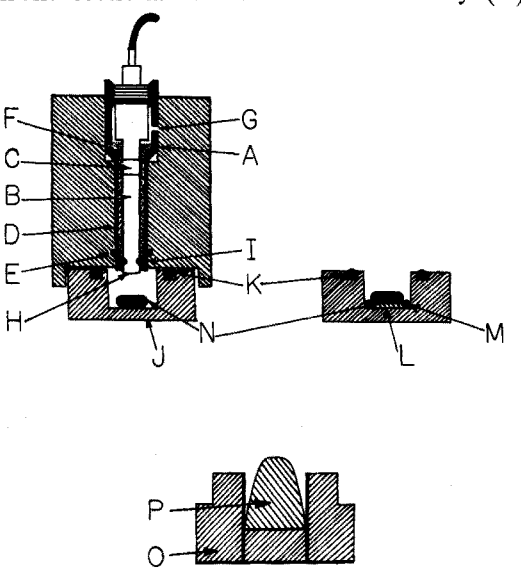

Fig. 1. Construction and parts of the enzyme air gap electrode (see text for details).

height of 60 mm into which fits snugly the glass (B) and reference (C) electrodes in a common Perspex tube (D). To accomplish this, a smooth coaxial hole (diameter 10 mm) was drilled, furnished with an O-ring (E). The reference electrode, Ag/AgCl, is surrounded by the reference solution (F; saturated AgCl in 0.1 *M* NaCl) contained within the Perspex tube, and introduced through a small hole (G). The pH-sensitive surface of the glass electrode (H) is covered by an electrolyte solution (see below). The liquid junction between the electrolyte and reference solution is achieved by using an O-ring (I) which is degreased and made hydrophilic before use.

The microchamber (J) used for enzyme studies was cylindrical and made of Perspex, diameter 42 mm and height 12 mm, with a cavity of diameter 16.5 mm and depth 9 mm, and fitted with an O-ring (K) to provide an air-tight fit to the air-gap electrode. The cavity was well polished with rounded corners and was used directly as the sample compartment for soluble and insolubilized enzyme studies.

The urea-specific electrode was constructed by placing 15 mg (10 units) of immobilized urease powder or gel at the bottom of the microchamber (L). The enzyme layer was covered with a round piece of nylon net (Nytal Nr 40 (9) HD, 100 μm, Swiss Silk Mfg. Co., CH-9425 Thal St. Gall) held in position with an O-ring (M) which exactly fits the inside diameter of the cavity (refer to Fig. 1).

Teflon-coated magnetic stirring bars (N) were used to stir all solutions.

The electrolyte layer was applied to the electrode by means of a Perspex electrode holder (O) containing the electrolyte solution. A cone-shaped polyurethane sponge (P), well soaked with the electrolyte solution, provides a fresh film layer to the electrode surface each time the air-gap electrode is placed on top of the electrode holder. The glass electrode (H) contacts the sponge (P) directly, and if the Teflon body (A) is rotated several times on the electrode holder and the sponge is pressed down once or twice with a stirring rod to provide fresh electrolyte, a fast return to base line is achieved.

The glass electrode (Radiometer E 5036/0) (H) has a flat pH-sensitive surface (*ca.* 12 mm^2 area) and combined reference electrode consisting of a silver chloride-covered silver strip (C). A 0.1 *M* sodium chloride solution saturated with silver chloride was used as reference solution.

A digital (Radiometer Model 52) or a non-digital (Radiometer Model 51) pH meter and a recorder (Servogor, RE511) were used for measuring and recording all electrode responses.

All pipettes used were Carlsberg micropipettes, 100 and 200 μl ($\pm 1\%$ accuracy; H. E. Pedersen, Denmark).

Reagents

The electrolyte solution was $1.0 \cdot 10^{-3}$ *M* ammonium chloride (AnalaR, BDH) saturated with wetting agent (Victawet 12, Stauffer Chemical Co., U.S.A.).

The buffer solution was 0.5 *M* tris(hydroxymethyl)aminomethane, (Sigma, St. Louis, Mo.) adjusted to pH 8.50 with hydrochloric acid.

Urease. Soluble urease (Boehringer, Mannheim, Germany; activity 100 units mg^{-1}) solutions were prepared at a concentration of 1 mg ml^{-1} in tris buffer, pH 8.5.

Immobilized urease used was from two sources: Boehringer Enzygel, (activity 650 units g^{-1}) and enzyme chemically bound to Enzacryll AA (Aldrich Chemical Co., Milwaukee, Wisc.) by diazo coupling by a procedure described previously[10] (activity 100 units g^{-1}).

Urea. The urea used for preparing standard calibration plots was that in freeze-dried blood (Monitrol I and II; Dade, Division of American Hospital Supply, Miami, Fla.). Dilution of Monitrol II (urea concentration $1.86 \cdot 10^{-2}$ *M* as analyzed with the AutoAnalyzer) with doubly distilled water gave the best electrode calibration for use in assaying serum samples.

Serum samples were obtained from the University Hospital of Copenhagen. The serum samples were fresh and were concurrently analyzed at the hospital (by the AutoAnalyzer method). The normal background ammonium ion content of blood (about $3–7.5 \cdot 10^{-5}$ *M*) did not present any interference in urea assays (urea about 3–30 m*M* in serum), but if the serum samples were over 1 day old, enough hydrolysis of species in blood to ammonium ion had occurred (as indicated by high blanks) to make the samples useless.

Procedures

Soluble enzyme. To 100 µl of soluble urease in 0.50 *M* tris buffer, pH 8.50, add 100 µl of blood serum to be assayed. Stir the solution and record the equilibrium pH (pH_e). Read the urea content of blood from a calibration plot of pH_e *vs.* log urea concentration obtained with Monitrol II standards. After each run, rinse the microcell with water and dry before the next measurement.

Enzyme electrode. Add 200 µl of 0.5 *M* tris buffer pH 8.5 to the microchamber followed by 200 µl of the serum to be assayed. Stir the solution and record the equilibrium pH. Read the urea content from a plot of pH_e *vs.* log

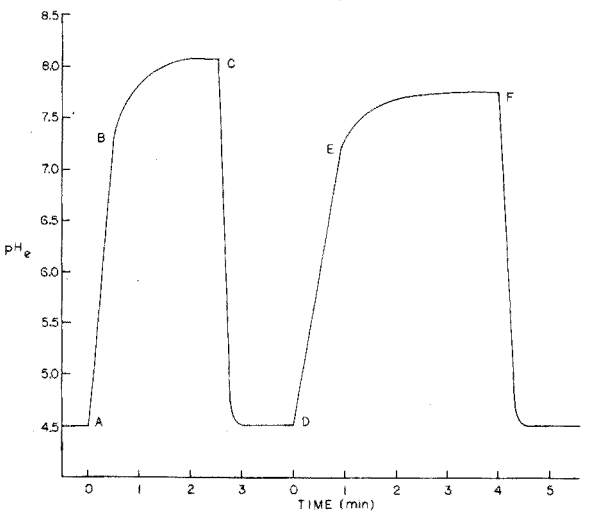

Fig. 2. Response curves for the enzyme electrode. (A) (D) Electrode placed on enzyme cell; (B) response to Monitrol II, 17.6 m*M* urea; (C) (F) electrode placed on electrolyte layer; (E) response to Monitrol II, 6.0 m*M* urea.

urea concentration as above, using Monitrol II standards. After each run, rinse the microchamber containing the immobilized enzyme under a distilled water tap for 5–10 s and pat the enzyme layer dry with a paper tissue. Renew the electrode surface by placing the electrode on the electrode holder (Fig. 2).

RESULTS AND DISCUSSION

Principle of air-gap electrode—response time

As ammonia is volatilized from solution according to Henry's Law, and diffuses to the electrode surface, it reacts with the ammonium ion present at the electrode surface with a resulting decrease in the hydrogen ion concentration. The equilibrium pH of the electrode, pH_e, at constant $[NH_4^+]$ at the electrode surface and at constant pH of the sample (held constant by the tris buffer pH 8.50), should be proportional to the log $[NH_4^+]$ of the sample:

$$pH_e = \log[NH_4^+]_{sample} + \text{constant} \quad (1)$$

Hansen and Růžička[9] have presented an excellent discussion of the theoretical and practical limits of detection as a function of pH, $[NH_4^+]_s$ and percent conversion of ammonium ion to ammonia. In this study an attempt was made to measure the urea–urease reaction directly, without the necessity of preincubation at low pH followed by measurement at high pH. To do this, a pH of 8.5 was chosen for the reaction, and an ammonium ion concentration of 10^{-3} *M* for the electrolyte layer. At a pH of 8.5, the velocity of the urea–urease reaction is still 0.5 V_{max}, and enough free ammonia is liberated to be efficiently measured (ratio of $[NH_3]/[NH_4^+]=0.18$ at pH 8.5). With an electrolyte concentration of 10^{-3} *M*, the practical limit of detection is about 10^{-4} *M*, and fast electrode response to the ammonia liberated from urea by urease is observed (Fig. 2). At high urea concentration (>10 mmol^{-1}) a stable pH_e is observed in 2 min at pH 8.5, whereas at urea concentrations of less than 10 mmol l^{-1}, a response time of 3–4 min is required. Since the response of the electrode to ammonia released from ammonium ion at pH 8.5 is less than 1 min at concentrations above 10^{-2} *M* and about 1 min at concentrations below 10^{-2} *M* for a 10^{-3} *M* ammonium electrolyte, the greater part of the electrode response time is due to the enzymatic reaction. As predicted theoretically, the electrode response time should increase as the substrate concentration decreases[11]. The equilibrium pH is quite stable, as seen in Fig. 2. To renew the electrode surface, the electrode is placed on the electrolyte layer, and a very fast (*ca.* 20 s) return to base line is observed.

Figure 3 (line A) shows the observed plot of pH_e *vs.* log $[NH_4^+]$ at pH 8.5. The plot is linear from 10^{-1} *M* to $5\cdot10^{-5}$ *M* with a slope of 0.95, which is close to the theoretical value of 1.00. The lower limit of detection (10^{-5} *M*) and the practical limit of detection (*ca.* 10^{-4} *M*) agree reasonably well with theory.

Effect of enzyme concentration

In order to study the efficiency of the enzyme reaction in producing measurable ammonia at pH 8.5, studies were first made with soluble enzyme.

The first enzyme tried was a preparation from Struers (Copenhagen) which had an activity of 5 units mg^{-1}. Linear plots of pH_e *vs.* log [urea] were obtained

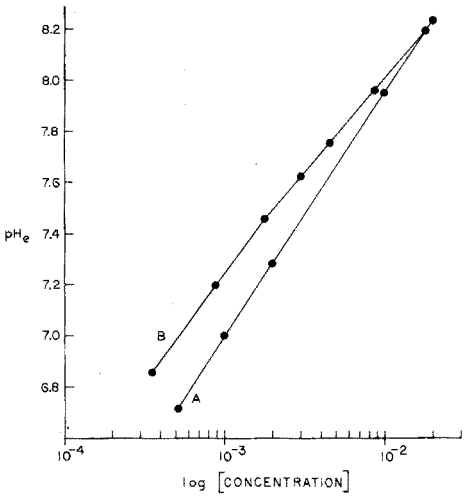

Fig. 3. Calibration curves for ammonium chloride (A) and Monitrol II (B) obtained with the microchamber. The curves for Monitrol II were obtained with 10 units of Enzygel-urease. Both lines were obtained at pH 8.5 with tris buffer, 0.50 *M*.

over the concentration range 10^{-4}–10^{-2} *M*, but with a slope of only 0.51, indicating a poor conversion of substrate to ammonia.

When a purified urease from Boehringer (100 units mg^{-1}) was used, better results were obtained. Linear plots of pH_e *vs.* log [urea] were obtained over the range of 10^{-4}–10^{-2} *M*, with a slope of 0.88 for pure urea and 0.75 for Monitrol II. Although the conversion to ammonia was not complete, the curve for Monitrol II was quite reproducible, and was used for the assay of 11 blood serum samples from the University Hospital in Copenhagen. The results obtained with the electrode agree with those obtained by the Hospital using the AutoAnalyzer with a difference of $\pm 3.5\%$ (Table I). Each sample was run 3 times, the relative standard deviation being 2.4% (an average difference of 0.01 pH in the measurement).

Finally, two types of immobilized enzymes were used, one a special Enzygel (Boehringer) preparation which had an activity of 0.65 units mg^{-1}, and the second a product prepared by binding urease to Enzacryl AA[10] (activity 0.10 units mg^{-1}). Both products worked well, yielding linear plots of pH_e *vs.* log [urea] over the concentration range 10^{-4} *M*–$2 \cdot 10^{-2}$ *M*. The curves leveled off at higher concentrations as predicted by the Michaelis–Menten equation, the reaction becoming independent of substrate concentration. Likewise, a leveling off at low concentration ($< 10^{-4}$ *M*) was observed because of the limit of detection of the electrode sensor used. Since the normal urea concentration of blood serum is between 3 and 20 m*M*, the range of the enzyme electrode is perfect for all uses. The Enzacryl AA-enzyme had so low an activity that large quantities of it had to be used (about 30 mg); this resulted in very long response times (5–7 min). When the Enzygel preparation was used, only 15 mg of enzyme was required (*ca.* 10 units) and fast response curves (2–4 min) were obtained. As discussed by Guilbault[11], about 10 units of an enzyme is needed for a good enzyme

TABLE I

ASSAY OF UREA IN BLOOD SERUM BY THE SOLUBLE ENZYME METHOD

Sample number	*[Urea] (mmol l^{-1})*		*Difference (%)*
	Electrode[a]	*AutoAnalyzer*	
1	6.0	6.5	−9.1
2	33.0	32.9	+0.3
3	19.9	20.5	−3.0
4	19.1	19.2	−0.5
5	24.0	22.3	+7.5
6	19.6	20.4	−4.0
7	10.2	10.5	−3.0
8	6.1	5.7	+6.5
9	5.4	5.3	+1.8
10	25.8	25.3	+1.9
11	35.8	35.9	−1.7
			Avg. ±3.5

[a] Average of three or more runs with average standard deviation of 2.4%.

electrode, and the use of smaller weights of purer chemically bound enzymes will give faster response curves than larger weights of less pure enzymes.

Figure 3 (line B) shows a calibration plot for Monitrol II urea standard determined with the urea air-gap enzyme electrode, compared with a plot for ammonium chloride (line A) obtained with an identical microcell (see Fig. 1), but without enzyme. Only below $2 \cdot 10^{-3}$ *M* is most of the urea in Monitrol II converted to ammonium ion, which is then sensed by the air-gap electrode (ΔpH_e between the Monitrol II and ammonium chloride lines is close to the theoretical value of 0.3 ΔpH, for two ammonium ions produced from each urea). At higher concentrations, the two curves become closer and closer indicating an incomplete conversion to ammonium ion. The slope of the Monitrol II calibration curve was 0.87 below $2 \cdot 10^{-3}$ *M* and 0.73 above $2 \cdot 10^{-3}$ *M* urea. The slope of the calibration plot for Monitrol I was closer to theoretical—slope 0.90—but the results obtained on assay of 20 blood serum samples from the University Hospital showed much better agreement with the AutoAnalyzer values when the Monitrol II curve was used. Eleven of these typical results are shown in Table II. An average difference of only ±2.2% was obtained, and the relative standard deviation of all the samples (3 runs or more on each sample) was only 2.0% (less than 0.01 pH unit difference).

Specificity of assay

None of the common ions present in blood, Na^+, K^+ or NH_4^+, interfered in the assay. The free ammonium ion content of normal blood is less than 0.1 mmol, generally less than 1% of the urea value. All of the blood samples assayed, as well as the Monitrol standards, were tested for their ammonium content, and all proved well within this 1% value, except for those blood samples which had been kept unrefrigerated for more than 24 h, or stored refrigerated for more than 3 days.

TABLE II

ASSAY OF UREA IN BLOOD SERUM WITH THE ENZYME ELECTRODE

Sample number	*[Urea] (mmol l^{-1})*		*Difference (%)*
	Electrode[a]	*AutoAnalyzer*	
1	10.0	10.1	−1.0
2	33.2	33.0	+0.6
3	17.0	17.4	−2.3
4	20.0	20.0	0.0
5	16.0	15.7	+1.9
6	12.0	11.3	+6.2
7	4.0	4.0	0.0
8	2.95	3.0	−1.6
9	12.2	12.0	+1.6
10	12.9	12.0	+7.5
11	11.2	11.0	+1.8
			Avg. ±2.2

[a] Average of three or more runs with average standard deviation of 2.0%.

Concentrations of sodium and potassium ions as high as 10^{-1} *M* had no effect on the electrode response, since the electrode responds only to free ammonia vaporized from solution. Thus all of the selectivity problems of previous urea enzyme electrodes[1–5] have been eliminated.

The selectivity of urease for urea has been discussed[11]; none of the other amines or amino acids or urea derivatives interfere.

When Monitrol II, which is freeze-dried blood, was used as a standard, excellent results were obtained. The results with Monitrol I and pure urea standards were not as good, probably because the higher urea level of Monitrol II (17.6 m*M* compared to 3.86 m*M* for I) allowed a better comparison to the blood samples assayed, which ranged from 3 to 36 m*M*.

Stability of enzyme electrode

Figure 4 shows the stability of the immobilized urease electrode over a

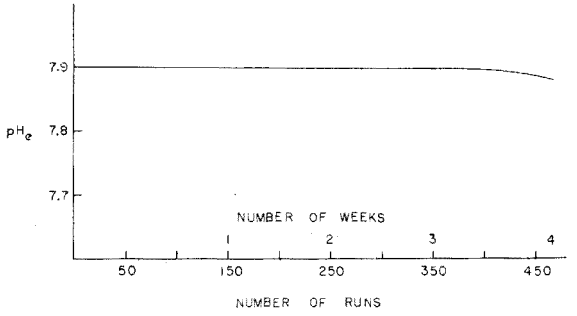

Fig. 4. Stability of Enzygel-urease electrode. pH_e response of Monitrol II, 9 m*M* urea, to 10 units of urease at pH 8.5 (tris buffer, 0.5 *M*) as a function of number of weeks from preparation and number of assays.

period of 4 weeks and over 460 assays. The stability is indicated by the equilibrium potential, pH_e, measured for each run over this period, and plotted *vs.* number of runs and time in weeks. The same reading for a 9 m*M* Monitrol II sample was obtained for 3 weeks and 350 assays, followed by a slight decrease up to 4 weeks or 460 assays. This is excellent stability, and indicates the economic benefit of this type of approach; the cost of each assay is about 2% of the cost by the AutoAnalyzer method. How long one electrode would last is uncertain; that it was useful for almost 500 assays seemed sufficient to show its excellent utility. Unfortunately, the response time of the enzyme electrode increases with age, going from about 3 min at 9 m*M* when first used, to as long as 5–6 min after 500 tests. This is due to an ageing of the immobilized enzyme.

The electrode cell was stored in a refrigerator overnight and used each day for at least 10 runs over this 4-week period. The electrode was stored both dry and in tris buffer pH 7.5, both with good results. Added stability might be achieved by addition of 10^{-3} *M* dithiothreitol to the buffer solution.

Other factors

Use of a 100-μm net to hold the enzyme layer proved optimal for fast speed of response. Smaller nets, cellophane and fine nylon dialysis membranes, though as useful in holding the enzyme layer, yielded slower response curves. The longest responses (10 min at 9 m*M*) were obtained with the cellophane (35 μm); the fine nylon dialysis membrane (50 μm) took about 5 min for a steady state response compared to about 2.5–3 min for the 100 μm net.

The pH_e observed varied quite drastically with the stirring rate; this is as expected and has been discussed by Guilbault[11] and Mascini and Liberti[12] for other enzyme electrodes. For this reason, the stirrer should always be adjusted to a moderate speed, and then switched on and off by a separate switch so that all samples are agitated in an almost identical manner.

In this assay, only 200 μl of blood serum is required, and is diluted with 200 μl of tris buffer pH 8.50, which is added to maintain the pH of the solution constant (below $\pm$0.01 pH) and provide the same ionic strength and buffer conditions for each assay. This 0.400 ml total volume is sufficient to provide a constant volume on the enzyme bed each time, so long as the enzyme layer, after washing, is patted dry with a paper tissue. A change in the total volume of the cell will of course introduce errors in the determination.

After use, the electrode surface can be regenerated very quickly by placing the electrode on the electrode holder. By gently pressing the sponge with electrolyte solution each time before placing the electrode on it, a very fast return to base line (Fig. 2) is observed. By simply holding the cell with the enzyme layer under a distilled water tap for 5–10 s, all of the unreacted substrate, products and buffer are washed out, and the cell is ready for the next measurement. It is estimated that, in all, less than 1 min total time is required from one measurement to the next. In order to obtain reproducible results each day, a standard of Monitrol II should be used to set the pH. However, it was found with the air-gap system that the same pH_e was observed each day over a month, within $\pm$0.01 pH.

Finally, some mention of the practical utility of the Růžička–Hansen air-gap electrode is in order. Compared with the Orion gaseous ammonia electrode,

the air gap has several advantages. First, the response of the air gap is faster, and this is especially true at low ammonia concentrations (below 10^{-3} *M*). Even for measurements at pH 8.5 where only a small fraction of the ammonium ion exists as free ammonia (9%), a 1–2 min response time was observed at concentrations as low as $5 \cdot 10^{-5}$ *M*. Secondly, the air-gap electrode is not affected by the solution measured since it is not in contact with it. Thus, proteins, blood cells, surfactants and other compounds which have been found to affect adversely the performance of the conventional ammonia membrane electrodes[6], have no effect on the air-gap electrode. It is rugged, and can be used continuously for long periods of time with no adverse affects. Thirdly, it is extremely simple in design and easy to operate and use. The surface electrolyte is easily renewed between measurements. A very fast (less than 30 s) return to base line is always observed. Finally, the electrode can be used for different systems, simply by changing the electrolyte layer. Within a minute the electrode can be adapted to CO_2 or SO_2 measurements. Thus, it is envisioned that enzyme electrodes based on the air-gap principle can be made for any system that releases ammonia or carbon dioxide and collaborative studies with Růžička and Hansen are now underway in these areas.

Conclusion

Compared to other electrode systems described by this author[1–5] and others[7,13] for urea assay, this type of approach appears the best. It is fast (3–5 min total time per assay), economical, reliable (accuracy and precision about 2%), specific (no interferences from Na^+, K^+, NH_4^+ or other substances in blood) and easy to do. 'An enzyme electrode can be easily made by placing 10 units of enzyme on the bottom of a Plexiglas microcell, covering it with a nylon net, and securing it with an O-ring. Since the immobilized enzyme is available commercially, anyone can make an electrode.

The authors wish to express their sincere appreciation and gratitude to Professors Růžička and Hansen for the loan of the air-gap electrodes used, and also for many valuable discussions and assistance. The financial support of the Danish Natural Science Research Council in the form of a Guest Professorship for the senior author and of his research in Denmark is gratefully acknowledged. Thanks are also extended to Dr. Jorgen Melchior Rasmussen of the University Hospital of Copenhagen for providing the serum samples. Finally, the authors thank Dr. Dieter Jaworek of Boehringer Mannheim GmbH, Tutzing, Germany, for providing the sample of high-purity, chemically bound Enzygel urease.

SUMMARY

A truly specific, simple enzyme electrode is described for the assay of urea in blood serum. The sensor used is the newly developed air-gap electrode of Růžička and Hansen, and has advantages of speed of response and specificity over earlier enzyme electrodes for urea. Potassium, sodium and ammonium ions and other organic and inorganic species present in blood do not interfere. Linear curves are obtained from $2 \cdot 10^{-2}$ *M* to $1 \cdot 10^{-4}$ *M* urea with slopes close to

Nernstian (about 0.90 pH/decade). Urea in blood was assayed with an accuracy of 2.2% and a precision of 2.0% with immobilized urease; only 3–5 min is required per assay. The electrode was used for a month and almost 500 assays with excellent results. Since the sensor never touches the sample solution, problems caused by blood components which block membrane pores are avoided.

REFERENCES

1 G. G. Guilbault and J. G. Montalvo, *J. Amer. Chem. Soc.*, 91 (1969) 2164, *Anal. Lett.*, 2 (1969) 283; *J. Amer. Chem. Soc.*, 92 (1970) 2533.
2 G. G. Guilbault, R. K. Smith and J. G. Montalvo, *Anal. Chem.*, 41 (1969) 600.
3 G. G. Guilbault and E. Hrabankova, *Anal. Chim. Acta*, 52 (1970) 287.
4 G. G. Guilbault and G. Nagy, *Anal. Chem.*, 45 (1973) 417.
5 G. G. Guilbault, G. Nagy and S. S. Kuan, *Anal. Chim. Acta*, 67 (1973) 195.
6 H. F. Proelss and B. W. Wright, *Clin. Chem.*, 19 (1973) 1162.
7 T. Anfält, A. Granelli and D. Jagner, *Anal. Lett.*, 6 (1973) 691.
8 J. Růžička and E. H. Hansen, *Anal. Chim. Acta*, 69 (1974) 129.
9 E. H. Hansen and J. Růžička, *Anal. Chim. Acta*, 71 (1974) 225.
10 G. G. Guilbault and G. Lubrano, *Anal. Chim. Acta*, 64 (1973) 439.
11 G. G. Guilbault in H. Weetall (Ed.), *Enzyme Electrodes, in Practical Uses of Immobilized Enzymes*, Marcel Dekker, New York, 1974.
12 M. Mascini and A. Liberti, *Anal. Chim. Acta*, 68 (1974) 177.
13 J.G. Montalvo, *Anal. Chim. Acta*, 65 (1973) 189.

Analytica Chimica Acta, 73 (1974) 367–373

ENZYME ELECTRODE FOR L-AMINO ACIDS AND GLUCOSE

M. NANJO and G. G. GUILBAULT

Department of Chemistry, University of New Orleans, New Orleans, Louisiana 70122 (U.S.A.)

(Received 11th June 1974)

Recently, an enzyme electrode based on the continuous amperometric detection of the decrease in dissolved oxygen during the enzymatic reaction has been described for the assay of uric acid[1]. Since other oxidases are useful for assays of clinically important substrates, glucose and L-amino acid oxidases were examined in a similar way to uricase, the direct decrease of dissolved oxygen being measured at a platinum electrode.

Glucose oxidase[2,3] and L-amino acid oxidase[4,5] have been used for enzyme electrodes, the hydrogen peroxide formed being detected. In this paper, the same type of enzyme electrodes were used to show a response to L-amino acids and glucose at negative potentials where dissolved oxygen was reduced to water. By monitoring the change in dissolved oxygen, the enzyme electrodes were found to be more sensitive than the hydrogen peroxide method which was measured at positive potentials.

EXPERIMENTAL

Immobilization of enzymes

L-Amino acid oxidase (100 mg of E.C. 1.4.3.2; Sigma Chemical Co.; Type I from *crotalus adamanteus venom*; 0.3 units/mg) and 100 mg of albumin (Sigma Chemical Co., from *bovine serum*) were added to 5.0 ml of 0.1 *M* phosphate buffer solution (pH 7.3) and mixed well; then 5 drops of glutaraldehyde (Sigma Chemical Co., aqueous 50% solution) were added to the mixture, and the solution was frozen with dry ice–acetone coolant.

The frozen copolymer was kept in a refrigerator for a day to dissolve the buffer solution and was washed with the same buffer solution. This immobilized L-amino acid oxidase was kept in a refrigerator until use. The same procedure was adopted for glucose oxidase (EC. 1.1.3.4; Sigma Chemical Co., Type II from *Asparagillus niger*, 13–18 EU/mg).

Construction of enzyme electrodes

Enzyme electrodes were prepared by the same method reported for uric acid[1] electrodes as follows. The base electrode, sensing dissolved oxygen was a platinum inlay electrode (Beckman 39273) consisting of a platinum disk (diameter 5 mm) supported by a plastic cylindrical body (diameter 10 mm). The immobilized enzyme copolymer was placed on the platinum surface and secured by nylon cloth and rubber O-rings. The electrodes were stored in the buffer solution at room temperature.

Apparatus

A Heath polarograph module (Model EUA 19-2) was combined with a Heath operational amplifier system at a constant potential. Currents were recorded with a Heath Recorder Model EU-205-11. A side-arm saturated calomel electrode was placed in contact with the enzyme electrode.

Procedures

The enzyme electrode procedure consisted simply of placing the electrode with a calomel electrode into a stirred 0.1 *M* phosphate buffer solution (10.0 ml, pH 7.3) at −0.6 V *vs.* SCE. When the current was at a constant level, the sample solution to be assayed, less than 0.5 ml, was pipeted into the buffer solution and the initial rate of change in the limiting current for dissolved oxygen, and the difference of currents between the initial and final oxygen levels (steady state current indicating the amount of consumed oxygen) were recorded. The rate and steady state current at +0.6 V *vs.* SCE for hydrogen peroxide were also measured for comparison with the dissolved oxygen method. These procedures were conducted at 30°C, by means of a water-jacketed cell. After each measurement, the electrode was rinsed with distilled water and dipped into fresh buffer solution for 1–2 min to recover the dissolved oxygen concentration around the enzyme and to eliminate the remaining reaction products.

The measurement time was only 4–5 min for a single assay, including washing time.

RESULTS AND DISCUSSION

L-Amino acid electrode response

The measurement of amino acids is important not only in biochemical analysis but also in industrial analysis. Many kinds of assay methods have been developed[6], but most of them lack good sensitivity, are not economical, and/or require long analysis times.

Several enzymatic methods based on L-amino acid oxidase and peroxidase have been reported[7–9]. Guilbault and Hrabankova[10] reported an enzyme electrode based on an ammonium ion-selective electrode to measure the ammonium ion produced by the following reaction:

$$RCHNH_2COOH + O_2 + H_2O \xrightarrow[\text{Oxidase}]{\text{L-Amino acid}} RCOCOOH + NH_3 + H_2O_2 \quad (1)$$

Attempts to detect the hydrogen peroxide formed with an iodide electrode with horseradish peroxidase and iodide ion was reported by Guilbault and Nagy[4]. The assay of L-amino acids by detecting hydrogen peroxide directly has also been reported[5]; a platinum electrode coupled with immobilized L-amino acid oxidase was used at a positive potential, where hydrogen peroxide is oxidized.

Another method of monitoring reaction (1) is by measuring the decrease in dissolved oxygen. This was first suggested by Hicks and Updike[11] who coated an oxygen electrode with physically entrapped enzyme. It is even better to detect the limiting current of the dissolved oxygen by a platinum electrode at a negative potential, −0.6 V *vs.* SCE. This proposed method has advantages over the oxygen

electrode method of Hicks and Updike[11] in that there is a faster speed of response and an insensitivity to proteins and other biological substances in blood which tend to block the pores of the membrane used in the oxygen electrode, making the latter inoperable in a short period of time. The proposed dissolved oxygen method was found to be more sensitive than measuring the hydrogen peroxide at positive potentials because peroxide is consumed in several ways during the enzymatic production. Especially in the case of reactions catalyzed by L-amino acid oxidase, the hydrogen peroxide formed has been reported to react non-enzymatically with the α-keto acid product in the absence of catalase[12]:

$$\mathrm{RCOCOO^- + H_2O_2 \rightleftharpoons R\text{-}\overset{\overset{\mathrm{O}}{\|}}{\mathrm{C}}O^- + CO_2 + H_2O} \qquad (2)$$

The rate of this successive reaction (2) is considered to lower the sensitivity of detection of hydrogen peroxide. However, the dissolved oxygen decrease predominates over the hydrogen peroxide increase because of the disappearance in reaction (2) of hydrogen peroxide which is also electroactive at the same negative potential, −0.6 V *vs.* SCE.

In Fig. 1, the enzyme electrode response of the current change at −0.6 V *vs.* SCE caused by dissolved oxygen consumption during the enzymatic reaction is shown. When L-amino acid solution is added to the buffer solution, (0.1 *M* phosphate buffer, pH 7.3), the L-amino acid diffuses into the enzyme layer and reacts with the immobilized enzyme. As the result of the reaction, dissolved oxygen is consumed and hydrogen peroxide is produced. At +0.6 V (at this potential and in pH 7.3 buffer, hydrogen peroxide gives a limiting current), the formation of hydrogen peroxide is also sensed, as shown in Fig. 1, curve II. The initial rates and steady-state currents were measured and plotted *vs.* the substrate concentration, in Figs. 2 and 3.

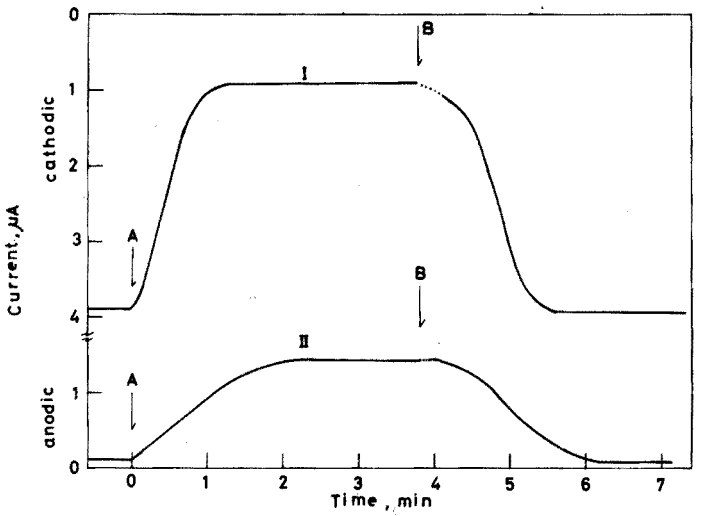

Fig. 1. Enzyme electrode responses at −0.6 V (I) and at +0.6 V *vs.* SCE (II). 0.1 *M* Phosphate buffer, pH 7.3, 30°C. Phenylalanine, 18.2 mg%, added at A and the electrode washed and dipped in fresh buffer solution at B.

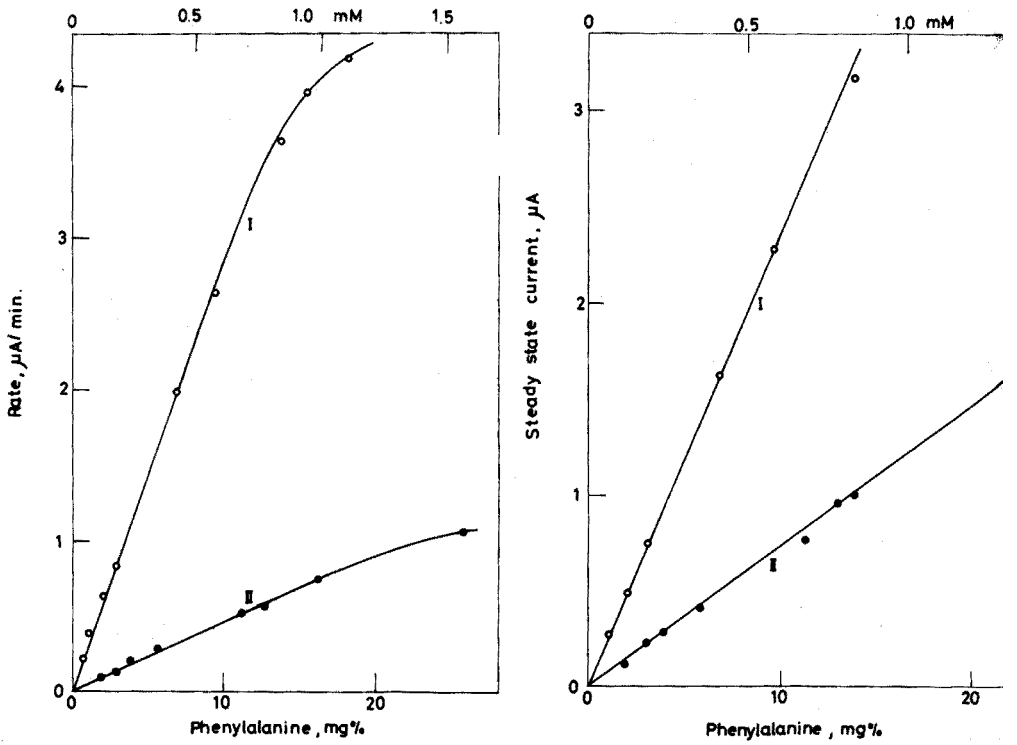

Fig. 2. Calibration curves for phenylalanine by rate method. 0.1 *M* Phosphate buffer, pH 7.3, 30°C. (I) −0.6 V *vs.* SCE; (II) +0.6 V *vs.* SCE.

Fig. 3. Calibration curves for phenylalanine by steady-state method. 0.1 *M* Phosphate buffer, pH 7.3, 30°C. (I) −0.6 V *vs.* SCE; (II) +0.6 V *vs.* SCE.

The sensitivity of the dissolved oxygen method was found to be higher than that of the hydrogen peroxide method for both methods. The rate of dissolved oxygen uptake is seven times faster than the hydrogen peroxide rate. The lowest limit of detection was found to be 1.0 mg% ($6 \cdot 10^{-5}$ *M*). This result indicates that the successive nonenzymatic reaction (2) exerts a serious effect on the rate of hydrogen peroxide formation.

Selectivity

L-Amino acid oxidase is specific for L-amino acids, but is not very selective for the side-chain. As a result, it catalyzes the oxidation of a considerable number of L-amino acids. Table I shows the substrate selectivity of the L-amino acid electrode. The selectivity of the dissolved oxygen method shows good agreement with the results of Greenstein *et al.*[13] and Ziller *et al.*[14].

The sensitivity of the dissolved oxygen method was found to be higher than that of the hydrogen peroxide method in the case of every L-amino acid. As a result of the selectivity of L-amino acid oxidase, this enzyme electrode is not as useful for amino acid sensing as the ninhydrin[15] or *p*-dimethylaminobenzaldehyde[16]

LE I

ECTIVITY OF L-AMINO ACID OXIDASE ELECTRODE

nino	*Methods*					
	Rate ($\mu A\ min^{-1}\ mM^{-1}$)		*Steady state current ($\mu A\ mM^{-1}$)*		*Oxygen uptake*	
	D.O.	H_2O_2	*D.O.*	H_2O_2	*Greenstein*[a]	*Ziller*[b]
	5.0	0.77	4.6	0.64	243	1.88
	5.0	0.77	4.5	0.86	225	1.76
	4.7	0.71	4.5	1.22	185	1.92
	4.7	0.25	4.5	—[c]	199	1.97
H	2.2	0.22	9.5[d]	0.78	63	1.02
	2.1	0.32	3.5	0.87	71	1.58
	0.44	0.05	1.3	0.43	0.4	
	0.39	0	1.2	0		0.82
	0.14	0	0.82	0	0.2	
	0.07	0	0.28	0	0.9	0.95
	0.11	0	0	0	9.0	0.79
	0	0	0	0	0	
e	0	0	0	0	0	
	0	0	0	0	0	
	0	0	0	0	0	

eenstein, μM of O_2/h per mg of N.
ller, number of O_2 atoms consumed per substrate, $1.0 \cdot 10^{-5}$ M.
y does not give a steady-state current because of slow rate.
SH consumes dissolved oxygen to form $(CyS)_2$.

reagents. However, it may be applicable as a detector of certain L-amino acids such as those six L-amino acids shown in Table I after a separation.

The L-amino acid oxidase electrode was found to be stable for over 4 months with little loss of activity; hence it is useful as a practical assay device.

Glucose electrode

The same procedure was adopted for the assay of glucose with glucose oxidase. The calibration curves, shown in Fig. 4, indicate that the lowest limit of detection is 1 mg% ($5 \cdot 10^{-6}$ M). This dissolved oxygen method is therefore more sensitive than the hydrogen peroxide method reported previously[2] and should also be useful for assay of blood glucose. This electrode is likewise stable over four months.

CONCLUSIONS

As reported in a previous paper on the uric acid electrode[1] and this paper on L-amino acid and glucose electrodes, the dissolved oxygen method has many merits. First, it is very simple to immobilize the enzyme, to construct the electrode and to measure substrate concentrations as low as 10^{-5}–10^{-6} M. Secondly, the only reagent required is the buffer solution (10 ml or less), and only a few minutes are necessary for one assay. Thirdly, no pretreatment of the electrode is required,

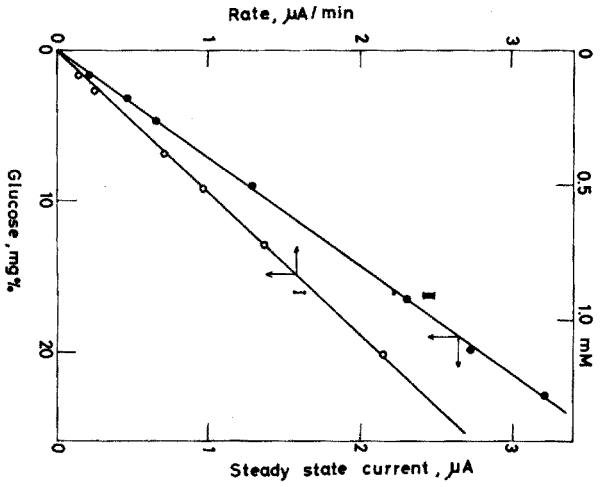

Fig. 4. Calibration curves for glucose at −0.6 V *vs.* SCE. 0.1 *M* Phosphate buffer, pH 7.3, 30°C. (I) Rate method; (II) steady-state method.

such as elimination of oxide films on the platinum electrode which is necessary for the hydrogen peroxide method, and there is no need for pretreatment of the sample solution, such as deproteinization as required by the spectrophotometric method. Moreover, the method is more sensitive than the hydrogen peroxide method because of the sensing of the dissolved oxygen starting material instead of the unstable product, hydrogen peroxide, which is consumed in several ways, such as catalase decomposition or reaction with other products.

The method eliminates the interference of other compounds present in blood which are easily oxidized on the platinum electrode at positive potentials, such as uric acid which gives a positive error in the hydrogen peroxide method.

Because the membrane present in the regular oxygen electrode is eliminated in this electrode, the speed of response is faster and the electrode is insensitive to protein material present in blood that tends to block the pores of the oxygen membrane electrode causing experimental difficulties.

This method should be very useful in the assay of other oxidase systems, such as cholesterol oxidase, xanthine oxidase, pyruvate oxidase, sulfite oxidase, and thiol oxidase.

The financial assistance of the National Science Foundation, NSF Grant No. GP-31518, is gratefully acknowledged. Also, the authors wish to thank Dr. S. S. Kuan for discussions on this report.

SUMMARY

New electrodes based on chemically bound enzymes are described for glucose and L-amino acids. The decrease in the dissolved oxygen content during the enzyme reaction is measured polarographically. The electrodes are stable for at least 4 months and give a response in less than 1 min. These electrodes are more sensitive than the hydrogen peroxide-based electrodes described previously, because

the unstable peroxide can be consumed in several ways such as catalase decomposition or reaction with other products.

REFERENCES

1 M. Nanjo and G. G. Guilbault, *Anal. Chem.*, 46 (1974).
2 G. G. Guilbault and G. J. Lubrano, *Anal. Chim. Acta*, 64 (1973) 439; 60 (1972) 254.
3 G. Nagy, L. H. von Storp and G. G. Guilbault, *Anal. Chim. Acta*, 66 (1973) 443.
4 G. G. Guilbault and G. Nagy, *Anal. Lett.*, 6 (1973) 301.
5 G. G. Guilbault and G. J. Lubrano, *Anal. Chim. Acta*, 69 (1974) 183.
6 G. G. Guilbault, *Anal. Chem.*, 42 (1970) 334R; 40 (1968) 459R.
7 H. V. Malmstadt and T. P. Hadjiioannou, *Anal. Chem.*, 35 (1963) 14.
8 L. A. Lichtenberg and D. Wellner, *Anal. Biochem.*, 26 (1968) 313.
9 G. G. Guilbault and J. E. Hieserman, *Anal. Biochem.*, 26 (1968) 1.
10 G. G. Guilbault and E. Hrabankova, *Anal. Chem.*, 42 (1970) 1779; *Anal. Chim. Acta*, 56 (1971) 285.
11 S. J. Updike and G. P. Hicks, *Nature (London)*, 214 (1967) 986.
12 A. Meister, D. Wellner and S. J. Scott, *J. Nat. Cancer Inst.*, 24 (1960) 31.
13 J. P. Greenstein, S. M. Birnbaum and M. C. Otey, *J. Biol. Chem.*, 204 (1953) 307.
14 E. A. Ziller and A. Maritz, *Helv. Chim. Acta*, 27 (1944) 1888.
15 H. Kalant, *Anal. Chem.*, 28 (1956) 265.
16 J. R. Spies and D. C. Chambers, *Anal. Chem.*, 20 (1948) 30.

Analytica Chimica Acta, 73 (1974) 375–382

SELECTIVITY OF NEUTRAL CARRIER–PVC MEMBRANE ELECTRODES

MARCO MASCINI and FRANCO PALLOZZI*
Istituto di Chimica Analitica, Università di Roma, 00185 Roma (Italy)
(Received 16th April 1974)

Neutral carrier electrodes are of practical importance in the determination of alkali and alkaline earth metal cations. The mechanism of operation has been investigated[1–4] and it has been experimentally demonstrated[2,3] that the selectivity coefficients of liquid membrane electrodes based on valinomycin and cyclic polyethers as neutral carriers can be predicted from the formation constants of the complex between the metal ion and the carrier, at least for monovalent cations.

These experimental studies have not included an examination of the influence of the solvent of the carrier on the pattern of selectivity and the selectivity coefficient values; and they disagree with the theoretical conclusion[1] that the selectivity depends on the desolvation energy of the cation from aqueous solution, and on the solvation energy in the carrier, which varies with the solvent used for the carrier. Simon and Morf[4] have discussed these discrepancies.

Recently, it has become popular to use PVC membrane electrodes[5–8] because a solid construction is convenient for practical purposes. In the study described here, the selectivity coefficients of cations with neutral carriers in PVC membrane electrodes were measured in order to obtain information on the influence of the solvents in such membranes and to compare such electrodes with liquid membrane electrodes. The effects of different plasticizers on the performance of a potassium-selective PVC membrane electrode has already been described, but these electrodes were based on tetra(*p*-chlorophenyl)borate[9].

In PVC membranes, the pore size is diminished to macromolecular dimensions, the viscosity of the organic liquid is increased, and convection is totally avoided. In this medium it seems probable that interaction between the neutral carrier molecules and the PVC matrix would occur, and a different mechanism of operation could be postulated. In the preparation of PVC neutral carrier membranes, it was soon found that it was necessary to add plasticizers with PVC to obtain Nernstian behaviour; various workers have recommended different plasticizers with good results[6–10]. The initial aim of this study was to obtain electrodes with reproducible behaviour and Nernstian slope, for only with such electrodes is it meaningful to measure selectivity coefficients.

EXPERIMENTAL

Neutral carriers and plasticizers

Valinomycin was obtained from Calbiochem; the cyclic polyethers (crown

* Laboratorio Inquinamento Atmosferico, Consiglio Nazionale delle Richerche.

compounds) dicyclohexyl-18-crown-6 and dibenzo-18-crown-6 were kindly donated by Dr. A. K. Fredsdorff (E. I. Du Pont de Nemours and Co.). The dicyclohexyl-18-crown-6 proved unsatisfactory in electrodes, because a long response time was necessary to obtain a stable potential and the results were poorly reproducible.

The plasticizers used were tributylphosphate, dibutylphthalate and diphenylether (Fluka). The PVC was obtained from Montedison as a powder.

Membrane preparation

The general procedure used to obtain PVC–neutral carrier membranes was to dissolve 0.15–0.20 g of PVC, 5–10 mg of neutral carrier and 0.1–0.4 g of plasticizer in 6 ml of tetrahydrofuran. In some cases, the plasticizer was omitted. The solution was poured on a Petri dish of 48 mm diameter. After evaporation of the tetrahydrofuran, a film 0.15 cm thick was obtained. Disk of 6 mm diameter were cut with a cork-borer and fixed to a PVC tube with an adhesive obtained by dissolving PVC in tetrahydrofuran.

Electrodes

The internal solution for the neutral carrier electrodes was of 10^{-3} *M* potassium chloride; a silver–silver chloride wire served as internal reference electrode. The external reference electrode was a saturated calomel electrode with a double junction and ammonium nitrate solution in the external chamber.

The electrochemical cell can be represented as follows:

$$\underbrace{\text{Ag.AgCl, 0.001 } M \text{ KCl}|\text{PVC membrane}|\text{sample}}_{\text{PVC membrane electrode}}\underbrace{||0.1\ M\ NH_4NO_3||KCl_{sat}Hg_2Cl_2(s)Hg}_{\text{ref. electrode}}$$

The PVC membrane electrode loaded with carrier was conditioned for 24 h in 10^{-3} *M* potassium nitrate after being assembled.

Measurement techniques

All measurements were made at 25°C. The calibration curves for electrodes in pure potassium(I) solution were obtained by sequential dilution of a 0.1 *M* potassium nitrate solution.

The selectivity coefficients were measured in mixed solutions of potassium(I) and interfering ion, by taking a constant background of potassium(I) ion and varying the concentration of interfering ion, as described by Toth and Pungor[11]. The curves were obtained in both directions, *i.e.* increasing the concentration of interfering ion and then decreasing it. In some cases, it was necessary to wait for hours to obtain a stable value of potential, and the reference electrode was then immersed in the solution intermittently to eliminate the leakage of ammonium ion. By extrapolating the two branches of the curve (one parallel to the abscissa and the other with a Nernstian or quasi-Nernstian slope) an interfering ion concentration (C_m^+) was obtained; the selectivity coefficient K_{KM} was the ratio C_{K^+}/C_{M^+} where C_{K^+} was the constant background concentration.

RESULTS AND DISCUSSION

The first problem was to obain Nernstian behaviour with neutral carriers

TABLE I

COMPOSITION OF PVC MEMBRANES TESTED

Composition number	*Carrier*	*Plasticizer*[a]
1	Valinomycin	—
2	Valinomycin	TBP
3	Valinomycin	TBP+D
4	Valinomycin	DBP
5	Dibenzo-18-crown-6	—
6	Dibenzo-18-crown-6	TBP
7	Dibenzo-18-crown-6	TBP+D
8	Dibenzo-18-crown-6	DBP

[a] TBP, tributylphosphate; D, diphenylether; DBP, dibutylphthalate.

embedded in PVC membranes; in Table I are reported the carriers and the plasticizer used with PVC. At least five electrodes of each preparation were prepared in order to obtain information on the influence of the neutral carrier concentration and of the polymer content. In practice, it was found that the components could be mixed in different proportions without modifying the behaviour of the electrode. But in all cases it was necessary to ensure that the plasticizer content sufficed to allow mobility of the carrier. The evaporation of the plasticizer with time (some months

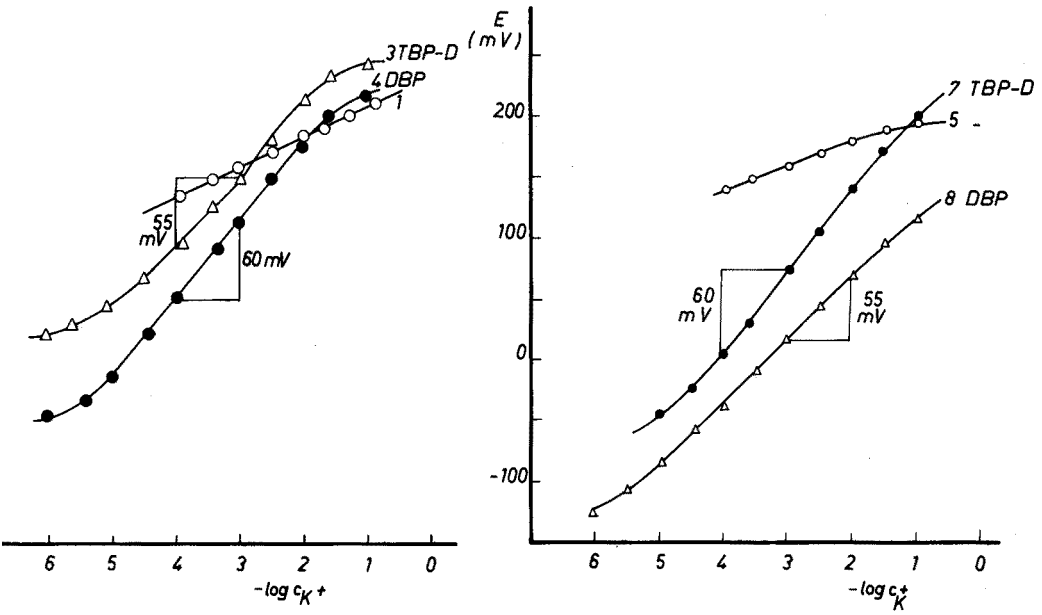

Fig. 1. Calibration curves for PVC membranes loaded with valinomycin. Numbers refer to Table I.

Fig. 2. Calibration curves for PVC membranes loaded with dibenzo-18-crown-6.

TABLE II

ELECTRODE PROPERTIES OF PVC MEMBRANES WITH NEUTRAL CARRIERS COMPARED WITH LIQUID MEMBRANES

Type	*Electrode*	*Plasticizer*[a]	*Range pK*	*Slope (mV/decade)*	*Values of K_{KM}; interfering ion*						
					Na^+	Rb^+	NH_4^+	Cs^+	Li^+	Ca^{2+}	Mg^{2+}
Valinomycin											
PVC	3[b]	TBP+D	1–2	40	$<2\cdot10^{-4}$	3	$1.2\cdot10^{-2}$	$2.6\cdot10^{-1}$	$\sim10^{-4}$	$\sim10^{-4}$	$\sim10^{-4}$
			2–5	55							
PVC	4[b]	DBP	1–2	40	$<2\cdot10^{-4}$	3	$2\cdot10^{-2}$	$5\cdot10^{-1}$	$\sim10^{-4}$	$\sim10^{-4}$	$\sim10^{-4}$
			2–5	60							
			5–6	30							
PVC	Ref. 6	DOA	1–4	57	$7\cdot10^{-5}$	4.8	$1.3\cdot10^{-2}$	$6\cdot10^{-1}$	$2\cdot10^{-4}$	$5\cdot10^{-5}$	$5\cdot10^{-5}$
PVC	Ref. 8	DPP	1–5	60	$3\cdot10^{-4}$						
Liquid	Ref. 2	—			$\sim10^{-4}$	2.5	$2\cdot10^{-2}$		$\sim5\cdot10^{-5}$		
Dibenzo-18-crown-6											
PVC	7[b]	TBP+D	1–2	40	$7\cdot10^{-2}$	10^{-1}	$<10^{-2}$	10^{-1}			
			2–5	55							
			5–6	35							
PVC	8[b]	DBP	1–4	60	$4.5\cdot10^{-1}$	10^{-1}	$6\cdot10^{-2}$	$9\cdot10^{-2}$			
			4–5	40							
PVC	Ref. 8	DPP	2.5–5	51	$7.7\cdot10^{-2}$						
Liquid	Ref. 3	—			$4\cdot10^{+2}$	0.3	$6\cdot10^{-2}$	$2.5\cdot10^{-1}$			

[a] D, diphenylether; TBP, tributylphosphate; DBP, dibutylphosphate; DOA, dioctyladipate; DPP, dipentylphthalate.
[b] Number refers to Table I.

at room temperature, or some hours in an oven) led to useless membranes, but a drop of plasticizer added to the PVC membrane was sufficient to restore the Nernstian behaviour. Accordingly, the percentages of polymer are not specified in the Table. Within the ranges described for the preparation of the membranes, the behaviour of the electrodes seemed reproducible and independent of the plasticizer content.

Figures 1 and 2 show the calibration curves for the different compositions in Table I. Valinomycin and dibenzo-18-crown-6 electrodes without plasticizer (curves 1 and 5) showed slopes of about 20 mV per decade; with only TBP as plasticizer (electrodes 2 and 6), the calibration curves obtained are not reported because of the poor reproducibility of the potential values. In all other cases, the slopes were near the Nernstian value in the range 10^{-2}–10^{-5} M, and these membrane electrodes can be utilized in the range 10^{-1}–10^{-6} M potassium ion. Diphenylether cannot be used alone as platicizer, being exuded from the membrane.

The second point of the research was to examine selectivity coefficients, and to establish if the values obtained were reasonably constant with different plasticizers and if they were comparable to the values obtained for liquid membrane electrodes.

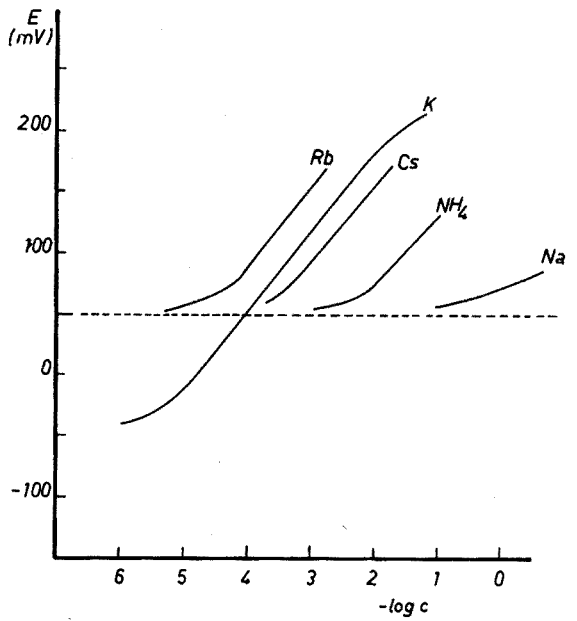

Fig. 3. Selectivity coefficient measurements for the valinomycin composition 3. $[K^+] = 10^{-4}$ M.

In Table II and in Figs. 3–6 are shown the results obtained with the different electrode compositions in PVC; Table II also shows some results published by different workers during the course of this work. The selectivity coefficients were determined by different techniques but the results appear to be quite similar. The results obtained by Rechnitz[2,3] with liquid membranes complete Table II.

As can be seen from the Figures, when the selectivity coefficients are quite low (*ca.* 10^{-4}), it is very difficult to obtain significant values. When the selectivity coefficient lies in the range 10–10^{-2}, extrapolation is much easier and more precise.

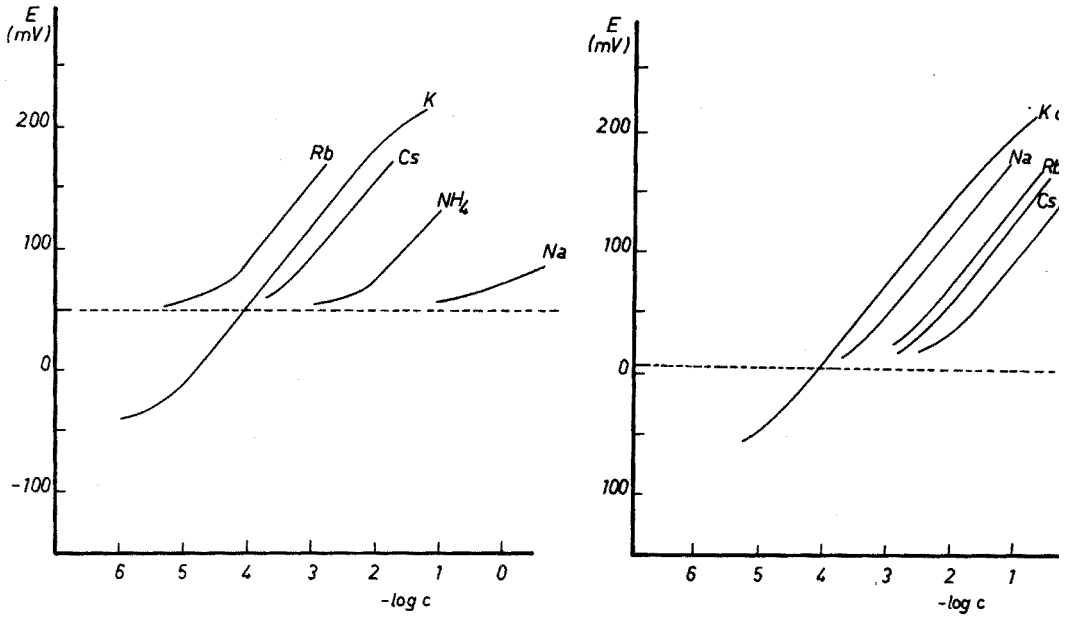

Fig. 4. Selectivity coefficient measurements for the valinomycin composition 4. $[K^+] = 10^{-4}$ *M*.

Fig. 5. Selectivity coefficient measurement for the dibenzo-18-crown-6 composition 7. $[K^+] = 10^{-4}$ *M*.

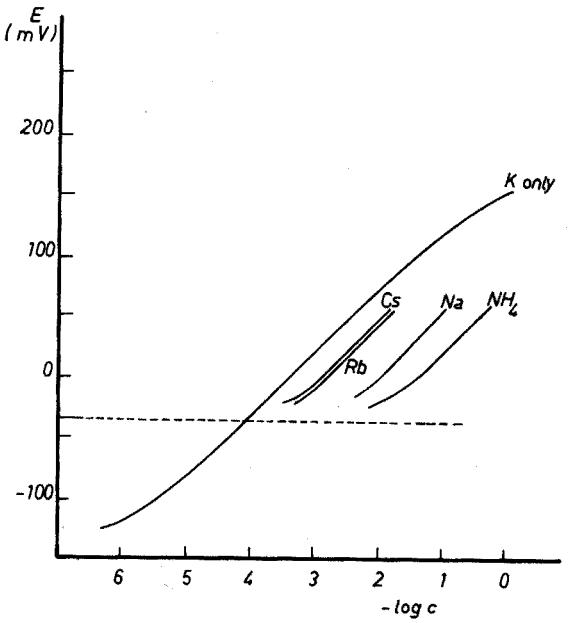

Fig. 6. Selectivity coefficient measurement for the dibenzo-18-crown-6 composition 8. $[K^+] = 10^{-4}$ *M*.

It is worth noting that the electrodes react in a near-Nernstian fashion with rubidium, caesium, ammonium and sodium ions, as well as potassium ions. The curves in Figs. 3–6 show some horizontal potassium response sections as well as sections which indicate the response to the interfering ion; the slopes of these latter portions are almost parallel to the potassium calibration curves (K only) which have slopes of 55–60 mV per decade change in activity (Table II). The fact that these electrodes can change rapidly, and quite reproducibly, from a potassium response to an interfering ion response during the course of a single experiment, is unusual, and seems to reflect an uncommonly high rate of ion-replacement phenomena with these neutral carriers. Similar rapid exchanges were not observed with the bivalent ions, calcium and magnesium, and in these cases the reproducibility of the tests was very poor.

Table II shows that there is no meaningful difference in selectivity coefficients between the liquid membrane electrodes and the PVC electrodes, no matter which plasticizer is used, when valinomycin serves as the neutral carrier. But significant differences are obtained when the neutral carrier is dibenzo-18-crown-6. It should be noted that the pattern of selectivity changes with the plasticizer—an effect which has also been found by Baum and Lynn[9] for a different type of potassium-selective electrode based on PVC. With TBP and diphenylether, the response decreases

TABLE III

RESULTS OBTAINED WITH POLYMERS OTHER THAN PVC

(DBP, dibutylphthalate; DB, dibenzo-18-crown-6)

Composition	*Amounts used (mg)*	*pK-Range*	*Slope*	*Selectivity constant*
Polymethylmethacrylate	150	5–4	42	Na^+ $9 \cdot 10^{-2}$
DBP	200	4–2	58	Rb^+ $1.3 \cdot 10^{-1}$
DB	5	2–1	20	Cs^+ $1.3 \cdot 10^{-1}$
Collodion	200 4–1	42 Poor reproducibility		
DB	5			
Polymethylmethacrylate	200			
DBP	200	High resistance		
DB	10			
Polybutylmethacrylate	400			
DBP	200	Sticking; exudes solvent		
DB	5			
Polybutylmethacrylate	600			
DBP	200	Sticking; high resistance		
DB	5			
Polystyrene	150 300	Poor mechanical properties		
DBP	100 or 150			
DB	5 5			
Polystyrene	600	High resistance; no response		
DBP	250			
DB	10			
Polyamide	200	Sticking		
DBP	100			
DB	5			

in the order: $K > Na > Rb > Cs > NH_4$, whereas with DBP, the order is $K > Cs > Rb > Na > NH_4$.

The selectivity reflects the ability of the cation to accommodate itself within the coordinating cavity of the neutral carrier, and this property depends on the interaction of the cation with the ligand dipoles and with the organic solvent for the neutral carrier. Thus the selectivity coefficient values do depend largely on the solvation energy of the cation in the cavity. The experimental results indicate that in the PVC–plasticizer medium, the solvation energy of the cation in valinomycin is not affected by interactions with the medium of the neutral carrier; in the case of the dibenzo-18-crown-6 electrodes, such interactions do contribute to the solvation energy. The experimental results conform with a comparison of molecular models: the potassium–dibenzo-18-crown-6 complex is quite rigid and is not susceptible to much deformation from the planar configuration[12] but the open configuration allows interaction perpendicularly to the plane; whereas with valinomycin the carrier surrounds the metal ion completely[13] so that no interaction is possible. However, some recent data[7] on valinomycin electrodes indicate that the potassium/sodium selectivity coefficient may change drastically with the type of polymer, the plasticizer and the percentage composition of the membrane; thus even with valinomycin it seems probable that some interactions exist.

In the present work, attempts were made to prepare electrodes with polymers other than PVC based on dibenzo-18-crown-6. The results are summarized in Table III; unfortunately these electrodes generally had poor mechanical properties and the results obtained were not reproducible.

SUMMARY

The selectivity coefficients of monovalent cations with neutral-carrier PVC membrane electrodes have been measured in order to establish the influence of solvent interactions in such media. The results are compared with those from liquid membrane electrodes. Valinomycin and dibenzo-18-crown-6 were used in PVC membranes with different plasticizers. Other polymeric membrane materials were less satisfactory than PVC.

REFERENCES

1 G. Eisenman in *Ion Selective Electrodes, NBS Special publication 314*, Washington, D.C., 1969, Ch. 1.
2 E. Eyal and G. A. Rechnitz, *Anal. Chem.*, 43 (1971) 1090.
3 G. A. Rechnitz and E. Eyal, *Anal. Chem.*, 44 (1972) 370.
4 W. Simon and W. E. Morf, *Ion Selective Electrodes, Symposium held at Matrafured, Hungary, 23–25 Oct. 1972*, p. 127.
5 G. J. Moody and J. D. R. Thomas, *Selective Ion-Sensitive Electrodes*, Merrow, London, 1971.
6 J. Růžička, E. H. Hansen and J. Chr. Tjell, *Anal. Chim. Acta*, 67 (1973) 155.
7 V. Fiedler and J. Růžička, *Anal. Chim. Acta*, 67 (1973) 179.
8 O. Ryba, E. Knižáková and J. Petránek, *Collect. Czech. Chem. Commun.*, 38 (1973) 497.
9 G. Baum and M. Lynn, *Anal. Chim. Acta*, 65 (1973) 393.
10 J. Pick, K. Toth, M. Vašak, E. Pungor and W. Simon, *Anal. Chim. Acta*, 64 (1973) 477.
11 K. Toth and E. Pungor, *Anal. Chim. Acta*, 37 (1969) 291.
12 G. Eisenman, S. M. Ciani and G. Szabo, *Fed. Proc.*, 27 (1968) 1289.
13 W. E. Morf and W. Simon, *Helv. Chim. Acta*, 54 (1971) 2683.

Analytica Chimica Acta, 73 (1974) 383–389

A PIEZOELECTRIC DETECTOR FOR ORGANOPHOSPHORUS PESTICIDES IN THE AIR

WALTER M. SHACKELFORD and GEORGE G. GUILBAULT

Department of Chemistry, University of New Orleans, New Orleans, Louisiana 70122 (U.S.A.)*

Received 11th June 1974)

Monitoring of air pollutants continues to be of increasing importance. Methods and equipment for monitoring various pollutants must be simple and rugged, yet selective and extremely sensitive. Previous work has shown that piezoelectric crystal detectors with coatings which are highly selective can provide the basis for analytical systems which are consistent with the above criteria[1,2]. These detectors consist of a vibrating quartz crystal which is coated with a substrate which selectively and reversibly adsorbs the desired pollutant when exposed to air contaminated with the pollutant. The frequency of vibration of the crystal depends on the weight of the coating and the weight of the material adsorbed onto the coating. Thus, the concentration of the pollutant in the air is measured by observing changes in the frequency of the vibrations of the coated crystal. Previous work[1,2] has shown that the theoretical limit of detection for a substrate coated crystal is about 10^{-12} g.

Organophosphorus pollutants

The monitoring of organophosphorus pollutants is of paramount importance for two reasons. First, organophosphorus pesticides to one degree or another are powerful cholinesterase inhibitors and as such are toxic to wildlife and humans, as well as to pests. Secondly, since organophosphorus pesticides are effective and have great persistence, their use and control requires diligent application of safeguards. Thus, there is the need for a rugged, portable, and sensitive monitor for airborne organophosphorus pesticides.

Almost all organophosphorus pesticides contain either the phosphoryl or thiophosphoryl groups. Although the reactions of compounds containing these groups are similar, in this study both a phosphoryl- and thiophosphoryl-containing compound were used for study. Diisopropyl methylphosphonate (DIMP) was also used as a model, as has been the practice in many studies of phosphoryl-containing compounds. DIMP, however, is an extremely weak cholinesterase inhibitor and was found to be a poor model for compounds with more vigorous action toward cholinesterase. Nevertheless, DIMP can be used as a model for the detection of actual phosphorus-containing pesticides.

The previous work concerning piezoelectric crystal detectors for organophosphorus compounds utilized metal complexes of the pesticides as an adsorptive

* A Member of the L.S.U. System (formerly L.S.U. in New Orleans).

substrate[3]. Although useful as detectors, these metal complexes lacked the sensitivity desirable in many cases of assay of organophosphorus compounds in the atmosphere. In this work, emphasis was placed on using compounds as substrates which had demonstrated reactivity toward cholinesterase inhibitors. Oximes have been shown to react with organophosphorus cholinesterase inhibitors in solution, and are used as antidotes for organophosphorus poisoning[4]. Thus, certain oximes which had been shown to have fast reaction rates with organophosphorus compounds were chosen for this study. Since many reactions between an oxime and an organophosphorus compound in the body are irreversible, it was felt that the study should also address itself to the problem of obtaining fast reversibility, which is needed for a workable piezoelectric crystal detector system.

EXPERIMENTAL

Equipment and chemicals

For this work an instrument was built from a modified design by Karasek and Gibbens[2]. The instrument consists of two modified Clapp oscillators, the signals from which are mixed, and the resultant difference frequency is fed through a pump diode circuit to either an ammeter or a recorder. The schematic drawing for this instrument is shown in Fig. 1. Power for the instrument was obtained from a Heathkit variable power supply (Model 1P-28) set at 9.0 V. The frequency of the two oscillators (reference and detector) was monitored with a digital frequency counter (Systron–Donner, Model 8050) which has an accuracy of ± 0.1 cycle. The output voltage was monitored by a potentiometric recorder (Bristol Dynamaster). For purposes of zeroing the detector oscillator with respect to the reference oscillator, an ammeter built into the instrument was used.

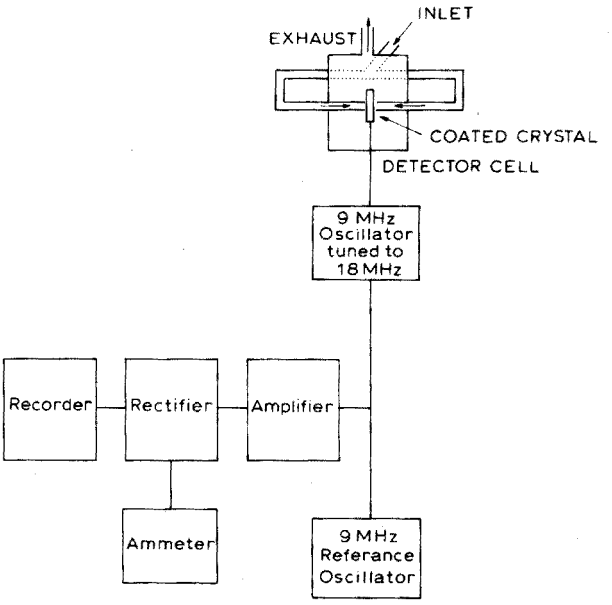

Fig. 1. Block diagram for flow system and instrument layout.

The piezoelectric crystals used were 9 MHz quartz crystals with a plated metal electrode on each side. The crystals were AT-cut and mounted in a HC 6/U holder (International Crystal Manufacturing Co., Oklahoma City). The chemicals used were reagent grade and not further purified. The organophosphorus compounds were degassed and further purified by a freeze–thaw method on a vacuum line. The gas flow cell which held the detector crystal was built after the design of Karmarkar and Guilbault[5].

Operating procedure

Air was drawn into the detector cell by means of an aspirator at rates of between 10 and 30 ml min^{-1}. The cell was isolated from the aspirator by a flow meter and a capillary stainless steel tube (12-in. long, 1/16-in. o.d.). Thus, small variations in pressure caused by irregularity of the flow of water were eliminated at the detector. Also, since the inlet to the detector and all tubing in the detector was 1/4-in. o.d. glass tubing, the pressure within the cell was always equal to the ambient pressure. Samples diluted with ambient air were injected into the flowing stream at the detector inlet and the resultant changes in frequency were recorded on the potentiometric recorder.

Samples were prepared by allowing purified organophosphorus compounds to come to equilibrium in 2-l flasks. From these stock samples, portions were removed with 10-ml glass syringes and then diluted appropriately before injection. Literature values for vapor pressures of the compounds studied were used after confirmation on the vacuum rack. The sample size for injection was standardized at 5 ml for convenience in injection as well as for optimal response at the flow rates used. Detector crystals were prepared by dropping 0.05 μl of a *ca.* 5.0% solution of the substrate in a volatile solvent on each electrode face; the solvent then evaporated leaving a thin coating of substrate on the crystal. The substrate application was reproducible within 1000 Hz which was well within the adjustment capabilities of the instrument. About 2 h was required for equilibration of the crystal after it was placed in the air stream of the cell. All samples were reversible within 5 min.

RESULTS

Oxime coatings

Two oximes of proven reactivity toward organophosphorus compounds were evaluated for use as substrates. 2-Pyridylaldoxime methiodide (2-PAM) has been used as a therapeutic agent[4], and isonitrilobenzoylacetone (IBA) as a reagent in the determination of organophosphorus compounds[6]. 2-PAM proved to be too volatile for use in a flowing gas stream detector. IBA, when used as the sodium salt, proved to be quite stable, selective, and sensitive. Unfortunately, the reaction taking place on the substrate surface was not reversible, and sensitivity decreased with each injection until only about 1% of the original sensitivity remained; at this point the sensitivity leveled off. To remedy this situation, the cobalt complex of IBA was made as described in the literature procedure[7]. The yellow complex was dissolved in methylene chloride and applied to the crystal as described above. The resultant detector was stable, selective, sensitive and completely reversible.

Further improvement in this substrate was made by adding a small amount of pesticide to the methylene chloride solution of the cobalt–IBA complex. This latter improvement increased sensitivity and added to the overall lifetime of the crystal. Whereas the cobalt–IBA complex alone could be expected to decrease in sensitivity by 1/3 in about a week, the improved substrate (cobalt–IBA–organophosphorus complex) required about three weeks for a similar loss in sensitivity.

In Table I the responses of the three coatings tried are shown. The organophosphorus compound detected here was dimethyldichlorovinyl phosphonate (DDVP), and diethyl-*p*-nitrophenylphosphonate (Paraoxon) was used in fabricating the most sensitive crystal substrate.

TABLE I

RESPONSE OF SUBSTRATE-COATED CRYSTALS TO 1 p.p.m. DDVP

	Fresh coating response (Hz)	*Response after one week (Hz)*
Na–IBA	16	—
Co–IBA	40	16
Co–IBA–Paraoxon	54	50

As previously mentioned, it is believed that the loss of sensitivity of the sodium–IBA crystal is due to the irreversible reaction of the organophosphorus compound with the substrate. This was evidenced by a lowering of frequency as the reaction occurred and then only a slight recovery. Upon injection of another sample, the drop in frequency decreased markedly. This decrease in response indicates that the active sites on the substrates are irreversibly occupied.

The loss in sensitivity by the cobalt–IBA substrate appears to be due to the effects of exposure to the flowing air stream for the indicated period. Monitoring of the frequency revealed a loss of about 700 Hz during exposure for one week. This loss of frequency is probably due to volatility of the substrate. The increase of sensitivity and lifetime of the cobalt–IBA–Paraoxon over that of the previous two detectors is thought to be due to the added sorption effect caused by the organophosphorus compound (Paraoxon) present in the substrate and to decreased volatility, respectively.

Detection of organophosphorus compounds

Figures 2, 3, and 4 give the response of the cobalt–IBA–Paraoxon detector to the three studied compounds, parathion, DDVP, and DIMP. From a comparison of the three Figures, it is evident that DIMP is not a good model for pesticides when this detector is used. The lack of response toward DIMP indicates that interference from organophosphorus compounds which are not pesticides is small. Parathion, which is a stronger cholinesterase inhibitor than DDVP, shows much more interaction with the detector than DDVP. Recovery time for the crystal when Parathion is the detected pesticide is longer than that for DDVP, but not inordinately so; also, recovery to the original frequency is complete. The relatively high vapor pressure of DDVP as compared to Parathion allows a much wider

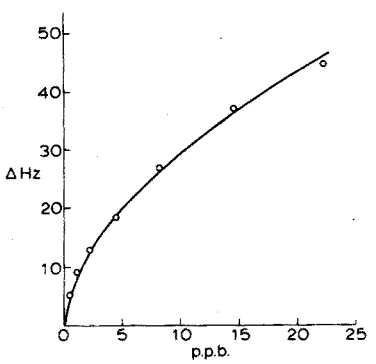

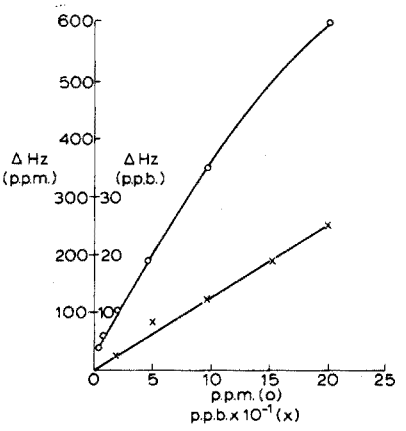

Fig. 2. Plot of change in frequency against concentration in air for Parathion.

Fig. 3. Plot of change in frequency against concentration in air for DDVP; (○) p.p.m. range values, (×) p.p.b. range values.

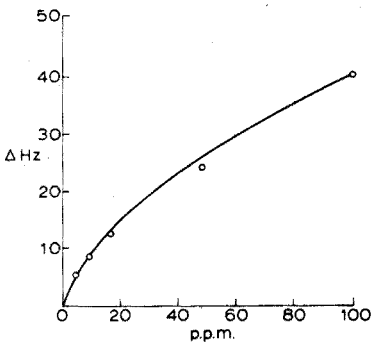

Fig. 4. Plot of change in frequency against concentration in air for DIMP.

range of detection in a calibration plot. In all three cases, the calibration plots tail off at higher concentrations. It is thought that this curvature is due to a change in the overall mechanism of sorption. At very low concentrations of sample, sorption is essentially between the substrate and the sample; whereas, at higher concentrations as the sites on the substrate are filled, adsorption on the previously sorbed layer occurs. This would account for the loss in sensitivity at higher levels of concentration. Since syringe dilution is not especially precise, the dilution technique may contribute to the curvature. Care was exercised, however, to increase the concentration of successive samples when calibrating. In this way, contamination from previous samples was minimized.

Interferences

In Table II, the various interferences which would be expected to exist in open air sampling are enumerated and their respective responses are shown. It is

TABLE II

RESPONSE OF SUBSTRATE-COATED CRYSTALS TO INTERFERENCES

Interference	*Concentration (p.p.m.)*	*Response (Hz)*
SO_2	1000	14
CO_2	1000	7
CO	1000	10
NO_2	100	20
NH_3	100	20

TABLE III

RESPONSE OF SUBSTRATE-COATED CRYSTALS TO OTHER PESTICIDES

Pesticide	*Response (Hz)*
Lindane	0
Heptachlor	0
DDD	2
Chlordane[a]	175
Karathane[a]	26

[a] Hydrocarbon solvent present.

evident that normal air pollutants pose little problem as interferences to this detector. It should be noted, however, that the responses to nitrogen dioxide and ammonia are only very slowly reversible, and that long exposure to concentrations of these greater than 100 p.p.m. can result in poisoning of the detector.

Water vapor interference is compensated for by use of the mixer circuit in the instrument. When the detector crystal is tuned to the reference crystal in the presence of air, the water vapor concentration in air is compensated for. At present this compensation is manually performed.

Air samples of chlorinated hydrocarbon pesticides at saturated vapor pressure concentrations gave practically no interference except when the pesticide was combined with a solvent. Table III shows the results of this interference study. Chlordane and Karathane contained hydrocarbon solvents and thus the response noted is due to high (>100 p.p.m.) solvent concentrations in the vapor. Heptachlor, which is an isomer of chlordane, gave no response, nor did Lindane. Both of these samples as well as that of DDD were free of solvent. The conclusion may be drawn that the vapors from these pesticides will not interfere with the detection of organophosphorus pesticides after solvent dissipation.

CONCLUSIONS

Piezoelectric crystals coated with metal complexes of oximes are sensitive, selective, and relatively durable detectors for organophosphorus pesticides. These

detectors may be combined with inexpensive portable instruments available today to provide convenient simple systems for field monitoring of pesticides at p.p.b. levels. Work is in progress to construct a new instrument with automatic compensation for moisture in the air, and new oxime complexes will be made to increase the selectivity of the detector.

The authors gratefully acknowledge the financial assistance of the Army Research Office (Grant No. ARO-RDRD-CH-11753-C), in carrying out this research.

SUMMARY

A quartz piezoelectric crystal coated with a substrate has been used for the detection of organophosphorus pesticides via selective sorption. The crystal is incorporated in a mixer circuit to allow read-out by either an ammeter or a recorder, and is sufficiently sensitive to allow detection of organophosphorus pesticides at levels of less than 10 p.p.b. AT-cut quartz crystals with fundamental frequencies of 9.0 MHz were coated with oxime substrates and subsequently investigated and evaluated for response to organophosphorus pesticides. This detector has a potential for use both as an air pollution sensor and a highly selective gas chromatography detector.

REFERENCES

1 W. H. King, Jr., *Anal. Chem.*, 36 (1964) 1735; *U.S. Patent*, 3, 164, 004 (5 January 1965); *Environ. Sci. Technol.*, 4 (1970) 1136; *Res. Develop.*, 20 (1969) 28.
2 F. W. Karasek and K. R. Gibbens, *J. Chromatogr. Sci.*, 9 (1971) 535.
3 E. P. Scheide and G. G. Guilbault, *Anal. Chem.*, 44 (1972) 1764.
4 R. I. Ellin and J. H. Wills, *J. Pharm. Sci.*, 53 (1964) 995.
5 K. H. Karmarkar and G. G. Guilbault, *Anal. Chim. Acta*, 71 (1974) 419.
6 E. J. Poziomek, E. V. Crabtree and D. N. Kramer, *Mikrochem. J.*, (1969) 150.
7 T. W. J. Taylor and E. K. Eubank, *J. Chem. Soc., London*, (1926) 2818.

Analytica Chimica Acta, 73 (1974) 391–398

SELECTION AND PREPROCESSING OF FACTORS FOR SIMPLEX OPTIMIZATION

LAURA A. YARBRO and STANLEY N. DEMING*

Department of Chemistry, Emory University, Atlanta, Georgia 30322 (U.S.A.)

(Received 18th May 1974)

Simplex optimization was developed as an alternative method of evolutionary operation[1–3], a procedure generally used in industry to optimize product yield. Spendley *et al.*[4] introduced simplex optimization as a method that is simple and efficient. The method is not based on factorial experiments and thus requires fewer experiments per move than evolutionary operation. Spendley *et al.*[4] foresaw the possible adaptation of this method to other areas of research and its easy implementation on digital computers. Long[5] was the first to propose the utility of the fixed-sized simplex to analytical chemistry.

Since its introduction in 1962, the simplex optimization method has undergone several modifications. Most of these modifications were implemented either to allow expansion of the simplex in directions that are favorable and contraction in directions that are unfavorable[6], or to provide the algorithm with a means of handling boundary conditions and constraints[7–9]. The mathematical details of the simplex method have been described previously[4–12].

The usual method of defining the initial simplex[5] has been to: (a) determine the relative significance of each factor and retain only the most significant factors for further study; (b) assign to each of these factors a step size that is inversely proportional to the factor's significance; and (c) calculate the vertices of the initial simplex.

The purpose of this paper is to discuss the definition of useful factors, the choice of initial step size, and the design of the initial simplex.

DEFINITION OF USEFUL FACTORS

Optimization methods based upon factorial designs generally require a large number of experiments; if k full factorial designs are needed to reach the optimum in a study involving n factors evaluated at m levels, then a minimum of $k(m^n)$ experiments is required. Thus, there is a strong incentive to study only the most significant factors.

The experimenter might already be sufficiently familiar with the system to select the significant factors[4]. If he is not, the traditional criterion for determining the significance of a factor has been the change in response caused by a given

* Author to whom correspondence should be addressed. Present address: Department of Chemistry, University of Houston, Houston, Texas 77004, U.S.A.

change in the level of the factor. Factorial experiments can be used to determine quantitatively the apparent effect of each factor on the overall response[5].

Long[5] has pointed out inadequacies in the use of two-level factorial experiments that might lead to the rejection of significant factors. The apparent change in response is not an absolute measure of a factor's effect because the response change is dependent on factor scaling and on the factor levels chosen for analysis. Long suggests that response could be normalized over the domain of a factor, or normalized with respect to the ability to control the factor's level.

Friedman and Savage[13] and Morgan and Deming[12] consider in detail two other problems associated with significant factor determination by factorial experiments. First, the difference in response for a continuous factor (*e.g.* pH, temperature, time, etc.) is dependent on the experimental levels examined. The levels might be so close together that the effect on the response would not be statistically significant. Yet, the levels might be too widely separated, in which case the optimum might be missed entirely and possibly no significant effect would be observed.

A second problem is the possible omission of a significant factor because of insufficient sensitivity of the experiments. When the null hypothesis is used to reject factors[14], a significant difference in response between experimental levels proves the null hypothesis false and the factor is retained as significant. However, when no significant difference is observed between experimental levels, care must be taken in asserting that the null hypothesis is true, for there might be differences in response that the experiment was unable to detect. This caution will probably result in a greater number of factors being included in the optimization process but the experimenter can be reasonably sure that a significant factor has not been omitted[12].

In the selection of factors for simplex optimization, all those factors which are thought to have a possible effect on the response should be included. Only those factors which are thoroughly understood to be insignificant should be rejected. If k simplex moves are needed to reach the optimum in a study involving n factors, then a minimum of only $k+(n+1)$ experiments is required. The inclusion of additional factors does not greatly increase the number of experiments required to reach the optimum.

The most useful manner of expressing each factor must be determined. Important considerations here are: (a) the undesirable possibility of a limiting reagent; (b) the possible interrelationships among factors; and (c) the ability to bound a factor.

Limiting reagent

Long[5] suggests that concentrations of a reagent less than the stoichiometrically required amount should not be included in a factor's domain because the response will of necessity increase proportionally with increasing concentration.

Interrelationships

When two factors are constrained (*e.g.*, a binary mixed solvent in which the mole fractions must add up to unity) they should be considered as one factor. If not handled in this way, dependent factors can create stationary ridges in the response surface which give an infinite number of combinations of the two factors

corresponding to optimum conditions[15]. Further, the experimenter must carefully choose the units by which the factor is expressed. For example, a seemingly useful factor might be the volume of a particular reagent added to a reaction mixture, the total volume of which is not held constant. Such a measure of factor level will produce inconsistent results because the effect is caused not by the total amount of the reagent present but rather by its concentration in the final reaction mixture.

Boundaries

Expressing the factor domains in bounded form facilitates an understanding of the region accessible to experimentation. An example of a naturally bounded factor is concentration which can vary from zero to saturation. Logarithmic transformations are often used to produce a domain throughout which unit changes are of equal importance. Such domains are not naturally bounded but the experimenter can often define a region of interest: pH, for example, is usually varied[16] between 0 and 14. Ratios are often troublesome because they range from zero to infinity; fractions of the whole can usually be employed instead.

When factors are expressed in different units or when they have different regions of interest, the following transformation[9] can be used to normalize the factor domains:

$$F = \frac{f - f_l}{f_h - f_l} \tag{1}$$

where F is the normalized value, f is the original value, f_l is the lowest value and f_h is the highest value in the original domain of the factor. The domain of all normalized factors ranges from 0 to 1.

After all of the useful factors have been defined, their bounds determined, and (optionally) their domains standardized, the initial simplex can be constructed. This involves the following: (a) choosing the initial step size; and (b) calculating the vertices of the initial simplex. These procedures interrelate and depend on the variation of the simplex method used. There are several possible choices for the initial step size and the feasibility of each can be understood in the context of the process that it optimizes.

CHOICE OF INITIAL STEP SIZE

The step size is the amount of change in a factor that occurs when a new vertex of the simplex is calculated. Each factor may be assigned a unique step size or the step size may be numerically identical for all factors. Depending on which variation of the simplex method is employed, the step size used in constructing the vertices of the initial simplex may be retained throughout the optimization process (fixed-size simplex[4]) or the step size may be changed as the optimization progresses (variable-size simplex[6]).

Traditional small step size

Evolutionary operation (EVOP) originated in an industrial environment where systems are operated at fixed levels of the various input factors. Any change

in these levels must be small to minimize the risk associated with producing material of unacceptable quality. Thus, traditional EVOP methods use factorial designs in which the differences in factor levels are small. For the same reason, simplex optimization in such environments uses a small step size and a fixed-size simplex. Perhaps because of this tradition, variable-size simplex optimization also uses a small initial step size.

Unique step size

Long[5] suggests that each factor can be assigned a unique step size such that these changes in the factors will produce equal changes in response. This can be stated

$$c_i\left(\frac{\partial R}{\partial F_i}\right) = K \tag{2}$$

where $\partial R/\partial F_i$ is the change in response with respect to factor F_i, and c_i is the number of units of factor i (unique step size) required to produce a specified change K in the response. As an example, for a given system a change of 10°C (c_1) in temperature (F_1) might be required to produce a change in response (K) equal to that produced by a change of 2 atm (c_2) in pressure (F_2).

Numerically identical step size

Factor scaling has been recommended[4] so that a unit change in each scaled factor will result in equal changes in response. Thus, it is possible to use a single step size for all factors. This can be stated

$$\left(\frac{\partial R}{\partial F_i'}\right) = K \tag{3}$$

which indicates that a unit change in the scaled factor F_i' produces a specified change K in the response. Scaling can be accomplished in the following way

$$F_i' = k_i \times F_i \tag{4}$$

The scaling factor k_i is related to the factor c_i. From eqns. (2) and (3)

$$c_i\left(\frac{\partial R}{\partial F_i}\right) = \left(\frac{\partial R}{\partial F_i'}\right) \tag{5}$$

Substituting eqn. (4) in eqn. (5) gives

$$c_i\left(\frac{\partial R}{\partial F_i}\right) = \left(\frac{\partial R}{\partial k_i F_i}\right) = \frac{1}{k_i}\left(\frac{\partial R}{\partial F_i}\right) \tag{6}$$

Therefore,

$$k_i = \frac{1}{c_i} \tag{7}$$

In the previous example, multiplying temperature by 0.1 ($1/c_1$) and pressure by 0.5 ($1/c_2$) will give scaled factors such that a unit change in either will produce the same change in response.

Large step size

The above three choices for the initial step size can be used with both the fixed-size and variable-size simplexes. A fourth option exists for the variable-size simplex.

Rather than starting with an initially small simplex that expands in the

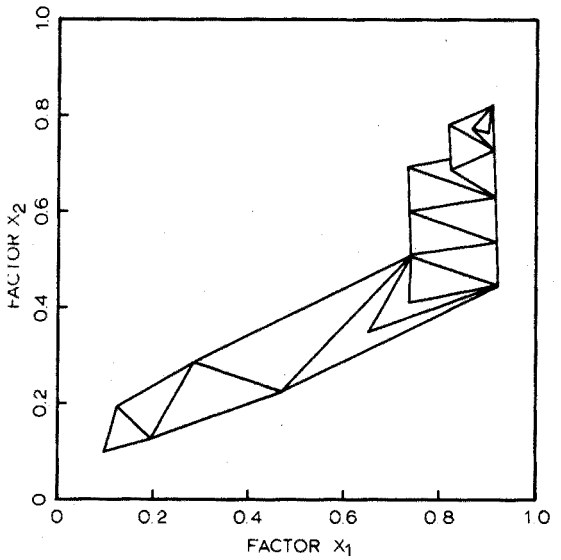

Fig. 1. Simplex optimization with a small initial simplex with origin of (0.1, 0.1). Nineteen vertices shown.

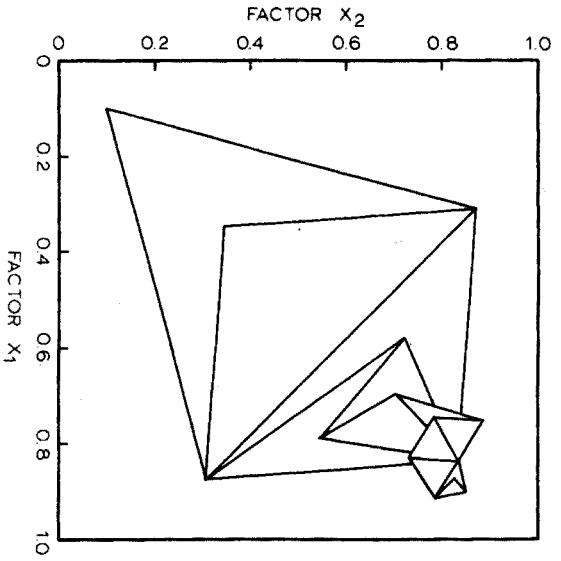

Fig. 2. Simplex optimization with a large initial simplex with origin of (0.1, 0.1). Fourteen vertices shown.

direction of the optimum, a large initial simplex which fills most of the factor space can be used. The optimum is then approached as the simplex collapses on itself. One of the advantages of this choice is that it provides information about a larger volume of the factor space. This is often useful when regression analysis is used as an aid in understanding or predicting response.

Figures 1 and 2 compare optimizations with a small initial simplex and a large initial simplex. The function optimized is

$$R = 1-(x_1-0.9)^2-(x_2-0.8)^2 \tag{8}$$

with optimum at (0.9, 0.8). The initial step size for the small simplex is 0.1; for the large simplex the initial step size is 0.8.

DESIGN OF INITIAL SIMPLEX

After the step sizes have been chosen, the vertices of the initial simplex can be calculated. Factors are treated as dimensions and each vertex is located by means of coordinates from each dimension. For n factors, there are $(n+1)$ vertices, each of which is located by n coordinates. The first vertex of the initial simplex usually consists of standard or accepted factor levels.

When the general framework of Spendley *et al.*[4] is used, the following matrix and accompanying equations can be used to calculate the initial simplex easily.

Vertex	*Dimensions*					
	1	2	3	4 ... $n-1$	n	
1	0	0	0	0 ... 0	0	
2	p	q	q	q ... q	q	
3	q	p	q	q ... q	q	
4	q	q	p	q ... q	q	
	.	.	.	. ... .	.	
n	q	q	q	q ... p	q	
$n+1$	q	q	q	q ... q	p	

where

$$p = \frac{s_n}{n2^{\frac{1}{2}}}((n+1)^{\frac{1}{2}}+n-1) \tag{9}$$

and

$$q = \frac{s_n}{n2^{\frac{1}{2}}}((n+1)^{\frac{1}{2}}-1) \tag{10}$$

The number of dimensions is n, and s_n is the step size for each dimension. The appropriate p's and q's are added to the value of their respective coordinates of

the first vertex. This design was used in calculating the initial simplexes shown in Figs. 1 and 2.

CONCLUSIONS

Factor selection and preprocessing are important aspects of optimization studies. When simplex optimization is used, the following points should be considered.

As many factors as can be handled conveniently should be included in the optimization. The inclusion of additional factors does not greatly increase the number of experiments required to reach the optimum. Determining the relative significance of each factor and retaining only the most significant factors for further study are unnecessary.

If the risk associated with poor response is minimal, a large initial simplex will provide information about a larger volume of the factor space. Assigning to each of the factors a step size that is inversely proportional to the factor's significance is unnecessary.

The vertices of the initial simplex can be easily calculated by a minor modification of the algorithm of Spendley *et al.*[4].

The authors thank P. G. King and S. L. Morgan for helpful discussions; and the National Science Foundation for its support through NSF Grant GP-32911.

SUMMARY

Factor selection and preprocessing are important aspects of optimization studies. When simplex optimization is used, as many factors as can be handled conveniently should be included in the optimization; additional factors do not greatly increase the number of experiments required to reach the optimum. If the risk associated with poor response is minimal, a large initial simplex will provide information about a larger volume of the factor space. It is unnecessary to assign to each of the factors a step size that is inversely proportional to the factor's significance. The vertices of the initial simplex can be easily calculated by a minor modification of a published algorithm.

REFERENCES

1 G. E. P. Box and K. B. Wilson, *J. Roy. Statist. Soc., Ser. B*, 13 (1951) 1.
2 G. E. P. Box, *Appl. Statistics*, 6 (1957) 81.
3 G. E. P. Box and N. R. Draper, *Evolutionary Operation*, Wiley, New York, 1969.
4 W. Spendley, G. R. Hext and F. R. Himsworth, *Technometrics*, 4 (1962) 441.
5 D. E. Long, *Anal. Chim. Acta*, 46 (1969) 193.
6 J. A. Nelder and R. Mead, *Computer J.*, 7 (1965) 308.
7 M. J. Box, *Computer J.*, 8 (1965) 42.
8 D. M. Himmelblau, *Applied Non-Linear Programming*, McGraw-Hill, New York, 1972.
9 D. L. Keefer, *Ind. Eng. Chem., Process Des. Develop.*, 12 (1973) 92.
10 G. S. G. Beveridge and R. S. Schechter, *Optimization: Theory and Practice*, McGraw-Hill, New York, 1970.

11 S. N. Deming and S. L. Morgan, *Anal. Chem.*, 45 (1973) 278A.
12 S. L. Morgan and S. N. Deming, *Anal. Chem.*, accepted for publication.
13 M. Friedman and L. J. Savage in C. Eisenhart, M. W. Hastay and W. A. Wallis (Eds.), *Techniques of Statistical Analysis*, McGraw-Hill, New York, 1957.
14 O. L. Davies, *The Design and Analysis of Industrial Experiments*, Hafner, New York, 1954.
15 G. E. P. Box, *Biometrics*, 10 (1954) 16.
16 H. Kaiser, *Anal. Chem.*, 42 (4) (1970) 26A.

Analytica Chimica Acta, 73 (1974) 399–401

SHORT COMMUNICATION

The determination of glutethimide by n.m.r. spectrometry

HASSAN Y. ABOUL-ENEIN

The Toxicology Center, Department of Pharmacology, College of Medicine, University of Iowa, Iowa City, Iowa 52242 (U.S.A.)

(Received 14th May 1974)

Glutethimide (2-ethyl-2-phenylglutarimide) is a sedative hypnotic agent chemically related to the barbiturates. Several analytical approaches have been successfully applied to the isolation and determination of glutethimide in biological fluids, such as serum and cerebrospinal fluid[1–3]. The u.v. spectrophotometric method described in NF XIII[4] for determination of glutethimide in tablet dosage form requires separation by column chromatography which renders the method lengthy. The acid–base titration method adopted by the British Pharmacopaeia[5] involves ether extraction of the drug from tablets, which also makes the method time-consuming. This paper describes a method based on n.m.r. spectrometry to determine glutethimide in tablet formulations. The method utilizes carbon tetrachloride as the solvent, and hexamethylcyclotrisiloxane is used as an internal standard. Known mixtures and commercial tablets were analyzed by this procedure, which proved to be simple, rapid (40 min) and accurate; the method provides a spectrum of the drug as confirmatory identification.

Experimental

A Varian T-60 n.m.r. spectrometer was used.

Glutethimide standard (USV Pharmaceutical Corp., Tuckahoe, N.Y.) and glutethimide tablets (Doriden 500-mg, tablets, USV Pharmaceutical Corp., Tuckahoe, N.Y.).

Procedure. Dry the tablets at 45° C over phosphorus pentoxide overnight in a desiccator. Place a tablet into a 50 ml stoppered flask. Carefully crack the tablet with the end of a spatula. Use a measured amount of carbon tetrachloride so that the final concentration of glutethimide will be about 20 mg ml^{-1}. Wash down the end of the spatula to ensure quantitative removal of the sample. Add an accurately weighed amount of hexamethylcyclotrisiloxane (K&K Laboratories) as internal standard, to the sample solution so that its final concentration is about 7 mg ml^{-1}, then add the remainder of the solvent to the flask. Stopper the flask and place it in a shaker for 10 min to effect dissolution. Filter through a cotton wad, and transfer about 0.4 ml of the clear solution to an analytical n.m.r. tube. Place the tube in the spectrometer, adjust the spin rate to eliminate spinning side band, and obtain a spectrum. All

peak field positions are referenced to hexamethylcyclotrisiloxane at 0.00 p.p.m. Integrate the peaks of interest (phenyl group at 7.3 δ and hexamethylcyclotrisiloxane at 0.00 δ) at least five times. The amount of glutethimide may be then calculated as follows:

$$\text{mg of glutethimide} = \frac{A_g}{A_h} \times \frac{EW_g}{EW_h} \times (\text{mg of hexamethylcyclotrisiloxane})$$

where A_g is the integral value of the signal representing glutethimide; A_h the integral value of the signal representing the internal standard; EW_g the molecular weight of glutethimide (5 = 43.45); and EW_h the molecular weight of internal standard (18 = 12.35).

Results and discussion

The n.m.r. of pure glutethimide shows a singlet at 7.3 δ for the phenyl protons, when hexamethylcyclotrisiloxane is used as a reference. This is an ideal peak for precise integration. The utility of this internal standard has been demonstrated previously[6–8]. It appears as a single signal at an extreme upfield position. The n.m.r. spectrum of glutethimide (Fig. 1) under the described analytical conditions is free of excipient peaks and provides identification of the active ingredient in addition to quantitative results. The results of the determination of a series of glutethimide standards (Table I) demonstrate good precision ($\pm 0.70\%$). Table II summarizes the analysis of commercial tablets; good agreement with the declared value was found. Measurements shown in both tables are within the NF monograph limits of 95.0–105.0%, for glutethimide and glutethimide tablets. The use of n.m.r. for quantitative analysis is attractive because it is a simple and rapid procedure.

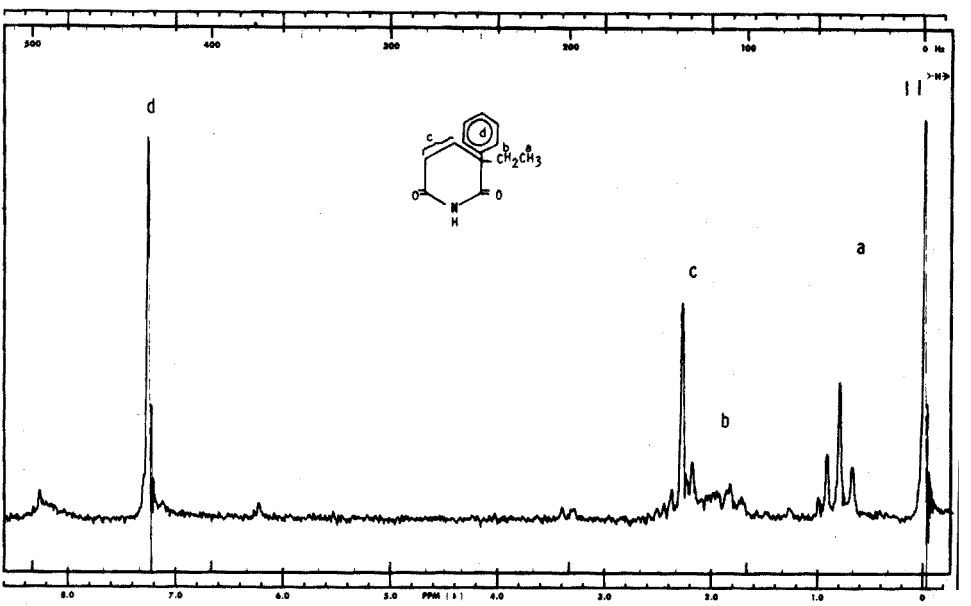

Fig. 1. N.m.r. spectrum of glutethimide(I) and hexamethylcyclotrisiloxane(II) in carbon tetrachloride.

TABLE I

ANALYSIS OF GLUTETHIMIDE STANDARDS BY N.M.R.

Sample	*Internal standard (mg)*	*Glutethimide*		
		Added (mg)	*Found (mg)*	*Recovered (%)*
1	39.57	50.58	50.32	99.48
2	103.73	45.10	44.89	99.53
3	114.46	76.50	75.98	99.32
4	65.33	52.39	52.33	99.88
5	30.12	45.53	45.76	100.50
6	19.26	49.49	48.99	98.99
7	17.64	70.50	70.02	99.32
8	17.24	72.80	73.67	101.20
9	14.59	71.98	71.62	99.50
10	15.65	70.92	70.13	98.89
				Mean 99.66
				s_r 0.70

TABLE II

ASSAY OF GLUTETHIMIDE IN PHARMACEUTICAL PREPARATIONS BY N.M.R.

Sample	*Internal standard (mg)*	*Percent of declared[a] amount*
1	75.5	98.70
2	108.45	101.06
3	120.24	99.60
4	84.84	98.97
5	54.47	99.22
6	42.96	97.89
7	45.94	98.97
		Mean 99.20
		s_r ±0.97

[a] Declared amount is 500 mg per tablet.

The author acknowledges Dr. L. J. Fischer and Dr. A. R. Hansen for their valuable suggestions. This work was supported by U.S.P.H.S. Grant GM 12675.

REFERENCES

1 A. R. Hansen and L. J. Fischer, *Clin. Chem.*, 20 (1974) 236.
2 I. Sunshine, R. Maes and R. Faracci, *Clin. Chem.*, 14 (1968) 595.
3 J. J. Ambre and L. J. Fischer, *Res. Commun. Chem. Pathol. Pharmacol.*, 4 (1972) 307.
4 *The National Formulary*, Mack, Easton, Pa., 13th edn., 1970, p. 329.
5 *The British Pharmacopoeia*, Pharmaceutical Press, London, 1968, p. 443.
6 S. Barcza, *J. Org. Chem.*, 28 (1963) 1941.
7 J. W. Truczan and B. A. Goldwitz, *J. Pharm. Sci.*, 61 (1972) 1309.
8 J. W. Truczan and B. A. Goldwitz, *J. Pharm. Sci.*, 62 (1973) 1705.

Analytica Chimica Acta, 73 (1974) 402–404

SHORT COMMUNICATION

A simple, rapid complexometric determination of titanium in the presence of other metals

MISS M. M. A. PERIK and P. J. D. ORANJE

Twente University of Technology, Department of Chemical Engineering, Laboratory for Inorganic Chemistry and Materials Science, Enschede (The Netherlands)

(Received 15th May 1974)

The determination of titanium in the presence of other metals, *e.g.* lead, by the usual gravimetric or titrimetric methods are very time-consuming[1,2], hence a rapid, titrimetric method was developed in which lead does not interfere. In our particular case, the method had to be applicable to the determination of titanium in complex compounds such as lead titanyl oxalate tetrahydrate ($PbTiO(C_2O_4)_2 \cdot 4\,H_2O$).

Various publications have presented methods based on the back-titration of an excess of EDTA with standard bismuth[3] or copper[4] solutions, in which the titanium–EDTA complex is stabilized with hydrogen peroxide.

Back-titration of the excess of EDTA with a standard lead solution and xylenol orange as indicator was examined here. Lead was used as titrant because, if this metal is present in the titanium solution to be analyzed, the titration remains straightforward and because the titration of lead with EDTA and xylenol orange as indicator is well known to be very accurate with a distinct colour change. If lead is present in the solution, it can be determined together with the titanium from the amount of EDTA solution consumed. The lead content may then be determined by a separate titration after masking of the titanium with lactic acid. The difference between the quantities of lead solution used in these titrations then gives the titanium content. Of course, it is necessary to ensure that no metal ions are present in the solution with the same complex-forming properties as titanium, *i.e.* reacting with both EDTA and lactic acid.

Experimental

Reagents. The 0.1 *M* EDTA solution was standardized against p.a. lead nitrate (Baker) and the 0.1 *M* lead nitrate solution against the EDTA solution. The titanium salt—$(NH_4)_2TiO(C_2O_4)_2 \cdot H_2O$—was prepared as described previously[5].

Procedure. To 40–300 mg of the titanium salt, dissolved in a small volume of 4 *M* sulphuric acid, add 3 drops of 30% (vol.) hydrogen peroxide and 10 ml of 0.1 *M* EDTA solution. Dilute the solution with water to about 100 ml. Add 3.5 g of hexamine as buffer, adjust the pH to 5.5 with ammonia liquor, and add 3 drops

of 0.5% (w/v) xylenol orange indicator solution. (After addition of the hydrogen peroxide, the solution turns orange-yellow and this changes to yellow after the pH adjustment.) Back-titrate the excess of EDTA with the standard 0.1 *M* lead(II) solution until a stable colour change to purple-red is reached.

If lead(II) is present, the method does not have to be changed. Because the lead sulphate formed originally is soluble in EDTA, the total metal content (Ti + Pb) is determined. The lead content is found by adding 5 ml of 90.4% (w/v) lactic acid solution instead of the hydrogen peroxide to the titration vessel. After this, the rest of the procedure described above is followed. The colour change is more pronounced in this case.

Results and discussion

All determinations were performed in triplicate, except for the determination of titanium in a perchloric acid solution in the presence of lead, which was done six times; the errors given in Table I correspond to half the difference between the extreme results. The titanium content of the standard titanium salt used was determined by calcining at about 900°C and weighing as TiO_2. The lead content in the lead nitrate added was simply calculated.

TABLE I

TITRATION OF TITANIUM UNDER DIFFERENT CONDITIONS

(In all cases, the theoretical result was 15.56% Ti)

Conditions	*% Ti found*
Ti salt in H_2SO_4, no Pb present	15.55 ± 0.03
Ti salt in H_2SO_4, Pb present	15.56 ± 0.02
Ti salt in $HClO_4$, no Pb present	15.56 ± 0.05
Ti salt in $HClO_4$, Pb present	15.00 ± 1.3
Ti salt in HCl, Pb present	15.58 ± 0.02

The results for titanium are very good, even when lead is present (Table I). This method was also tested in the presence of various acids; the results were reasonably good except for the determination of titanium in the presence of perchloric acid and lead. The use of the other acids has one drawback: the solutions are brown-yellow instead of clear yellow, making the colour change less easy to see.

The effectiveness of the masking agent and the accuracy of the method was proved by the determination of lead in lead nitrate in the presence of titanium. The results obtained were 62.54 ± 0.05% lead in sulphuric acid solution, and 62.56 ± 0.11% lead in nitric acid solution (calculated 62.56%).

The hydrogen peroxide and the lactic acid must be added to the relatively concentrated acid solutions before neutralization, otherwise the titanium may precipitate as hydroxide, which is only slightly soluble in EDTA. The results show that when these precautions are followed, the accuracy is good, except for the determination in perchloric acid in the presence of lead, the cause of which is not clear. The spread is small, when compared with that of gravimetric methods where it usually is of the order of at least ± 1% relative.

Moreover, the total time necessary for the determination of both titanium and lead is only 15 min, compared to at least one and a half days for the gravimetric method.

The authors wish to thank P. J. Gellings for his stimulating interest and G. M. H. van de Velde for helpful suggestions and discussions.

REFERENCES

1 R. S. Ramakrishna and H. D. Gunawardena, *Talanta*, 20 (1973) 21.
2 A. I. Vogel, *Quantitative Inorganic Analysis*, Longmans, London, 3rd edn., 1961.
3 B. Bieber and Z. Věcěra, *Collect. Czech. Chem. Commun.*, 26 (1961) 2081 (note).
4 D. H. Wilkins, *Anal. Chim. Acta*, 20 (1959) 113.
5 G. M. H. van de Velde, S. Harkema and P. J. Gellings, *Inorg. Nucl. Chem. Lett.*, 9 (1973) 1169.

Analytica Chimica Acta, 73 (1974) 405–408

SHORT COMMUNICATION

Simultaneous extractive photometric determination of gold(III) and palladium(II) with *syn*-phenyl-α-pyridylketoxime

C. K. BHASKARE and S. G. KAWATKAR
Inorganic Chemistry Laboratories, Shivaji University, Kolhapur-416004, (India)
(Received 10th May 1974)

Reliable analytical procedures for the determination of gold(III) and palladium(II) are available[1], but very little work has appeared on the simultaneous determinations of these elements. Ripon and Pop[2] have reported assays with ascorbic acid. Bobtelsky and Eisenstadter[3] gave a detailed account of the diethyldithiocarbamates of gold and palladium and their use in microdeterminations. There is, however, no simple spectrophotometric technique available for this purpose.

Binary alloys of gold and palladium are widely used in the chemical industry, in electrical engineering, in jewelry[4], as catalysts[5], for preparing thermocouples[6], for electrical contacts[7] and as high-temperature solders[4]. Gold and palladium alloys are used for electrodeposition[8] and the determination of the composition of the plating baths is analytically important.

syn-Phenyl-α-pyridylketoxime (PPK) forms orange and yellow complexes with gold[9] and palladium[10] at pH 9, the absorption maxima of chloroform extracts being 455 nm and 410 nm, respectively. A new method for the simultaneous photometric determination of the two elements is described below.

Experimental

Reagents. PPK was synthesized[11] from 2-benzoylpyridine. The product was crystallized several times from ethanol with norite, to give the pure *syn*-form as colourless prisms (m.p. 151–152°C). The reagent was used as a 10 mg ml^{-1} solution in 95% ethanol.

Stock solutions of gold or palladium containing 0.6328 mg Au ml^{-1} or 0.4411 mg Pd ml^{-1}, respectively, were prepared by dissolving A.R. grade gold metal or palladium chloride (both from Johnson-Matthey), and were standardized by conventional procedures[1]. Further dilutions were made as required.

Chloroform (BDH) was distilled before use, and double-distilled conductivity water was used throughout.

Aqueous 1 *M* sodium carbonate (A.R. grade) was used for adjusting the pH.

Apparatus. Spectrophotometric measurements were made with a Carl Zeiss Spekol grating spectrophotometer equipped with a ZV booster amplifier and EGS and EG photocells; 10.0-mm matched glass cuvettes were used. The pH values

were measured with a Philips pH meter PR 9405 L and a glass–calomel combined electrode.

Procedure. Dilute an aliquot containing up to 80 μg of gold(III) and up to 50 μg of palladium(II) to 10 ml, add 2.0 ml of reagent, and adjust the pH to 9.0 with carbonate solution. Transfer the solution to a small separatory funnel, add 3.0 ml of chloroform and shake for 5 min. Transfer the organic layer to a 10-ml measuring flask through a small plug of dry cotton. Extract again with 3.0 ml of chloroform. Dilute the combined organic layers to the mark with chloroform. Measure the absorbances in triplicate at 410 nm and 455 nm. Determine the concentrations of the two elements by solving the appropriate simultaneous equations (see below).

Analysis of a binary alloy. Dissolve a few mg of the alloy in aqua regia and boil to expel the nitrogen oxide fumes. Evaporate twice with concentrated sulphuric acid and further dilute with water in a volumetric flask. Treat the solution as above for the determination of the constituents.

Analysis of plating bath. Carefully evaporate a suitable aliquot of the bath to dryness on a steam bath and treat with 1.0 ml of concentrated nitric acid and 3.0 ml of concentrated sulphuric acid. Again evaporate to dryness and repeat the procedure twice more to destroy organic matter and nitrogen oxides. Then dilute to a known volume and analyse suitable aliquots as above.

Results and discussion

The absorption spectra of the gold and palladium complexes are given in Fig. 1. Gold(III) forms a yellowish orange complex which can be extracted[9] with

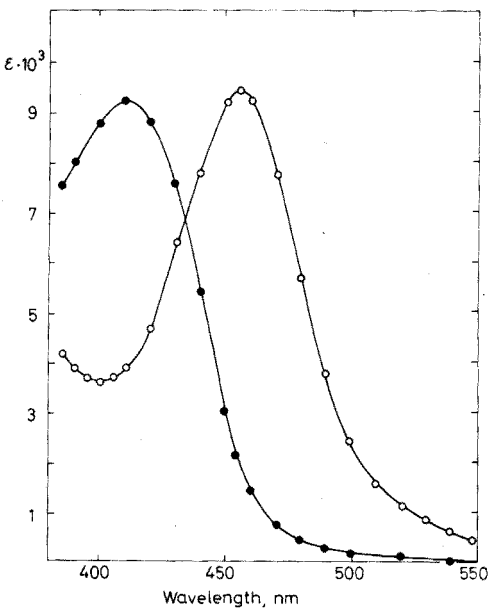

Fig. 1. Variation of molar absorptivity with wavelength for the palladium complex (●), and the gold complex (○).

TABLE I

SPECTROPHOTOMETRIC PROPERTIES OF GOLD AND PALLADIUM COMPLEXES

Complexes at pH 9.0	λ_{max}	ε_{455}	ε_{410}	*Colour*
Au(III)	455	$9.419 \cdot 10^3$	$3.891 \cdot 10^3$	Orange
Pd(II)	410	$2.145 \cdot 10^3$	$9.249 \cdot 10^3$	Yellow

chloroform at pH 9.0. Palladium forms a yellow complex under the same conditions[10]. The reagent does not absorb in the visible region. The spectrophotometric properties of the complexes are summarized in Table I. It was shown that two extractions sufficed for quantitative transference of both metals.

The simultaneous determinations of gold(III) and palladium(II) are possible, because the complexes can be completely extracted under the same conditions and have well separated absorption maxima, and the absorbances are additive.

The relationships

$$A_{410} = \varepsilon_{410}^{Pd}[Pd] + \varepsilon_{410}^{Au}[Au]$$
$$A_{455} = \varepsilon_{455}^{Pd}[Pd] + \varepsilon_{455}^{Au}[Au]$$

were used to develop the following simultaneous equations:

$$[Au] \cdot 10^4 = 1.174A_{455} - 0.272A_{410}$$
$$[Pd] \cdot 10^4 = 1.196A_{410} - 0.496A_{455}$$

Several synthetic mixtures were prepared and analysed. The results are summarized in Table II. The maximum standard deviations found were $\pm 1.06\%$ for gold(III) and $\pm 1.04\%$ for palladium(II).

TABLE II

ANALYSES OF SYNTHETIC MIXTURES

Samples	*Au(III)* ($\cdot 10^{-5}$ *M*)		*Pd(II)* ($\cdot 10^{-5}$ *M*)		*Sr (%)*	
	Taken	*Found*	*Taken*	*Found*	*Au*	*Pd*
I	1.285	1.269	4.194	4.248	+0.58	+1.04
II	5.140	5.099	4.194	4.180	−0.02	+0.42
III	6.425	6.354	3.355	3.328	+0.72	−0.07
IV	6.425	6.425	4.194	4.194	0.00	0.00
V	3.855	3.782	4.194	4.138	−0.32	−0.58
VI	6.425	6.406	1.678	1.646	−1.06	−0.07
VII	6.425	6.372	2.516	2.470	−0.04	−1.00

Analysis of plating baths. The method can be used to determine the composition of the plating baths used for simultaneous electrodeposition of gold and palladium alloy. The plating baths contain cyanides, ethylenediamine, tartrates, or EDTA[8], which interfere strongly. By using a mixture of nitric acid and sulphuric acid, the interfering constituents can be completely decomposed. Several plating

bath solutions were analysed as described under *Experimental*; the results obtained were within $\pm 0.5\%$ of the values obtained by other methods.

Interferences. Platinum metals, copper, iron, nickel and cobalt interfere and must be absent. Procedures can be developed for three-component systems under favourable conditions.

We are grateful to the University authorities for research facilities. One of us (SGK) thanks the U.G.C. for the award of a travel grant.

REFERENCES

1 E. B. Sandell, *Colorimetric Determination of Traces of Metals*, Interscience, New York, 3rd edn., 1965, pp. 497, 714.
2 R. Ripan and G. Pop, *Rev. Roum. Chim.*, 12 (1967) 13.
3 M. Bobtelsky and J. Eisenstadter, *Anal. Chim. Acta*, 16 (1957) 479.
4 E. M. Savitskii, V. P. Polyakova and M. A. Tylkina, *Palladium alloys*, Primary Sources Publishers, New York, 1969.
5 J. H. Sinfelt, A. E. Barnett and G. W. Bembinski, *U.S. Patent* 3,442,973, 1969; *Chem. Abstr.*, 71 (1969) 41018w.
6 Engelhard Industries, Inc., *British Patent* 1,079,141, 1967; *Chem. Abstr.*, 68 (1968) 32711c.
7 T. P. Belousova and S. A. Telezhkin, *New Materials in Electrical Instrument Making*, Izd. Ontipribor, 1965.
8 S. N. Vinogradov, N. T. Kudryavtsev and N. F. Kulagina, *U.S.S.R. Patent 302,396*, 1971; *Chem. Abstr.*, 75 (1971) 104552w.
9 B. Sen, *Anal. Chim. Acta*, 21 (1959) 35.
10 B. Sen, *Anal. Chem.*, 31 (1959) 791.
11 E. H. Huntress and H. C. Walter, *J. Amer. Chem. Soc.*, 70 (1948) 3704.

Analytica Chimica Acta, 73 (1974) 409–412

SHORT COMMUNICATION

Studies in the tetraarylborates

Part VI. The preparation and reagent properties of sodium tetrakis(*m*-chlorophenyl) borate

FRANK JARZEMBOWSKI, FRANK CASSARETTO, HARVEY POSVIC and CARL E. MOORE
Loyola University, Department of Chemistry, 6525 North Sheridan Road, Chicago, Illinois 60626 (U.S.A.)
(Received 25th March 1974)

In a continuation of the study of substituent effects on reagent stability and selectivity[1–5], sodium tetrakis(*m*-chlorophenyl)borate has been synthesized. Sodium tetrakis(*m*-chlorophenyl)borate is similar to sodium tetraphenylborate in selectivity in its reaction with large cations and is superior to tetraphenylborate in respect to stability and precipitate formation.

Synthesis of sodium tetrakis(m-chlorophenyl)borate

The following sequence of reactions is employed in the preparation of sodium tetrakis (*m*-chlorophenyl)borate:

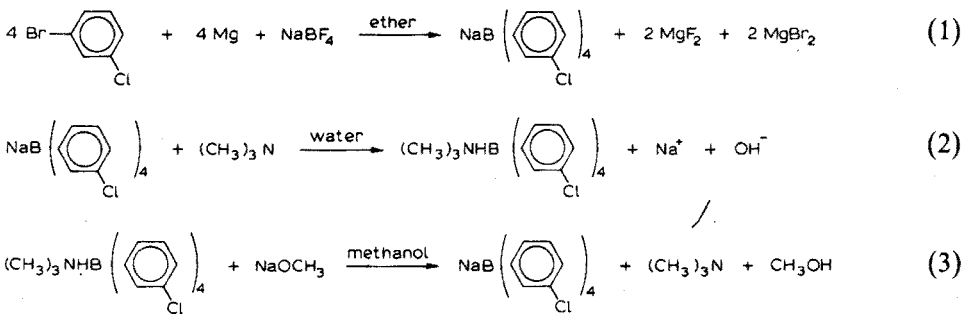

The reaction apparatus consists of a 1-l three-necked (ground glass) flask equipped with a 125-ml dropping funnel, a 600-ml dropping funnel, a water-cooled reflux condenser, and a teflon-coated magnetic stirring bar. Dry the apparatus by heating gently over a Bunsen flame while blowing nitrogen through the glassware. Place dry magnesium turnings (12.69 g; 0.522 mole) and sodium fluoroborate (14.3 g; 0.131 mole) in the flask. Place 550 ml of anhydrous ethyl ether in the 600-ml funnel. In the 125-ml funnel place 100 g (0.522 mole) of *m*-bromochlorobenzene and 50 ml of anhydrous ethyl ether. Sweep the assembly with dry nitrogen, and then add about 50 ml of the anhydrous ether in order to cover the magnesium turnings.

To initiate the Grignard reaction, add 5 ml of the *m*-bromochlorobenzene solution to the reaction vessel. After reaction begins, quickly add the remaining 500 ml of anhydrous ether and maintain rapid stirring. Partially immerse the flask in an ice water bath and add the remaining *m*-chlorobromobenzene dropwise over a period of about 5 h. Maintain gentle reflux for another hour. Stop the gas flow and rapid stirring. If necessary, allow the reaction mixture to stand overnight in a dry ice–acetone bath before proceeding with isolation and purification.

Transfer the reaction mixture to a 2-l beaker containing 200 ml of water and about 50 g of crushed ice. Add another 200 ml of water containing 4 g of sodium carbonate and 1 g of sodium hydroxide. Saturate the aqueous layer with sodium chloride and separate the ether layer. Extract the aqueous layer three times with 100-ml portions of ether. Add about 900 ml of distilled water to the combined ether solutions (about 1 l) and carefully warm until all the ether has evaporated. Filter the resulting cloudy, aqueous solution containing the required reagent several times through celite until a clear filtrate results. Extract the celite with 500 ml of water, filter and combine the aqueous filtrates (about 1500 ml). Treat this aqueous solution with 300 ml of aqueous 2.5% (w/v) trimethylamine solution while stirring and filter the resulting white precipitate of trimethylammonium tetrakis(*m*-chlorophenyl)borate by suction. Dissolve the precipitate in methanol, filter through celite, and recrystallize from a methanol–water solution. (Yield: 27.8 g.) After a second recrystallization and drying under vacuum at 80°C, the trimethylammonium tetrakis-(*m*-chlorophenyl)borate (m.p. 164–165°C) gave the following elemental analysis results (in %): C, 62.64; H, 5.01; N, 2.79; Cl, 27.57. Calculated: C, 62.71; H, 5.07; N, 2.71; Cl, 27.42.

Preparation of sodium tetrakis(m-chlorophenyl)borate

Dissolve 10 g (0.019 mole) of the trimethylammonium salt and 2.05 g (0.038 mole) of sodium methoxide in about 300 ml of anhydrous methanol. Heat and stir until all the trimethylamine has been evolved (*ca.* 3 h); remove the remaining methanol under vacuum. Dissolve the residue in 200 ml of distilled water and filter. Saturate this solution with sodium chloride and extract with ether. Remove the ether under vacuum, leaving a white powder. Dissolve this in anhydrous ether and filter through 10 g of basic alumina. Remove the anhydrous ether under vacuum and air-dry the white residue, sodium tetrakis(*m*-chlorophenyl)borate, at room temperature overnight. Then powder the sodium tetrakis(*m*-chlorophenyl)borate and dry under vacuum at 80°C for 1 h. (Yield: 8.35 g.) Elemental analysis gave the following results (in %): C, 60.09; H, 3.38; Cl, 29.66. Calculated: C, 60.05; H, 3.36; Cl, 29.54.

Reagent properties of the tetrakis(m-chlorophenyl)borate anion

Some of this reagent was dissolved in distilled water and subsequently used to precipitate the potassium ion. The potassium salt after recrystallization from a methanol–water solution and drying for 1 h at 100°C, gave the following elemental analysis (in %): C, 58.40; H, 3.31; Cl, 28.85. Calculated: C, 58.10; H, 3.25; Cl, 28.58.

Qualitative testing was done with a 1% solution of the sodium salt. Approximately 1 ml of the reagent was added to 1 ml of a 0.1 *M* solution of the ion to be tested. Silver gave a heavy flocculant precipitate. Cesium, rubidium, potassium and

ammonium gave heavy, dense precipitates. Lead and copper showed a trace of precipitate formation, and no precipitates were observed for cadmium, manganese, barium, and nickel. The alkali metals were detectable at the concentrations 0.01 mg K ml^{-1}, 0.002 mg Rb ml^{-1}, and 0.002 mg Cs ml^{-1}.

The reagent was investigated for its ability to precipitate "onium" compounds by testing several compounds containing a basic nitrogen atom and a few quaternary ammonium salts. A number of these compounds dissolved in either distilled water or dilute hydrochloric acid, gave precipitates with the reagent. Typical analytical results are summarized in Table I.

TABLE I

PROPERTIES OF PRECIPITATES FORMED WITH TETRAKIS(*m*-CHLOROPHENYL) BORATE

Material tested	*M.p.* (°C)	*% Nitrogen*	
		Found	*Calc.*
Ammonium chloride	198–204 Decomposes	3.04	2.95
Trimethylamine	164–165	2.79	2.71
Tetramethylammonium bromide	222.5	2.56	2.64
Dimethylaminoethanol	128	2.60	2.56
1-Ethylpyridinium bromide	210	2.74	2.48
Methylene blue chloride	201–205	5.49	5.67

Sodium tetrakis(m-chlorophenyl)borate as a reagent for potassium

The precipitation of potassium from a pure potassium chloride solution was carried out in the following manner. Samples containing 33.44 mg, 16.35 mg, and 8.36 mg K ml^{-1} were prepared, diluted to 50 ml, and heated to about 70°C. A 2% solution of the reagent was filtered through a column containing 2 g of basic alumina and added dropwise to the samples. A calculated 15% excess of the reagent was used in each case. After cooling to room temperature, the precipitates were placed in an ice bath for 1 h. The fine, dense precipitate was then transferred to a tarred medium-porosity crucible and washed with three 5-ml portions of distilled water cooled to about 5°C. The crucible was dried at 100°C for 2 h and the recovery of potassium was calculated from the theoretical gravimetric factor of 0.07882. The results are shown in Table II.

The solubility of potassium tetrakis(*m*-chlorophenyl)borate in water was found by atomic absorption to be 0.0992 g l^{-1}; the sample was held at a constant temperature of 24°C for 138 h before the determination. Sodium tetrakis(*m*-chlorophenyl)borate forms sparingly soluble precipitates with K^+, Rb^+, and Cs^+. It appears to be a suitable gravimetric reagent for potassium. The reagent forms a fine, dense precipitate similar in appearance to that of barium sulfate, which is readily filterable through both medium- and fine-porosity crucibles. The reagent appears to have greater stability in aqueous solution than sodium tetraphenylborate. It also has possible utility as a reagent for "onium" compounds with which it forms well-defined crystalline precipitates. A 1% solution of sodium tetrakis(*m*-chloro-

TABLE II

RECOVERY OF POTASSIUM FROM PURE POTASSIUM CHLORIDE SOLUTIONS

K Taken (mg)	*K found*[a] *(mg)*	*Average recovery (%)*
33.44	33.32±0.08[b]	99.7
16.35	16.09±0.14	98.5
8.36	8.14±0.05	97.4

[a] Average of 5 results.
[b] Standard deviation.

phenyl)borate has remained active for a period of seven months with no visible appearance of decomposition.

Conclusions

Sodium tetrakis(*m*-chlorophenyl)borate has been synthesized and shown to be suitable as a gravimetric reagent for potassium, being in some ways superior to sodium tetraphenylborate. The salts formed with nitrogen-containing compounds offer possibilities for both qualitative and quantitative analysis.

REFERENCES

1 F. P. Cassaretto, J. J. McLafferty and C. E. Moore, *Anal. Chim. Acta*, 32 (1965) 376.
2 C. E. Moore, F. P. Cassaretto, H. Posvic and J. J. McLafferty, *Anal. Chim. Acta*, 35 (1966) 1.
3 J. T. Vandeberg, C. E. Moore, F. P. Cassaretto and H. Posvic, *Anal. Chim. Acta*, 44 (1969) 175.
4 M. Meisters, C. E. Moore and F. P. Cassaretto, *Anal. Chim. Acta*, 44 (1969) 287.
5 M. Meisters, J. T. Vandeberg, F. P. Cassaretto, H. Posvic and C. E. Moore, *Anal. Chim. Acta*, 49 (1970) 481.

Analytica Chimica Acta, 73 (1974) 413–415

SHORT COMMUNICATION

Potentiometric determination of copper(II) with iron(II) in phosphoric acid medium and in presence of thiocyanate

N. KRISHNAMURTY and Y. PULLARAO
Department of Chemistry, Andhra University, Waltair (India)
(Received 13th June 1974)

No procedure for the direct titration of copper(II) with iron(II) solution has been described in the literature. Belcher and West[1] determined copper(II) by adding an excess of iron(II) ammonium sulphate and ammonium thiocyanate and titrating the produced iron(III) with mercury(I) nitrate; iron(III) interferes in this method. Later, Belcher and West[1] used the above method to determine copper as copper(I) thiocyanate gravimetrically in 0.5 *M* hydrochloric acid and sulphuric acid media. Gopala Rao and Sagi[2] found that the formal redox potential of the Fe(III)/Fe(II) couple decreases as the concentration of phosphoric acid increases. In view of the above observations, a direct titration of copper(II) with iron(II) in phosphoric acid medium and in the presence of thiocyanate was tried; details of a successful procedure are given below.

Experimental

Apparatus. Measurements were made with an OSAW Crompton potentiometer (Ambala, India); a bright platinum rod served as indicator electrode and a saturated calomel electrode as reference electrode, the latter being connected via a saturated potassium chloride salt bridge.

The titration vessel was fitted with a hard rubber stopper having five holes, one for the microburette, the second for the platinum electrode, the third for one limb of the salt bridge, and the fourth and fifth for the flow of carbon dioxide. As the potential of the Fe(III)/Fe(II) couple falls in phosphoric acid medium[2], iron(II) is liable to atmospheric oxidation, hence a carbon dioxide atmosphere is essential.

Reagents. These were of analytical-reagent grade. All solutions were prepared from boiled-out distilled water. Iron(II) ammonium sulphate solution (0.1 *M*) was prepared in 0.5 *M* sulphuric acid; as a precaution, this solution was stored under carbon dioxide. A 0.1 *M* copper(II) sulphate solution was used for testing.

Preliminary tests. The effect of phosphoric acid concentration on the potentiometric titration of copper(II) with iron(II) solution in the absence and in the presence of thiocyanate was studied. The presence of thiocyanate remarkedly improved the value of the potential jump at the equivalence point, and also caused the immediate formation of stable potentials on addition of iron(II).

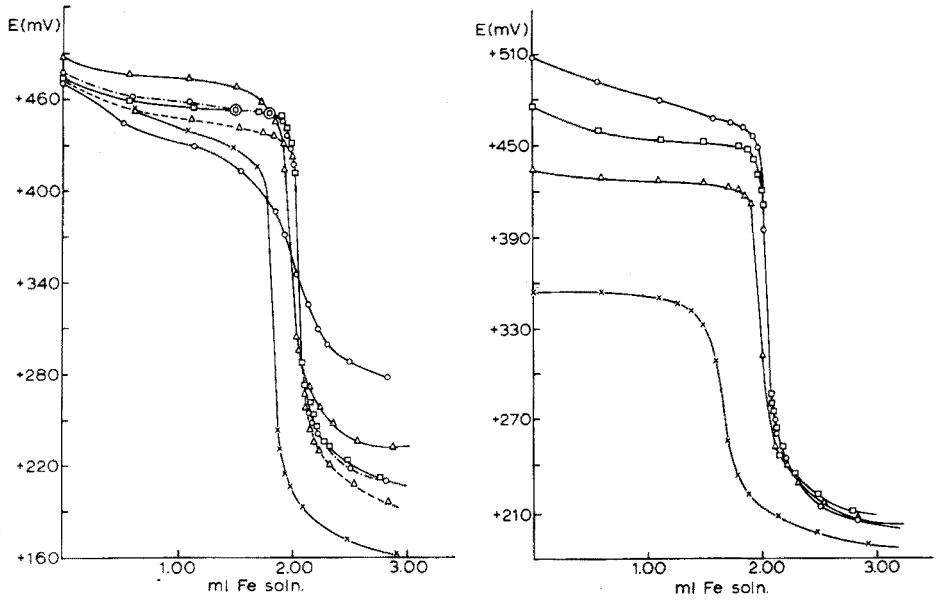

Fig. 1. Potentiometric titration of copper(II) with standard iron(II) solution at various phosphoric acid concentrations in a total volume of 30.0 ml and in presence of 0.50 ml 10% KSCN. H_3PO_4 concentrations: (○—○), 1.0 *M*; (△—△), 4.0 *M*; (○—·—○), 6.0 *M*; (⊡), 7.0 *M*; (△---△), 7.5 *M*; (×), 9.0 *M*.

Fig. 2. Potentiometric titration of copper(II) with standard iron(II) solution in 7.0 *M* phosphoric acid medium and at varying concentrations of thiocyanate in a total volume of 30.0 ml. Amount of 10% KSCN added: (○), 0.25 ml; (⊡), 0.60 ml; (△), 1.0 ml; (×), 5.0 ml.

The effect of phosphoric acid at a fixed concentration of thiocyanate, and the effect of thiocyanate concentration at a fixed phosphoric acid concentration on the potentiometric titration curves are shown in Figs. 1 and 2.

Recommended procedure. Transfer an appropriate amount of syrupy phosphoric acid to the titration vessel to give an overall phosphoric acid concentration of 7 *M* in a final volume of 30 ml. Add 0.5 ml of 10% potassium thiocyanate solution. Pass carbon dioxide through the solution for 10 min, and then add the test solution containing 6–25 mg of copper. Record the potentials in the usual way during the titration with 0.1 *M* iron(II) solution. A sharp break of *ca.* 120 mV per 0.04 ml of iron(II) solution is observed at the end-point. The potentials attain steady values quickly even after the equivalence point.

A typical titration curve in 7 *M* phosphoric acid medium is shown in Fig. 1. Some results are presented in Table I. The mean percentage error relative to the iodimetric method was found to be 0.3%.

Application

The method was tested for the determination of copper in alloys such as Cu–Ni alloy and brass. These alloys were dissolved in concentrated nitric acid and made up to a known volume (after metastannic acid had been removed in the

TABLE I

TITRIMETRIC DETERMINATION OF COPPER(II) WITH IRON(II) SOLUTION

Amount of copper(II) (mg) found		*% Error*
Iodimetric method	*Proposed method*	
6.20	6.23	0.48
10.35	10.39	0.39
14.17	14.20	0.21
18.78	18.82	0.21
24.61	24.66	0.20

case of brass); copper(II) was then titrated. The results obtained were: for brass, 59.62% Cu (59.29% by iodimetry); and for Cu–Ni alloy, 76.03% Cu (74.80% by iodimetry).

Results and discussion

Chloride, sulphate, acetate, oxalate, borate, tartrate, citrate, nitrate, Ni^{2+}, Cd^{2+}, Ba^{2+}, Co^{2+}, Mn^{2+}, Zn^{2+}, Hg_2^{2+}, Pb^{2+}, Al^{3+}, As^{3+} and Fe^{3+} did not interfere. Sb^{5+} and nitrite interfered.

From the potentiometric titration curve, the formal redox potential of the Cu(II)/Cu(I) couple was 700 mV at an overall concentration of 7.24 *M* phosphoric acid containing 0.015 *M* sulphuric acid. From similar titration curves, the formal redox potential of the Cu(II)/Cu(I) couple did not vary significantly with varying phosphoric acid concentration.

In the determination of copper(II) by the method of Belcher and West[1], iron(III) interferes, and these procedures[1] do not allow a direct titration.

The advantage of the present method is that copper(II) can be titrated in presence of iron(III). The determination of copper(II) in alloys is very simple, when compared to the iodimetric methods[3,4].

We are grateful to the Council of Scientific and Industrial Research for the award of Junior Research fellowship to one of us (Y.P.R.).

REFERENCES

1 R. Belcher and T. S. West, *Anal. Chim. Acta*, 5 (1951) 364; 6 (1952) 337.
2 G. Gopala Rao and S. R. Sagi, *Talanta*, 9 (1962) 715; *Z. Anal. Chem.*, 196 (1963) 448.
3 D. N. Grindley, *An Advanced Course in Practical Inorganic Chemistry*, Butterworths, London, 1964, p. 109.
4 A. I. Vogel, *Quantitative Inorganic Analysis*, Longmans, London, 1961, pp. 358, 629.

Analytica Chimica Acta, 73 (1974) 416–419

SHORT COMMUNICATION

Méthode de préparation de sels anhydres de lanthanides pour la polarographie en solvants non aqueux aprotiques

J. MASSAUX* et G. DUYCKAERTS

Laboratoire de Chimie Analytique et Nucléaire, Université de Liège au Sart Tilman, B-4000 Liège (Belgique)

(Reçu le 31 mai 1974)

La polarographie des lanthanides dans les solvants non aqueux, aprotiques et anhydres se heurte à la difficulté de la préparation de sels de lanthanides exempts d'eau et à anion non complexant du type perchlorate. Il est bien connu, en effet, que de très faibles quantités d'eau influencent fortement le potential de demi-vague, surtout lorsqu'il s'agit de milieux à faible pouvoir solvatant, comme le carbonate de propylène (C.P.)[1].

L'obtention de perchlorates anhydres de lanthanides n'est pas simple: par chauffage direct du perchlorate hydraté, on n'obtient pas le sel exempt d'eau[2]; on peut utiliser la méthode proposée par Starke[3] qui consiste à faire réagir chimiquement l'eau résiduelle avec le 2,2-diméthoxypropane selon l'équation suivante:

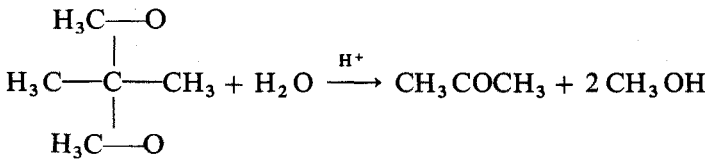

Ce dernier procédé n'est pas sans danger et il ne conduit pas au résultat escompté, surtout en présence de perchlorates.

On peut obtenir des complexes anhydres du type $LnS_x(ClO_4)_3$ avec certains solvants comme la diméthylformamide (DMF)[4], la diméthylsulfoxyde (DMSO)[5], l'hexaméthylphosphorotriamide (HMPT)[6]. Cette méthode aisée ne marche qu'avec des molécules à fort pouvoir solvatant, capables de déplacer l'eau liée.

Nous avons ainsi été amenés à rechercher un acide capable de donner facilement des sels anhydres de lanthanides et possédant des propriétés chimiques voisines de celles des perchlorates. Le réactif que nous proposons est l'acide trifluorométhanesulfonique CF_3SO_3H; le mode opératoire pour la préparation de sels anhydres est le suivant: un excès d'oxyde de lanthanide est chauffé dans l'acide en question jusqu'à neutralisation de la solution; celle-ci est filtrée puis évaporée à sec, le sel obtenu est séché sous vide à 100°C durant une nuit.

* Aspirant du Fonds National de la Recherche Scientifique.

Nous avons préparé par cette méthode $La(CF_3SO_3)_3$, $Sm(CF_3SO_3)_3$, $Eu(CF_3SO_3)_3$, $Yb(CF_3SO_3)_3$.

L'absence d'eau a été vérifiée par titrage complexiométrique du métal[7] d'une part et par titrage Karl Fischer dans l'alcool anhydre d'autre part. Les résultats obtenus sont consignés dans le tableau I.

TABLEAU I

L'ANALYSE DES SELS ANHYDRES DE LANTHANIDES

Nature du sel	*% Théor. en métal*	*% Trouvé*	*mg H_2O l^{-1} dans l'éthanol pur*	*Conc. en sel dans l'éthanol ($\cdot 10^{-2}$ M)*	*mg H_2O l^{-1} dans la sol. du sel*
$La(CF_3SO_3)_3$	23,71	23,6	73	1,23	85
$Eu(CF_3SO_3)_3$	25,37	25,5	80	1,10	94
$Yb(CF_3SO_3)_3$	27,90	27,8	70	0.94	80
$Sm(CF_3SO_3)_3$	25,17	25,20	96	0,92	110

Les sels obtenus se dissolvent aisément dans des solvants aprotiques tels que le carbonate de propylène, le DMSO, la DMF, le HMPT, l'acétonitrile, nous avons préparé des solutions $5 \cdot 10^{-2}$ *M* de $Eu(CF_3SO_3)_3$ dans la DMSO et le carbonate de propylène (CP); ils ont un comportement électrochimique voisin de celui des perchlorates ainsi qu'il ressort des résultats que nous avons obtenus en milieu Et_4NClO_4 0.1 *M* et qui sont comparés à ceux trouvés dans la littérature pour les perchlorates (tableau II).

Remarques concernant le tableau II

$E_{\frac{1}{2}}$(SCE) représente le potentiel de demi-vague rapporté à l'électrode au calomel saturée en KCl, tandis que $E_{\frac{1}{2}}(Co^{3+}/Co^{2+})$ exprime le potentiel de demi-vague rapporté au $E_{\frac{1}{2}}$ du couple perchlorate de cobalticinium–cobaltocène déterminé dans le même milieu.

On peut constater en général une concordance très satisfaisante: les $E_{\frac{1}{2}}$(SCE) que nous obtenons avec les trifluorométhanesulfonates sont systématiquement plus négatifs par rapport à ceux donnés dans la littérature pour les perchlorates; il est vraisemblable que cette différence soit partiellement attribuable au système de jonction utilisé pour l'électrode de référence. En effet, si nous comparons les $E_{\frac{1}{2}}$ obtenus pour les deux types de sels dans la DMSO dans nos conditions expérimentales, on peut constater que la concordance est très satisfaisante.

Si enfin l'on compare les valeurs de $\Delta E_{\frac{1}{2}}$, c'est-à-dire la différence entre les $E_{\frac{1}{2}}$ des deux vagues polarographiques ($M^{3+} \rightarrow M^{2+}$ et $M^{2+} \rightarrow M^0$), on peut observer que les différences trouvées entre les perchlorates et les trifluorométhanesulfonates sont beaucoup plus faibles et on peut affirmer que, dans les limites des erreurs expérimentales, les deux sels se comportent de façon identique.

En conclusion, ces sels de lanthanides offrent une possibilité intéressante pour l'étude polarographique des lanthanides en milieu non-aqueux aprotique parfaitement anhydre.

TABLEAU II

COMPORTEMENT ÉLECTROCHIMIQUE DES SELS OBTENUS

Solvant	*Espèce dissoute*	$E_{\frac{1}{2}}^{1}$(*SCE, V*) (*III/II*)	$E_{\frac{1}{2}}^{2}$(*SCE, V*) (*II/0*)	$E_{\frac{1}{2}}^{1}(Co^{3+/2+}, V)$	$E_{\frac{1}{2}}^{2}(Co^{3+/2+}, V)$	$(E_{\frac{1}{2}}^{2}-E_{\frac{1}{2}}^{1})$	*Réf.*
DMSO	$Eu(DMSO)_7(ClO_4)_3$	−0,877	−2,185	+0,051	−1,257	1,308	[a]
	$Eu(ClO_4)_3$	−0,85	−2,15	—	—	1,30	8
	$Eu(CF_3SO_3)_3$	−0,871	−2,180	+0,049	−1.262	1,311	[a]
	$Yb(DMSO)_7(ClO_4)_3$	−1,551	−2,286	−0,618	−1,353	0,735	[a]
	$Yb(CF_3SO_3)_3$	−1,550	−2,284	−0,622	−1,356	0,734	[a]
CP	$Eu(ClO_4)_3$	+0,05	−1,72	—	—	1,77	1
	$Eu(CF_3SO_3)_3$	−0,01	−1,76	+1,02	−0,73	1,75	[a]
	$Yb(ClO_4)_3$	−0,68	−1,76	—	—	1,08	1
	$Yb(CF_3SO_3)_3$	−0,685	−1,80	+0,345	−0,77	1,115	[a]
	$Sm(ClO_4)_3$	−1,13	−1,70	—	—	0,57	1
	$Sm(CF_3SO_3)_3$	−1,126	−1,74	−0,096	−0,71	0,614	[a]

[a] Indiquent nos mesures.

Nous remercions le F.N.R.S. pour l'intérêt apporté à nos travaux et le soutien financier accordé à notre laboratoire.

BIBLIOGRAPHIE

1 G. Peychal-Heiling et V. Gutmann, *Z. Anal. Chem.*, 248 (1969) 6.
2 I. M. Kolthoff et J. F. Coetzee, *J. Amer. Chem. Soc.*, 79 (1957) 1852.
3 K. Starke, *J. Inorg. Nucl. Chem.*, 11 (1959) 77.
4 C. E. Higgins et W. H. Baldwin, *Chem. Div. Ann. Progr. Rep. ORNL-4791*, May 20, 1972, p. 46.
5 V. N. Krishnamurthy et S. Soundarajan, *J. Inorg. Nucl. Chem.*, 29 (1967) 517.
6 J. T. Donoghue, E. Fernandez, J. A. McMillan et D. A. Peters, *J. Inorg. Nucl. Chem.*, 31 (1969) 1431.
7 *Méthodes d'analyses complexométriques par les Titriplex*, Merck, Darmstadt, R.F.A., p. 45.
8 V. Gutmann et G. Peychal-Heiling, *Monatsh. Chem.*, 100 (1969) 1423.

Analytica Chimica Acta, 73 (1974) 420–423

SHORT COMMUNICATION

The determination of carbonate impurities in nickel hydroxide

TOM ALMGREN
Department of Analytical Chemistry, University of Göteborg, Fack, 402 20 Göteborg 5 (Sweden)
(Received 1st July 1974)

The carbon dioxide membrane electrode responds to carbon dioxide concentration in accordance with the Nernst equation

$$E = E^0 + RTF^{-1}(\ln 10) \log[CO_2]$$

For every increment of v ml of a t M standard solution of sodium carbonate added to an acidified sample solution (v_0 ml), the molar concentration of carbon dioxide is

$$[CO_2] = (v + v_i)t/(v_0 + v)$$

where v_i (ml of standard solution) is equivalent to the amount of carbonate in the sample. From these two equations a Gran function, F, proportional to $(v + v_i)$ may be derived:

$$F = (v_0 + v)\ 10 \exp(E + E_k)F/RT(\ln 10) \propto v + v_i$$

where E_k is an arbitrary constant chosen so that the calculations of F are simplified. A plot of F *versus* v, extrapolated to $F = 0$, gives $v = -v_i$ (Fig. 1). The initial molar concentration of carbon dioxide in the sample, and thus the amount of carbonate in the sample, is calculated from the following equation

$$[CO_2] = v_i\, t/v_0$$

The proposed method has been applied to the determination of carbonate impurities in nickel hydroxide intended for storage batteries.

Experimental

Chemicals. Hydrochloric acid, analytical-grade and stored in an ampoule; anhydrous sodium carbonate, analytical grade.

Apparatus. A CO_2–membrane combination electrode (Radiometer E5036/0); pH-meter (Orion Research 701).

Trials. The four samples analysed were made for NiFe storage batteries and were composed of about 80 % nickel hydroxide with graphite, barium sulphate and nickel carbonate as minor constituents. Portions (10–100-mg) of the samples were acidified with hydrochloric acid of various concentrations (0.025–0.1 M) in order to establish optimal conditions. The measurements were made with slow magnetic

stirring. Addition of 0.035 *M* carbonate standard was made in 1-ml portions and the time to reach stable e.m.f. readings was noted for the different conditions. In order to avoid very high osmotic force between the electrode and sample solutions, the ionic strength in the former was in some experiments increased from about 0.025 *M* to 0.1 *M* with sodium chloride.

Results

The best precision was obtained when 50 mg of sample was treated with 100 ml of 0.025 *M* hydrochloric acid. Table I gives the results of these analyses in comparison with the values determined by a method given by Treadwell[1] based on the addition of acid, collecting the carbon dioxide released and weighing it in an adsorption tube. When stronger acid was used, which would be more favourable kinetically, the electrode was poisoned and showed a rapid increase in e.m.f. This also occurred when the ionic strength was increased as described above. The time for analysis was estimated to be about 20 min including four standard additions.

TABLE I

PERCENTAGE CARBONATE AS DETERMINED BY THE PROPOSED METHOD (I) AND BY THE METHOD DESCRIBED BY TREADWELL (II)

Sample	$\%CO_3^{2-}$ *(II)*[a]	*Average*	$\%\ CO_3^{2-}$ *(II)*[a]	*Number of stand. additions used to evaluate* v_i
1	3.7			
1	3.6	3.7±0.1	3.1	4
1	3.8			
2	3.9	3.9	4.0	4
3	1.5	1.8±0.3	1.8	
3	2.1			
4	3.1	3.35±0.25	3.5	2
4	3.6			2

[a] Values obtained by Mrs. Ingegärd Alfelt, Jungner AB.

Figure 2 shows a measurement started directly after acidification. The time to obtain stable e.m.f. values is of course much less after the first standard addition (about 2 min). An example of the calculations is given in Table II. The values are plotted in Fig. 1.

Discussion

The fact that the electrode is poisoned in hydrochloric acid stronger than about 0.05 *M* is probably due to hydrogen chloride molecules passing through the membrane. The time of analysis is thus determined by the rate of dissolution of nickel carbonate in weak (0.025 *M*) hydrochloric acid. It is possible, however, to speed up the analysis by acidifying several samples at one time and then analysing them sequentially. A sample can probably stand for at least 1 h without any appreciable loss of carbon dioxide, if no stirring is applied. The average time of analysis for

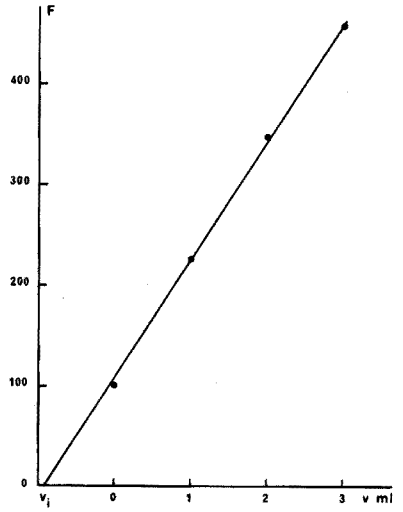

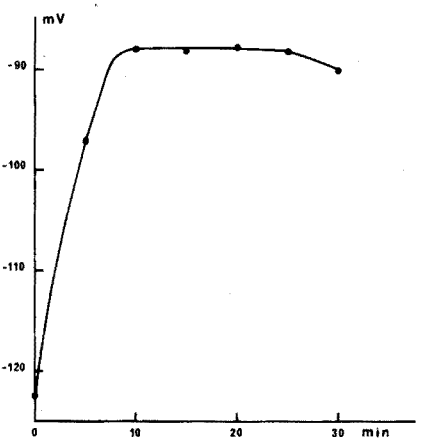

Fig. 1. Gran extrapolation of v ml of 0.035 M sodium carbonate with data from Table II.

Fig. 2. Carbon dioxide electrode response during stirring after acidification of the sample of nickel hydroxide.

TABLE II

EXAMPLE OF CALCULATIONS OF F *VERSUS* v

(Giving $v_i = 0.90$ ml (Fig. 1))

v (ml)	v_0+v (ml)	E (mV)	$E+90.5$ (mV)	$\frac{E+90.5}{59}$	$10\exp\left(\frac{E+90.5}{59}\right)$	$(v_0+v)10\exp\left(\frac{E+9}{59}\right)$
0	100	−90.5	0	0.000	1	100
1	101	−69.8	20.7	0.352	2.25	227
1	102	−59.0	31.5	0.533	3.41	348
3	103	−52.3	38.2	0.648	4.45	458

four samples acidified at the same time and measured one after the other was about 10 min, including two standard additions to each sample. Carbon dioxide was not removed from the hydrochloric acid, which may contain an equilibrium CO_2 concentration of 10^{-5} M at 25°C. This is equivalent to 0.06 mg of carbonate, which should be compared with the 1–2 mg of carbonate in the 50-mg sample. Since the precision of the method is only 0.05–0.15 mg of carbonate, it did not seem worthwhile to remove carbon dioxide from the hydrochloric acid. The present method can also be adapted directly to similar problems; the major limitations are the kinetics of the dissolution of carbonate in the material. The amount of hydrochloric acid and standard solution added should be adapted to the amount of carbonate in the sample.

The author wishes to thank Professor David Dyrssen for valuable discussions,

Mrs. Ingegärd Alfelt for pleasant cooperation, and Enrica Ratti-Moberg for reviewing the English text.

REFERENCE

1 F. P. Treadwell, *Kurzes Lehrbuch der Analytischen Chemie, II Quantitative Analyse*, Franz Deuticke; Leipzig u. Wien, 1917.

Analytica Chimica Acta, 73 (1974) 424–426

ANNOUNCEMENT

Analytical chemistry division, IUPAC, 1974–75

Following the elections at the XXVII Conference of IUPAC at Munich, Germany in 1973, the composition of the Division Committee, responsible for the administration of the Division, is as follows:

President: Prof. N. Tanaka (Japan)
Vice-President: Prof. W. Kemula (Poland)
Secretary: Mr. R. W. Fennell, Materials Department, Royal Aircraft Establishment, Farnborough, Hampshire GU14 6TD, UK
Members: Prof. D. N. Hume (USA)
Prof. H. Kaiser (Germany)
Prof. I. M. Kolthoff (USA)
Prof. O. Samuelson (Sweden)
Prof. B. Tremillon (France)
Prof. T. S. West (UK)
Prof. Yu. A. Zolotov (USSR)

The main work of the Division is performed by its seven Commissions, whose projects are listed below.

Commission V.1. Analytical reactions and reagents
Chairman: Prof. R. Belcher (UK)
Secretary: Prof. F. Pellerin, Hopital General Emile Roux, F-95600 Eaubonne, France
Projects: 1.1 Methods of analysis of food additives (CEE Contract)
1.2 Methods for determination of carbonyl
1.3 Redox indicators
1.4 Complexiметric indicators
1.5 Acid–base indicators for non-aqueous titration
1.6 Methods for polyphenols
1.7 Primary standards
1.8 Colorimetric and fluorimetric determination of steroids

Commission V.2. Microchemical techniques and trace analysis
Chairman: Dr. O. G. Koch (Germany)
Secretary: Dr. M. Pinta, Office de la Recherche scientifique et technique Outre-Mer, 70–74 route d'Aulnay, F-93140 Bondy, France
Projects: 2.1 Study on accuracy and precision of the determination of metals in organic compounds
2.2 Determination of C, H and N in organometallic compounds
2.3 Standard reference materials for trace analysis
2.4 Contamination in trace analysis
2.5 Trace analysis of surfaces

2.6 Stability of solutions used as trace analytical standards
2.7 Volatility losses of trace elements in destruction of organic substances
2.8 Applicability of high pressure decomposition in the trace analysis of biological materials
2.9 Analysis of organoboron compounds
2.10 Determination of minor impurities in analytical reagents
2.11 Sensitivities of trace analytical methods

Commision V.3. Analytical nomenclature
Chairman: Prof. H. M. N. H. Irving (UK)
Secretary: Dr. H. Zettler, Norddeutsche Affinerie, Postfach 67, Alsterterrasse 2, D-2000 Hamburg 36, German Federal Republic
Projects: 3.1 Nomenclature of scales of working
3.2 List of synonyms and trivial names
3.3 Development and publication of methods of analysis
3.3.1 Spectrophotometric procedures
3.3.2 Gravimetric procedures
3.3.3 Ion selective electrode procedures
3.4 Nomenclature of liquid–liquid extraction
3.5 Nomenclature of kinetic methods of analysis
3.6 Nomenclature of ion-selective electrodes
3.7 Selectivity index
3.8 Criteria for sensitivity, detection limits, precision and accuracy
3.9 Nomenclature of data processing
3.10 Compendium of analytical nomenclature
3.11 Nomenclature of sampling
3.12 Information storage and retrieval

Commission V.4. Spectrochemical and other optical procedures for analysis
Chairman: Prof. V. A. Fassel (USA)
Secretary: Mr. B. F. Scribner, National Bureau of Standards, US Department of Commerce, Washington DC 20234, USA
Projects: 4.1 Nomenclature of analytical x-ray spectroscopy
4.2 Systematic classification of spectromechanical excitation sources
4.3 Nomenclature of analytical molecular fluorescence spectroscopy

Commission V.5. Electroanalytical chemistry
Chairman: Prof. R. G. Bates
Secretary: Prof. J. F. Coetzee, Department of Chemistry, University of Pittsburgh, Pittsburgh, Pennsylvania 51260, USA
Projects: 5.1 Purification of electrolytes
5.2 Half-wave potentials in dimethylformamide
5.3 Symbols and terminology for electroanalytical techniques
5.4 Pretreatment of solid electrodes
5.5 Conditional diffusion coefficients
5.6 Standard potentials in fused salts
5.7 Purification of background electrolytes

5.8 Diffusion coefficients in mercury
5.9 Sign convention for currents
5.10 Conditional equilibrium constants
5.11 Recommendations on reporting of electroanalytical data
5.12 Selectivity of ion selective electrodes
5.13 Indicator and reference electrodes in non-aqueous solvents
5.14 Half-wave potentials in propylene carbonate and hexamethylphosphoramide
5.15 Purification of dimethylformamide
5.16 Application and potentialities of electroanalytical methods in environmental analysis

Commission V.6. Equilibrium data
Chairman: Prof. G. H. Nancollas (USA)
Secretary: Dr. S. Ahrland, Department of Inorganic and Physical Chemistry, Chemical Center, University of Lund, POB 740, S-220 07 Lund 7, Sweden
Projects: 6.1 Stability constants
6.2 Distribution equilibria
6.3 Critical surveys
6.4 Ionic media
6.5 Information retrieval (data flagging)
6.6 Symbols for mixed ligand complex constants
6.7 Solubility data

Commission V.7. Analytical radiochemistry and nuclear materials
Chairman: Dr. M. B. A. Crespi (Argentina)
Secretary: Dr. J. C. White, Analytical Chemistry Division, Oak Ridge National Laboratory, POB X, Oak Ridge, Tennessee 37830, USA
Projects: 7.1 Light element analysis
7.2 Trace analysis reference materials for radiochemical analysis
7.3 Reference materials for uranium analysis
7.4 Analysis of nuclear materials
7.5 Nomenclature for radioanalytical chemistry
7.6 Nuclear methods for analysis of key elements in environmental pollution
7.7 Nuclear methods for analysis of fissile and fertile elements
7.8 Nuclear methods for analysis of molecular compounds in environmental pollution
7.9 Critical compilation of radioanalytical data
7.10 Non-nuclear methods of analysis of fissile and fertile elements
7.11 Charged-particle-induced x-ray fluorescence
7.12 Separations in radioanalytical chemistry
7.12.1 Ion exchange
7.12.2 Liquid–liquid extraction
7.12.3 Precipitation and adsorption
7.12.4 Miscellaneous
7.13 State of the art of thorium analysis

ERRATUM

M. I. Karayannis, S. M. Tzouwara-Karayannis and T. P. Hadjiioannou, Kinetic Study and Analytical application of the Iodate–Arsenite reaction in strongly acidic Solutions, *Anal. Chim. Acta*, 70 (1974) 351–357.

1) Number 2.303 in equations (13) and (14) should be replaced by 0.4343.

2) p. 353 line 2 should read:

... the hydrogen ion concentration were kept constant at 0.150 *M* and 1.00 *M*, respectively ...

ANALYTICA CHIMICA ACTA, VOL. 73 (1974)

AUTHOR INDEX

ANALYTICA CHIMICA ACTA, VOL. 73 (1974)

SUBJECT INDEX

on of the ed
ally complete descript
included in this category; these

INFORMATION FOR AUTHORS
ANALYTICA CHIMICA ACTA

e paper in double-spaced typing on one side c
of 4 cm, on pages of uniform size. If any var
used (e.g. Xerox), authors should ensure tha
nd that the paper used can be written on wit
re advised to retain at least one copy of the p
preceded by a sheet of manuscript paper car
er, (b) the name and full postal address of the
e sent, (c) the number of pages, tables and fi
title for page headings, not exceeding 45 cha

e given every latitude, consistent with clarity and bre
papers. Inexperienced authors may, however, welco
is provided in the Handbooks for Authors issued b
an Chemical Society. Authors writing in English will
as Gowers *Complete Plain Words* and Fowler's *Moc*

d initial layout

headed by a concise but informative ti
address of the laboratory wh
different from that
ort shou

INFORMATION FOR AUTHORS

General

Analytica Chimica Acta publishes papers which report significant advances in methods techniques, knowledge or understanding in any area of analytical chemistry. Submission c a paper implies that the work described has not been, and will not be,published elsewhere (except as an abstract, or as part of a lecture, review or academic thesis).

Three types of papers are published: regular papers, short communications, and review Reviews are written by invitation of the editors, who welcome suggestions for subjects. Short communications are usually complete descriptions of limited investigations, but preliminary notes may also be included in this category; these should as a rule not exceed four printed pages.

Submission of Papers

Papers may be written in English, French or German. Authors should submit two copies of the paper in double-spaced typing on one side of the paper only, with a margin of 4 cm, on pages of uniform size. If any variety of machine copying is used (e.g. Xerox), authors should ensure that both copies are easily legible and that the paper used can be written on with both ink and pencil. Authors are advised to retain at least one copy of the paper. Typescripts should be preceded by a sheet of manuscript paper carrying (a) the title of the paper, (b) the name and full postal address of the person to whom proofs are to be sent, (c) the number of pages, tables and figures, and (d) a short running title for page headings, not exceeding 45 characters.

Authors are given every latitude, consistent with clarity and brevity, in the style and form of their papers. Inexperienced authors may, however, welcome some guidance. Very useful advice is provided in the Handbooks for Authors issued by the Chemical Society and American Chemical Society. Authors writing in English will find much of value in books such as Gowers *Complete Plain Words* and Fowler's *Modern English Usage.*

Title and initial layout

Papers should be headed by a concise but informative title. This is followed by the names of the authors, and the address of the laboratory where the work was carried out. If the present address of an author is different from that mentioned, it should be given in a footnote. Acknowledgements of financial support should not be made in footnotes. The same procedure applies to regular papers and short communications.

Summary

A regular paper should have a summary on a separate page. This summary (50–250 words) should comprise a brief *factual* account of the contents of the paper, with emphasis on new information. Uncommon abbreviations, jargon and reference numbers must not be used. Papers written in French or German should be followed by a Résumé or

Zusammenfassung. All French and German papers also carry summaries in English, and authors are encouraged to provide translations where necessary.

Short communications do not require summaries.

Introduction

The first paragraphs of the paper should contain accounts of the reasons for the work, any necessary historical background (as briefly as possible), and preliminary experimental work. The principal results of the work should be summarized as early as possible.

Experimental

The description of the experimental methods may be given after the introductory material, or after the discussion of results, depending on the nature of the paper. Detailed experimental descriptions should, however, be restricted to one section of the paper, and not scattered throughout the text. Working procedures should be given in the imperative mood; sufficient detail should be given to allow any reasonably experienced worker to carry out the procedure. Detailed descriptions of well known techniques and equipment are unnecessary, as are simple preparations of reagents or solutions, and lists of common chemicals. Names of manufacturers need be given only if the product differs essentially from that of other manufacturers.

Results and Discussion

These may be treated together or separately. In discussing results, unnecessary repetition of experimental detail, unsupported elaboration of hypotheses, and verbose exposition of ideas should be avoided. Chemical formulae should not be used in the text unless confusion is likely to arise from the use of names; a slip in proof-reading will probably have a less dramatic effect on meaning if chemical names rather than formulae are used. Formulae should however be used for brevity in Tables and Figures.

Acknowledgements

These should be kept as short as possible, and placed, without a heading, at the conclusion of the text.

References

The references should be collected at the end of the paper, numbered in the order of their appearance in the text (*not* arranged alphabetically), and typed on a separate sheet. If the paper forms part of a series, the reference to the previous part should appear as the first reference, the number being cited at the title of the paper. References given in Tables should be numbered according to the position of the Table in the text. Every reference listed must be cited in the text. Care should be taken that reference numbers in the text do not become confused with numerical data, and textual rearrangement should be made where necessary. Numerals referring to equations are placed in parentheses.

In the list of references, the following forms should be adopted:

(a) *Journals*

G. Dryhurst and P.J. Elving, Anal. Chem., 40 (1968) 492.
N. Zaman, E. Merciny and G. Duyckaerts, Anal. Chim. Acta, 56 (1971) 261.

The title of the journal must be abbreviated as in the *Chemical Abstracts List of Periodical*

(b) *Books*

C.A. Parker, Photoluminescence of Solutions, Elsevier, Amsterdam, 1968, p.476.

or, for edited books:

R.E. Thiers, in D. Glick (Ed.), Methods of Biochemical Analysis, Vol. 5, Interscience-Wiley, New York, 1957, p. 273.

Titles of papers are unnecessary. Citations of reports which are not widely available (e.g. reports from government research centres) should be avoided if possible. Authors' initials should not be used in the text, unless real confusion could be caused by their omission. If the reference cited contains three of more names, only the first author's name followed by et al. (e.g. Zaman et al.) should be used in the text; but in the reference list, the initials and names of *all* authors must be given.

Tables

All Tables should be numbered with Roman numerals, and have brief descriptive headings; they should be typed on separate pages, because it may not be possible to print them exactly where they are cited in the text. The layout of Tables should be given serious thought, so that the reader can quickly grasp the significance of the results.

Tables with only two or three headings are printed best horizontally, e.g.

Hg^{2+} added (μg)	1.0	2.0	3.0	5.0
% Extraction	95.0	99.8	99.5	89.0

Column headings should be brief, because their width is usually the limiting factor for the number of columns which can be accommodated on a page.

Experimental information which is relevant to all the results in the Table is best given in parenthesis immediately after the heading. No column should contain the same number throughout its length. Footnotes to Tables are best denoted by superscript a, b, c . . . The units used should be clearly stated. Confusion can arise from the use of powers in column headings. The following usage is recommended: e.g. if molar absorptivities are listed, the heading should be $\epsilon(\times 10^4$ l mole^{-1}cm$^{-1})$ so that a number 2.32 in the column becomes 23 200.

Figures

Figures should be prepared in black waterproof drawing ink on drawing or tracing paper of the same size as that on which the paper is typed. One original and two photostat (or other) copies are required. Attention should be given to any lettering (which should be kept to a minimum) and to spacing on axes of graphs, in order to ensure that numbers, etc., remain legible after reduction for printing. Preferably, lettering and numbers should be written in pencil. Axes of a graph should be clearly labelled.

The following standard symbols should be used in graphs:

▽ ▽ ■ □ ● + x ○

Straight-line graphs are not usually admissible, because they can readily be described in the text, by means of an equation. Explanatory information should be placed not in the figure, but in the legend.

Legends to figures should be typed on a separate sheet of paper. All Figures should be numbered with Arabic numerals, and require descriptive legends.

Photographs should be glossy prints and be as rich in contrast as possible; colour photographs cannot be accepted. In general, line diagrams are more informative than photographs of equipment.

Nomenclature, Abbreviations and Symbols

In general, the recommendations of the International Union of Pure and Applied Chemistry (I.U.P.A.C.) should be followed, and attention should be given to the recommendations of the Analytical Chemistry Division in the journal *Pure and Applied Chemistry*.

The following units are recommended:

Basic SI Units

metre	m	candela	cd
kilogram	kg	mole	mol
second	s	(an Avogadro number of any	
ampere	A	particle: atoms, molecules,	
degree Kelvin	K	ions, electrons, etc.)	

Derived SI Units

joule	J	$kg\ m^2\ s^{-2}$	farad	F	$A\ s\ V^{-1}$
newton	N	$J\ m^{-1}$	weber	Wb	V s
watt	W	$J\ s^{-1}$	henry	H	$V\ s\ A^{-1}$
coulomb	C	A s	tesla	T	$V\ s\ m^{-2}$
volt	V	$J\ A^{-1}\ s^{-1}$	hertz	Hz	s^{-1}
ohm	Ω	$V\ A^{-1}$	degree Celsius	°C	K−273.15

Other Units

litre	l	10^{-3} m^3	hour	h	3.6×10^2 s
gram	g	10^{-3} kg	dyne	dyn	10^{-5} N
poise	P	10^{-3} m^{-1} s^{-1}	atmosphere	atm	101.325 kN m^{-2}
electron volt	eV	1.6021×10^{-19} J	molar	*M*	mol l^{-1}
calorie	cal	4.184 J	molal	*m*	mol kg^{-1}
minute	min	60 s	curie	Ci	37×10^9 s^{-1}

Prefixes to Abbreviations for the names of units indicating

Multiples		Sub-multiples			
tera ($\times 10^{12}$)	T	milli ($\times 10^{-3}$)	m	pico ($\times 10^{-12}$)	p
giga ($\times 10^9$)	G	micro ($\times 10^{-6}$)	μ	femto ($\times 10^{-15}$)	f
mega ($\times 10^6$)	M	nano ($\times 10^{-9}$)	n	atto ($\times 10^{-18}$)	a
kilo ($\times 10^3$)	k				

The use of nanometre (nm) for the expression of analytical wavelengths has now superseded mμ or Å, both of which should be avoided.

Symbols, formulae and equations should be written with great care, capitals and lower case letters being distinguished where necessary. Particular care should be taken in writing mathematical expressions containing superscripts and subscripts, and in proof-reading such equations, Greek letters and unusual symbols employed for the first time should be defined by name in the left-hand margin.

The solidus / may be used in equations to economize vertical space, but its use should be consistent. For example:

$$A/b = x^2/(u + v)^{5/6}$$

It is recommended that natural or Naperian logarithms should be denoted by ln while decadic logarithms should be denoted by log.

In analytical chemistry, the term normality (N) serves many useful purposes and will be retained. It should not however, be used, if no ambiguity is introduced by the use of molarity (M). The term formality (F) should be avoided.

Unusual abbreviations require definition when first used in a paper. Abbreviations for long chemical names may be useful, especially in equations, tables or figures. The need for abbreviations can often be avoided in the text by the use of pronouns or expressions such as the reagent, the enzyme or the medium.

Ambiguity in expressing dilution can be avoided by the use of e.g. (1 + 2) rather than 1 : 2 which could mean either one part diluted with 2 parts or one part diluted to twice its volume.

In accordance with I.U.P.A.C. rules, the mass number, atomic number, number of atoms and ionic charge should be designated by a left upper index, a left lower index, a right lower index and a right upper index, respectively, placed round the atomic symbol. For example, the phosphate ion should be designated as PO_4^{3-} (*not* PO_4^{-3} or PO_4^{---}), and phosphorus-32 as ^{32}P (*not* P^{32} or P-32).

The Stock notation for the indication of stoichiometric valency states (and indirectly the proportion of the constituents) is recommended. Examples are iron(III) chloride in preference to ferric chloride, and potassium hexacyanoferrate(II) in preference to potassium ferrocyanide. This I.U.P.A.C. rule is valid for French and German as well as English usage.

(Continued from page 4 of cover)

CONTENTS

(Continued on inside back cover)